

# **Antibiofilm Activity of Novel Antimicrobial Peptides and Liposomal Encapsulation as a Promising Approach to Enhance Their Efficacy**

**Ahmed M. Amer**



Thesis for the degree Philosophiae Doctor  
PhD programme in Health Sciences  
Department of Life Sciences and Health  
Faculty of Health Sciences  
OsloMet – Oslo Metropolitan University  
Autumn 2025

CC-BY-SA versjon 4.0

OsloMet Avhandling 2025 nr. 50

ISSN 2535-471X

ISBN 978-82-8364-695-5

OsloMet – storbyuniversitetet

Universitetsbiblioteket

Skriftserien

St. Olavs plass 4,

0130 Oslo,

Telefon (47) 64 84 90 00

Postadresse:

Postboks 4, St. Olavs plass

0130 Oslo

Trykket hos Byråservice

Trykket på Scandia 2000 white, 80 gram på materiesider/200 gram på coveret

## Acknowledgements

First and foremost, I thank God for granting me the strength, patience, and perseverance to complete this work. The research presented in this thesis was conducted within the Disease and Environmental Exposures research group, Department of Life Sciences and Health, Oslo Metropolitan University (OsloMet). I am deeply grateful for the PhD scholarship funded by the Faculty of Health Sciences, which made this work possible.

I am sincerely grateful to my supervisors, **Sanko Nguyen** and **Colin Charnock**, for their invaluable guidance, constructive feedback, and constant encouragement throughout this project. I am especially grateful to **Sanko** for granting me the freedom and space to explore my own research ideas, for supporting my initiatives in the laboratory, and for always encouraging independent thinking while providing steady guidance when needed. To **Colin**, I owe special thanks for your expertise in microbiology, which was essential to the success of this work. I truly appreciate your constant availability, whether to provide hands-on help in the lab or simply to lend a listening ear whenever I needed to share and work through challenges (and occasionally question my life choices).

My sincere and heartfelt thanks go to the Head of Pharmacy Studies, **Anne Berit Walter**, and my colleagues in the department for their support, insightful discussions, and for fostering a positive and inclusive working environment. I am grateful to **Vigdis Aas** and **Ellen Hagesæther** for their assistance with cell culture work, to **Ane Meisland** and **Niclas Karlsson** for their help with the HPLC–MS instrument, and to **Björg Siw Møller Tannæs** for your support in the chemistry laboratory. I also deeply appreciate **Martina Martin Tzanova** for the many conversations and companionship, and **Ane Gedde-Dahl** for providing valuable assistance, offering wise advice, and keeping me company during the late working hours past 17:00 when most offices were already closed. I am also grateful to **Elisabeth Henrohn** and **Marthe Rambøl Bjørknes** for their help with teaching duties and for making those times more enjoyable, despite the challenges involved.

My sincere thanks are also extended to the Biomedical Laboratory Sciences staff, particularly **Eldri Undlien Due, Hege Tunsjø, Farzana Riasat, and Oliwia Witezak** for their consistent readiness to assist whenever I needed help in the lab. I would also like to thank our collaborators at AgriBiotix – **Tage Thorstensen** and **Kirill Ovchinnikov** – for providing Micrococcin P1 as well as their technical support and assistance, without which this project would not have been successful.

A special thanks goes to my fellow PhD candidates for their support and shared experiences. To those who joined me along this journey – **Helene Marie Haldorsen Gombos, Katrine Heger, Ketil Hegerstrøm Haugli, Madhavi Bhandari, Marthe Tofthagenand** and especially my officemate **Ragna Tingstad**, for the countless conversations, mutual encouragement, and laughter we shared. To those who completed their PhD during my time here – **Alice Shwe, Rønnaug Eline Larsen, Maria Aukrust Naqvi** and **Yngvild Kristine Bergsholm Rochette** – your achievements were an inspiration. And to the new colleagues just embarking on their PhD path – **Ali Reza Afshari, Christiansen Stian, Tommy Emil Dzus** – I wish you success in your own journeys.

Finally, I am forever indebted to my family – my parents **Mohamed Medhat** and **Wafaa Fouad** and my brothers **Amr, Taher** and **Adham** – for their unconditional love, patience, and unwavering belief in me. Your support has been the foundation that sustained me through this challenging yet rewarding period of my life.

With gratitude,

*Ahmed Amer*

Oslo, April 2025



# Abstract

Biofilms are structured communities of microorganisms embedded within a self-produced extracellular matrix. Biofilm-associated infections are difficult to treat, as the extracellular matrix acts as both a physical and chemical barrier that hinders the penetration of antimicrobial agents. Treatment challenges are further compounded by the emergence of antimicrobial resistant strains. Together, these factors highlight the urgent need for novel antimicrobial agents suitable for clinical use, as well as effective delivery systems capable of targeting microbes within the biofilm. Antimicrobial peptides (AMPs) offer a promising alternative due to their diverse mechanisms of action and ability to target drug-resistant microbes. However, their clinical application is hindered by suboptimal physicochemical and pharmacokinetic properties.

This thesis explores the antimicrobial and antibiofilm activity of novel AMPs, namely teixobactin analogues and micrococcin P1 (MP1), and liposomal encapsulation as a strategy to enhance their delivery and efficacy against biofilm-forming pathogens. Initially, cholesterol-free fusogenic liposomes with varying surface charges were developed, and their ability to fuse with microbial cells and penetrate the biofilm matrix was assessed. All liposomal formulations demonstrated fusion with different microbial cells, highlighting their potential for AMP delivery. Moreover, cationic liposomes showed the strongest interaction and retention within biofilms. Subsequently, MP1 was incorporated into cholesterol-free fusogenic liposomes formulated using phospholipids with varying acyl chain lengths. Liposomes with longest acyl chains exhibited higher MP1 entrapment efficiency and enhanced the peptide's antimicrobial and antibiofilm activity. Furthermore, MP1-loaded liposomes effectively disrupted *Staphylococcus aureus* biofilms formed on biomedical surfaces.

Finally, this thesis evaluated the antimicrobial and antibiofilm activities of three teixobactin analogues. The natural teixobactin compound represents a novel class of antibiotics with a unique mechanism of action and has attracted considerable interest as a potential drug candidate. While all three analogues demonstrated promising efficacy against biofilm-forming pathogens, one showed comparatively stronger effects and is proposed as a lead candidate for further liposomal encapsulation.

In conclusion, this work highlights the potential of fusogenic liposomes as an advanced delivery system for novel AMPs targeting biofilms, offering a promising strategy for combating biofilm-associated infections.

# Sammendrag

Biofilmer er strukturerte samfunn av mikroorganismer som er omsluttet i en egenprodusert ekstracellulær matriks. Infeksjoner assosiert med biofilm er utfordrende å behandle, ettersom den ekstracellulære matriksen fungerer både som en fysisk og kjemisk barriere som hemmer penetrasjon av antimikrobielle midler. Behandlingsutfordringene forsterkes ytterligere av fremveksten av antimikrobiell resistens. Samlet sett understreker disse faktorene det akutte behovet for nye antimikrobielle midler som egner seg for klinisk bruk, samt effektive leveringssystemer som kan målstyres mot mikrober inni biofilmen. Antimikrobielle peptider (AMP-er) representerer et lovende alternativ grunnet deres varierte virkningsmekanismer og evne til å angripe resistente mikroorganismer. Deres kliniske anvendelse begrenses imidlertid av suboptimale fysikalsk-kjemiske og farmakokinetiske egenskaper.

Denne avhandlingen undersøker den antimikrobielle og antibiofilmaktiviteten til nye AMP-er, nærmere bestemt teixobactin-analoger og micrococcin P1 (MP1), samt liposomal innkapsling som en strategi for å forbedre leveringen og effekten deres mot biofilmdannende patogener. Innledningsvis ble det utviklet kolesterolfrie fusogene liposomer med ulik overflateladning, og deres evne til å fusjonere med mikrobielle celler og penetrere biofilmmatrisen ble evaluert. Alle liposomformuleringene demonstrerte fusjon med ulike mikrobielle celler, noe som understreker deres potensiale som legemiddelleveringssystem for AMP-er. Kationiske liposomer utviste sterkest interaksjon med og retensjon i biofilmen. Deretter ble MP1 innkapslet i kolesterolfrie fusogene liposomer formulert med fosfolipider med varierende acylkjedelengde. Liposomer med lengst acylkjeder viste høyere innkapslingseffektivitet for MP1 og forbedret både den antimikrobielle og antibiofilmaktiviteten til peptidet. Videre viste MP1-liposomer effektiv forstyrrelse av biofilmer dannet av *Staphylococcus aureus* på biomedisinske overflater.

I denne avhandlingen ble den antimikrobielle og antibiofilmaktiviteten til tre teixobactin-analoger også evaluert. Det naturlige stoffet teixobactin? representerer en ny klasse antibiotika med en unik virkningsmekanisme og har vakt betydelig interesse som lovende legemiddelkandidat. Alle tre analogene viste lovende effekt mot biofilmdannende patogener, men én av dem utpekte seg med relativ sterkere effekt og foreslås som en mulig kandidat for videre formulering med liposomer.

Dette arbeidet har løftet frem potensialet til fusogene liposomer som et avansert legemiddelleveringssystem for nye AMP-er rettet mot biofilmer. Dette kan være en lovende strategi for å bekjempe biofilmassosierte infeksjoner.

# Table of Contents

List of Abbreviations .....	3
List of papers and manuscripts .....	6
1. Introduction .....	7
1.1. Biofilms and their clinical relevance.....	7
1.1.1. The biofilm development cycle.....	8
1.1.2. Challenges associated with biofilm infection management .....	12
1.2. Antimicrobial peptides and their application in biofilm treatment .....	14
1.2.1. Classes and mechanisms of action of AMPs .....	14
1.2.2. Teixobactin and micrococcin P1 as potential antibiofilm agents.....	18
1.2.3. Limitations to the clinical application of AMPs .....	21
1.3. Liposomes as a promising approach for biofilm treatment .....	23
1.3.1. Preparation and classification of liposomes .....	23
1.3.2. Liposomes in biofilm management.....	27
1.3.3. Fusogenic liposomes .....	30
2. Aim of the work .....	32
3. Methodological considerations .....	33
3.1. Materials.....	34
3.1.1. Antimicrobial peptides .....	34
3.1.2. Phospholipids.....	35
3.1.3. Microbial strains .....	36
3.1.4. Medical-grade surfaces for biofilm studies .....	36
3.2. Preparation and physicochemical characterization of liposomes .....	36
3.2.1. Preparation of fusogenic liposomes .....	36
3.2.2. Measurement of liposomal size and polydispersity index.....	37
3.2.3. Determination of liposomal zeta potential .....	39
3.2.4. Quantification of drug entrapment efficiency .....	39
3.3. Biocompatibility testing of fusogenic liposomes.....	40
3.4. Liposomal fusion with microbial cells.....	41

3.5. Evaluation of antimicrobial and antibiofilm activity.....	43
3.5.1. Minimum inhibitory concentration assay .....	43
3.5.2. Minimum bactericidal concentration assay.....	44
3.5.3. Effect of antimicrobial agents on bacterial growth curves.....	44
3.5.4. Inhibition of biofilm formation.....	44
3.5.5. Treatment of preformed biofilms.....	45
3.5.6. Microscopic Analysis of Biofilms.....	45
4. Synopsis of the papers .....	47
Paper I.....	47
Paper II.....	49
Paper III.....	51
5. Discussion .....	53
5.1. Main findings .....	53
5.2. Significance of the results and future perspectives .....	60
6. Concluding remarks.....	63
References .....	64

# List of Abbreviations

ATCC – American Type Culture Collection

AMP – Antimicrobial Peptide

AMR – Antimicrobial Resistance

Arg – Arginine

BIC – Biofilm Inhibitory Concentration

CFU – Colony Forming Unit

CLSI – Clinical and Laboratory Standards Institute

CLSM – Confocal Laser Scanning Microscopy

CPP – Critical Packaging Parameter

CV – Crystal Violet

DAPC – 1,2-Diarachidoyl-sn-glycero-3-phosphatidylcholine

DAPI – 4',6-Diamidino-2-phenylindole

DLS – Dynamic Light Scattering

DLVO – Derjaguin-Landau-Verwey-Overbeek

DMSO – Dimethyl Sulfoxide

DNA – Deoxyribonucleic Acid

DOPC – 1,2-Dioleoyl-sn-glycero-3-phosphatidylcholine

DOPE – 1,2-Dioleoyl-sn-glycero-3-phosphatidylethanolamine

DOPG – 1,2-Dioleoyl-sn-glycero-3-phospho-(1'-rac-glycerol)

DOTAP – 1,2-Dioleoyl-3-trimethylammonium-propane

DPPC – 1,2-Dipalmitoyl-sn-glycero-3-phosphatidylcholine

DSPC – 1,2-Distearoyl-sn-glycero-3-phosphatidylcholine

DSM – Deutsche Sammlung von Mikroorganismen (German Collection of Microorganisms)

EE% – Entrapment Efficiency Percentage

EF-G – Elongation Factor G

EMA – European Medicines Agency

ELS – Electrophoretic Light Scattering

EPS – Extracellular Polymeric Substances

EUCAST – European Committee on Antimicrobial Susceptibility Testing

FDA – Food and Drug Administration

FRET – Förster Resonance Energy Transfer

Gln – Glutamine

GUV – Giant Unilamellar Vesicle

HPLC-MS – High-Performance Liquid Chromatography-Mass Spectrometry

Leu – Leucine

LUV – Large Unilamellar Vesicle

MBC – Minimum Bactericidal Concentration

MDR – Multidrug Resistance

MIC – Minimum Inhibitory Concentration

MLV – Multilamellar Vesicle

MP1 – Micrococcin P1

MRSA – Methicillin-Resistant *Staphylococcus aureus*

NBD – 7 nitro-2,1,3-benzoxadiazole-4-yl

Nle – Norleucine

Nva – Norvaline

PBS – Phosphate-Buffered Saline

PDI – Polydispersity Index

PEG – Polyethylene Glycol

PTFE – Polytetrafluoroethylene

PTMs – Post-Translational Modifications

PVC – Polyvinyl Chloride

QS – Quorum Sensing

RBCs – Red Blood Cells

Rh – Rhodamine

SAR – Structure-Activity Relationship

SUV – Small Unilamellar Vesicle

T<sub>m</sub> – Phase Transition Temperature

TEM – Transmission Electron Microscopy

TB – Teixobactin analogue

TSA – Tryptic Soy Agar

TSB – Tryptic Soy Broth

TTC – Triphenyl tetrazolium Chloride

VRE – Vancomycin-Resistant *Enterococcus*

# List of papers and manuscripts

## Paper I

Ahmed M. Amer, Colin Charnock, Sanko Nguyen

**The Impact of Surface Charge on the Interaction of Cholesterol-Free Fusogenic Liposomes with Planktonic Microbial Cells and Biofilms**

*International Journal of Pharmaceutics*, 669, article 125088 (2025).

DOI: <https://doi.org/10.1016/j.ijpharm.2024.125088>

## Paper II

Ahmed M. Amer, Colin Charnock, Kirill V. Ovchinnikov, Tage Thorstensen, Sanko Nguyen

**Phospholipid Acyl Chain Length Modulation: A Strategy to Enhance Liposomal Drug Delivery of the Hydrophobic Bacteriocin Micrococcin P1 to Biofilms.**

*European Journal of Pharmaceutical Sciences*, 211, article 107149 (2025).

DOI: <https://doi.org/10.1016/j.ejps.2025.107149>

## Paper III

Ahmed M. Amer, Colin Charnock, Sanko Nguyen

**Novel Teixobactin Analogues Show Promising In Vitro Activity on Biofilm Formation by *Staphylococcus aureus* and *Enterococcus faecalis***

*Current Microbiology*, 81, 349 (2024).

DOI: <https://doi.org/10.1007/s00284-024-03857-9>



# 1. Introduction

## 1.1. Biofilms and their clinical relevance

Biofilms are microbial communities embedded in a self-produced extracellular matrix [1]. They can form on both living and non-living surfaces, including surfaces within the human body, where they can impact health [1, 2]. Biofilms are not limited to surface formation; bacterial aggregates that are not surface attached (e.g. pellicles) are also recognized as biofilms [3, 4]. Resident microbes in biofilms benefit from enhanced tolerance to antimicrobial agents and increased protection against environmental harsh conditions [2, 5].

Biofilm aggregates were first described in the late seventeenth century by Anton van Leeuwenhoek, who characterized them as bacterial clusters adhering to surfaces [4, 5]. The term "film" was first used in the mid-1930s to describe bacterial aggregates forming on surfaces submerged in water [6, 7]. In medical microbiology, the first reported link between biofilm formation and human disease emerged in the 1970s, when researchers observed *Pseudomonas aeruginosa* aggregates in sputum samples and lung autopsies from cystic fibrosis patients [4]. Since then, biofilm formation has been linked to a wide range of infections, including periodontitis, chronic otitis media, infective endocarditis, chronic wounds and recurrent urinary tract infections, among others [8]. Furthermore, medical devices and implants, such as catheters, orthopaedic implants and heart valves, are susceptible surfaces for biofilm development [8]. Biofilms formed on implanted medical devices contribute to approximately 60–70% of hospital-acquired infections [9].

The transition of microbial cells from the planktonic (free-floating) state to biofilm formation is a complex process triggered by changes in the surrounding environment. Factors such as shifts in nutrient availability, temperature, pH and oxygen concentration play a critical role in initiating this transition [10]. These changes lead to an increase in the intracellular concentration of the second messenger cyclic diguanylate monophosphate (cyclic-di-GMP), which in turn activates the production of adhesins and extracellular polymeric substances (EPS) essential for biofilm attachment, maturation, and structural integrity [11]. Once microbial cells manage to form biofilms, the infection often becomes chronic and more challenging to treat compared with infections associated with planktonic microbial cells [3]. Biofilm infections have also been reported to play a significant role in promoting the emergence of antimicrobial resistance

(AMR) by various mechanisms [2, 12]. For instance, biofilm formation is frequently linked to hypermutator bacterial phenotypes, which can exhibit mutation rates up to 1,000 times higher than normal, thereby increasing the likelihood of AMR development [13]. Additionally, the presence of diverse microbial species within the biofilm promotes the transfer of resistance genes via mobile genetic elements, such as plasmids [12]. Moreover, biofilm infections are often managed by administering high doses of antibiotic combinations over extended periods, an approach that may further contribute to the development of antimicrobial resistance [2].

Although most reports highlight the role of bacterial biofilms in infections, fungal biofilms on medical devices are also increasingly being recognized as a major contributor to hospital-acquired infections [14]. Bacterial species commonly detected in infection-related biofilms include *Pseudomonas aeruginosa*, *Escherichia coli*, *Staphylococcus aureus* and *Enterococcus faecalis*; whereas *Candida* species are the most frequently isolated fungi from biofilms [15, 16]. The following two subsections will provide a description of the biofilm formation process, and the challenges encountered in treating biofilm-associated infections.

### ***1.1.1. The biofilm development cycle***

Biofilm development and composition are influenced by both the microbial species involved and environmental conditions. For example, single-species biofilms of *P. aeruginosa* can form as mushroom-shaped microcolonies in glucose-based media and as flat biofilms when grown in the presence of citrate as a carbon source [2]. Moreover, biofilms in clinical settings are rarely monomicrobial. They are rather polymicrobial and can include various bacteria and fungi coexisting within a shared EPS matrix, which adds complexity to the biofilm structure [16, 17]. Polymicrobial biofilm formation can involve multiple biofilm-forming species during the initial stages, while other microbial cells may adhere later, particularly species lacking biofilm-forming properties. In such cases, the species that first colonize the surface are often referred to as the founding species [18]. Regardless of the microorganism or environmental conditions, biofilm development typically progresses through four key stages as shown in **Figure 1** [11]. Both bacterial and fungal cells share the same main stages in biofilm formation and development [14]. The following section will describe each stage of biofilm development

depicted in the figure, illustrated with examples from the most studied and clinically relevant biofilm-forming microbial species.

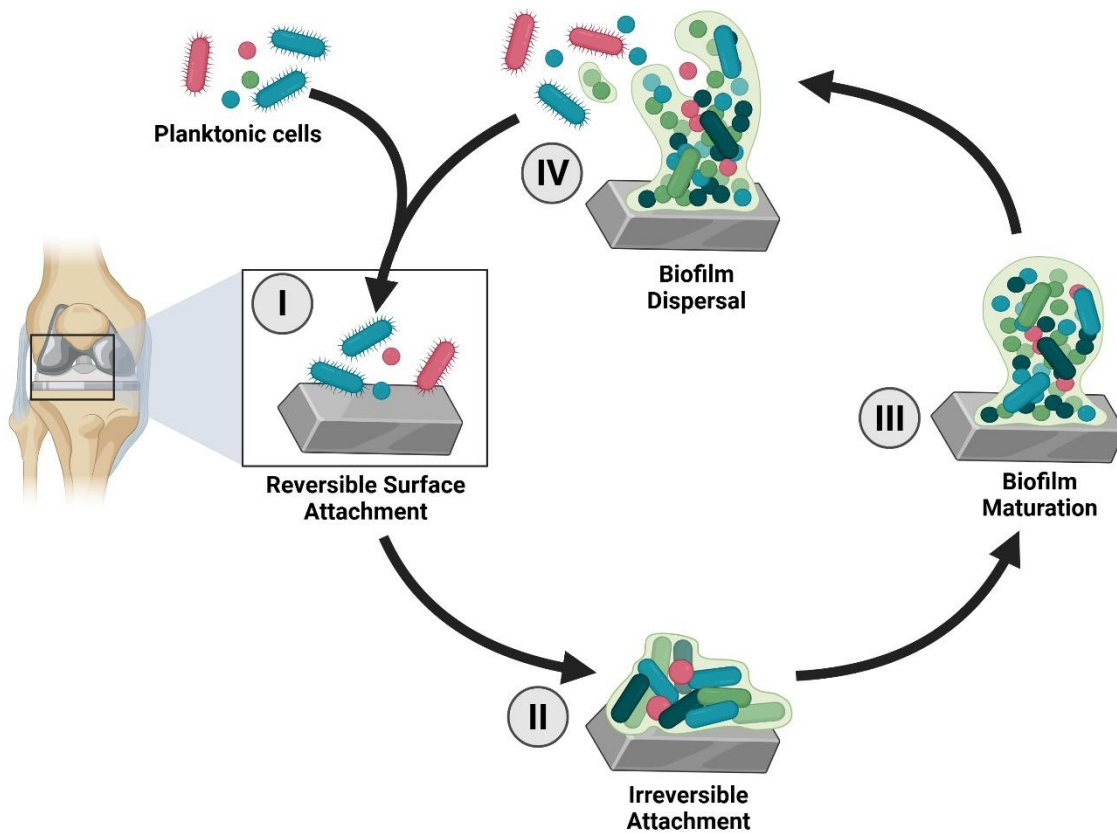


**Figure 1.** Illustration of the main stages of biofilm development and dispersal depicted using a prosthetic knee joint as an example. The figure is created in BioRender.com.

### *I. Initial reversible attachment:*

Microbial cell motility plays a crucial role in the initial phase of biofilm development, by facilitating physical contact with surfaces suitable for cellular attachment. This motility may arise from specialized appendages (e.g. flagella) or from passive mechanisms like Brownian motion in species lacking motility structures, such as species of *Streptococcus* and *Klebsiella* [18]. Cell attachment is influenced by the physicochemical properties of the surface, such as roughness, hydrophilicity, surface energy, and electrical potential. For instance, irregular or rough surfaces promote bacterial adhesion and colonization, thereby creating favourable conditions for biofilm development [19]. Conversely, certain studies report that nanoscale surface roughness has an inhibitory effect on microcolony formation

[20]. The interaction between microbial cells and material surfaces is governed by the principles of colloidal physics, as described by the Derjaguin–Landau–Verwey–Overbeek (DLVO) theory [21, 22]. According to this theory, repulsive electrostatic forces may arise between the surface charge of microbial cells and a material surface. However, these forces are counterbalanced by attractive van der Waals interactions, facilitating the adhesion process [21, 23]. During the final stage of adhesion, bacterial cell wall deformation strengthens attachment by positioning cytoplasmic molecules closer to the surface, facilitating interaction via van der Waals attractive forces [22]. The extended DLVO theory also considers acid–base interactions, which lower the energy barrier and render the adhesion process irreversible [21, 23]. Once microbial cells make contact with a surface, they employ various mechanisms to maintain attachment. These include the production of adhesin proteins, such as lectin. Adhesins facilitate the binding of the cells to the surface and promote stable attachment [18, 24]. Additionally, the bacterial capsule, primarily produced for cell protection, has been shown to facilitate surface adhesion and contribute to biofilm establishment. *Staphylococcus* and *Streptococcus* are examples of bacterial genera in which this mechanism plays a key role [18]. Moreover, irreversible surface adhesion is also reported to involve appendages such as adhesive pili [25]. Once attachment is established, microbial cells proliferate and produce the EPS matrix, which promotes further aggregation and marks the transition into the second stage of the biofilm development cycle [3, 25].

## *II. Irreversible attachment and microcolony formation:*

The production of an EPS matrix is a crucial step in the biofilm formation process [26]. EPS is involved in cellular attachment, cell-to-cell communication and the development of antimicrobial tolerance [11]. The EPS matrix functions as a scaffold offering structural integrity and its secretion starts immediately after surface attachment [15]. EPS is a broad term encompassing a diverse range of components, the composition varies depending on the microbial cells forming the biofilm [26]. It generally includes polysaccharides, extracellular DNA, proteins and lipids [27]. Polysaccharides are the most prevalent organic molecules in the biofilm matrix, constituting typically 50 to 90% of the total biofilm mass [15]. The composition of polysaccharides in a biofilm varies depending on the microbial species present. For example, poly-N-acetylglucosamine is commonly

produced by bacterial species such as *S. aureus*, *S. epidermidis* and *E. coli*, while alginate is produced by *P. aeruginosa*. On the other hand, the fungi *Aspergillus fumigatus* and *Candida* spp. produce polysaccharides such as galactosaminogalactan and glucans, respectively [14]. Regardless of their chemical composition, polysaccharides generally serve similar functions, including surface attachment and maintaining biofilm architecture [28].

### *III. Biofilm maturation:*

After irreversible surface attachment, further microbial aggregation and microcolony growth lead to biofilm maturation. A biofilm microcolony is generally regarded as mature when it reaches a thickness of approximately 100  $\mu\text{m}$  [15, 29]. Once established, mature biofilms are extremely resistant to antimicrobial treatments and mechanical removal [22]. Maturation is characterized by development of active coordination between the cells within the biofilm. At this stage, gene expression and protein production are regulated at the level of the entire microbial community rather than at the individual cellular level, promoting the expression of biofilm-specific genes [15]. Intercellular communication within the biofilm occurs primarily through quorum sensing (QS), which is a cell-to-cell biochemical communication mechanism enabling microorganisms to detect the density of nearby cells and adjust gene expression accordingly [30, 31]. Some QS molecules not only enable communication within the same species but also influence other bacterial and fungal species, demonstrating intraspecies, interspecies and inter-kingdom signalling. For instance, the “diffusible signal factor” family of QS molecules, produced by many gram-negative bacteria, mediates interactions across species and kingdoms [32]. QS plays a critical role in biofilm development by regulating the cellular production of key factors, such as extracellular DNA, surface proteins, lectins and biosurfactants, which contribute to the biofilm’s structure and integrity [11]. During biofilm maturation, the EPS strengthens cell adhesion and cohesion, leading to densely packed microbial aggregates and a highly structured biofilm [22].

As maturation progresses, physiological heterogeneity develops within the biofilm, with microbial subpopulations exhibiting diverse phenotypes. This phenomenon can arise from adaptation to localized environmental conditions [33]. For instance, oxygen concentration

varies within the biofilm matrix, with the lowest levels often found near the biofilm core [26]. Alternatively, the emergence of subpopulations can result from cellular migration, as observed in the example of *P. aeruginosa*, where motile subpopulations migrate toward the biofilm surface, while non-motile subpopulations remain in close proximity to the point of attachment [34]. The presence of heterogeneous subpopulations can also be driven by changes in gene expression, particularly the expression of biofilm-specific genes [15, 33]. Persister cells are an example of biofilm subpopulations, commonly found in mature biofilms. These cells exhibit enhanced resistance to antimicrobial agents due to their dormant state, making them less susceptible to treatment [33]. Physiological heterogeneity in biofilms serve as a protective mechanism, allowing survival of subpopulations under extreme conditions or antibiotic treatments. For example, studies on *P. aeruginosa* show that tobramycin and ciprofloxacin primarily impact bacteria in the cap region of mushroom-shaped biofilms, while colistin affects bacteria in the stalk region [34].

#### *IV. Biofilm dispersal:*

Biofilm dispersal is a crucial phase of the biofilm life cycle. At this stage, microbial cells spread from the initial site of colonization to other areas within the body, thereby contributing to the progression of the infection [15]. This phenomenon has also been referred to as metastatic seeding, as it shows similarities to the metastatic behaviour of cancer cells [35]. Biofilm dispersal is initiated in response to environmental changes, such as nutrient limitations, which stimulate the production of enzymes that degrade the biofilm matrix and facilitate cell dispersal [11, 29]. For instance, *P. aeruginosa* produces alginate lyase, while *E. coli* produces N-acetyl-heparosan lyase to degrade the EPS matrix. Additionally, this phase involves the upregulation of flagella proteins, enabling bacterial motility and facilitating the colonization of new sites [29].

### ***1.1.2. Challenges associated with biofilm infection management***

Biofilm-associated infections are characterized by persistent inflammation and ongoing tissue damage [5, 36]. Mature biofilms are highly resistant to antimicrobial treatment, making the prevention of initial microbial attachment to surfaces a critical strategy for combating biofilm-

related infections [22]. Current approaches to biofilm management are primarily prophylactic, aiming to inhibit microbial cell attachment and prevent the initiation of biofilm formation [5]. One approach involves using biofilm-resistant materials in medical implants, which are designed with various strategies to prevent biofilm formation. These strategies include surface modifications to prevent microbial cell attachment, incorporation of antimicrobial agents, or a combination of both [30]. For example, hydrophilic coatings with heparin or polyethylene glycol (PEG) have shown to significantly reduce microbial adhesion [30]. Additionally, coatings of stainless steel and titanium implants with hydrophobic polycationic materials have been reported to effectively prevent *S. aureus* biofilm formation [37]. Administration of antibiotics following implant surgeries is among the common prophylactic approaches, aiming to target planktonic cells before surface attachment [5].

Once a biofilm is fully formed, antibiotic monotherapy is typically not sufficient and administration of high-dose combination therapy of antibiotics for a prolonged duration is the most common treatment approach [38]. Biofilm tolerance to antimicrobial treatment can be attributed to several factors. A primary contributor is the EPS matrix, which restricts the diffusion of antimicrobial agents into the biofilm core. Additionally, the EPS matrix contains enzymes and chemical compounds capable of degrading or neutralizing susceptible antimicrobial agents [39]. Furthermore, the transition of cells into a dormant state and the resulting alterations in their metabolic activity render certain antimicrobial agents, such as those targeting cell wall synthesis, ineffective [29]. Due to these factors, microbial cells within biofilms have been reported in some instances to exhibit up to a thousand times higher tolerance to antimicrobial treatments compared to planktonic cells [14, 40].

Mechanical removal of biofilms is implemented when feasible. This typically involves the removal or replacement of biofilm-contaminated implants or medical devices [38]. However, this approach is not always possible, particularly when biofilms colonize the host tissue instead of implant surfaces (e.g. endocardial and pulmonary tissues). Alternative mechanical disruption methods, such as ultrasound-mediated microbubble technology, have gained attention. This approach utilizes gaseous cores encased in stabilizing shells to induce mechanical forces, facilitating biofilm disruption and enhancing antimicrobial penetration [41].

Various novel approaches have been investigated to enhance the eradication of mature biofilms, either as standalone strategies or in combination with conventional antimicrobials. Notable methods include the use of quorum-sensing inhibitors, EPS matrix degrading enzymes and antimicrobial peptides (AMPs) [39]. Among these, AMPs stand out as a promising approach and are presented in the following section.

## **1.2. Antimicrobial peptides and their application in biofilm treatment**

AMPs are small molecules composed typically of fewer than 100 amino acids with an amphiphilic structure [42, 43]. In 1940, gramicidin became the first AMP to undergo clinical testing but was found unsuitable for systemic use due to its high toxicity [44]. Since then, over 5,000 AMPs have been identified and reported [45]. AMPs have emerged as a promising alternative to conventional antimicrobials with a potential broad range of clinical applications [46]. They exhibit potent and rapid action against a variety of pathogenic microbial species, including multidrug-resistant (MDR) pathogens [47]. Moreover, some AMPs, particularly those with multiple target molecules and mechanisms of action, have been reported to exhibit a low tendency for resistance development [47, 48]. In addition to their antimicrobial properties, certain AMPs can exhibit antibiofilm activity. They have been reported to inhibit biofilm formation through various mechanisms, such as downregulating essential genes involved in microbial attachment and quorum sensing or disrupting established biofilms by breaking down the EPS matrix [46, 49, 50]. The spectrum of antibiofilm activity encompasses various clinically relevant biofilm-forming microbes, such as *E. coli*, *P. aeruginosa*, *S. epidermidis*, *Acinetobacter baumannii* and *S. aureus*, including methicillin-resistant *Staphylococcus aureus* (MRSA) strains [46, 49].

### **1.2.1. Classes and mechanisms of action of AMPs**

AMPs have been variously classified according to their chemical structure, spectrum of activity or source. They can be categorized structurally into four main types: linear  $\alpha$ -helical peptides,



$\beta$ -sheet peptides, linear extended structures, and hybrid  $\alpha$ -helix/ $\beta$ -sheet peptides [49, 50]. Additionally, more complex structures, such as cyclic peptides and thioether-bridged structures, contribute to the diversity of AMPs and can be grouped into a separate fifth class as demonstrated in **Figure 2-A**. This structural complexity has been further enriched by recent advancements in the development of synthetic AMPs [48, 49]. Increased knowledge of AMP structural diversity has enhanced the understanding of their structure-activity relationships (SAR) [48]. This insight forms the basis for rational peptide design, as key physicochemical properties, such as amino acid sequence, charge, and hydrophobicity, determine their antimicrobial activity [51].

Based on their spectrum of activity, AMPs can be classified into various classes such as antibacterial, antifungal and antiviral peptides. In addition to their antimicrobial properties, some AMPs have been shown to exhibit immunomodulatory effects and have potential applications in anti-inflammatory and anticancer treatments [42, 46]. Antibacterial peptides account for more than half of the identified AMPs, while approximately 25% exhibit antifungal activity [49]. Their antibacterial action encompasses both gram-positive and gram-negative bacteria, including various MDR strains [44]. Antifungal peptides have shown significant activity against various clinically relevant fungal species, including *Candida albicans* and *Aspergillus flavus*, indicating their potential for therapeutic applications [49]. The remaining AMPs are categorized into smaller groups, such as antiviral, anticancer and anti-inflammatory [49].

Regarding the classification of AMPs by origin, they are naturally produced by various life forms, including animals, plants, insects, fungi and bacteria, serving as a primary defence mechanism [51]. In animals, AMPs such as defensins and cathelicidins are primarily found in epithelial tissues and body fluids, where they exhibit antimicrobial activity against pathogenic microbes [49, 51]. Animal-derived AMPs constitute the largest group, accounting for approximately 70% of all identified antimicrobial peptides [52]. In microorganisms, AMPs perform different roles by mediating interactions within their shared environment. For instance, bacterial AMPs often function as toxins, promoting the survival of the producing bacteria by targeting and eliminating closely related competing microbial species [43].

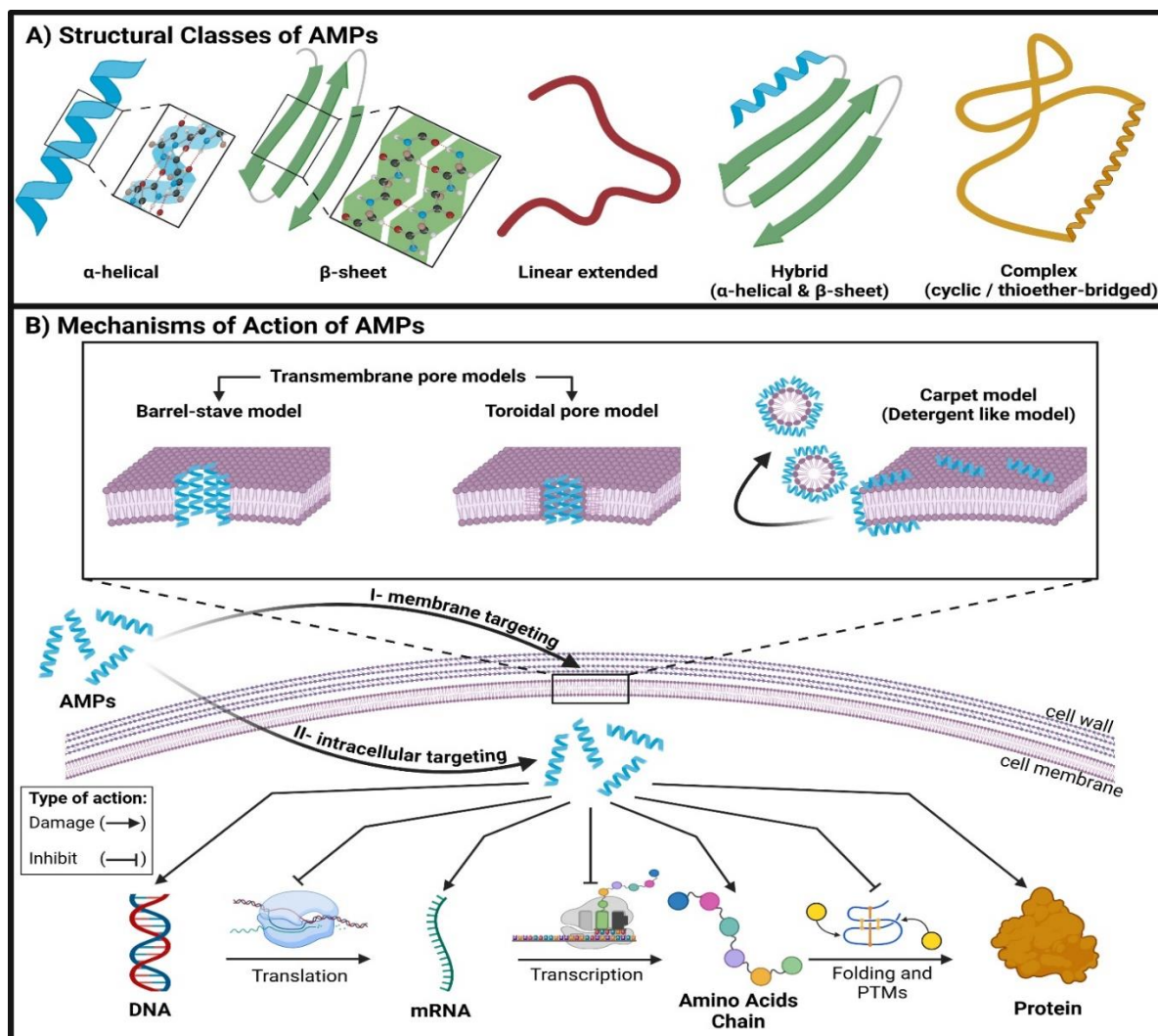


**Figure 2.** A) The main structural categories of antimicrobial peptides (AMPs). B) Illustration of the various mechanisms of action of AMPs: (I) disruption of the microbial cell membrane through the barrel-stave, toroidal pore, or carpet model, leading to membrane damage; and (II) penetration of the cell envelope to target intracellular components, thereby inhibiting essential cellular processes (e.g. translation, transcription, protein folding and posttranscriptional modifications (PTMs)) or damaging critical targets necessary for microbial cell survival (e.g. DNA, mRNA, amino acids and proteins). The figure is created in BioRender.com and adapted from [53, 54].

Bacteria-derived AMPs are categorized based on their biosynthetic origin into ribosomally synthesized AMPs (commonly referred to as bacteriocins) and non-ribosomally synthesized AMPs [55, 56]. Both types are produced by gram-positive and gram-negative bacteria. However, bacteriocins are more commonly associated with gram-positive bacteria [57]. Bacteriocins from gram-positive and gram-negative bacteria vary significantly in structure,

mechanism of action and spectrum of activity [57]. Colicin, the first bacteriocin to be discovered, was isolated from *E. coli* in 1925. Since then, numerous bacteriocins have been discovered, forming a diverse group of AMPs. Bacteriocins also includes gramicidin, the first peptide-based topical antibiotic, which was isolated from *Bacillus brevis* and demonstrated broad spectrum of activity against gram-positive and gram-negative bacteria [57]. Bacteriocins produced by gram-positive bacteria are usually classified into four categories [43, 56, 58]:

- Class I: lantibiotics  
Small (<5 kDa), heat stable, post-translationally modified and contain thioether bridges in their structure (e.g. nisin).
- Class II: non-lantibiotics  
Small (<10 kDa), heat stable and lack post-translational modifications (e.g. pediocin).
- Class III: large bacteriocins  
Large (>30 kDa) and heat labile (e.g. helveticin J).
- Class IV: complex bacteriocins  
Uniquely structured and may contain lipid or carbohydrate moieties.

However, recent efforts to classify bacteriocins from gram-positive bacteria have proposed the inclusion of two additional classes: sactipeptides (Class V) and thiopeptides (Class VI). A key distinction between sactipeptides and lantibiotics is the involvement of the  $\alpha$ -carbon in thioether bridge formation in sactipeptides, compared to the  $\beta$ -carbon in lantibiotics class [59]. Thiopeptides are post-translationally modified thiazole-containing bacteriocins. They possess a central pyridine ring and a core macrocyclic ring with substituents such as thiazole, oxazole and thiazoline [60]. Finally, bacteriocins produced by gram-negative bacteria are less diverse and classified into two main classes based on their molecular weight: colicins, which are large (>10 kDa), and microcins, which are smaller (<10 kDa) and more tolerant to thermal and enzymatic degradation [58].

AMPs in general exert their antibacterial effects either by disrupting the cellular membrane or by targeting essential intracellular components as shown in **Figure 2-B**. The specific mode of action of each peptide is determined by its physicochemical properties and its interaction with the target molecule [51]. The intracellular mode of action of AMPs involves disrupting processes crucial for cellular viability, such as nucleic acid replication, gene expression and

protein synthesis, eventually leading to cell death [53, 61]. In the membrane disruption mode, AMPs interact with the bacterial envelope, with cationic peptides often initiating this process through electrostatic attraction. This interaction can lead to pore formation and altered membrane curvature, resulting in ion leakage, membrane depolarization and cell lysis. AMPs utilize mechanisms such as “barrel-stave”, “toroidal pore” and “carpet formation” to destabilize the bacterial membrane [53].

The barrel-stave model involves AMP insertion vertically in the membrane, followed by aggregating to form channels that lead to cytoplasmic outflow and cell death (e.g. alamethicin) [49]. The toroidal pore model also involves vertical insertion of AMPs into the membrane, disrupting the hydrophobic/hydrophilic arrangement of the lipid bilayer and creating ring-shaped pores that compromise the membrane integrity (e.g. magainin and lactacin Q) [62]. Finally, in the carpet-like model, peptides align parallel to the membrane, forming a coating that disrupts its integrity in a detergent-like manner (e.g. human cathelicidin LL-37) [51].

Similar mechanisms are observed with antifungal AMPs. Some directly target the fungal cell membrane by interacting with ergosterol, a sterol specific to fungi [49]. Others disrupt essential intracellular processes, such as inhibiting biosynthetic pathways for key fungal cell wall components or interfering with ergosterol-related genes. These disruptions compromise structural integrity, eventually leading to fungal cell death (e.g. echinocandin and caspofungin) [47].

### ***1.2.2. Teixobactin and micrococcin P1 as potential antibiofilm agents***

Two types of antimicrobial peptides, analogues of the naturally occurring teixobactin and micrococcin P1 (MP1), were explored in this thesis for their potential as antibiofilm agents. Teixobactin is a non-ribosomally synthesized, positively charged depsipeptide, whereas MP1 is a ribosomally synthesized bacteriocin [59, 63].

Teixobactin, discovered in 2015, is produced by a previously uncultivated gram-negative bacterium provisionally designated as *Eleftheria terrae* [64]. It is a cyclic depsipeptide containing 11 amino acids (**Figure 3-A**). Position 10 is occupied by L-allo-enduracididine,

which is derived from arginine through post-translational modification and has proven difficult to synthesize [65]. Teixobactin represents a new antibiotic class, exerting its antimicrobial activity by disrupting cell wall synthesis. It targets intracellular precursors, lipid II and lipid III, which are essential for the production of peptidoglycan and teichoic acid, respectively [64-66]. Its dual-targeting mechanism of action is believed to pose a barrier to the development of bacterial resistance [65]. The C-terminal enduracididine motif enables teixobactin to bind to the pyrophosphate-sugar moiety of lipid II, while the N-terminus interacts with the pyrophosphate of a second lipid II molecule, promoting the formation of a  $\beta$ -sheet structure of the teixobactin-target complex [67]. The formation of  $\beta$ -sheet structures initiates further aggregation into stable fibrillar assemblies, which have been reported to remain stable for hours and effectively sequestering lipid II [67]. The interaction with lipid III is reported to involve a similar mechanism, initiated by teixobactin binding to the pyrophosphate groups of lipid III [68].

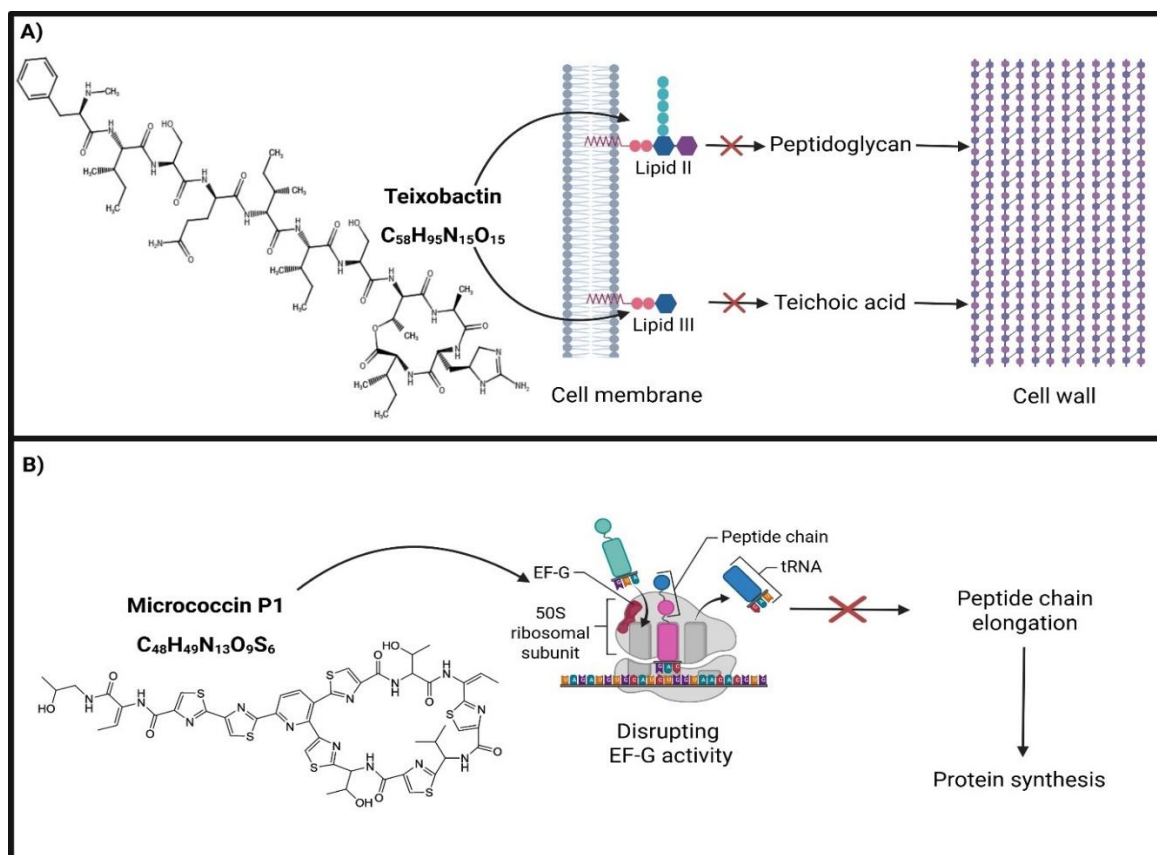


**Figure 3.** Chemical structure, molecular formula and mechanism of action of A) teixobactin and B) micrococccin P1 (MP1). Teixobactin inhibits cell wall synthesis by binding to lipid II and lipid III, which are respectively the precursors for peptidoglycan and teichoic acid. MP1 prevents protein synthesis by interfering with the activity of elongation factor-G (EF-G). The figure is created in BioRender.com.

Teixobactin has been found to be highly effective against various clinically-important gram-positive bacteria, including *S. aureus*, *E. faecalis*, *Streptococcus pneumoniae* and *Clostridium difficile* [69]. The spectrum of activity also extends to MDR strains, such as methicillin-resistant *Staphylococcus aureus* (MRSA) and vancomycin-resistant *Enterococci* (VRE). However, it is ineffective against gram-negative bacteria due to its inability to penetrate their outer membrane [64]. Teixobactin demonstrates favourable pharmacokinetics, safety and efficacy in murine infection models. It is currently undergoing preclinical evaluation for drug development by NovoBiotic Pharmaceuticals in Cambridge, USA [69, 70].

Several research groups have chemically synthesized teixobactin analogues, and a primary focus has been the replacement of L-allo-enduracididine with more common and readily available amino acids [65, 71]. Some of these analogues maintained comparable antimicrobial activity to the parent compound [65], along with reported antibiofilm activity [72, 73]. For instance, the analogue L-Chg10-teixobactin showed 80% inhibition of *E. faecalis* biofilm formation at a concentration of 0.13 µg/mL [72]. Another study reported promising antibiofilm activity of D-Arg4-Chg10-teixobactin, Arg3-D-Arg4-Chg10-teixobactin and Nle10-teixobactin analogues against preformed *S. aureus* and *S. epidermidis* biofilms [73].

Micrococcin P1 (MP1) is a post-translationally modified thiopeptide with a molecular weight of 1144 Da, and featuring a 26-membered ring structure (**Figure 3-B**). Micrococcin, the first thiopeptide discovered, was isolated from a *Micrococcus* species in 1948. It was later also isolated from *Bacillus pumilus* and renamed micrococcin P. The *B. pumilus* micrococcin was shown to be a mixture of two compounds, micrococcin P1 and P2, with P1 comprising approximately 90% of the composition [74]. Subsequently, MP1 was found to be produced by certain members of other genera, including *Staphylococcus* and *Micrococcus* [59]. MP1 disrupts protein synthesis by targeting the 50S ribosomal subunit and interacting with elongation factor-G (EF-G), thereby inhibiting peptide chain elongation. Additionally, it inhibits translation initiation by destabilizing the interaction between the ribosome, tRNA and the initiation factor [75]. MP1 produced by *Staphylococcus equorum*, exhibited bacteriostatic activity against a broad spectrum of gram-positive bacteria, including 130 out of 135 strains belonging to the genera *Listeria*, *Enterococcus*, *Staphylococcus* and a number of other bacterial species [76]. MP1 shows also antimicrobial activity against MRSA and VRE [77, 78]. Studies on MP1's antibiofilm activity demonstrate synergy in combination with other antimicrobial

agents (e.g. penicillin G and garvicin KS) against preformed *S. aureus* biofilms [79, 80]. Moreover, MP1 exhibited no cytotoxicity towards various human cell lines, including embryonic kidney cells, monocytic cells, hepatic cells, and skin keratinocytes [81, 82].

Chemical synthesis of MP1 employing a variety of strategies has been documented in the literature [77, 83, 84]. However, the total chemical synthesis remains economically impractical for large-scale production and drug development [85, 86]. The complexity and challenges of total thiopeptide chemical synthesis can be attributed to the presence of multiple heterocycles and chiral centres [77]. As a result, semisynthetic and biosynthetic approaches have become the primary focus for producing thiopeptide derivatives [85, 86]. For instance, a cost-efficient production method for MP1 was reported using *S. equorum*. This approach, gave high and stable MP1 production and yielded 98% pure MP1 [86].

### ***1.2.3. Limitations to the clinical application of AMPs***

Despite significant advancements in the discovery and isolation of AMPs, only ten peptide-based antimicrobial agents have been approved for clinical use by the United States Food and Drug Administration (FDA) as of 2024 [87]. The clinical development of AMPs has faced significant challenges due to various factors. The isolation of natural AMPs presents issues related to safety, quality, and production yield. Although chemical synthesis methods are available for some AMPs, large-scale production remains economically challenging [42]. Over the past few decades, only limited efforts have been made to overcome these obstacles. This is primarily due to the perceived marginal advantages of AMPs over conventional antibiotics and the complexities of the regulatory approval process. Moreover, inherent chemical properties of AMPs may lead to suboptimal pharmacokinetics and stability challenges, further restricting their clinical value [42]. For instance, despite their promising antimicrobial properties, bacteriocins have not yet been utilized in pharmaceutical applications due to their instability, proteolytic degradation, poor water solubility and low bioavailability [88, 89]. To date, nisin remains the only bacteriocin approved for use, with its application restricted to food preservation [89].

To address the previously mentioned limitations, chemical modifications of the peptide structure have been explored [47, 90]. These modifications can enhance AMP stability and efficacy through strategies such as hydrocarbon stapling, which reinforces secondary structure, and hybridization with cell-penetrating peptides to boost antimicrobial activity [52]. Additionally, amino acid modifications can improve the proteolytic stability and lower toxicity, whereas conjugation with fatty acids or sugar moieties has been reported to enhance both pharmacokinetics and antimicrobial activity [47, 91]. However, chemical modifications do not always enhance all peptide properties simultaneously, as improving one aspect may compromise another. For instance, incorporating D-amino acids can extend a peptide's plasma half-life but often reduces its biological efficacy [92].

Studies have shown that employing advanced nanosized delivery systems can effectively overcome various limitations of AMPs. A wide range of nanocarriers, such as liposomes, micelles, metallic nanoparticles, mesoporous nanoparticles, dendrimers, polymeric nanoparticles, nanofibers and carbon nanotubes have demonstrated the potential to enhance the antimicrobial efficacy, stability, and target specificity of AMPs [47, 52]. For instance, conjugation of colistin with gold nanoparticles improved its interaction with the cellular envelope of *A. baumannii*, while silver nanoparticles enhanced colistin activity against *E. coli*, *K. pneumoniae*, and *P. aeruginosa* [93, 94]. Incorporating the bacteriocin nisin into solid lipid nanoparticles has been reported to enhance its antimicrobial and antibiofilm activity against the oral pathogen *Treponema denticola* [95]. Loading the cathelicidin LL-37 peptide into anionic mesoporous silica nanoparticles, minimized its degradation by proteases produced by *P. aeruginosa* and human immune cells [96].

Among the various nanosized drug delivery systems, liposomes stand out as a highly effective, biocompatible and versatile delivery system. They can encapsulate both hydrophilic and hydrophobic drugs, protect AMPs from degradation and control the drug release. Furthermore, liposomal formulations enhance the proteolytic stability of peptide drugs and improve their bioavailability [47, 52]. Given their advantages as nanocarriers for peptide drugs, liposomes were selected as a nanosized delivery system for AMPs investigated in this thesis.



## **1.3. Liposomes as a promising approach for biofilm treatment**

Liposomes are self-assembled vesicles composed of one or more phospholipid bilayer membranes encapsulating an aqueous core. The term ‘liposomes’ was introduced in 1961 by Alec D. Bangham during his studies on phospholipids and blood clotting [97]. In the 1970s, G. Gregoriadis proposed their use as drug carriers, and liposomal preparations eventually entered the market in the 1990s [97]. Liposomes were the first nanosized delivery system to receive clinical approval from the United States FDA and the European Medicines Agency (EMA), marked by the introduction of the liposomal formulation of the anticancer drug doxorubicin in 1995 [98-100]. Since then, interest in liposomes has grown significantly, with liposomal formulations accounting for 44% of all nanomedicine products in clinical trials between 2016 and 2021 [99]. By 2022, the number of approved liposomal products for clinical use, excluding generics, had reached 14. These products cover various therapeutic indications, including multiple types of cancer and microbial infectious diseases (e.g. amphotericin B and amikacin liposomal products) [101]. More details on liposomes are provided in the following sections.

### ***1.3.1. Preparation and classification of liposomes***

Phospholipids are the primary structural components of liposomal vesicles. The amphiphilic nature of phospholipids, characterized by a hydrophilic phosphate head group and hydrophobic carbon chain tails, plays a crucial role in directing liposome formation [102]. When amphiphilic molecules interact with aqueous solutions, they spontaneously self-assemble into supramolecular structures. This phenomenon is primarily driven by the hydrophobic effect, which minimizes unfavourable interactions between hydrophobic regions and water, thereby making the self-assembly process thermodynamically favourable [103]. The shape of the resulting assembled structure depends on the properties of the amphiphilic molecules, such as the hydrophobic chain length and the polar head size. The "critical packing parameter" helps to predict the self-assembly behaviour and the resulting structure (e.g. micelles or bilayers vesicles) [104]. The bulky hydrophobic chains of phospholipids favour the assembly into

bilayers over micelle formation, as illustrated in **Figure 4**. The assembly process initiates by planar bilayer formation followed by bending and closure into vesicles [103].

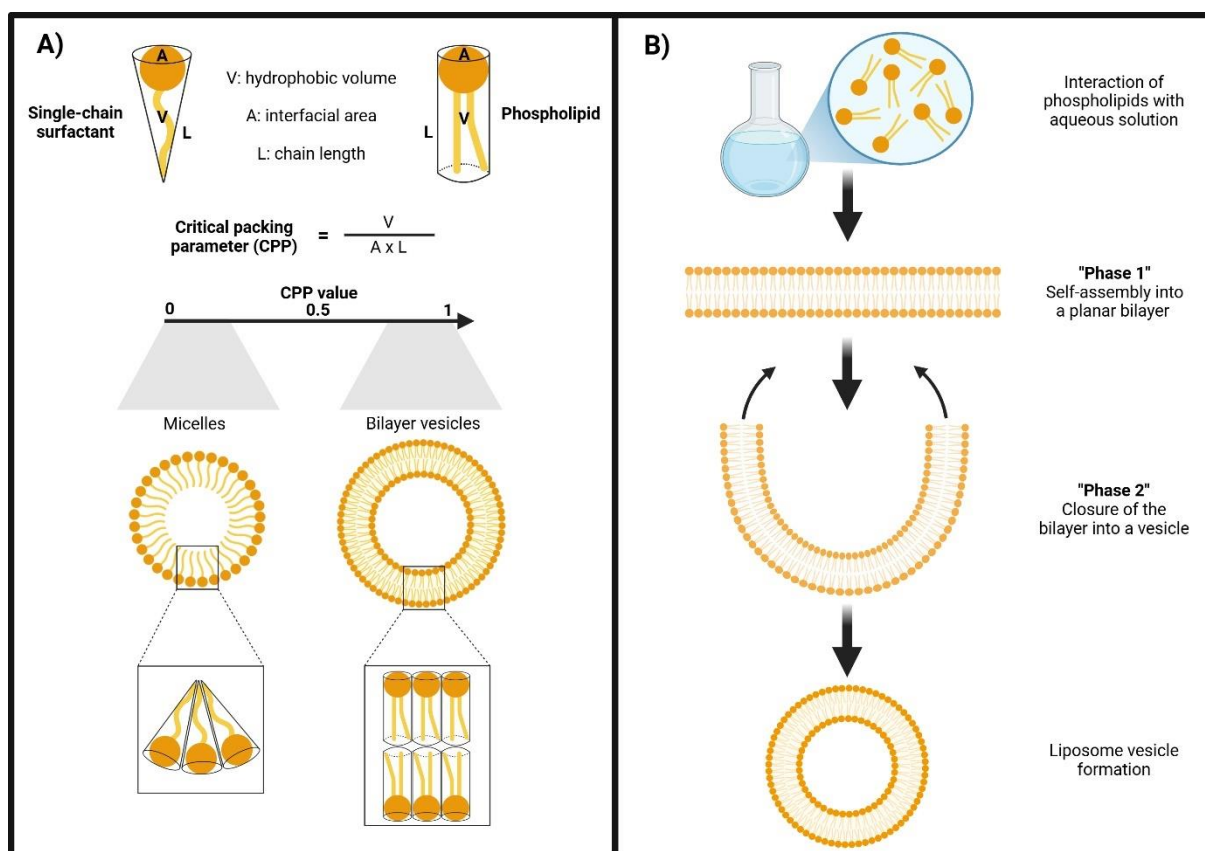


**Figure 4.** A) Factors affecting the self-assembly process of amphiphilic compounds, which can be either single-chain surfactant or a phospholipid with two chains. The critical packing parameter (CPP) value can predict the type of the assembled structure. Values less than 0.5 result in micelle formation, while values around 1 typically result in bilayer formation. B) The process of phospholipid self-assembly upon contact with aqueous solution, which starts by formation of a planar bilayer (phase 1) followed by closure into a vesicle (phase 2). The figure is created in BioRender.com and adapted from Eugster and Luciani [103].

Liposomes can be classified based on their size and lamellarity into either multilamellar vesicles (MLVs) or unilamellar vesicles. MLVs consist of multiple lipid bilayers separated by aqueous layers and typically exceed several hundred nanometres in size [105]. Unilamellar vesicles, on the other hand, are characterized by a single lipid bilayer and are further divided into small unilamellar vesicles (SUVs), ranging from 20-100 nm, and large unilamellar vesicles (LUVs), which are larger than 100 nm in diameter. Unilamellar vesicles with diameters greater than one

$\mu\text{m}$  are referred to as giant unilamellar vesicles (GUVs) [106]. Preparation conditions significantly influence vesicle size and morphology. Preparation of liposomes typically involves two main steps: the assembly of the liposomes, followed by size reduction and control to achieve a uniform liposomal structure and a monodisperse size distribution [103]. Several techniques have been developed for the first step, with some of the most commonly used methods being:

#### *I. Thin-film hydration:*

The thin-film hydration technique is one of the simplest approaches. It involves dissolving the lipids in an organic solvent, which is then evaporated to create a thin lipid film. The film is subsequently rehydrated with an aqueous solution to produce liposomes. This approach has some drawbacks, including vesicles size variability, low encapsulation efficiency for hydrophilic drugs, risk of residual organic solvents, and limited scalability [105].

#### *II. Reverse-phase evaporation:*

In this method, a small amount of water is added to an organic lipid solution to create a water-in-oil emulsion. Gradual evaporation of the organic solvent leads to the assembly of phospholipids into liposomal vesicles. While this method provides high encapsulation efficiency for hydrophilic drugs, it shares similar drawbacks with the thin-film hydration method, including size variability, residual organic solvent, and limited scalability [103].

#### *III. Ethanol injection:*

This method involves dissolving lipids in ethanol to create a lipid solution, which is then rapidly injected into an aqueous phase. This process results in the self-assembly of lipid molecules into bilayer vesicles [107]. A key advantage of this method is the ability to control liposome size and uniformity through process parameters, such as lipid concentration and ethanol injection flow rate, eliminating the need for an additional size reduction step. Following liposome formation, ethanol is removed by stirring the mixture at room temperature. However, the potential presence of residual organic solvent remains a limitation of this technique [108].

After the assembly of liposomal vesicles, a size reduction step is often required to optimize the preparation and achieve the desired vesicle size range. Ultrasound is effective in breaking down large multilamellar liposomes into small SUVs through cavitation, a process in which gas bubbles are generated and collapsed, creating significant local pressure changes [109]. Sonication can be performed using either probe or bath sonication. While probe sonication delivers direct energy input, it can cause localized temperature increases that may degrade the encapsulated drug or liposomal components. In contrast, bath sonication offers better temperature control [105]. Despite its simplicity, sonication requires optimization of several parameters, such as ultrasound intensity, amplitude, frequency, output power and duration, which influences the final liposomal size [109].

The membrane extrusion method provides superior size control and narrower size distribution compared to sonication, as it is possible to control the membrane pore size [109]. During extrusion, the liposomal preparation is passed through a polycarbonate membrane at a temperature exceeding the phase transition temperature ( $T_m$ ) of the phospholipids, which is the point at which phospholipids transition from a gel phase to a liquid-crystalline phase [110]. At  $T_m$ , the phospholipids in the bilayer become less tightly packed facilitating the breakdown of large vesicles as they pass through the membrane pores [109, 110]. Although extrusion offers precise vesicle size control, it faces challenges with respect to scalability and potential membrane pore clogging. Additionally, extrusion requires multiple cycles to achieve the desired size range, which can be time-consuming [103, 109]. Finally, high-shear homogenization provides a scalable alternative for size reduction by forcing the suspension through an orifice under high pressure. However, this method may lead to a broader size distribution [103].

Liposomes can also be categorized according to their composition. For instance, conventional liposomes are typically composed of phosphatidylcholine as the primary phospholipid, along with cholesterol. The inclusion of cholesterol enhances liposomal stability by increasing the membrane rigidity [107]. Modifications to liposomal composition have been made to enhance functionality or overcome limitations. For example, surface-modified liposomes with polyethylene glycol (PEG), referred to as "PEGylated" or "stealth" liposomes, were designed to evade detection by macrophages. This modification helps address rapid clearance by the immune system and extends liposomal plasma circulation time [100]. Additionally, charged phospholipids, with either a positive or negative net charge, have been incorporated into

liposomes to enhance their physical stability. This stabilization is achieved through electrostatic repulsion between liposomal vesicles, which prevents aggregation as described by DLVO theory [103, 111]. Furthermore, the liposomal charge can enhance drug entrapment through electrostatic attraction between the drug molecules and the oppositely charged liposomes [103]. For instance, cationic liposomes are a distinct class prepared using positively charged lipids. They were developed to enhance the encapsulation efficiency of negatively charged drugs via electrostatic interactions [107].

### ***1.3.2.Liposomes in biofilm management***

Liposomes can enhance the treatment of biofilm-related infections by encapsulating antimicrobial agents, improving their penetration into biofilms and protecting them from premature degradation within the biofilm matrix [112, 113]. Furthermore, their direct interaction with microbial cell envelopes enables the intracellular delivery of high drug concentrations, thereby enhancing the antimicrobial activity of the encapsulated drug [112-114]. Liposomal encapsulation have demonstrated efficacy against various antibiotic resistant gram-negative and gram-positive bacteria [112]. The efficacy of liposomes in combating biofilms is influenced by their physicochemical properties, including size, composition, and encapsulation efficiency [115]. For example, nanoparticles smaller than 500 nm have been shown to effectively penetrate the EPS matrix due to their ability to navigate through the dense network of polysaccharides and proteins [116, 117]. **Figure 5** illustrates the underlying principle of liposome-based biofilm treatment.

Biofilm-specific traits, including the EPS structure and the microbial makeup, must also be considered, as they influence the interaction between biofilms and liposomes. These interactions are governed by electrostatic, hydrophobic, and steric forces, which affect liposomal adhesion to the biofilm matrix and facilitate penetration and drug delivery [113]. Cationic nanoparticles typically exhibit enhanced interaction with the biofilm matrix due to the prevalence of negatively charged components within the EPS, such as extracellular DNA [118]. Thus, cationic liposomes have been reported to show deeper diffusion and stronger binding to the biofilm matrix [113]. This interaction contributes to the enhanced retention of cationic

liposomes within biofilms, as demonstrated in a comparative study evaluating the interactions of cationic and anionic liposomes with *P. aeruginosa* biofilms [119].

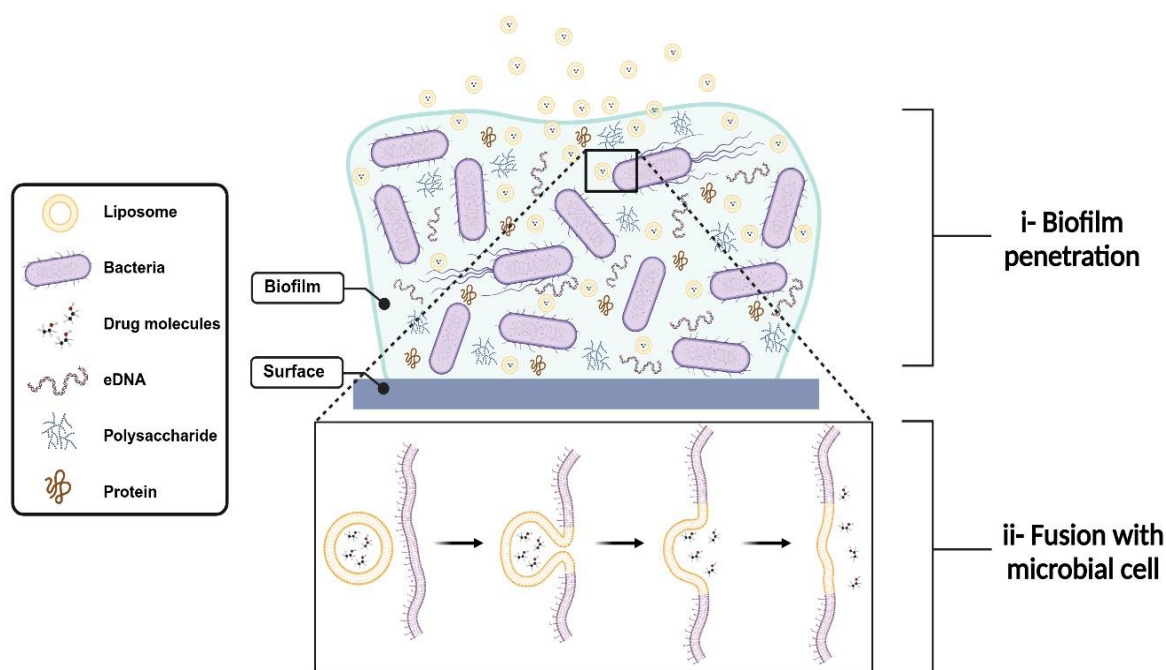


**Figure 5.** A graphical representation of the mechanism of action of liposomes following administration to a biofilm. (i) Liposomes penetrate the biofilm matrix while protecting the encapsulated drug from degradation. (ii) Fusion with microbial cells facilitates the release of the antimicrobial agent, achieving high intracellular concentrations. The figure is created in BioRender.com.

Several studies have demonstrated that incorporating antimicrobial agents into liposomal formulations enhances biofilm disruption compared to the application of free drugs [120-122]. For example, the inclusion of fluconazole in conventional 1,2-dipalmitoyl-sn-glycero-3-phosphocholine (DPPC)/cholesterol liposomal preparations improved its activity against *C. albicans* biofilms. This activity was further enhanced by adding a quorum sensing inhibitor to the liposomal formulation [123]. Similarly, a liposomal preparation of meropenem showed superior efficacy in eradicating biofilms of various *P. aeruginosa* isolates compared to free meropenem [124]. The antibiofilm activity of liposomes can be further enhanced through various strategies: One approach involves the dual incorporation of two antimicrobial agents or the combination of an antibiofilm agent, such as a quorum-sensing inhibitor, with an

antimicrobial drug [113]. Another effective strategy is the functionalization of the liposomal surface to improve interactions with biofilms. This can be achieved by covalently attaching lectins, such as concanavalin A, to the liposomal surface [114]. The targeting mechanism of lectin-functionalized liposomes is based on the selective binding of concanavalin A to  $\alpha$ -mannopyranosyl and  $\alpha$ -glucopyranosyl residues, which are commonly present in the EPS matrix of certain biofilms [114]. For instance, coating metronidazole-loaded liposomes with concanavalin A was reported to enhance their antibiofilm activity against *Streptococcus mutans* periodontal biofilm compared to both free metronidazole and uncoated metronidazole liposomes [125]. In addition to the biofilm-specific advantages, liposomes are generally considered biocompatible, biodegradable and non-immunogenic, making them ideal for drug delivery [109]. Moreover, liposomes possess a versatile structure that can be easily modified for a wide range of therapeutic applications. For example, they can function as sustained-release depots or facilitate targeted drug delivery, thereby minimizing host cell exposure to the drug and reducing side-effects [97, 99].

Despite their many advantages, liposomes also have some characteristic weaknesses and limitations, such as premature drug leakage and physical instability. These limitations can be addressed through various strategies, including modifying the liposomal composition to enhance membrane rigidity and prevent drug leakage [97, 103]. Increasing the proportion of charged phospholipids can also improve physical stability by enhancing the electrostatic repulsion forces between the vesicles and minimizing liposomal aggregation [109]. Additionally, freeze-drying techniques can eliminate physical instability, enabling long-term storage of liposomal formulations in a solid state, which can be reconstituted immediately prior to administration [103, 109]. The disadvantage of rapid clearance of conventional liposomes from the bloodstream by the immune system can be mitigated through the use of PEGylated liposomes [97].

Furthermore, modifying the liposomal composition by incorporating fusogenic phospholipids, such as 1,2-dioleoyl-sn-glycero-3-phosphatidylethanolamine (DOPE), enhances their ability to fuse with biological membranes. This modification takes advantage of the structural similarity between liposomal bilayers and cell membranes, thereby increasing the potential for liposome-cell membrane fusion [126, 127]. This is further discussed in the next section.

### 1.3.3. *Fusogenic liposomes*

The interaction between liposomes and cells is critical for ensuring precise drug targeting, thereby achieving the intended therapeutic efficacy. This interaction has been extensively studied with mammalian cells due to its importance for drugs targeting intracellular ligands, such as anticancer agents [128]. Liposomes can either be internalized by endocytosis or fuse directly with the cell membrane. Fusion offers distinct advantages over other uptake mechanisms as it bypasses lysosomal degradation and enables the direct release of high drug concentrations into the cytosol [128-130]. Liposomes can be further modified to enhance their ability to utilize the fusion pathway over other cellular uptake mechanisms. This can be achieved by incorporating specific types of phospholipids that increase membrane fluidity, making the liposomal membrane more prone to fusion [129]. These modified liposomes are referred to as “fluidosomes” or “fusogenic liposomes”.

In general, phospholipids exhibiting fusogenic properties have specific structural features, including relatively small polar head groups and unsaturated hydrophobic tails. These structural properties promote the transition from a stable lamellar phase to a more dynamic hexagonal phase, which enhances membrane fluidity and promotes fusion [107]. As the degree of unsaturation in phospholipid acyl chains increases, bending rigidity decreases, facilitating curvature adaptation, which enhances liposomal fusogenicity [129]. Examples of such fusogenic phospholipids include 1,2-dioleoyl-sn-glycero-3-phosphatidylcholine (DOPC) and DOPE [107]. An increase in the proportion of DOPE in liposomal formulations has been reported to enhance fusion with bacterial cells. In contrast, higher cholesterol content was found to reduce fusion efficiency [131]. These effects can be attributed to the influence of each component on liposomal membrane fluidity: DOPE promotes membrane fluidity, facilitating fusion, whereas cholesterol stabilizes the membrane and increases rigidity, thereby hindering the fusion process [131]. While increased fusogenicity enhances liposome-cell membrane fusion, it may reduce membrane stability, leading to a higher risk of premature drug release [112].

While numerous studies have investigated the mechanisms of liposomal fusion with mammalian cells, fusion with microbial cells remains less understood [113]. Several reports have documented the fusion of fusogenic liposomes with bacterial cells [127, 131-133].



However, the exact mechanism underlying this interaction has yet to be fully elucidated. A recent study investigating the fusion mechanism of positively charged fusogenic liposomes with *E. coli* (gram-negative) and *B. subtilis* (gram-positive) revealed distinct interactions depending on bacterial cell envelope structure [134]. In *E. coli*, liposomes fused directly with the outer membrane, whereas in *B. subtilis*, they first attached to the cell wall before their lipid components were internalized. The findings suggest that the mode of interaction of liposomes can vary across bacterial species, underscoring the need for species-specific investigations [134]. Moreover, greater fusion with gram-negative bacterial cells has been reported in the literature compared to gram-positive bacteria. This is attributed to the structural similarity between liposomal vesicles and the outer membranes of gram-negative bacteria, as both contain phospholipids [133].

Despite uncertainties regarding the molecular mechanism of liposomal fusion with microbial cells, the ability of fusogenic liposomes to enhance the antimicrobial activity of various agents has been reported in the literature. For instance, studies have demonstrated that tobramycin-loaded fusogenic liposomes exhibit superior antimicrobial activity against *P. aeruginosa* compared to free tobramycin [131, 132]. Similarly, enhanced activity was observed in a study evaluating aminoglycosides including amikacin, gentamicin and tobramycin against *P. aeruginosa* strains after encapsulation in fusogenic liposomes [135]. Another study reported greater antimicrobial efficacy of fusidic acid-loaded fusogenic liposomes compared to both free fusidic acid and fusidic acid-conventional liposomes, against *S. aureus* and *S. epidermidis* [136]. Notably, fusogenic liposomes not only enhanced antimicrobial activity against susceptible bacteria but also enabled antibiotics to cross the outer membrane of gram-negative bacteria [136, 137]. This could potentially allow the use of antibiotics that are normally ineffective against these bacteria due to their impermeable outer membrane. For instance, fusidic acid-loaded fusogenic liposomes demonstrated antimicrobial activity against *K. pneumoniae* and *E. coli* strains, which are inherently resistant to fusidic acid [136]. Similarly, vancomycin-loaded fusogenic liposomes showed enhanced activity against various gram-negative bacterial species [137].

## 2. Aim of the work

There is a need for new and innovative strategies to treat biofilm-related infections, particularly those caused by antimicrobial-resistant microbes. Efficient drug delivery is crucial for targeting microbes embedded within the biofilm matrix. Formulating AMPs into suitable and effective pharmaceutical forms is an overarching aim of the present work. Specifically, this thesis explores the potential of fusogenic liposomes as a nanocarrier system for novel AMPs in the treatment of biofilm-associated infections. Additionally, the study investigates the antibiofilm potential of new AMPs, as the rise in multidrug-resistant bacteria has created an urgent need for alternative therapeutic agents. The work is divided into three research papers. The main aim of each paper was to:

- develop cholesterol-free fusogenic liposomes and investigate the effect of liposomal surface charge on their interaction with planktonic microbial cells and established biofilms. **(Paper I)**
- develop and optimise fusogenic liposomes for the entrapment of micrococcin P1, with the goal of enhancing its antimicrobial and antibiofilm activity. **(Paper II)**
- investigate the antimicrobial and antibiofilm activity of three novel teixobactin analogues against clinically relevant bacterial strains, with the aim of identifying the most promising candidate for further development into a liposomal delivery system. **(Paper III)**

### 3. Methodological considerations

This section provides an overview of the materials and methods used in the scientific papers comprising this thesis, including the rationale for the chosen approaches, their limitations, and potential areas for refinement. A detailed description of each method can be found in the respective paper where it was applied. The studies incorporate various physicochemical and antimicrobial techniques and **Figure 6** outlines the methods used in each research paper.

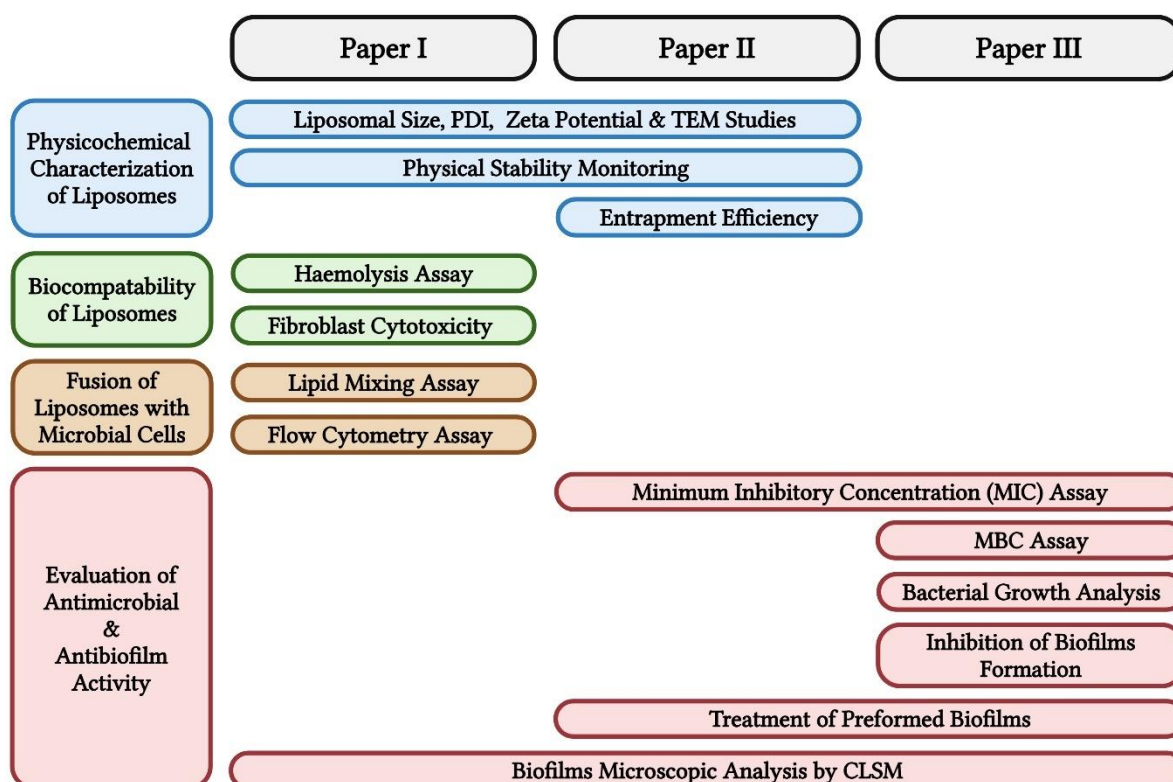


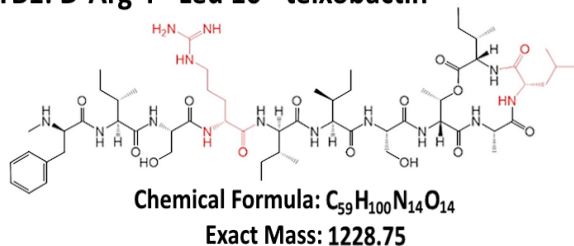
**Figure 6.** Overview of the experimental approaches and methods used across the three research papers involved in this study. (CLSM: Confocal Laser Scanning Microscopy, MBC: Minimum Bactericidal Concentration, MIC: Minimum Inhibitory Concentration, PDI: Polydispersity Index, TEM: Transmission Electron Microscopy).

## 3.1. Materials

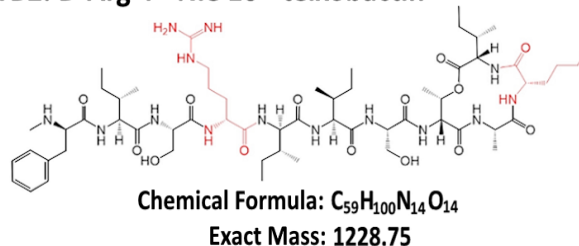
### 3.1.1. Antimicrobial peptides

This thesis investigates two types of AMPs: MP1 (**Paper II**) and three teixobactin analogues (**Paper III**). MP1 isolated from *S. equorum* with 98% purity as determined by high-performance liquid chromatography-mass spectrometry (HPLC-MS) and was provided by AgriBiotix AS, Norway. The teixobactin analogues (TB1, TB2, and TB3) were chemically synthesized by the University of Liverpool with >90% purity as determined by HPLC-MS and feature modifications to the natural teixobactin structure. Specifically, each analogue includes a different substitution at position 10, where the L-allo-enduracididine residue is replaced with either leucine (Leu), norleucine (Nle), or norvaline (Nva). The chemical structures of all AMPs are shown in **Figure 7**.

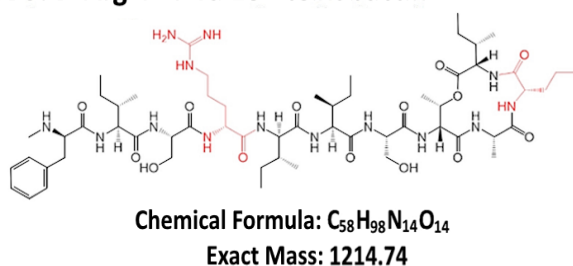
**TB1: D-Arg 4 - Leu 10 - teixobactin**



**TB2: D-Arg 4 - Nle 10 - teixobactin**



**TB3: D-Arg 4 - Nva 10 - teixobactin**



**MP1: Micrococцин P1**

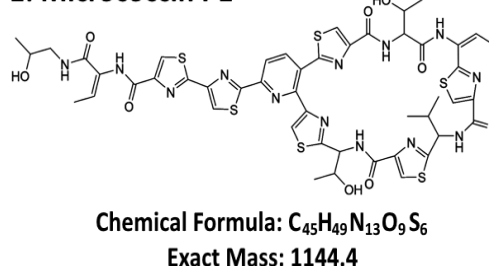


**Figure 7.** Chemical structures of the three teixobactin analogues (TB1, TB2, and TB3) and micrococцин P1 (MP1) investigated in this study. Substitutions from the natural teixobactin structure are highlighted in red. In all analogues, the L-allo-enduracididine residue at position 10 is replaced by leucine (Leu), norleucine (Nle), or norvaline (Nva), as indicated. Additionally, the glutamine (Gln) residue at position 4 is substituted with arginine (Arg) in each analogue.

### 3.1.2. Phospholipids

Lipids used in the various liposomal formulations prepared in this thesis, along with their relevant key properties are presented in **Table 1**.

**Table 1.** Function, transition temperature ( $T_m$ ) and net charge at physiological pH of the phospholipids used in preparation of the fusogenic liposomes, as reported by the supplier Avanti Polar Lipids (Alabaster, AL, USA).

Function	Phospholipid	Net charge at pH 7.4	$T_m$ (°C)
Membrane stabilization	DPPC	Neutral	41
	(1,2-Dipalmitoyl-sn-glycero-3-phosphatidylcholine)		
	DSPC	Neutral	55
	(1,2-Distearoyl-sn-glycero-3-phosphatidylcholine)		
	DAPC	Neutral	66
	(1,2-Diarachidoyl-sn-glycero-3-phosphatidylcholine)		
Fusion promoter	DOPE	Neutral	-16
	(1,2-Dioleoyl-sn-glycero-3-phosphatidylethanolamine)		
Charge modulation	DOPG	Anionic	-18
	(1,2-Dioleoyl-sn-glycero-3-phospho-(1'-rac-glycerol))		
	DOTAP	Cationic	<5
	(1,2-Dioleoyl-3-trimethylammonium-propane)		

### **3.1.3. Microbial strains**

The bacterial and fungal strains used in this study included both reference strains and clinical isolates. *S. aureus* (ATCC 29213), *E. coli* (ATCC 25922), and *E. faecalis* (ATCC 29212) were purchased from the American Type Culture Collection (ATCC, Rockville, MD, USA). *S. aureus* (DSM 2569) and *C. albicans* (DSM 1386) were purchased from the Leibniz Institute DSMZ-German Collection of Microorganisms and Cell Cultures GmbH (Braunschweig, Germany). A bioluminescent *S. aureus* Xen 29 strain, derived from ATCC 12600, was purchased from Revvity (MA, USA). Additionally, clinical isolates of *S. aureus* (P14 and P20) and *E. faecalis* (P40) were collected from the eyes of patients diagnosed with severe dry eye disease in a study conducted at Oslo Metropolitan university, as previously described [138].

### **3.1.4. Medical-grade surfaces for biofilm studies**

Biofilms of *S. aureus* and *E. faecalis* were formed on one-centimetre rods of medical-grade polymers commonly used in medical applications. Polytetrafluoroethylene (PTFE), used in catheter production (Zeus Company, USA), and polyvinyl chloride (PVC), used for intravenous infusion tubing (B. Braun, Germany), were selected for the present work.

## **3.2. Preparation and physicochemical characterization of liposomes**

### **3.2.1. Preparation of fusogenic liposomes**

Fusogenic liposomes were prepared using a standard thin film hydration method, followed by membrane extrusion to obtain uniformly sized unilamellar vesicles. The phospholipid DOPE was incorporated in all liposomal preparations to confer fusogenic properties. Saturated phospholipids DPPC, DSPC and DAPC were added to enhance membrane rigidity and stabilize the liposomes. Additionally, charged phospholipids DOPG and DOTAP were included to provide anionic and cationic surface charges, respectively.

The pH of the liposome hydration medium was adjusted from the physiological pH of 7.4 in **Paper I** to 9.0 in **Paper II**. This was based on preliminary screening work which indicated that higher pH values enhance MP1 entrapment. The observed effect is likely due to increased ionization of anionic groups in MP1 at higher pH, which strengthens electrostatic interactions with the cationic DOTAP incorporated in the liposomal formulation.

Additionally, the DOTAP concentration was increased from 10 mol% in **Paper I** to 25 mol% in **Paper II**. The lower DOTAP concentration led to physical instability when the phospholipid acyl chain length was increased from 16 to 20 carbons, resulting in liposome aggregation and size enlargement after preparation. Increasing the DOTAP concentration to 25 mol% improved physical stability by providing sufficient electrostatic repulsion. This effect was visually observable, as shown in **Figure 8**.

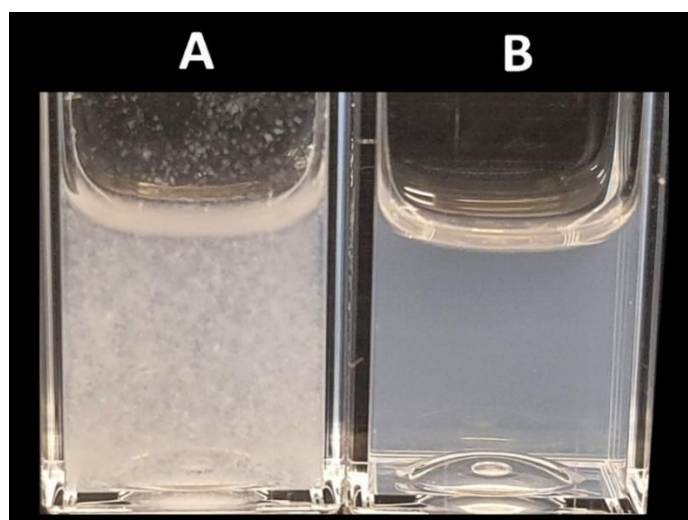


**Figure 8.** Physical appearance of DAPC-based fusogenic liposomes immediately after preparation, formulated with (A) 10 mol% and (B) 25 mol% of DOTAP.

### ***3.2.2. Measurement of liposomal size and polydispersity index***

The size and size distribution of nanosized delivery systems are critical parameters influencing drug encapsulation efficiency, *in vitro* stability, cellular uptake and biodistribution [103, 139]. For systemic administration, liposomes should ideally range between 50 and 200 nm to navigate capillaries and tissue effectively [103]. Additionally, for biofilm treatment, particle size plays a

crucial role in penetration, with optimal penetration reported for nanoparticles smaller than 500 nm [115]. The polydispersity index (PDI) is a key parameter used to assess the uniformity of particle size distribution and is calculated from dynamic light scattering (DLS) data. Generally, a PDI value below 0.2 indicates a monodisperse sample [139]. The particle size and PDI of fusogenic liposomes were measured using DLS technique with a Zetasizer Ultra instrument (Malvern Panalytical Ltd, UK), which determines the hydrodynamic diameter by analysing fluctuations in scattered light from particles undergoing Brownian motion [140]. Measurements were conducted in triplicate at 25°C, with a backscattering angle of 173° and a refractive index of 1.33. The physical stability of the liposomes, monitored via size and PDI measurements, was assessed over a period of one year in **Paper I** and two months in **Paper II**, with the liposomal preparations stored at 4°C under nitrogen.

DLS offers advantages such as minimal sample preparation and broad size range coverage. However, it has limitations including a bias toward larger particles in heterogeneous samples, a lack of particle shape information, and inconsistencies in data processing algorithms across different instruments [140]. Moreover, the hydrodynamic diameter determined by DLS is affected not only by particle size but also by other factors, such as dispersant medium composition and ionic strength [141]. Therefore, maintaining consistent measurement parameters, such as sample dilution procedures and instrument settings, is crucial for ensuring reliable stability studies.

Unlike the DLS technique, electron microscopy typically offers more precise size measurements, focusing on actual particle size rather than hydrodynamic diameter. However, it requires complex sample preparation and is time-consuming, making it unsuitable for routine size distribution analysis [140]. Additionally, electron microscopy can only provide size data for a limited number of particles, whereas DLS enables screening of a much larger particle population [140]. Caution is required when interpreting electron microscopy results for liposomes, as their vesicular structure may be altered during sample dehydration [142]. In contrast, DLS measurements are performed in solution, preserving the integrity of the vesicles.

Fusogenic liposomes imaging was conducted using transmission electron microscopy (TEM). TEM micrographs of selected liposomal preparations were acquired using a modified negative-staining embedding technique, adapted from a previously published protocol [143]. Cryo-TEM,



which better preserves the native structure of liposomes, is more suitable for analysing liposome lamellarity and morphology but is more expensive and time-consuming [144]. Although dehydration during TEM preparation can distort liposomal morphology, it was deemed sufficient for confirming liposome formation and validating DLS size measurements.

### ***3.2.3. Determination of liposomal zeta potential***

Zeta potential is the electric potential at the slipping plane within the electrical double layer of a colloidal particle, relative to a point in the surrounding bulk medium. It is calculated by determining the electrophoretic mobility of the particle within the medium [145]. The zeta potential is influenced by the surface charge density of the particles and the composition of the surrounding liquid. This parameter is essential in colloidal systems, as it influences particle stability and interactions [146]. Particles with a zeta potential of  $\pm 30$  mV or higher are generally regarded stable, as the electrostatic repulsive forces between the particles are sufficiently strong to prevent aggregation [109]. The electrophoretic light scattering (ELS) technique was employed in **Papers I** and **II** to measure the electrophoretic mobility and calculate the zeta potential of the fusogenic liposomes, using a Zetasizer Ultra instrument (Malvern Panalytical Ltd, UK). Zeta potential measurements were conducted at the same time intervals as those used for size and PDI measurements.

### ***3.2.4. Quantification of drug entrapment efficiency***

The entrapment efficiency (EE%) of MP1 was determined using HPLC-MS. Prior to quantification, the free untrapped drug was removed. This purification step can be performed using various techniques, such as ultracentrifugation, ultrafiltration, dialysis, or chromatography, although each approach has its own challenges [103]. Ultracentrifugation may be inefficient, particularly for small liposomes, and can compromise liposomal integrity, while dialysis is time-consuming and may lead to drug leakage [147]. Ultrafiltration is prone to drug adsorption on the membrane surface and membrane clogging due to lipid accumulation.

Chromatographic methods, such as size exclusion chromatography, introduce risks of liposome disruption due to lipid interactions with the column matrix [147].

In **Paper II**, size exclusion chromatography was selected for purification, utilizing PD-10 preppacked columns (Sephadex G-25). To mitigate the drawbacks of this technique and optimize liposome recovery, empty liposomes were first eluted through the column to prevent potential disruption caused by lipid interactions with the column packing. Before injecting the samples into the HPLC-MS, liposomes were treated with 1% Triton X-100 and sonicated to disrupt the liposomal membrane and release the entrapped MP1. The chemical stability of entrapped MP1 was evaluated over two months of storage at 4°C.

### **3.3. Biocompatibility testing of fusogenic liposomes**

As phospholipids are fundamental components of biological membranes, liposomes exhibit inherent compatibility with biological systems due to their phospholipid-based composition. Therefore, liposomes are generally considered biocompatible and biodegradable [110]. The biocompatibility of the prepared fusogenic liposomes was assessed in **Paper I** through two different approaches: haemolysis testing and fibroblast cytotoxicity assay.

Direct interaction between nanosized drug delivery systems and red blood cells (RBCs) can disrupt the cell membrane, potentially causing haemolysis [148]. Therefore, a haemolysis assay was conducted as an initial screening for hemocompatibility. However, since RBCs are not the only cellular components of blood, a comprehensive hemocompatibility assessment should also consider interactions with other blood components, such as white blood cells and platelets. RBCs from healthy donors were isolated by centrifugation and resuspended in phosphate-buffered saline (PBS). They were incubated with serially diluted liposomes in a 96-well plate, and haemolysis was assessed by measuring haemoglobin release at 405 nm. The assay was performed using liposomal concentrations from 0.625 to 15 mM. Negative controls included RBCs in PBS, while positive controls were treated with 1% Triton X-100 to induce haemolysis.

A cytotoxicity study was performed on adult human dermal fibroblasts (C-12302, PromoCell, Heidelberg, Germany). Cells were seeded into 96-well plates and exposed to different

concentrations of liposomes (1.25, 2.5, 5, 10, and 15 mM) for 20 hours. Cytotoxicity was assessed using the Alamar Blue assay, with 1% Triton X-100 added to the positive control wells to induce cytotoxicity and growth medium added to the negative control wells. The cell viability assay measures the irreversible enzymatic conversion of Alamar Blue to resazurin by live cells, which is then determined fluorometrically at an excitation wavelength of 560 nm and emission at 600 nm.

### 3.4. Liposomal fusion with microbial cells

The ability of the prepared liposomes with various surface charges to fuse with microbial cells (*S. aureus*, *E. coli* and *C. albicans*) was evaluated in **Paper I** via two experimental approaches, namely the lipid mixing assay and flow cytometry. The underlying principle of each assay employed in this study is illustrated in **Figure 9**. Including conventional liposomes as controls for comparison with the developed cholesterol-free fusogenic liposomes could have been considered. However, the impact of cholesterol incorporation on liposomal fusion has already been well-documented in literature, confirming its negative effect on the fusogenic properties [131, 133].

The lipid mixing assay is a fluorescence-based technique widely used to investigate membrane fusion and lipid exchange between membranes. It relies on Förster Resonance Energy Transfer (FRET) between two fluorescent probes, typically nitro-2,1,3-benzoxadiazole-4-yl (NBD) as the donor and lissamine rhodamine B (Rh) as the acceptor [149]. Initially, the close proximity of the fluorophores enables FRET, where excitation of NBD facilitates energy transfer to Rh, leading to Rh fluorescence emission. When the labelled liposomal fuses with unlabelled microbial membranes, the fluorescent probes become diluted, reducing FRET efficiency and Rh fluorescence. This decrease provides a quantitative measure of liposomal fusion events [131, 133]. Selected liposomal formulations were prepared with incorporation of 0.2 mol% of each fluorescent probe and mixed with microbial cells in 96-well plates. Fluorescence intensity of Rh was measured at time point zero, after 30 minutes and 3 hours of incubation. To determine the maximum change in FRET, Triton X-100 was added at the final measurement to disrupt the liposomal membrane and release the probes.

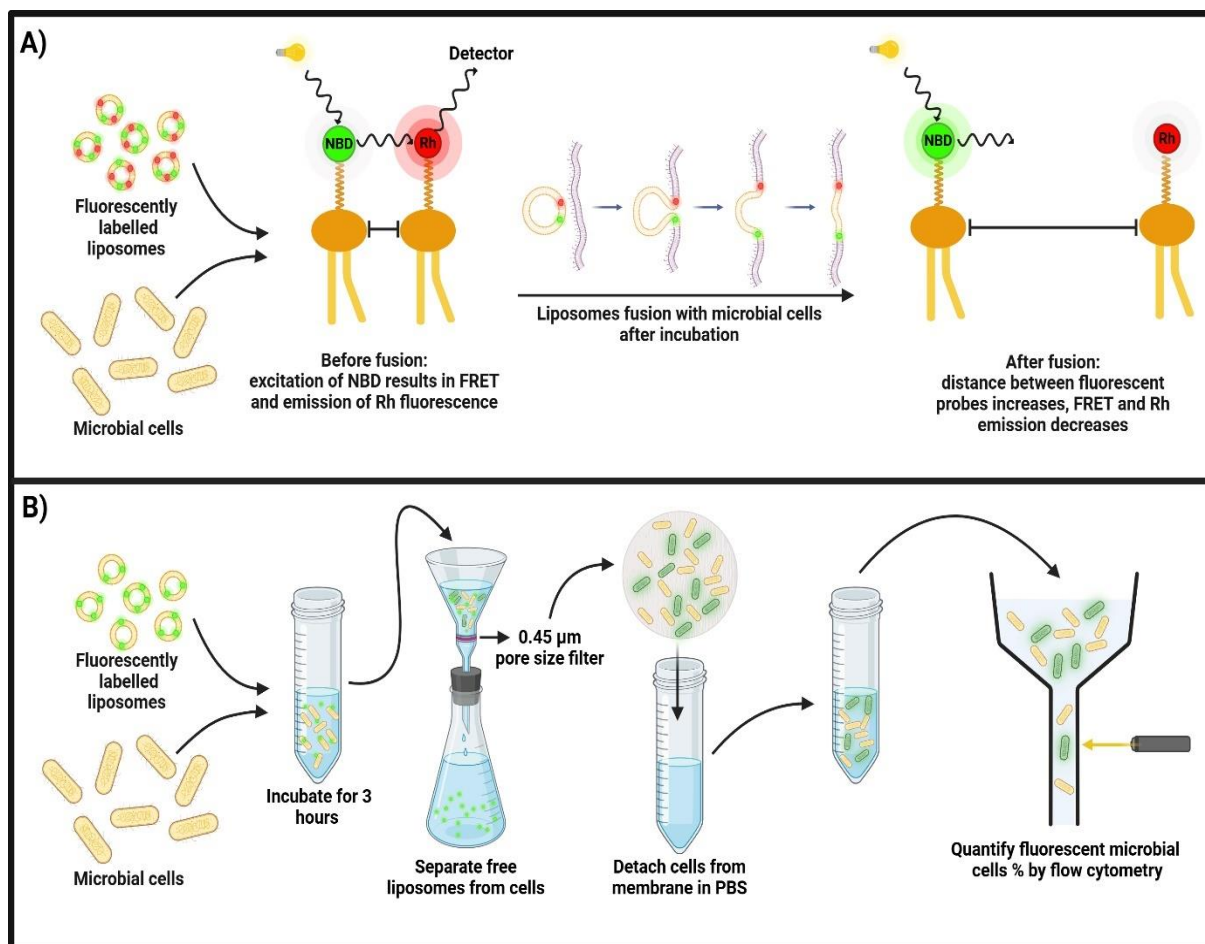


**Figure 9.** Schematic representation of the experimental principles of (A) the lipid mixing assay and (B) the flow cytometry assay, illustrating their application in detecting liposomal fusion with planktonic microbial cells. The figure is created in BioRender.com.

To assess the liposomal fusion with flow cytometry, the formulations were labelled with a green fluorescent cell membrane labelling kit (PKH67) and incubated with microbial cells for 3 hours. The experiment followed previously published protocols with minor modifications. While earlier methods relied on sucrose cushion centrifugation to separate microbial cells from free liposomes [132, 135], this approach was found to be ineffective due to the potential retention of liposomes with microbial cells, leading to inaccurate measurements. To ensure effective separation, microbial cells were retained on 0.45 µm polycarbonate membranes, detached in PBS, and then analysed by flow cytometry. The extent of liposomal fusion was determined by calculating the percentage of fluorescent cells relative to the total cell count.

## 3.5. Evaluation of antimicrobial and antibiofilm activity

### 3.5.1. Minimum inhibitory concentration assay

The minimum inhibitory concentration (MIC) is defined as the lowest concentration ( $\mu\text{g/mL}$ ) of an antimicrobial agent that prevents visible growth of the tested microorganism [150]. MIC values are used to determine whether a microbial strain is resistant or susceptible to an antimicrobial agent, based on established clinical breakpoints published by the European Committee on Antimicrobial Susceptibility Testing (EUCAST) or the Clinical and Laboratory Standards Institute (CLSI) [151]. These breakpoints are determined by various factors, including the pharmacokinetic and pharmacodynamic properties of the antimicrobial agent. Consequently, direct comparison of MIC values between different antimicrobial agents is not appropriate for assessing relative susceptibility [151].

In this work, the broth microdilution method was performed following CLSI guidelines to determine MIC values for MP1 and MP1-loaded liposomes (**Paper II**) and for teixobactin analogues (**Paper III**). As neither MP1 nor teixobactin analogues have yet reached clinical application, no established breakpoints are currently available. For teixobactin analogues, MIC values were compared to evaluate the impact of chemical structural modifications on antimicrobial activity (**Paper III**). For MP1, MIC values of free MP1 and MP1-loaded liposomal formulations were compared, to assess whether liposomal encapsulation had a positive or negative impact on antimicrobial activity *in vitro* (**Paper II**). Vancomycin was included as a quality control measure in both studies to ensure the validity of the experimental procedures. Breakpoints for vancomycin have been reported by CLSI for the ATCC reference bacterial strains, *S. aureus* (ATCC 29213) and *E. faecalis* (ATCC 29212), which were used in the quality control assessments.

Stock solutions of teixobactin, teixobactin analogues, MP1, and vancomycin were made in dimethyl sulfoxide (DMSO) and serially diluted according to CLSI guidelines [152]. MP1-loaded liposomes were diluted based on their entrapment efficiency determined by HPLC-MS to yield similar concentration ranges. MIC testing was conducted in 96-well plates using ATCC reference strains and clinical isolates of *S. aureus* and *E. faecalis*, according to CLSI guidelines and MIC values were visually determined after 18 hours of incubation at 37°C.

### 3.5.2. Minimum bactericidal concentration assay

The minimum bactericidal concentration (MBC), also referred to as the minimal lethal concentration, is defined as the lowest concentration of an antimicrobial agent required to kill  $\geq 99.9\%$  of viable microorganisms after 24 hours of incubation [153]. MBC was determined in **Paper III** for the teixobactin analogues. Following MIC determination, the contents of wells without visible bacterial growth were transferred onto tryptic soy agar (TSA) plates and incubated overnight at 37 °C. Colony counts were then used to determine the MBC. The MBC/MIC ratio was calculated for each analogue-strain combination to classify the compounds as either bactericidal or bacteriostatic, with a ratio of  $\leq 4$  generally indicating bactericidal activity [154].

### 3.5.3. Effect of antimicrobial agents on bacterial growth curves

The effect of teixobactin analogues and vancomycin on planktonic growth was evaluated using *S. aureus* (ATCC 29213) and *E. faecalis* (ATCC 29212) in **Paper III**. Bacterial growth responses vary based on the antimicrobial agent mechanism of action, for instance, agents targeting the cell wall or cell membrane have been reported to delay growth onset [155]. Bacterial suspensions ( $\approx 10^5$  CFU/mL) in tryptic soy broth (TSB) + 1% glucose were treated with teixobactin analogues or vancomycin at concentrations equivalent to  $\frac{1}{2} \times \text{MIC}$ , MIC, and  $2 \times \text{MIC}$ . Optical density was measured every 15 minutes for 16 hours at 37°C using a plate reader (Victor<sup>3</sup>, Perkin Elmer, USA) at 590 nm. Growth curves were analysed to determine the exponential phase onset and doubling time.

### 3.5.4. Inhibition of biofilm formation

In **Paper III**, teixobactin analogues were evaluated for their ability to inhibit *S. aureus* and *E. faecalis* biofilm formation at concentrations ranging from  $\frac{1}{2} \times \text{MIC}$  to  $4 \times \text{MIC}$ . Bacterial suspensions were incubated statically in 96-well polypropylene plates with TSB + 1% glucose overnight at 37°C in the presence of the antimicrobial agents. Biofilm formation was first assessed visually, and wells showing significant growth reduction were further analysed using

colony counting, crystal violet (CV) staining, and triphenyl tetrazolium chloride (TTC) activity staining. The biofilm inhibitory concentration (BIC<sub>90</sub>) was defined as the lowest concentration achieving >90% inhibition. Using both CV and activity staining provided complementary insights into biofilm inhibition. CV staining measures total biofilm mass, including cells and extracellular matrix, while activity staining selectively detects viable cells based on metabolic activity [156, 157]. Combining these methods ensured a comprehensive evaluation of both biofilm matrix and bacterial cell viability.

### ***3.5.5. Treatment of preformed biofilms***

The ability of MP1, MP1-loaded liposomes, and teixobactin analogues to treat established biofilms was evaluated in **Papers II** and **III** using various quantitative and qualitative approaches. Biofilms of *S. aureus* and *E. faecalis* were allowed to form on various materials, including 96-well polystyrene plates and biomedical materials such as PTFE and PVC. Bacterial inoculums were cultured in TSB + 1% glucose for three days to allow biofilm formation, followed by treatment for 24 hours with various concentrations of each antimicrobial agent.

In **Paper II**, the antibiofilm activity of MP1 and MP1-loaded liposomes was assessed against a bioluminescent strain of *S. aureus* (Xen 29), and biofilm eradication was quantified by measuring changes in biofilm metabolic activity detected as bioluminescence. In **Paper III**, biofilm inactivation by teixobactin analogues was evaluated using colony counting as a quantitative assay measuring the reduction in CFU numbers after treatment compared to the control. Additionally, activity staining by TTC was employed as a qualitative screening method, where the intensity of colour development was scored visually.

### ***3.5.6. Microscopic Analysis of Biofilms***

Biofilms of *S. aureus* were grown in 4-well chamber slides using TSB supplemented with 1% glucose. Bacterial inoculum was prepared by suspending colonies from overnight TSA cultures in saline at 0.5 McFarland, and diluting in TSB to  $\approx 10^5$  CFU/mL. The suspension was incubated

for 72 hours with daily medium replacement. Before treatment, biofilms were washed twice with sterile water. Confocal laser scanning microscopy (CLSM) was employed to analyse biofilms after treatment. In **Papers I and II**, the ability of fusogenic liposomes to penetrate the biofilm was assessed by labelling the liposomes with rhodamine-phosphatidylethanolamine, while biofilm cells were visualized using 4',6-diamidino-2-phenylindole (DAPI).

Additionally, CLSM was used to evaluate the eradication of *S. aureus* biofilm. In **Paper II**, this was assessed following treatment with MP1 and MP1-loaded fusogenic liposomes. In **Paper III**, the evaluation was carried out after treatment with teixobactin analogue TB3. Live/dead cell staining, consisting of Syto 9 and propidium iodide, was employed to differentiate between viable (green) and dead (red) cells. The reduction in cellular viability was quantified by calculating the percentage of dead cells relative to the total cell count after incubation with the antimicrobial agent for 24 hours.



## 4. Synopsis of the papers

### Paper I

#### **The Impact of Surface Charge on the Interaction of Cholesterol-Free Fusogenic Liposomes with Planktonic Microbial Cells and Biofilms**

Ahmed M. Amer, Colin Charnock, Sanko Nguyen

International Journal of Pharmaceutics, 2025

#### Aim of the study:

Based on previous reports in the literature highlighting the negative impact of cholesterol on liposomal fusion, this study aimed to enhance the fusogenic properties of liposomes by formulating cholesterol-free variants with different surface charges and investigating their interactions with both planktonic microbial cells and established biofilms.

#### Materials and methods:

Cholesterol-free fusogenic liposomes with varying surface charges were prepared using the thin-film hydration method, incorporating DOPE as the fusion-promoting phospholipid. Their physical properties, including size, polydispersity index (PDI), and zeta potential, were characterized using light scattering techniques and long-term stability was assessed over one year of storage at 4°C. Liposomal fusion with microbial cells, including yeast-like fungal cells (*C. albicans*), gram-positive (*S. aureus*) and gram-negative (*E. coli*) bacteria, was evaluated using both the lipid mixing assay and flow cytometry. Additionally, the influence of surface charge on liposomal interaction and penetration into preformed *S. aureus* biofilms was examined via confocal laser scanning microscopy (CLSM). Finally, biocompatibility was assessed through cytotoxicity testing on human skin fibroblasts and haemolysis assays.

#### Results and discussion:

Monitoring the physical stability of the prepared liposomes revealed that they remained stable for over a year, except for two cationic formulations, which exhibited size enlargement and aggregation over time. The incorporation of DPPC effectively compensated for the absence of

cholesterol, ensuring the structural stability of the liposomes. Fusion experiments using lipid mixing and flow cytometry assays revealed that liposomal fusion efficiency was highest with the gram-negative species (*E. coli*), followed by the gram-positive species (*S. aureus*). Fusion was lowest with the yeast-like fungi (*C. albicans*). Among the formulations, neutral liposomes exhibited the greatest fusion capacity, followed by cationic and anionic liposomes. The results suggest that liposomal fusion is a multifactorial process influenced by the chemical composition of both the liposomes and microbial cell envelopes.

Furthermore, confocal microscopy studies demonstrated that all liposomal formulations, regardless of charge, were capable of penetrating *S. aureus* biofilms. Cationic liposomes showed enhanced interaction and retention within the biofilm matrix, likely due to electrostatic interactions with the abundant negatively charged compounds present in the biofilm matrix. Biocompatibility assessments demonstrated that the prepared fusogenic liposomes exhibited minimal cytotoxicity toward human skin fibroblasts, maintaining cell viability above 90% across all tested concentrations. Furthermore, haemolysis studies confirmed that the liposomal formulations did not induce red blood cell damage, as no haemoglobin leakage was detected.

### Conclusion:

The cholesterol-free fusogenic liposomes developed in this study, with varying surface charges, demonstrate strong potential as drug delivery platforms against biofilm-associated infections. Surface charge and phospholipid composition influenced the fusion with microbial cells and interaction with preformed biofilm. Cationic liposomes exhibited greater interaction and retention within *S. aureus* biofilm.

## Paper II

### **Phospholipid Acyl Chain Length Modulation: A Strategy to Enhance Liposomal Drug Delivery of the Hydrophobic Bacteriocin Micrococcin P1 to Biofilms**

Ahmed M. Amer, Colin Charnock, Kirill V. Ovchinnikov, Tage Thorstensen, Sanko Nguyen  
European Journal of Pharmaceutical Sciences, 2025

#### Aim of the study:

This study aimed to develop fusogenic liposomes for the entrapment of micrococcin P1 to enhance its antimicrobial and antibiofilm efficacy. It also investigated the influence of phospholipid acyl chain length on drug entrapment efficiency, liposomal stability and antibiofilm activity.

#### Materials and methods:

Fusogenic liposomes were prepared using the thin-film hydration method, incorporating phospholipids with varying acyl chain lengths (C16, C18, and C20). MP1 was entrapped by dissolving it in the organic phase during the lipid film formation step. Both empty and MP1-loaded liposomes were characterised in terms of vesicle size, PDI, and zeta potential, with stability monitored over two months of storage at 4°C. Entrapment efficiency was determined using HPLC-MS, while the chemical stability of entrapped MP1 was assessed over the same two months period. The antimicrobial activity of MP1-loaded liposomes was evaluated using MIC assays against various *S. aureus* strains, including clinical isolates. Additionally, the ability of liposomal entrapment to enhance MP1 activity against preformed *S. aureus* biofilms was investigated. Biofilms were first allowed to form in 96-well plates and on biomedical-grade PTFE before undergoing treatment. Confocal laser scanning microscopy (CLSM) was further employed to visualise *S. aureus* biofilms following treatment with MP1 and MP1-loaded liposomes.

#### Results and discussion:

This study demonstrated the successful development of fusogenic liposomes as a drug delivery system for the hydrophobic antimicrobial peptide MP1. Liposomal entrapment significantly

improved the aqueous stability of MP1. Additionally, MP1-loaded liposomes exhibited enhanced antimicrobial activity, reducing the MIC values against the tested *S. aureus* strains by 4- to 16-fold compared to free MP1. Increasing the phospholipid acyl chain length from 16 to 20 carbons not only improved MP1 entrapment but also enhanced the antibiofilm efficacy. This improvement could be partially attributed to the ability of longer-chain phospholipids to disrupt biofilm integrity, as demonstrated by the activity of empty liposomes against preformed biofilms in 96-well plates. Furthermore, CLSM confirmed the antibiofilm activity of MP1-loaded liposomes. At a concentration of 0.25 µg/mL, MP1-loaded fusogenic liposomes (MP1-DAPC) incorporating 20-carbon acyl chains reduced biofilm cell viability by approximately 55%, while free MP1 at the same concentration achieved only 15% reduction.

Despite the improved antibiofilm activity, the longer acyl chains compromised the physical stability of the liposomes. While MP1-loaded liposomes formulated with 16-carbon acyl chain (DPPC) remained stable for two months, those incorporating 20-carbon acyl chain (DAPC) were stable for only two weeks. Stability was improved by increasing the concentration of the cationic phospholipid DOTAP from 25 mol% to 50 mol% in the liposomal composition.

### Conclusion:

These findings highlight the potential of fusogenic liposomes for enhancing the aqueous stability, antimicrobial and antibiofilm activity of MP1. However, while increasing the phospholipid acyl chain length improved drug entrapment and antibiofilm activity, it also compromised the liposomal stability, emphasizing the need for formulation optimization to balance efficacy and stability.

## Paper III

### **Novel Teixobactin Analogues Show Promising In Vitro Activity on Biofilm Formation by *Staphylococcus aureus* and *Enterococcus faecalis***

Ahmed M. Amer, Colin Charnock, Sanko Nguyen

Current Microbiology, 2024

#### Aim of the study:

This study aimed to evaluate the antimicrobial and antibiofilm activity of three novel teixobactin analogues to identify the most promising candidate for further liposomal encapsulation.

#### Materials and methods:

Three newly developed teixobactin analogues (TB1, TB2 and TB3) were evaluated for their antimicrobial and antibiofilm efficacy against *S. aureus* and *E. faecalis*. The three analogues differ in the amino acid residue at position 10, where TB1 contains leucine (Leu), TB2 contains norleucine (Nle), and TB3 contains norvaline (Nva). The methodologies employed included determining MIC and MBC to assess the antibacterial activity of each analogue. Additionally, the effect of the analogues on the growth curves of planktonic cells was investigated by monitoring bacterial growth over 16 hours. Furthermore, the study investigated the ability of these analogues to prevent biofilm formation and to eradicate bacterial cells within preformed biofilms on medical-grade materials, specifically polyvinyl chloride (PVC) and polytetrafluoroethylene (PTFE). Antibiofilm activity was evaluated using colony counting, crystal violet staining, and metabolic activity staining (TTC). Additionally, CLSM was employed to visualise bacterial cell inactivation within the biofilm matrix and to quantify changes in biofilm biovolume.

#### Results and discussion:

All three analogues exhibited promising antibacterial activity, with MIC values comparable to those of the natural teixobactin compound. The MBC assay further confirmed the bactericidal nature of the compounds against the *S. aureus* strain tested, with MBC/MIC ratios  $\leq 4$ .

Regarding biofilm inhibition, the teixobactin analogues effectively reduced biofilm formation in 96-well polypropylene plates. All three analysis methods (colony counting, crystal violet staining and metabolic activity staining) yielded consistent results for *S. aureus*, while the activity staining results for *E. faecalis* were inconclusive, as no colour development was observed. The teixobactin analogue TB3, which contains a norvaline substitution at position 10, demonstrated higher activity than the other two analogues. The antibiofilm activity of the teixobactin analogues against preformed *S. aureus* biofilms on biomedical materials (PVC and PTFE) showed the highest activity with the TB3 analogue, followed by TB2 and TB1. These results were consistent across both colony counting and activity staining. Further CLSM analysis of TB3 treated biofilms showed a dose-dependent reduction in cellular viability and biovolume. Treatment with 8 µg/mL for 24 hours reduced viable cell counts by 65% and total biovolume by 75%.

#### Conclusion:

The study demonstrates that teixobactin analogues show considerable potential for addressing biofilm-associated infections and could be candidates for pharmaceutical development. Additionally, the findings underscore the influence of the position-10 substitution on the antimicrobial and antibiofilm activity of teixobactin analogues.

## 5. Discussion

### 5.1. Main findings

This research provides key insights into the development of fusogenic liposomes and antimicrobial peptide-based approaches for combating microbial biofilm infections. The findings in **Paper I** demonstrate that cholesterol-free fusogenic liposomes effectively fuse with microbial cells while maintaining long-term physical stability. Previous studies have shown that incorporating cholesterol can impair the fusogenic properties of liposomes [131, 133]. Therefore, cholesterol-free formulations are expected to exhibit enhanced fusion with microbial cells. A key finding of this study was that these liposomes remained physically stable despite the absence of cholesterol, which is typically required to maintain vesicle rigidity. Notably, the inclusion of DPPC at 50 mol% effectively compensated for the lack of cholesterol, ensuring structural stability during long-term storage. The stabilising effect of DPPC on fusogenic liposomes is likely due to its relatively high phase transition temperature (41 °C), which may have contributed to maintaining membrane rigidity during storage at 4 °C throughout the one-year stability study.

The ability of liposomes to fuse with microbial cells is crucial for enhancing the antimicrobial activity of the incorporated drug. Fusion facilitates the intracellular delivery of high drug concentrations, thereby enhancing antimicrobial effectiveness [112-114]. Regardless of surface charge, all fusogenic liposomes prepared in **Paper I** demonstrated the ability to fuse with various microbial cells, although the fusion efficiency varied depending on both the liposomal properties and the microbial cell type. The fusion efficiency followed a certain trend: neutral liposomes exhibited the highest fusion ability, followed by cationic, and then anionic liposomes.

Electrostatic interactions are often considered the primary driver of fusion, as they facilitate the interaction of cationic liposomes to negatively charged microbial cell surfaces. In contrast, anionic liposomes are thought to require divalent cations to overcome electrostatic repulsion and facilitate fusion [133]. However, the findings reported in this thesis challenge this assumption, as anionic liposomes were able to fuse in the absence of divalent cations. This suggests that, alongside electrostatic interactions, the composition of the microbial cell envelope and the properties of the liposomal membrane also play crucial roles in driving the fusion process.

The enhanced fusion ability of neutral liposomes is likely due to their higher DOPE content (50 mol%), compared to the 40 mol% in charged liposomes. The decision to replace part of the DOPE with charged phospholipids (DOTAP or DOPG) in the preparation of cationic and anionic liposomes was based on their similar acyl chain structures, despite differences in headgroups. In contrast, substituting DPPC with charged phospholipids would have introduced greater variability due to its distinct headgroup, shorter acyl chains, and lack of unsaturation. This consideration is particularly relevant as the curvature of the phospholipid membrane, which is critical for fusion, is influenced by the nature of the headgroup, as well as the length and unsaturation of the acyl chains [158]. Unsaturated phospholipids such as, phosphatidylethanolamine (e.g. DOPE) exhibit negative membrane curvature, resulting in membrane protrusion toward the hydrocarbon chains as shown in **Figure 10** [159]. Moreover, the smaller headgroup of DOPE further enhances negative membrane curvature, promoting the fusion process [134]. In contrast, phosphatidylcholine (e.g. DPPC) forms nearly planar monolayers, resulting in an overall curvature close to zero [159].

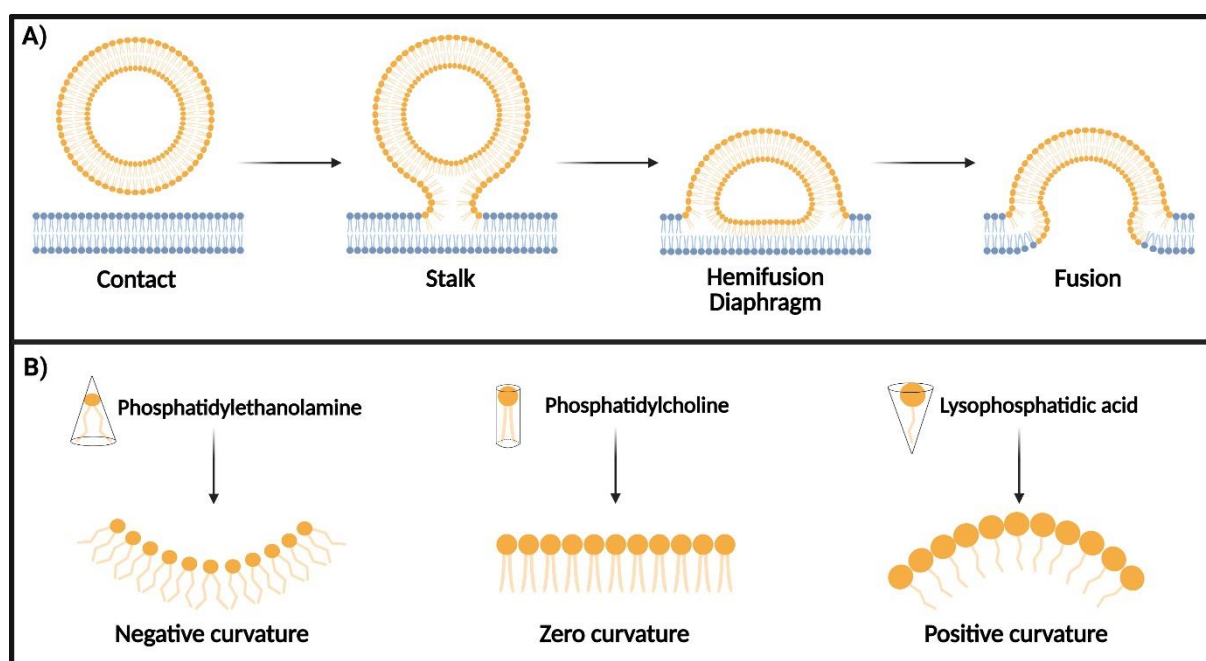


**Figure 10.** (A) Schematic representation of the fusion process according to the "stalk model." The process begins with the liposomes encountering biological membranes, leading to the formation of a stalk, followed by hemifusion diaphragm intermediates, and eventually resulting in complete fusion with the membrane. (B) Illustration of how the structure of phospholipids influences membrane curvature when incorporated into liposome preparations, which in turn affects the fusogenic ability of the liposomes. The figure is created in BioRender.com and adapted from [134, 158].



Several hypotheses have been proposed to explain the mechanism of liposome fusion with biological membranes. Based on simulations and theoretical studies, the "stalk model", illustrated in **Figure 10**, is the most widely accepted fusion mechanism [158]. According to this model, fusion starts with a point-like membrane protrusion that forms an hourglass-shaped stalk between the membranes undergoing fusion. The stalk then expands into a hemifusion diaphragm, which eventually leads to complete fusion [134, 158, 159]. Alternatively, the stalk may directly progress to complete fusion, bypassing the hemifusion diaphragm stage. The negative membrane curvature induced by DOPE plays a crucial role in forming the stalk intermediate, which is a key step in the fusion process [158, 159].

The fusion efficiency measured using the two analytical methods in **Paper I** showed that fusion was highest with *E. coli* (a gram-negative bacterium), followed by *S. aureus* (a gram-positive bacterium) and finally *C. albicans* (a fungal species). A similar trend has been reported in the literature where the extent of liposomal fusion with various gram-negative and gram-positive bacteria was investigated [131, 133]. However, the work in **Paper I** is the first to investigate fusion with fungal cells. The higher fusion observed with gram-negative bacteria has been attributed in the literature to the partial structural similarity between liposomes and the outer membrane of gram-negative bacteria, as both contain phospholipids [131, 133, 160]. It is important to note that, while some differences in the present study were statistically significant ( $P < 0.05$ ), this was not the case for all comparisons among the microbial strains and liposomes with varying surface charges. For instance, flow cytometry was unable to detect *C. albicans* cells undergoing liposomal fusion, likely due to weak fluorescence signals resulting from the low number of fusion events per cell. Increasing the exposure time of fungal cells to liposomes or increasing the liposomes concentration could potentially improve the detection in future studies.

The limited ability of antimicrobial agents to penetrate biofilms is a major challenge contributing to the tolerance of biofilm-associated infections to treatment [39]. Investigating the ability of fusogenic liposomes to overcome this barrier (**Paper I**) provided valuable insights into improving treatment strategies. The results from CLSM analysis indicate that the surface charge of liposomes did not affect their ability to penetrate *S. aureus* biofilms. All liposomal preparations, regardless of charge, were able to penetrate through all layers of the biofilm matrix. However, cationic liposomes showed superior interaction with the EPS matrix and

better retention within the biofilm. This aligns with previous studies on conventional cationic liposomes, where enhanced biofilm interaction was attributed to electrostatic attraction with the negatively charged components, which are predominant in the biofilm matrix [119]. These findings suggest that while charge does not influence the penetration of liposomes into biofilms, it plays a crucial role in ensuring prolonged retention and localized drug delivery within the biofilm, which is essential for sustained antimicrobial activity.

Despite the high ability of fusogenic liposomes to interact with biological membranes, preliminary biocompatibility testing (**Paper I**) demonstrated their tolerability. Haemolysis analysis and cell viability assays on human skin fibroblasts revealed no detectable toxicity, suggesting the potential of the liposomes for clinical applications. However, further comprehensive evaluations are necessary to confirm their safety before clinical use.

The ability of the developed fusogenic liposomes to enhance the antimicrobial and antibiofilm activity of AMPs was demonstrated in **Paper II** by incorporating MP1 into positively charged fusogenic liposomes. Additionally, the study investigated the effect of increasing the phospholipid acyl chain length from 16 to 20 carbons on the physicochemical properties of the liposomes, MP1 entrapment, and antibiofilm efficacy. Increasing the phospholipid acyl chain length negatively impacted the physical stability of the liposomes, as evidenced by size enlargement and increased PDI in liposomes prepared with the 20-carbon acyl chain phospholipid DAPC. These liposomes remained stable for only two weeks, whereas those containing the 16-carbon DPPC maintained stability for two months. The stability of DAPC liposomes further declined after MP1 incorporation. This is likely due to the ability of entrapped peptides to destabilize the liposomes by altering the properties and curvature of the liposomal membrane, potentially leading to liposome fusion and aggregation [158, 161]. Increasing the DOTAP content from 25 mol% to 50 mol% while reducing DAPC from 37.5 mol% to 25 mol% extended liposome stability to two months. However, this increase in DOTAP was not reflected in the zeta potential measurements, as both formulations exhibited similar zeta potential values. Additionally, the study demonstrated that extending the phospholipid acyl chain length from 16 to 20 carbons improved MP1 entrapment efficiency, from  $16.4 \pm 6.2\%$  to  $21.0 \pm 5.7\%$ . This enhancement might be due to the stronger hydrophobic interactions between MP1 and the longer acyl chains of DAPC.

Incorporating MP1 into liposomes enhanced its antimicrobial activity against various *S. aureus* strains, including clinical isolates, when tested without Tween 80 in the growth medium. This suggests that the liposomes effectively mimic the recently proposed natural process whereby MP1 is secreted into bacterial membrane vesicles, allowing the peptide to overcome its hydrophobicity [162]. This mechanism enables MP1 to diffuse through the aqueous environment, reach its target cells, and release the peptide upon fusion. Liposomal entrapment of MP1 significantly reduced the minimum inhibitory concentration (MIC) against various *S. aureus* strains, with reductions ranging from 4- to 16-fold. The antimicrobial activity showed a slight enhancement when the phospholipid acyl chain length was increased. Specifically, the MIC value decreased by 2- to 4-fold with DAPC (20C) liposomes compared to DPPC (16C) liposomes, across the tested *S. aureus* strains. Additionally, when testing in the presence of Tween 80, the MIC values for free MP1 and MP1-loaded liposomes were similar, indicating that liposomal entrapment did not impair the antimicrobial activity of MP1. The addition of Tween 80 likely mitigated the hydrophobic limitations of free MP1, enhancing its solubility and activity.

The screening of antibiofilm activity for empty liposomes (**Paper II**) against preformed *S. aureus* Xen 29 biofilms using bioluminescence measurements showed a concentration-dependent decrease in biofilm metabolic activity. This reduction was likely due to a decrease in biofilm mass rather than direct cellular toxicity, as empty liposomes did not show antimicrobial activity in the MIC assay. Notably, DAPC-based liposomes caused the most significant reduction in metabolic activity compared to other liposome types, suggesting that the phospholipid acyl chain length influences the interaction between liposomes and the biofilm matrix. These findings align with reports in the literature highlighting the ability of phosphatidylcholine and various amphiphilic molecules to disrupt the biofilm matrix [163-165].

MP1-loaded DAPC liposomes demonstrated notable antibiofilm activity, with a 50% reduction in metabolic activity at 8×MIC and up to an 80% reduction at 32×MIC against *S. aureus* Xen 29 biofilms preformed in 96-well plate. This was in contrast to free MP1, which showed no antibiofilm activity at 8×MIC. However, at higher concentrations ( $\geq 16\times\text{MIC}$ ), the difference in activity between free MP1 and MP1-loaded DAPC liposomes became insignificant. Additionally, MP1-loaded liposomes prepared with shorter acyl chains, such as DPPC and DSPC, demonstrated antibiofilm activity comparable to or inferior to that of free MP1.

These findings highlight the promising potential of MP1-loaded DAPC liposomes for antibiofilm applications, which was further investigated using biofilms formed on the biomedically relevant material PTFE. In the first round of testing, MP1-loaded DAPC liposomes reduced biofilm metabolic activity by approximately 70% at a concentration of 0.25 µg/mL, whereas free MP1 showed no effect at the same concentration. In the second round of testing, both free MP1 and MP1-loaded liposomes exhibited antibiofilm activity at 0.5 µg/mL, reducing biofilm activity by about 70% and 85%, respectively. Overall, the antibiofilm activity of MP1-loaded DAPC liposomes was less pronounced against biofilms preformed on PTFE compared to the results observed in the 96-well plate. This is likely due to the thinner biofilm formed on PTFE, as this material is known to exhibit resistance to biofilm formation [166, 167]. Further analysis using live/dead cell staining and CLSM revealed that the liposomal formulation was more effective than free MP1 in the eradication of *S. aureus* biofilm. MP1-loaded DAPC liposomes demonstrated a significantly greater reduction in cell viability (55%) at 0.25 µg/mL than that achieved with free MP1 (15%). Additionally, MP1-loaded DAPC liposomes resulted in more biofilm matrix disruption, as evidenced by CLSM images.

Given the increasing threat of antimicrobial resistance and the emergence of multidrug-resistant strains, this thesis investigated the potential antibiofilm activity of novel AMPs. Three teixobactin analogues were evaluated for their antimicrobial and antibiofilm activity in **Paper III**, with future plans to incorporate the most promising candidate into liposomal formulations. The three analogues exhibited promising antimicrobial activity against the tested *S. aureus* and *E. faecalis*, with MIC values of 1-2 µg/mL and 2-4 µg/mL, respectively, including clinical isolates. MBC analysis confirmed a bactericidal effect against *S. aureus*, whereas the analogues were only bacteriostatic against *E. faecalis*. The observed *E. faecalis* tolerance is likely attributed to an intrinsic resistance mechanism against cell wall-targeting antibiotics [168].

Growth curve analysis provided insights beyond MIC values, revealing how teixobactin analogues influence bacterial growth dynamics. The results supported the MIC findings, showing no growth at concentrations  $\geq$  MIC and a measurable delay in the exponential phase onset at  $\frac{1}{2} \times$  MIC for both *S. aureus* and *E. faecalis*. The teixobactin analogue TB3 caused the most significant delay, with more than 16 hours. The delayed onset of the exponential phase may reflect a bacterial defense mechanism known as “tolerance by lag”, a phenomenon observed with antibiotics that target the integrity of cell envelope [155, 169]. Doubling time

calculations indicated a more pronounced effect on *S. aureus* than *E. faecalis*, aligning with the MBC/MIC results. Among the three analogues tested, TB3 exhibited greatest inhibitory effects, likely due to the hydrophobic side chain length at position 10. This aligns with previous studies indicating that substitution with norvaline at position 10 enhances antimicrobial activity of teixobactin analogues [170].

The antibiofilm activity of the novel analogues was evaluated by assessing their ability to inhibit biofilm formation and eradicate preformed biofilms. TB1 and TB2 inhibited biofilm formation at 2×MIC for both *S. aureus* (4 µg/mL) and *E. faecalis* (8 µg/mL), while TB3 exhibited slightly higher activity, by reducing biofilm formation at 1–2×MIC for *S. aureus* (2–4 µg/mL) and 1×MIC for *E. faecalis* (4 µg/mL). Results were consistent across all three analytical methods: CV staining reflected total biofilm biomass, colony counting assessed viable cell numbers, and activity staining indicated the metabolic activity of the cells.

Furthermore, the analogues exhibited antibiofilm activity against preformed *S. aureus* biofilms on clinically relevant surfaces, PVC and PTFE. TB3 showed the highest activity, followed by TB2 and TB1. The agreement between the results of activity staining and colony counting suggests the potential use of the former as a reliable and rapid screening method. Additionally, the higher hydrophobicity of teixobactin analogues may enhance their adsorption to plastic surfaces, contributing to their antibiofilm efficacy. TB3, the most effective analogue, was further analysed using CLSM, revealing a dose-dependent reduction in biofilm viability and biovolume. Biofilm treatment for 24 hours with 8 µg/mL TB3 reduced viable cells by 65% and biovolume by 75% relative to the control, confirming significant biofilm disruption.

These findings identify TB3 as a promising candidate for further pharmaceutical development and incorporation in liposomal drug delivery systems. Moreover, the results support the proposed SAR of teixobactin analogues, particularly the influence of hydrophobic side chain length at position 10.

## 5.2. Significance of the results and future perspectives

Biofilms present a major challenge in clinical settings due to their resistance to conventional antimicrobial therapies [2, 5]. The EPS matrix within the biofilm, along with factors such as antimicrobial degradation, cell dormancy, and altered metabolic activity, significantly contribute to the enhanced tolerance of biofilms to antimicrobial agents [29, 39]. The cholesterol-free fusogenic liposomes developed in this thesis offer a promising strategy to address these challenges. Excluding cholesterol can enhance fusion with microbial cells, as its presence in liposomes has previously been shown to hinder this process [131, 133]. Despite the absence of cholesterol, these liposomes remained physically stable for over a year and were able to penetrate preformed biofilms and fuse with various planktonic microbial cells (bacteria and fungi), suggesting their potential as an effective approach for combating biofilm-associated microbial infections.

Despite ongoing research into the mechanism of liposomal fusion with microbial cells, many questions remain unanswered. Visualizing the fusion intermediates is a major challenge in deciphering the fusion process due to their transient nature [158]. The findings reported in this thesis may contribute to a better understanding of the parameters underpinning liposomal fusion with various microbial cell types, particularly highlighting the role of liposomal membrane composition and the impact of phospholipid charge.

Studies in the literature report the promising antimicrobial activity of MP1. However, its hydrophobic nature and susceptibility to chemical degradation as a peptide, limit its potential for pharmaceutical development [81, 171]. The work presented in this thesis marks the first attempt to develop an MP1-loaded liposomal drug delivery system, and to investigate the effect of MP1 liposomal entrapment on the antimicrobial and antibiofilm activity. The developed fusogenic liposomes incorporating the 20-carbon acyl chain phospholipid (DAPC) were found to exhibit dual functionality. They served as an effective drug delivery system for MP1 while also exhibiting antibiofilm properties by disrupting the biofilm matrix. However, the mechanism by which empty DAPC liposomes disrupts the biofilm matrix require further investigation to be fully elucidated.

As demonstrated by the results in the present work, DAPC-based fusogenic liposomes show promise as a foundation for developing antibiofilm nanosized drug delivery systems. However, their limited physical stability necessitates further optimization. This trade-off between stability and antibiofilm efficacy, highlights the need for additional research to develop liposomal formulations that effectively balance both properties for pharmaceutical applications.

The results obtained with the teixobactin analogues underscore their promising potential as novel AMPs for biofilm treatment. The observed differences in activity among the analogues contribute to a deeper understanding of teixobactin's SAR, aiding the rational design of more effective analogues in the future. While efforts to bring natural teixobactin to clinical application are ongoing [69, 70], the ease of production of TB3 and its promising antibiofilm activity, highlight its potential for pharmaceutical development. Future studies should investigate its efficacy against a wider range of bacteria and focus on the development of suitable liposomal formulations.

Overall, the work presented in this thesis confirms the antibiofilm efficacy of the tested AMPs and reports the successful incorporation of MP1 into fusogenic liposomes. The MP1-loaded liposomes effectively eradicated biofilm forming bacteria *in vitro*. Interpretation and any extrapolation of the results to the clinical setting should be approached with caution, as all biofilm experiments were conducted *in vitro* and on abiotic surfaces. While this is relevant to infections associated with medical implants, many biofilm-related infections, such as those in cystic fibrosis and skin wounds, originate from biofilm formation on biotic host surfaces [172]. The host interaction with microbial cells plays an essential role in microbial cell adherence and biofilm formation, which *in vitro* testing models lack. For instance, the interaction of the host proteins fibrinogen and fibronectin with the *S. aureus* fibrinogen/fibronectin-binding proteins plays a role in *S. aureus* biofilm formation *in vivo* [173]. Additionally, the host immune response influences biofilm development. For example, reactive oxygen species produced by the immune system trigger microbial stress responses, leading to increased biofilm EPS matrix production [174]. It has also been demonstrated that certain inflammatory cytokines promote *S. aureus* biofilm growth in a concentration-dependent manner [175]. Furthermore, the host immune response may contribute to collateral host tissue damage, as has been observed in *P. aeruginosa* lung infections in cystic fibrosis [176]. Future work should include *in vivo* animal models, such as the foreign-body mouse model, to provide a more physiologically relevant

approach [172]. As an alternative, *ex vivo* models, including explanted tissues and reconstructed human epidermis, are emerging as viable tools for studying host-microbe interactions while avoiding *in vivo* studies ethical concerns [177].

It should also be noted that the tested biofilms were developed from a single microbial species. However, clinical biofilms are mostly polymicrobial, which adds complexity to their structure and responses to treatment [16, 17]. Testing AMPs and liposome activity against co-cultured biofilms would be more representative of clinical conditions. However, this requires careful study design, as the interactions between microbial species can introduce variability, making it challenging to maintain experimental control across testing replicates.

To sum up, future research should focus on evaluating the *in vivo* and *ex vivo* activity of the developed fusogenic liposomes against biofilms, to assess their therapeutic potential in a clinically relevant setting that includes biofilm-host cell interactions. Additionally, further studies are needed to elucidate the precise mechanism by which longer acyl chain phospholipids influence biofilm integrity, and to provide a scientific rationale for their observed antibiofilm activity. Efforts should also continue towards the pharmaceutical development of MP1, with the aim of achieving an optimal balance between the physical stability of DAPC-liposomes and their antibiofilm efficacy. Lastly, an optimized liposomal formulation of TB3 should be developed to enhance its antibiofilm activity and stability as steps towards its formulation and clinical use.



## 6. Concluding remarks

This study highlights the potential of fusogenic liposomes as an effective delivery system for antimicrobial peptides (AMPs) in the treatment of biofilm-associated infections. The findings contribute to the development of AMP-based therapies and enhance the understanding of fusogenic liposomes as a promising drug delivery approach.

### **Paper I:**

Demonstrated the feasibility of developing physically stable, cholesterol-free fusogenic liposomes, capable of penetrating the biofilm matrix and fusing with clinically relevant biofilm-forming microbial cells. It also highlighted the impact of liposomal charge on fusion efficiency and biofilm penetration, with cationic liposomes exhibiting stronger retention within the biofilm matrix.

### **Paper II:**

Described the development of MP1-loaded fusogenic liposomes, which enhanced the antimicrobial and antibiofilm activity of MP1. Additionally, it investigated the influence of phospholipid acyl chain length on biofilm interactions, demonstrating the ability of DAPC-liposomes to effectively disrupt the biofilm matrix.

### **Paper III:**

Evaluated novel teixobactin analogues and identified TB3 as a promising candidate for further pharmaceutical development, emphasizing the role of structure-activity relationship in teixobactin antibiofilm activity.

# References

- 1 . Schulze A, Mitterer F, Pombo JP, Schild S (2021) Biofilms by bacterial human pathogens: Clinical relevance - development, composition and regulation - therapeutical strategies. *Microb Cell* 8(2):28-56.
- 2 . Liu HY, Prentice EL, Webber MA (2024) Mechanisms of antimicrobial resistance in biofilms. *npj Antimicrobials and Resistance* 2(1):27.
- 3 . Sauer K, Stoodley P, Goeres DM, Hall-Stoodley L, Burmølle M, Stewart PS, Bjarnsholt T (2022) The biofilm life cycle: expanding the conceptual model of biofilm formation. *Nat Rev Microbiol* 20(10):608-620.
- 4 . Høiby N (2017) A short history of microbial biofilms and biofilm infections. *APMIS* 125(4):272-275.
- 5 . Shree P, Singh CK, Sodhi KK, Surya JN, Singh DK (2023) Biofilms: Understanding the structure and contribution towards bacterial resistance in antibiotics. *Medicine in Microecology* 16:100084.
- 6 . Henrici AT (1933) Studies of Freshwater Bacteria: I. A Direct Microscopic Technique. *J Bacteriol* 25(3):277-287.
- 7 . Zobell CE, Allen EC (1935) The Significance of Marine Bacteria in the Fouling of Submerged Surfaces. *J Bacteriol* 29(3):239-251.
- 8 . Pinto H, Simões M, Borges A (2021) Prevalence and Impact of Biofilms on Bloodstream and Urinary Tract Infections: A Systematic Review and Meta-Analysis. *Antibiotics* 10(7):825.
- 9 . Bryers JD (2008) Medical biofilms. *Biotechnology and bioengineering* 100(1):1-18.
- 10 . Toole G, Kaplan HB, Kolter R (2000) Biofilm Formation as Microbial Development. *Annual Review of Microbiology* 54(Volume 54, 2000):49-79.
- 11 . Tolker-Nielsen T (2015) Biofilm Development. *Microbial Biofilms*, pp 51-66.
- 12 . Roberts MG, Burgess S, Toombs-Ruane LJ, Benschop J, Marshall JC, French NP (2021) Combining mutation and horizontal gene transfer in a within-host model of antibiotic resistance. *Mathematical Biosciences* 339:108656.
- 13 . Uruén C, Chopo-Escuin G, Tommassen J, Mainar-Jaime RC, Arenas J (2020) Biofilms as Promoters of Bacterial Antibiotic Resistance and Tolerance. *Antibiotics (Basel)* 10(1)
- 14 . Ramage G, Rajendran R, Sherry L, Williams C (2012) Fungal Biofilm Resistance. *International Journal of Microbiology* 2012(1):528521.
- 15 . Sharma S, Mohler J, Mahajan SD, Schwartz SA, Bruggemann L, Aalinkeel R (2023) Microbial Biofilm: A Review on Formation, Infection, Antibiotic Resistance, Control Measures, and Innovative Treatment. *Microorganisms* 11(6):1614.
- 16 . Mountcastle SE, Cox SC, Sammons RL, Jabbari S, Shelton RM, Kuehne SA (2020) A review of co-culture models to study the oral microenvironment and disease. *Journal of Oral Microbiology* 12(1):1773122.
- 17 . Harriott MM (2019) Biofilms and Antibiotics. *Reference Module in Biomedical Sciences*, Elsevier.
- 18 . Floyd KA, Eberly AR, Hadjifrangiskou M (2017) Adhesion of bacteria to surfaces and biofilm formation on medical devices. *Biofilms and Implantable Medical Devices*, Woodhead Publishing, pp 47-95.

- 19 . Ul Haq I, Krukiewicz K (2023) Antimicrobial approaches for medical implants coating to prevent implants associated infections: Insights to develop durable antimicrobial implants. *Applied Surface Science Advances* 18:100532.
- 20 . Medilanski E, Kaufmann K, Wick LY, Wanner O, Harms H (2002) Influence of the Surface Topography of Stainless Steel on Bacterial Adhesion. *Biofouling* 18(3):193-203.
- 21 . Wu S, Altenried S, Zogg A, Zuber F, Maniura-Weber K, Ren Q (2018) Role of the Surface Nanoscale Roughness of Stainless Steel on Bacterial Adhesion and Microcolony Formation. *ACS Omega* 3(6):6456-6464.
- 22 . Zheng S, Bawazir M, Dhall A, Kim H-E, He L, Heo J, Hwang G (2021) Implication of Surface Properties, Bacterial Motility, and Hydrodynamic Conditions on Bacterial Surface Sensing and Their Initial Adhesion. *Frontiers in Bioengineering and Biotechnology* 9
- 23 . Zhang X, Zhou X, Xi H, Sun J, Liang X, Wei J, Xiao X, Liu Z, Li S, Liang Z, Chen Y, Wu Z (2019) Interpretation of adhesion behaviors between bacteria and modified basalt fiber by surface thermodynamics and extended DLVO theory. *Colloids and Surfaces B: Biointerfaces* 177:454-461.
- 24 . Paharik AE, Horswill AR (2016) The Staphylococcal Biofilm: Adhesins, Regulation, and Host Response. *Microbiol Spectr* 4(2)
- 25 . Tian F, Li J, Nazir A, Tong Y (2021) Bacteriophage – A Promising Alternative Measure for Bacterial Biofilm Control. *Infection and Drug Resistance* 14(null):205-217.
- 26 . Monds RD, O'Toole GA (2009) The developmental model of microbial biofilms: ten years of a paradigm up for review. *Trends in Microbiology* 17(2):73-87.
- 27 . Harper DR, Parracho HMRT, Walker J, Sharp R, Hughes G, Werthén M, Lehman S, Morales S (2014) Bacteriophages and Biofilms. *Antibiotics* 3(3):270-284.
- 28 . Balducci E, Papi F, Capiálbi DE, Del Bino L (2023) Polysaccharides' Structures and Functions in Biofilm Architecture of Antimicrobial-Resistant (AMR) Pathogens. *International Journal of Molecular Sciences* 24(4):4030.
- 29 . Gupta P, Sarkar S, Das B, Bhattacharjee S, Tribedi P (2016) Biofilm, pathogenesis and prevention—a journey to break the wall: a review. *Archives of Microbiology* 198(1):1-15.
- 30 . Arciola CR, Campoccia D, Speziale P, Montanaro L, Costerton JW (2012) Biofilm formation in Staphylococcus implant infections. A review of molecular mechanisms and implications for biofilm-resistant materials. *Biomaterials* 33(26):5967-5982.
- 31 . Kindler O, Pulkkinen O, Cherstvy AG, Metzler R (2019) Burst statistics in an early biofilm quorum sensing model: the role of spatial colony-growth heterogeneity. *Scientific Reports* 9(1):12077.
- 32 . He Y-W, Deng Y, Miao Y, Chatterjee S, Tran TM, Tian J, Lindow S (2023) DSF-family quorum sensing signal-mediated intraspecies, interspecies, and inter-kingdom communication. *Trends in Microbiology* 31(1):36-50.
- 33 . Stewart PS, Franklin MJ (2008) Physiological heterogeneity in biofilms. *Nature Reviews Microbiology* 6(3):199-210.
- 34 . Parsek MR, Tolker-Nielsen T (2008) Pattern formation in *Pseudomonas aeruginosa* biofilms. *Current Opinion in Microbiology* 11(6):560-566.
- 35 . Archer NK, Mazaitis MJ, Costerton JW, Leid JG, Powers ME, Shirtliff ME (2011) *Staphylococcus aureus* biofilms. *Virulence* 2(5):445-459.
- 36 . Bjarnsholt T (2013) The role of bacterial biofilms in chronic infections. *APMIS* 121(s136):1-58.

- 37 . Schaer TP, Stewart S, Hsu BB, Klibanov AM (2012) Hydrophobic polycationic coatings that inhibit biofilms and support bone healing during infection. *Biomaterials* 33(5):1245-1254.
- 38 . Wu H, Moser C, Wang H-Z, Høiby N, Song Z-J (2015) Strategies for combating bacterial biofilm infections. *International Journal of Oral Science* 7(1):1-7.
- 39 . Zhao A, Sun J, Liu Y (2023) Understanding bacterial biofilms: From definition to treatment strategies. *Frontiers in Cellular and Infection Microbiology* 13:1137947.
- 40 . Ceri H, Olson ME, Stremick C, Read RR, Morck D, Buret A (1999) The Calgary Biofilm Device: new technology for rapid determination of antibiotic susceptibilities of bacterial biofilms. *J Clin Microbiol* 37(6):1771-1776.
- 41 . Dong Y, Li J, Li P, Yu J (2018) Ultrasound Microbubbles Enhance the Activity of Vancomycin Against *Staphylococcus epidermidis* Biofilms In Vivo. *Journal of Ultrasound in Medicine* 37(6):1379-1387.
- 42 . Mishra M (2024) Antimicrobial Peptides as Future Therapeutics: Challenges and Possibilities. In: Baindara P, Mandal SM (eds) *Evolution of Antimicrobial Peptides: From Self-Defense to Therapeutic Applications*, Springer Nature Switzerland. Cham, pp 1-21.
- 43 . Bin Hafeez A, Jiang X, Bergen PJ, Zhu Y (2021) Antimicrobial Peptides: An Update on Classifications and Databases. *International Journal of Molecular Sciences* 22(21):11691.
- 44 . Lewies A, Du Plessis LH, Wentzel JF (2019) Antimicrobial Peptides: the Achilles' Heel of Antibiotic Resistance? *Probiotics and Antimicrobial Proteins* 11(2):370-381.
- 45 . Wan F, Wong F, Collins JJ, de la Fuente-Nunez C (2024) Machine learning for antimicrobial peptide identification and design. *Nature Reviews Bioengineering* 2(5):392-407.
- 46 . Girdhar M, Sen A, Nigam A, Oswalia J, Kumar S, Gupta R (2024) Antimicrobial peptide-based strategies to overcome antimicrobial resistance. *Archives of Microbiology* 206(10):411.
- 47 . Somase V, Desai SA, Patel VP, Patil V, Bhosale K (2024) Antimicrobial Peptides: Potential Alternative to Antibiotics and Overcoming Limitations for Future Therapeutic Applications. *International Journal of Peptide Research and Therapeutics* 30(4):45.
- 48 . Koehbach J, Craik DJ (2019) The Vast Structural Diversity of Antimicrobial Peptides. *Trends in Pharmacological Sciences* 40(7):517-528.
- 49 . Huan Y, Kong Q, Mou H, Yi H (2020) Antimicrobial Peptides: Classification, Design, Application and Research Progress in Multiple Fields. *Frontiers in Microbiology* 11:582779.
- 50 . Patrúlea V, Borchard G, Jordan O (2020) An Update on Antimicrobial Peptides (AMPs) and Their Delivery Strategies for Wound Infections. *Pharmaceutics* 12(9):840.
- 51 . Hernández-Aristizábal I, Ocampo-Ibáñez ID (2021) Antimicrobial Peptides with Antibacterial Activity against Vancomycin-Resistant *Staphylococcus aureus* Strains: Classification, Structures, and Mechanisms of Action. *International Journal of Molecular Sciences* 22(15):7927.
- 52 . Yang M, Liu S, Zhang C (2023) Antimicrobial peptides with antiviral and anticancer properties and their modification and nanodelivery systems. *Current Research in Biotechnology* 5:100121.
- 53 . Bucataru C, Ciobanasu C (2024) Antimicrobial peptides: Opportunities and challenges in overcoming resistance. *Microbiological Research* 286:127822.
- 54 . Zou F, Tan C, Shinali TS, Zhang B, Zhang L, Han Z, Shang N (2023) Plant antimicrobial peptides: a comprehensive review of their classification, production, mode of action, functions, applications, and challenges. *Food & Function* 14(12):5492-5515.

- 55 . Chikindas ML, Weeks R, Drider D, Chistyakov VA, Dicks LMT (2018) Functions and emerging applications of bacteriocins. *Current Opinion in Biotechnology* 49:23-28.
- 56 . Dini I, De Biasi M-G, Mancusi A (2022) An Overview of the Potentialities of Antimicrobial Peptides Derived from Natural Sources. *Antibiotics* 11(11):1483.
- 57 . Mihaylova-Garnizova R, Davidova S, Hodzhev Y, Satchanska G (2024) Antimicrobial Peptides Derived from Bacteria: Classification, Sources, and Mechanism of Action against Multidrug-Resistant Bacteria. *International Journal of Molecular Sciences* 25(19):10788.
- 58 . Negash AW, Tsehai BA (2020) Current Applications of Bacteriocin. *International Journal of Microbiology* 2020(1):4374891.
- 59 . de Freire Bastos MdC, Miceli de Farias F, Carlin Fagundes P, Varella Coelho ML (2020) Staphylococcins: an update on antimicrobial peptides produced by staphylococci and their diverse potential applications. *Applied Microbiology and Biotechnology* 104(24):10339-10368.
- 60 . Chan DCK, Burrows LL (2021) Thiopeptides: antibiotics with unique chemical structures and diverse biological activities. *The Journal of Antibiotics* 74(3):161-175.
- 61 . Aljohani AB, Al-Hejin AM, Shori AB (2023) Bacteriocins as promising antimicrobial peptides, definition, classification, and their potential applications in cheeses. *Food Science and Technology* 43:e118021.
- 62 . Seyfi R, Kahaki FA, Ebrahimi T, Montazersaheb S, Eyvazi S, Babaeipour V, Tarhriz V (2020) Antimicrobial Peptides (AMPs): Roles, Functions and Mechanism of Action. *International Journal of Peptide Research and Therapeutics* 26(3):1451-1463.
- 63 . Luong HX, Ngan HD, Thi Phuong HB, Quoc TN, Tung TT (2022) Multiple roles of ribosomal antimicrobial peptides in tackling global antimicrobial resistance. *R Soc Open Sci* 9(1):211583.
- 64 . Ling LL, Schneider T, Peoples AJ, Spoering AL, Engels I, Conlon BP, Mueller A, Schäberle TF, Hughes DE, Epstein S, Jones M, Lazarides L, Steadman VA, Cohen DR, Felix CR, Fetterman KA, Millett WP, Nitti AG, Zullo AM, Chen C, Lewis K (2015) A new antibiotic kills pathogens without detectable resistance. *Nature* 517(7535):455-459.
- 65 . Qi Y-K, Tang X, Wei N-N, Pang C-J, Du S-S, Wang K (2022) Discovery, synthesis, and optimization of teixobactin, a novel antibiotic without detectable bacterial resistance. *Journal of Peptide Science* 28(11):e3428.
- 66 . Matheson E, Jin K, Li X (2019) Establishing the structure-activity relationship of teixobactin. *Chinese Chemical Letters* 30(8):1468-1480.
- 67 . Shukla R, Lavore F, Maity S, Derks MGN, Jones CR, Vermeulen BJA, Melcrová A, Morris MA, Becker LM, Wang X, Kumar R, Medeiros-Silva J, van Beekveld RAM, Bonvin A, Lorent JH, Lelli M, Nowick JS, MacGillavry HD, Peoples AJ, Spoering AL, Ling LL, Hughes DE, Roos WH, Breukink E, Lewis K, Weingarth M (2022) Teixobactin kills bacteria by a two-pronged attack on the cell envelope. *Nature* 608(7922):390-396.
- 68 . Morris MA, Vallmitjana A, Grein F, Schneider T, Arts M, Jones CR, Nguyen BT, Hashemian MH, Malek M, Gratton E, Nowick JS (2022) Visualizing the mode of action and supramolecular assembly of teixobactin analogues in *Bacillus subtilis*. *Chemical Science* 13(26):7747-7754.
- 69 . Lewis K, Lee RE, Brötz-Oesterhelt H, Hiller S, Rodnina MV, Schneider T, Weingarth M, Wohlgemuth I (2024) Sophisticated natural products as antibiotics. *Nature* 632(8023):39-49.
- 70 . Lok C (2015) Mining the microbial dark matter. *Nature* 522(7556):270-273.

- 71 . Gunjal VB, Thakare R, Chopra S, Reddy DS (2020) Teixobactin: A Paving Stone toward a New Class of Antibiotics? *Journal of Medicinal Chemistry* 63(21):12171-12195.
- 72 . Jarkhi A, Lee AHC, Sun Z, Hu M, Neelakantan P, Li X, Zhang C (2022) Antimicrobial Effects of L-Chg10-Teixobactin against *Enterococcus faecalis* In Vitro. *Microorganisms* 10(6):1099.
- 73 . Parmar A, Lakshminarayanan R, Iyer A, Goh ETL, To TY, Yam JKH, Yang L, Newire E, Robertson MC, Prior SH, Breukink E, Maddar A, Singh I (2023) Development of teixobactin analogues containing hydrophobic, non-proteogenic amino acids that are highly potent against multidrug-resistant bacteria and biofilms. *European Journal of Medicinal Chemistry* 261:115853.
- 74 . Ciufolini MA, Lefranc D (2010) Micrococcin P1: Structure, biology and synthesis. *Natural Product Reports* 27(3):330-342.
- 75 . Ongpipattanakul C, Desormeaux EK, DiCaprio A, van der Donk WA, Mitchell DA, Nair SK (2022) Mechanism of Action of Ribosomally Synthesized and Post-Translationally Modified Peptides. *Chem Rev* 122(18):14722-14814.
- 76 . Carnio MC, Hölzel A, Rudolf M, Henle T, Jung G, Scherer S (2000) The macrocyclic peptide antibiotic micrococcin P(1) is secreted by the food-borne bacterium *Staphylococcus equorum* WS 2733 and inhibits *Listeria monocytogenes* on soft cheese. *Appl Environ Microbiol* 66(6):2378-2384.
- 77 . Christy MP, Johnson T, McNerlin CD, Woodard J, Nelson AT, Lim B, Hamilton TL, Freiberg KM, Siegel D (2020) Total Synthesis of Micrococcin P1 through Scalable Thiazole Forming Reactions of Cysteine Derivatives and Nitriles. *Organic Letters* 22(6):2365-2370.
- 78 . Wolden R, Ovchinnikov KV, Venter HJ, Oftedal TF, Diep DB, Cavanagh JP (2023) The novel bacteriocin romsacin from *Staphylococcus haemolyticus* inhibits Gram-positive WHO priority pathogens. *Microbiol Spectr* 11(6):e0086923.
- 79 . Kranjec C, Kristensen SS, Bartkiewicz KT, Brønner M, Cavanagh JP, Srikantam A, Mathiesen G, Diep DB (2021) A bacteriocin-based treatment option for *Staphylococcus haemolyticus* biofilms. *Scientific Reports* 11(1):13909.
- 80 . Kranjec C, Ovchinnikov KV, Grønseth T, Ebineshan K, Srikantam A, Diep DB (2020) A bacteriocin-based antimicrobial formulation to effectively disrupt the cell viability of methicillin-resistant *Staphylococcus aureus* (MRSA) biofilms. *npj Biofilms and Microbiomes* 6(1):58.
- 81 . Liu Y, Liu Y, Du Z, Zhang L, Chen J, Shen Z, Liu Q, Qin J, Lv H, Wang H, He L, Liu J, Huang Q, Sun Y, Otto M, Li M (2020) Skin microbiota analysis-inspired development of novel anti-infectives. *Microbiome* 8(1):85.
- 82 . Degiacomi G, Personne Y, Mondésert G, Ge X, Mandava CS, Hartkoorn RC, Boldrin F, Goel P, Peisker K, Benjak A, Barrio MB, Ventura M, Brown AC, Leblanc V, Bauer A, Sanyal S, Cole ST, Lagrange S, Parish T, Manganelli R (2016) Micrococcin P1 – A bactericidal thiopeptide active against *Mycobacterium tuberculosis*. *Tuberculosis* 100:95-101.
- 83 . Lefranc D, Ciufolini MA (2009) Total Synthesis and Stereochemical Assignment of Micrococcin P1. *Angewandte Chemie International Edition* 48(23):4198-4201.
- 84 . Akasapu S, Hinds AB, Powell WC, Walczak MA (2019) Total synthesis of micrococcin P1 and thiocillin I enabled by Mo(vi) catalyst. *Chemical Science* 10(7):1971-1975.
- 85 . Li C, Kelly WL (2010) Recent advances in thiopeptide antibiotic biosynthesis. *Nat Prod Rep* 27(2):153-164.

- 86 . Ovchinnikov KV, Kranjec C, Telke A, Kjos M, Thorstensen T, Scherer S, Carlsen H, Diep DB (2021) A Strong Synergy Between the Thiopeptide Bacteriocin Micrococcin P1 and Rifampicin Against MRSA in a Murine Skin Infection Model. *Frontiers in Immunology* 12:676534.
- 87 . Cresti L, Cappello G, Pini A (2024) Antimicrobial Peptides towards Clinical Application—A Long History to Be Concluded. *International Journal of Molecular Sciences* 25(9):4870.
- 88 . Heinzinger LR, Pugh AR, Wagner JA, Otto M (2023) Evaluating the Translational Potential of Bacteriocins as an Alternative Treatment for *Staphylococcus aureus* Infections in Animals and Humans. *Antibiotics* 12(8):1256.
- 89 . Soltani S, Hammami R, Cotter PD, Rebuffat S, Said LB, Gaudreau H, Bédard F, Biron E, Drider D, Fliss I (2020) Bacteriocins as a new generation of antimicrobials: toxicity aspects and regulations. *FEMS Microbiology Reviews* 45(1):fuaa039.
- 90 . Vladkova TG, Smani Y, Martinov BL, Gospodinova DN (2024) Recent Progress in Terrestrial Biota Derived Antibacterial Agents for Medical Applications. *Molecules* 29(20):4889.
- 91 . Bellavita R, Braccia S, Galdiero S, Falanga A (2023) Glycosylation and Lipidation Strategies: Approaches for Improving Antimicrobial Peptide Efficacy. *Pharmaceuticals* 16(3):439.
- 92 . Wang L, Wang N, Zhang W, Cheng X, Yan Z, Shao G, Wang X, Wang R, Fu C (2022) Therapeutic peptides: current applications and future directions. *Signal Transduction and Targeted Therapy* 7(1):48.
- 93 . Muenraya P, Sawatdee S, Srichana T, Atipairin A (2022) Silver Nanoparticles Conjugated with Colistin Enhanced the Antimicrobial Activity against Gram-Negative Bacteria. *Molecules* 27(18):5780.
- 94 . Miller SE, Bell CS, McClain MS, Cover TL, Giorgio TD (2016) Colistin-functionalized nanoparticles for the rapid capture of *Acinetobacter baumannii*. *Journal of Biomedical Nanotechnology* 12(9):1806-1819.
- 95 . Radaic A, Malone E, Kamarajan P, Kapila YL (2022) Solid Lipid Nanoparticles Loaded with Nisin (SLN-Nisin) are More Effective Than Free Nisin as Antimicrobial, Antibiofilm, and Anticancer Agents. *J Biomed Nanotechnol* 18(4):1227-1235.
- 96 . Braun K, Pochert A, Lindén M, Davoudi M, Schmidtchen A, Nordström R, Malmsten M (2016) Membrane interactions of mesoporous silica nanoparticles as carriers of antimicrobial peptides. *Journal of Colloid and Interface Science* 475:161-170.
- 97 . Sharma VK, Agrawal MK (2021) A historical perspective of liposomes-a bio nanomaterial. *Materials Today: Proceedings* 45:2963-2966.
- 98 . Puri S, Mazza M, Roy G, England RM, Zhou L, Nourian S, Anand Subramony J (2023) Evolution of nanomedicine formulations for targeted delivery and controlled release. *Advanced Drug Delivery Reviews* 200:114962.
- 99 . Giordani S, Marassi V, Zattoni A, Roda B, Reschiglian P (2023) Liposomes characterization for market approval as pharmaceutical products: Analytical methods, guidelines and standardized protocols. *Journal of Pharmaceutical and Biomedical Analysis* 236:115751.
- 100 . Barenholz Y (2012) Doxil® — The first FDA-approved nano-drug: Lessons learned. *Journal of Controlled Release* 160(2):117-134.
- 101 . Liu P, Chen G, Zhang J (2022) A Review of Liposomes as a Drug Delivery System: Current Status of Approved Products, Regulatory Environments, and Future Perspectives. *Molecules* 27(4):1372.

- 102 . Abbasi H, Kouchak M, Mirveis Z, Hajipour F, Khodarahmi M, Rahbar N, Handali S (2023) What We Need to Know about Liposomes as Drug Nanocarriers: An Updated Review. *Adv Pharm Bull* 13(1):7-23.
- 103 . Eugster R, Luciani P (2025) Liposomes: Bridging the gap from lab to pharmaceuticals. *Current Opinion in Colloid & Interface Science* 75:101875.
- 104 . Lombardo D, Kiselev MA, Caccamo MT (2019) Smart Nanoparticles for Drug Delivery Application: Development of Versatile Nanocarrier Platforms in Biotechnology and Nanomedicine. *Journal of Nanomaterials* 2019(1):3702518.
- 105 . Gbian DL, Omri A (2022) Lipid-Based Drug Delivery Systems for Diseases Managements. *Biomedicines* 10(9):2137.
- 106 . Sforzi J, Palagi L, Aime S (2020) Liposome-Based Bioassays. *Biology* 9(8):202.
- 107 . Barba AA, Bochicchio S, Dalmoro A, Lamberti G (2019) Lipid Delivery Systems for Nucleic-Acid-Based-Drugs: From Production to Clinical Applications. *Pharmaceutics* 11(8)
- 108 . Fu Y, Saraswat A, Vartak R, Patki M, Patel K (2022) Chapter 4 - Liposomal formulation: opportunities, challenges, and industrial applicability. In: Mehra NK, Srivastava S, Madan J, Singh Pk (eds) *Multifunctional Nanocarriers*, Elsevier. pp 79-102.
- 109 . Dymek M, Sikora E (2022) Liposomes as biocompatible and smart delivery systems – the current state. *Advances in Colloid and Interface Science* 309:102757.
- 110 . Pande S (2023) Liposomes for drug delivery: review of vesicular composition, factors affecting drug release and drug loading in liposomes. *Artificial Cells, Nanomedicine, and Biotechnology* 51(1):428-440.
- 111 . Sainaga Jyothi VGS, Bulusu R, Venkata Krishna Rao B, Pranothi M, Banda S, Kumar Bolla P, Kommineni N (2022) Stability characterization for pharmaceutical liposome product development with focus on regulatory considerations: An update. *International Journal of Pharmaceutics* 624:122022.
- 112 . Wang D-Y, van der Mei HC, Ren Y, Busscher HJ, Shi L (2020) Lipid-Based Antimicrobial Delivery-Systems for the Treatment of Bacterial Infections. *Frontiers in Chemistry* 7:872.
- 113 . Panthi VK, Fairfull-Smith KE, Islam N (2024) Liposomal drug delivery strategies to eradicate bacterial biofilms: Challenges, recent advances, and future perspectives. *International Journal of Pharmaceutics* 655:124046.
- 114 . Rukavina Z, Vanić Ž (2016) Current Trends in Development of Liposomes for Targeting Bacterial Biofilms. *Pharmaceutics* 8(2):18.
- 115 . Liu Y, Shi L, Su L, van der Mei HC, Jutte PC, Ren Y, Busscher HJ (2019) Nanotechnology-based antimicrobials and delivery systems for biofilm-infection control. *Chemical Society Reviews* 48(2):428-446.
- 116 . Fayed B (2024) Nanoparticles in the battle against *Candida auris* biofilms: current advances and future prospects. *Drug Delivery and Translational Research* 15(5):1496–1512.
- 117 . Malaekheh-Nikouei B, Fazly Bazzaz BS, Mirhadi E, Tajani AS, Khameneh B (2020) The role of nanotechnology in combating biofilm-based antibiotic resistance. *Journal of Drug Delivery Science and Technology* 60:101880.
- 118 . Fulaz S, Vitale S, Quinn L, Casey E (2019) Nanoparticle-Biofilm Interactions: The Role of the EPS Matrix. *Trends in Microbiology* 27(11):915-926.



- 119 . Ibaraki H, Kanazawa T, Chien W-Y, Nakaminami H, Aoki M, Ozawa K, Kaneko H, Takashima Y, Noguchi N, Seta Y (2020) The effects of surface properties of liposomes on their activity against *Pseudomonas aeruginosa* PAO-1 biofilm. *Journal of Drug Delivery Science and Technology* 57:101754.
- 120 . Fang J-Y, Chou W-L, Lin C-F, Sung CT, Alalaiwe A, Yang S-C (2021) Facile biofilm penetration of cationic liposomes loaded with DNase I/Proteinase K to eradicate *Cutibacterium acnes* for treating cutaneous and catheter infections. *International Journal of Nanomedicine*:8121-8138.
- 121 . Hou Y, Wang Z, Zhang P, Bai H, Sun Y, Duan J, Mu H (2017) Lysozyme Associated Liposomal Gentamicin Inhibits Bacterial Biofilm. *International Journal of Molecular Sciences* 18(4):784.
- 122 . Alzahrani NM, Booq RY, Aldossary AM, Bakr AA, Almughem FA, Alfahad AJ, Alsharif WK, Jarallah SJ, Alharbi WS, Alsudir SA, Alyamani EJ, Tawfik EA, Alshehri AA (2022) Liposome-Encapsulated Tobramycin and IDR-1018 Peptide Mediated Biofilm Disruption and Enhanced Antimicrobial Activity against *Pseudomonas aeruginosa*. *Pharmaceutics* 14(5):960.
- 123 . Bandara HMHN, Hewavitharana AK, Shaw PN, Smyth HDC, Samaranyake LP (2020) A novel, quorum sensor-infused liposomal drug delivery system suppresses *Candida albicans* biofilms. *International Journal of Pharmaceutics* 578:119096.
- 124 . Zahra M-J, Hamed H, Mohammad R-Y, Nosratollah Z, Akbarzadeh A, Morteza M (2017) Evaluation and study of antimicrobial activity of nanoliposomal meropenem against *Pseudomonas aeruginosa* isolates. *Artificial Cells, Nanomedicine, and Biotechnology* 45(5):975-980.
- 125 . Vyas SP, Sihorkar V, Dubey PK (2001) Preparation, characterization and in vitro antimicrobial activity of metronidazole bearing lectinized liposomes for intra-periodontal pocket delivery. *Pharmazie* 56(7):554-560.
- 126 . Ferreira M, Pinto SN, Aires-da-Silva F, Bettencourt A, Aguiar SI, Gaspar MM (2021) Liposomes as a Nanoplatfrom to Improve the Delivery of Antibiotics into *Staphylococcus aureus* Biofilms. *Pharmaceutics* 13(3):321.
- 127 . Kolašinac R, Kleusch C, Braun T, Merkel R, Csiszár A (2018) Deciphering the Functional Composition of Fusogenic Liposomes. *Int J Mol Sci* 19(2):346.
- 128 . Gandek TB, van der Koog L, Nagelkerke A (2023) A Comparison of Cellular Uptake Mechanisms, Delivery Efficacy, and Intracellular Fate between Liposomes and Extracellular Vesicles. *Advanced Healthcare Materials* 12(25):2300319.
- 129 . Pavlov RV, Akimov SA, Dashinimaev EB, Bashkirov PV (2024) Boosting Lipofection Efficiency Through Enhanced Membrane Fusion Mechanisms. *International Journal of Molecular Sciences* 25(24):13540.
- 130 . Kube S, Hersch N, Naumovska E, Gensch T, Hendriks J, Franzen A, Landvogt L, Siebrasse J-P, Kubitscheck U, Hoffmann B, Merkel R, Csiszár A (2017) Fusogenic Liposomes as Nanocarriers for the Delivery of Intracellular Proteins. *Langmuir* 33(4):1051-1059.
- 131 . Ma Y, Wang Z, Zhao W, Lu T, Wang R, Mei Q, Chen T (2013) Enhanced bactericidal potency of nanoliposomes by modification of the fusion activity between liposomes and bacterium. *International Journal of Nanomedicine* 8(null):2351-2360.
- 132 . Sachetelli S, Khalil H, Chen T, Beaulac C, Sénéchal S, Lagacé J (2000) Demonstration of a fusion mechanism between a fluid bactericidal liposomal formulation and bacterial cells. *Biochimica et Biophysica Acta (BBA) - Biomembranes* 1463(2):254-266.

- 133 . Wang Z, Ma Y, Khalil H, Wang R, Lu T, Zhao W, Zhang Y, Chen J, Chen T (2016) Fusion between fluid liposomes and intact bacteria: study of driving parameters and in vitro bactericidal efficacy. *Int J Nanomedicine* 11:4025-4036.
- 134 . Scheeder A, Brockhoff M, Ward EN, Kaminski Schierle GS, Mela I, Kaminski CF (2023) Molecular Mechanisms of Cationic Fusogenic Liposome Interactions with Bacterial Envelopes. *Journal of the American Chemical Society* 145(51):28240-28250.
- 135 . Mugabe C, Halwani M, Azghani AO, Lafrenie RM, Omri A (2006) Mechanism of enhanced activity of liposome-entrapped aminoglycosides against resistant strains of *Pseudomonas aeruginosa*. *Antimicrob Agents Chemother* 50(6):2016-2022.
- 136 . Nicolosi D, Cupri S, Genovese C, Tempera G, Mattina R, Pignatello R (2015) Nanotechnology approaches for antibacterial drug delivery: Preparation and microbiological evaluation of fusogenic liposomes carrying fusidic acid. *International Journal of Antimicrobial Agents* 45(6):622-626.
- 137 . Nicolosi D, Scalia M, Nicolosi VM, Pignatello R (2010) Encapsulation in fusogenic liposomes broadens the spectrum of action of vancomycin against Gram-negative bacteria. *International Journal of Antimicrobial Agents* 35(6):553-558.
- 138 . Naqvi M, Fineide F, Utheim TP, Charnock C (2024) Culture- and non-culture-based approaches reveal unique features of the ocular microbiome in dry eye patients. *The Ocular Surface* 32:123-129.
- 139 . Danaei M, Dehghankhold M, Ataei S, Hasanzadeh Davarani F, Javanmard R, Dokhani A, Khorasani S, Mozafari MR (2018) Impact of Particle Size and Polydispersity Index on the Clinical Applications of Lipidic Nanocarrier Systems. *Pharmaceutics* 10(2):57.
- 140 . Edwards KA, Baeumner AJ (2006) Analysis of liposomes. *Talanta* 68(5):1432-1441.
- 141 . Gordillo-Galeano A, Mora-Huertas CE (2021) Hydrodynamic diameter and zeta potential of nanostructured lipid carriers: Emphasizing some parameters for correct measurements. *Colloids and Surfaces A: Physicochemical and Engineering Aspects* 620:126610.
- 142 . Robson A-L, Dastoor PC, Flynn J, Palmer W, Martin A, Smith DW, Woldu A, Hua S (2018) Advantages and Limitations of Current Imaging Techniques for Characterizing Liposome Morphology. *Frontiers in Pharmacology* 9:80.
- 143 . Webster P, Webster A (2014) Cryosectioning fixed and cryoprotected biological material for immunocytochemistry. *Electron Microscopy: Methods and Protocols*:273-313.
- 144 . Li T, Nowell CJ, Cipolla D, Rades T, Boyd BJ (2019) Direct Comparison of Standard Transmission Electron Microscopy and Cryogenic-TEM in Imaging Nanocrystals Inside Liposomes. *Molecular Pharmaceutics* 16(4):1775-1781.
- 145 . Gholizadeh S, Shehata Draz M, Zarghooni M, Sanati-Nezhad A, Ghavami S, Shafiee H, Akbari M (2017) Microfluidic approaches for isolation, detection, and characterization of extracellular vesicles: Current status and future directions. *Biosensors and Bioelectronics* 91:588-605.
- 146 . Németh Z, Csóka I, Semnani Jazani R, Sipos B, Haspel H, Kozma G, Kónya Z, Dobó DG (2022) Quality by Design-Driven Zeta Potential Optimisation Study of Liposomes with Charge Imparting Membrane Additives. *Pharmaceutics* 14(9)
- 147 . Jose J, Kanniyappan H, Muthuvijayan V (2022) A novel, rapid and cost-effective method for separating drug-loaded liposomes prepared from egg yolk phospholipids. *Process Biochemistry* 115:80-91.

- 148 . de la Harpe KM, Kondiah PPD, Choonara YE, Marimuthu T, du Toit LC, Pillay V (2019) The Hemocompatibility of Nanoparticles: A Review of Cell–Nanoparticle Interactions and Hemostasis. *Cells* 8(10):1209.
- 149 . François-Martin C, Pincet F (2017) Actual fusion efficiency in the lipid mixing assay - Comparison between nanodiscs and liposomes. *Scientific Reports* 7(1):43860.
- 150 . Andrews JM (2001) Determination of minimum inhibitory concentrations. *J Antimicrob Chemother* 48 Suppl 1:5-16.
- 151 . Kowalska-Krochmal B, Dudek-Wicher R (2021) The Minimum Inhibitory Concentration of Antibiotics: Methods, Interpretation, Clinical Relevance. *Pathogens* 10(2):165.
- 152 . (2020, 30th Edition) Clinical and Laboratory Standards Institute (CLSI). M100: Performance Standards for Antimicrobial Susceptibility Testing.
- 153 . (1999, 1st Edition) Clinical and Laboratory Standards Institute (CLSI). M26-A: Methods for Determining Bactericidal Activity of Antimicrobial Agents.
- 154 . Mogana R, Adhikari A, Tzar MN, Ramliza R, Wiart C (2020) Antibacterial activities of the extracts, fractions and isolated compounds from *Canarium patentinervium* Miq. against bacterial clinical isolates. *BMC Complementary Medicine and Therapies* 20(1):55.
- 155 . Theophel K, Schacht VJ, Schlüter M, Schnell S, Stingu C-S, Schaumann R, Bunge M (2014) The importance of growth kinetic analysis in determining bacterial susceptibility against antibiotics and silver nanoparticles. *Frontiers in Microbiology* 5:544.
- 156 . Etayash H, Qian Y, Pletzer D, Zhang Q, Xie J, Cui R, Dai C, Ma P, Qi F, Liu R, Hancock REW (2020) Host Defense Peptide-Mimicking Amphiphilic  $\beta$ -Peptide Polymer (Bu:DM) Exhibiting Anti-Biofilm, Immunomodulatory, and in Vivo Anti-Infective Activity. *Journal of Medicinal Chemistry* 63(21):12921-12928.
- 157 . Latka A, Drulis-Kawa Z (2020) Advantages and limitations of microtiter biofilm assays in the model of antibiofilm activity of *Klebsiella* phage KP34 and its depolymerase. *Scientific Reports* 10(1):20338.
- 158 . Joardar A, Pattnaik GP, Chakraborty H (2022) Mechanism of Membrane Fusion: Interplay of Lipid and Peptide. *The Journal of Membrane Biology* 255(2):211-224.
- 159 . Chernomordik LV, Kozlov MM (2008) Mechanics of membrane fusion. *Nature Structural & Molecular Biology* 15(7):675-683.
- 160 . Silhavy TJ, Kahne D, Walker S (2010) The bacterial cell envelope. *Cold Spring Harb Perspect Biol* 2(5):a000414.
- 161 . Xia Y, Sun J, Liang D (2014) Aggregation, Fusion, and Leakage of Liposomes Induced by Peptides. *Langmuir* 30(25):7334-7342.
- 162 . Liu Y, Liu Q, Zhao L, Dickey SW, Wang H, Xu R, Chen T, Jian Y, Wang X, Lv H, Otto M, Li M (2022) Essential role of membrane vesicles for biological activity of the bacteriocin micrococcin P1. *J Extracell Vesicles* 11(4):e12212.
- 163 . Percival SL, Mayer D, Kirsner RS, Schultz G, Weir D, Roy S, Alavi A, Romanelli M (2019) Surfactants: Role in biofilm management and cellular behaviour. *Int Wound J* 16(3):753-760.
- 164 . Simões M, Pereira MO, Vieira MJ (2005) Action of a cationic surfactant on the activity and removal of bacterial biofilms formed under different flow regimes. *Water Research* 39(2):478-486.

- 165 . Chen X, Stewart PS (2000) Biofilm removal caused by chemical treatments. *Water Research* 34(17):4229-4233.
- 166 . Demling A, Elter C, Heidenblut T, Bach F-W, Hahn A, Schwestka-Polly R, Stiesch M, Heuer W (2010) Reduction of biofilm on orthodontic brackets with the use of a polytetrafluoroethylene coating. *European Journal of Orthodontics* 32(4):414-418.
- 167 . Berry JA, Biedlingmaier JF, Whelan PJ (2000) In Vitro Resistance to Bacterial Biofilm Formation on Coated Fluoroplastic Tympanostomy Tubes. *Otolaryngology–Head and Neck Surgery* 123(3):246-251.
- 168 . Darnell RL, Knottenbelt MK, Todd Rose FO, Monk IR, Stinear TP, Cook GM (2019) Genomewide Profiling of the *Enterococcus faecalis* Transcriptional Response to Teixobactin Reveals CroRS as an Essential Regulator of Antimicrobial Tolerance. *mSphere* 4(3):e00228-00219.
- 169 . Bertrand RL (2019) Lag Phase Is a Dynamic, Organized, Adaptive, and Evolvable Period That Prepares Bacteria for Cell Division. *J Bacteriol* 201(7):e00697-00618.
- 170 . Jin K, Po KHL, Kong WY, Lo CH, Lo CW, Lam HY, Sirinimal A, Reuven JA, Chen S, Li X (2018) Synthesis and antibacterial studies of teixobactin analogues with non-isostere substitution of enduracididine. *Bioorganic & Medicinal Chemistry* 26(5):1062-1068.
- 171 . Park J, Kim LH, Lee JM, Choi S, Son YJ, Hwang HJ, Shin SJ (2023) In vitro and intracellular activities of novel thiopeptide derivatives against macrolide-susceptible and macrolide-resistant *Mycobacterium avium* complex. *Microbiol Spectr* 11(5):e0182523.
- 172 . Alves-Barroco C, Botelho AMN, Américo MA, Fracalanza SEL, de Matos APA, Guimaraes MA, Ferreira-Carvalho BT, Figueiredo AMS, Fernandes AR (2022) Assessing in vivo and in vitro biofilm development by *Streptococcus dysgalactiae* subsp. *dysgalactiae* using a murine model of catheter-associated biofilm and human keratinocyte cell. *Frontiers in Cellular and Infection Microbiology* 12:874694.
- 173 . Speziale P, Pietrocola G, Foster TJ, Geoghegan JA (2014) Protein-based biofilm matrices in *Staphylococci*. *Frontiers in Cellular and Infection Microbiology* 4:171.
- 174 . da Cruz Nizer WS, Adams ME, Allison KN, Montgomery MC, Mosher H, Cassol E, Overhage J (2024) Oxidative stress responses in biofilms. *Biofilm* 7:100203.
- 175 . Di Domenico EG, Cavallo I, Bordinon V, Prignano G, Sperduti I, Gurtner A, Trento E, Toma L, Pimpinelli F, Capitanio B, Ensoli F (2018) Inflammatory cytokines and biofilm production sustain *Staphylococcus aureus* outgrowth and persistence: a pivotal interplay in the pathogenesis of Atopic Dermatitis. *Sci Rep* 8(1):9573.
- 176 . Moser C, Pedersen HT, Lerche CJ, Kolpen M, Line L, Thomsen K, Høiby N, Jensen PØ (2017) Biofilms and host response – helpful or harmful. *APMIS* 125(4):320-338.
- 177 . Cleaver L, Garnett JA (2023) How to study biofilms: technological advancements in clinical biofilm research. *Frontiers in Cellular and Infection Microbiology* 13:1335389.

## **Publications**



# Paper I

Ahmed M. Amer, Colin Charnock, Sanko Nguyen

**The Impact of Surface Charge on the Interaction of Cholesterol-Free Fusogenic Liposomes with Planktonic Microbial Cells and Biofilms**

*International Journal of Pharmaceutics*, 669, article 125088 (2025).

DOI: <https://doi.org/10.1016/j.ijpharm.2024.125088>







# The impact of surface charge on the interaction of cholesterol-free fusogenic liposomes with planktonic microbial cells and biofilms

Ahmed M. Amer<sup>\*</sup>, Colin Charnock, Sanko Nguyen<sup>ID</sup>

Department of Life Sciences and Health, Oslo Metropolitan University (OsloMet), Oslo, Norway

## ARTICLE INFO

### Keywords:

Fusogenic liposomes  
Liposomal charge  
Biocompatibility  
Bacteria  
Fungi  
Biofilm

## ABSTRACT

This study focused on the development of cholesterol-free fusogenic liposomes with different surface charge with the aim of improving biofilm penetration. *In vitro* assessments of the liposomes included physical stability, biocompatibility, fusion with microbial cells, and the ability to penetrate established biofilms. Using dynamic light scattering, cholesterol-free, fusogenic liposomes were found to be < 200 nm in size with small size distribution (PDI < 0.1) and physically stable for a year when stored at 4 °C. Transmission electron microscopy (TEM) images confirmed vesicular sizes for selected liposomal formulations. Liposomal ability to fuse with microbial cells was assessed using lipid mixing and flow cytometer assays. Fusion levels were found to be higher with *Escherichia coli* compared to *Staphylococcus aureus* and *Candida albicans* regardless of the liposomal charge. Neutral liposomes exhibited highest fusion, followed by cationic and anionic liposomes, respectively. Our investigations demonstrated that fusion is a multifactorial process influenced by the chemical composition of the liposomes, the liposomal surface charge, and components of the microbial cell envelope. Penetration and retention within preformed *S. aureus* biofilms were assessed for liposomes with various surface charges. All liposomes, regardless of surface charge, were capable of penetrating and diffusing through the biofilm matrix. However, cationic liposomes displayed greatest interaction and retention. Biocompatibility was confirmed through haemolysis and cytotoxicity studies. The cholesterol-free fusogenic liposomes developed in this study demonstrated promising potential as drug delivery systems for incorporating antimicrobial agents for biofilm treatment.

## 1. Introduction

Biofilms are surface-attached microbial communities. They consist of sessile cells embedded in a self-produced extracellular polymeric substances (EPS) (Bjarnsholt 2013). Approximately 80 % of microbial infections are associated with biofilm formation, often linked to medical devices or persistent clinical conditions such as wound infections and cystic fibrosis (da Silva et al. 2021). Biofilm formation increases microbial tolerance to antimicrobial treatment due to limited drug diffusion through the biofilm matrix, antimicrobial agent degradation and altered metabolic activities of sessile cells (Sharma et al. 2023). Microbial cells embedded in the biofilm matrix are often 100 to 1000 times more tolerant for antibiotic treatment compared with planktonic cells (Panthi et al. 2024). *Pseudomonas aeruginosa*, *Escherichia coli*, *Staphylococcus aureus* and *Enterococcus faecalis* are among the most commonly reported bacterial species in biofilms (Sharma et al. 2023) whereas *Candida* spp. are the fungi most often isolated from biofilm infections

(Costa et al. 2022). In clinical settings, biofilms are a polymicrobial co-cultured environment with different microbial species, adding more complexity to the biofilm structure and composition (Mountcastle et al. 2020).

In recent years, various types of nanoparticulate drug delivery systems have been developed for combating microbial biofilms. They include lipid-based, polymeric, and metal nanoparticles. Encapsulation of antimicrobials in nanosized drug delivery systems have demonstrated notably improved antibiofilm activity (Malaek-Nikouei et al. 2020) providing drug protection against chemical degradation in the biofilm matrix, better biofilm penetration and targeted drug release (Al-Wrafy et al. 2022). Liposomes have demonstrated the most promising outcomes, and this can be attributed to some distinct advantages (Rukavina and Vanić 2016, Malaek-Nikouei et al. 2020, Ferreira et al. 2021, Makhoul et al. 2023): Liposomes are versatile and can encapsulate both hydrophilic and hydrophobic drugs within their structure, while their surface can be easily modified to target specific sites. Additionally, they

<sup>\*</sup> Corresponding author at: Pilestredet 50, Oslo 0167, Norway.

E-mail address: [ahmedame@oslomet.no](mailto:ahmedame@oslomet.no) (A.M. Amer).

generally exhibit both biocompatible and biodegradable properties when composed of biosimilar lipids (Rukavina and Vanić 2016). Liposome-encapsulated antibiotics have demonstrated effectiveness in overcoming microbial resistance mechanisms such as enzymatic degradation, efflux mechanisms, and impermeability of the cell envelope (Ghosh and De 2023). Moreover, the phospholipid bilayer structure of liposomes, which mimics biological membranes, can promote fusion with microbial cells (Ferreira et al. 2021). This distinctive capability can be improved by incorporating fluid-state phospholipids, such as dioleoylphosphatidylethanolamine (DOPE), into the liposomal formulation. This addition increases the flexibility of the liposomes, making them more prone to membrane fusion and creating what are known as fusogenic liposomes (Kolašinac et al. 2018).

Studies on the activity of fusogenic liposomes against microbes often involve the inclusion of liposomal formulations incorporating cholesterol (Furneri et al. 2000, Nicolosi et al. 2015, Patil et al. 2019, Scriboni et al., 2019, Ibaraki et al. 2020). The presence of cholesterol in the liposomal formulation has been shown to affect the membrane rigidity, thickness, fluidity and stability (Kaddah et al. 2018). Multiple studies have shown that liposomal membrane rigidity increases proportionally with cholesterol content, limiting molecular mobility within the lipid bilayer due to its steroid ring structure (Arriaga et al. 2009, Najafinobar et al. 2016, Kaddah et al. 2018). Increased membrane rigidity in fusogenic liposomes can prevent premature leakage of entrapped drugs, promoting *in vitro* stability of the delivery systems. However, reduced membrane flexibility may negatively influence fusogenicity, making finding a balance challenging. Based on testing with *P. aeruginosa*, it has been reported that incorporating cholesterol into fusogenic liposomes inhibits fusion with bacterial cells (Ma et al. 2013). In another study, liposomal fusion with *P. aeruginosa* was significantly decreased after adding only 10 % cholesterol to the liposome composition (Wang et al. 2016). Moreover, the physicochemical properties of the liposomes critically affect the antibiofilm activity. The influence of liposomal size and surface charge on delivery to biofilms has been reported in several studies (Rukavina and Vanić 2016, Al-Wrafy et al. 2022). According to Dong et al. (Dong et al. 2015), cationic liposomes with particle size < 200 nm showed better biofilm penetration than anionic liposomes and larger multilamellar liposomes (> 1000 nm). In another study of *P. aeruginosa* biofilms, cationic liposomes demonstrated the highest retention in the biofilm, while anionic liposomes showed better permeation through the biofilm matrix (Ibaraki et al. 2020).

In the present study, fusogenic liposomes with different surface charge (cationic, anionic, and neutral) and devoid of cholesterol were prepared, characterized, and their physicochemical properties were evaluated. A long-term (one year) *in vitro* stability study was also conducted. Hemocompatibility and skin fibroblast cytotoxicity tests were performed to assess the potential applications of these liposomes for parenteral and topical administration, respectively. The fusogenic behaviour of the liposomes against planktonic microbial cells was evaluated by two different methods. These were: lipid mixing assay and flow cytometry. Finally, the ability of the liposomes to permeate and remain within the biofilm matrix was assessed in order to determine their potential both physically and temporally as delivery systems against biofilms. The study was conducted on three different, clinically important types of microbial cells: *E. coli* representing gram negative bacteria, *S. aureus* representing gram positive bacteria, and *C. albicans* representing fungi (yeast-like). To the best of our knowledge, this is the first research work to investigate the interaction of fusogenic liposomes with fungal cells and with established biofilm. Moreover, we report the development of cholesterol-free fusogenic liposomes which remained physically stable throughout a year of monitoring.

## 2. Materials and methods

### 2.1. Materials

The lipids dipalmitoylphosphocholine (DPPC), dioleoyl-trimethylammoniumpropane (DOTAP), 1,2-dioleoyl-*sn*-glycero-3-phosphoethanolamine-N-(7-nitro-2-1,3-benzoxadiazol-4-yl) (18:1 NBD-PE) and 1,2-dioleoyl-*sn*-glycero-3-phosphoethanolamine-N-(lissamine rhodamine B sulfonyl) (18:1 Liss Rhod-PE) were purchased from Avanti Polar Lipids (Alabaster, AL, USA). Dioleoylphosphoethanolamine (DOPE) and dioleoylphospho-*rac*-glycerol (DOPG) were kindly provided by Lipoid GmbH (Ludwigshafen, Germany). PKH67 green fluorescent cell membrane labelling kit, 4',6-diamidino-2-phenylindole (DAPI), Triton X-100, Polysorbate 80, sodium dihydrogen phosphate monohydrate, disodium hydrogen phosphate dihydrate and phosphate buffered saline (PBS) tablets were purchased from Sigma-Aldrich (St. Louis, MO, USA). Tryptic soy agar (TSA), tryptic soy broth (TSB) and AlamarBlue™ Cell Viability Reagent were purchased from ThermoFisher Scientific (Sunnyvale, CA, USA). High purity chloroform and methanol were purchased from VWR BDH Chemical (Norway). Water involved in liposomal preparation and rinsing processes was purified by the Milli-Q® water purification system (Merck Millipore, Germany). *Escherichia coli* (ATCC 25922) was purchased from American Type Culture Collection (Rockville, MD, USA). *Staphylococcus aureus* (DSM 2569) and *Candida albicans* (DSM 1386) were purchased from Leibniz Institute DSMZ-German Collection of Microorganisms and Cell Cultures GmbH (Braunschweig, Germany).

### 2.2. Preparation of fusogenic liposomes

Fusogenic liposomes were prepared by a thin film hydration–extrusion method according to the specified lipid composition in Table 1. The phospholipid DOPE was included in all liposomal formulations to provide fusogenic properties, while DPPC was incorporated to enhance membrane rigidity and stabilize the liposomes. DOTAP and DOPG were utilized to provide cationic and anionic surface charges, respectively, to the liposomes. The preparation procedures were carried out as described in the literature (Lombardo and Kiselev 2022), phospholipids were dissolved in a chloroform:methanol mixture (2:1) and the solutions were evaporated to dryness in a rotary evaporator. The thin films were further dried under vacuum overnight to ensure complete removal of organic residues. The following day, films were hydrated with intermittent shaking for 2 h at 65 °C using 5 mM phosphate buffer (pH 7.4). The hydration buffer was prepared by dissolving the required amounts of sodium dihydrogen phosphate and disodium hydrogen phosphate in Milli-Q water to achieve 5 mM buffer, pH 7.4. The buffer was then filtered through a 0.2 µm syringe filter before use. After allowing the preparations to equilibrate overnight at 4 °C, size reduction was then performed at 65 °C using 200 nm polycarbonate membranes (Avanti Polar Lipids, USA) and a Mini-Extruder (Avanti Polar Lipids, USA). Liposomal preparations were extruded 11 times to ensure the formation of large unilamellar vesicles (LUV). Liposomal dispersions were stored at 4 °C throughout the entire study period.

### 2.3. Characterization of fusogenic liposomes

The liposomal preparations were diluted 1:10 with 5 mM phosphate buffer, pH 7.4, prior to measurements. Particle size and polydispersity index (PDI) were determined using a dynamic light scattering (DLS) technique (Zetasizer Ultra, Malvern Panalytical Ltd, UK). Measurements were performed three times for each sample at 25 °C with backscattering

at 173° angle and 1.33 as refractive index. The zeta potential was measured based on electrophoretic light scattering (ELS) principles using the same instrument. Measurements were performed at 25 °C with 1.33 as refractive index. Liposomal characterization was performed after 24 h of preparation and at different time intervals over one year to evaluate the long-term stability of the preparations (n = 3 for each formulation). The liposomal formulations were stored at 4 °C during the stability study.

Transmission electron microscopy (TEM) micrographs of selected liposomal preparations were obtained using a negative-staining embedding electron microscopy technique. Samples were prepared according to a previously published protocol (Webster and Webster 2014), with some modifications. The samples were adsorbed onto a carbon-coated copper grid (300 mesh). The grid was glow discharged to create a charge opposite to that of the liposomes. From each liposomal formulation, a 5 µl drop was applied on the grid. After 30 s contact time, the grid was washed twice each time for one min with Milli-Q water. Samples were placed on a 20 µl drop of 1 % (w/v) uranyl acetate for 30 s, followed by another 30 s exposure to a fresh 20 µl drop of the same solution. For embedding, the grids were transferred to a 20 µl drop containing a mixture of uranyl acetate 0.4 % (w/v) and 1.8 % (w/v) of methylcellulose, directly followed by 2 min incubation on a second drop of the same mixture. For drying, the grids were picked up in 3.5 mm metal loops to produce a thin layer of methylcellulose by gently dragging the loop's edge across a filter paper to remove excess liquid volume. Subsequently, the thin layer of methylcellulose solution was allowed to air dry before imaging using a transmission electron microscope (JEM-1400, JEOL Ltd, Japan) at 120 kV.

#### 2.4. Determination of liposomal fusion by lipid mixing assay

Liposomal fusion with microbial cells was studied by measuring the decrease in fluorescence resonance energy transfer (FRET) between the two fluorescent probes (NBD-PE and Rhod-PE) incorporated in the liposomes as previously reported (Wang et al. 2016). Selected fusogenic liposomal formulations (FL1, FL4, and FL7) were prepared based on the lipid composition outlined in Table 1, with the addition of 0.2 mol% of each fluorescent probe during the lipid film formation step. The total of 0.4 mol% contributed by the fluorescent probes was subtracted from the DOPE content, as the probes have a similar chemical structure to DOPE. The total phospholipid concentration was 10 mM and the liposomes were prepared as described in section 2.2.

Inoculums of *E. coli*, *S. aureus* and *C. albicans* were made from overnight cultures on TSA grown aerobically at 37 °C by suspending well-isolated colonies in PBS until 0.5 McFarland was obtained. The suspension was then diluted with PBS to get a final concentration of 10<sup>6</sup> CFU/ml. Using 96-well plates (Corning® polystyrene flat bottom plates, USA), 100 µl of each microbial inoculum was mixed with 100 µl of each fluorescent-labelled liposomal formulation (n = 6). As controls, some wells contained only liposomes without microorganisms while others contained only microorganisms without liposomes. The fluorescence intensity was measured using a VICTOR® Nivo plate reader (PerkinElmer, USA) with excitation at 480 nm and emission at 600 nm at time point zero. The plate was incubated at 37 °C with orbital shaking at 80 rpm and measurements were repeated after 30 min and 3 h of incubation. After the last measurement, the final fluorescence intensity (F<sub>max</sub>) was determined by adding 0.2 % v/v Triton X-100 to solubilize the liposomes and obtain the maximum change in FRET for each well. Percentage fusion at each time point for a well was then calculated using the following equation:

$$\%Fusion = (F_t - F_o) / (F_{max} - F_o) \times 100 \quad (1)$$

where F<sub>t</sub> is the fluorescence intensity at a certain time point and F<sub>o</sub> is the initial fluorescence intensity measured for the same well. The experiment was performed three times as independent triplicates. Analysis of variance (ANOVA) was used to determine significant differences (P-value < 0.05 was considered significant).

#### 2.5. Determination of liposomal fusion by flow cytometry

The experiment was performed according to previously reported protocols (Sachetelli et al. 2000, Mugabe et al. 2006) with slight modifications. Selected liposomal formulations were prepared as previously described (section 2.2) except for using Milli-Q water as the hydration medium to avoid micelle formation of PKH67 during the labelling step. PKH67 was prepared according to the labelling kit instructions and then mixed with the liposomes to yield a final concentration of 2.5 µM of PKH67. The tubes were incubated under orbital shaking (Genie Temp-Shaker 100, Scientific Industries, USA) at 80 rpm for 5 min after which the liposomes were separated from unbound PKH67 using Sephadex G-25 resin desalting columns (PD-10 Cytiva, USA) with 5 mM phosphate buffer as the elution medium. The final concentration of liposomes after elution was 10 mM.

Inoculums of *E. coli*, *S. aureus* and *C. albicans* were prepared as previously described (section 2.4) with a final concentration of 10<sup>6</sup> CFU/ml. Microbial suspensions were then mixed 1:1 with labelled liposomes (n = 4) and incubated at 37 °C for 3 h under gentle shaking using a tube rotator (Boekel scientific, USA) at 18 rpm. Following incubation, samples were passed through 0.45 µm polycarbonate membranes to trap microbial cells and to remove unfused liposomes from the samples. Membranes were washed first with 50 ml of a mixture of 0.9 % NaCl + 5 % Tween 80 (% w/v), followed by 200 ml of 0.9 % NaCl. Each membrane was then carefully placed in a tube with 2.5 ml PBS + 1 % (w/v) paraformaldehyde to detach the cells from the membrane under orbital shaking at 50 rpm for 1 min. Samples were then measured using a flow cytometer (CytoFlex, Beckman Coulter, CA, USA) to determine the number of fluorescent cells in each sample using the fluorescein isothiocyanate (FITC) filter with excitation at 488 nm and emission at 525 nm. The extent of fusion was determined by calculating the percentage of fluorescent cells of the total number of cells detected per sample. Analysis of variance (ANOVA) was used to determine significant differences; a P-value < 0.05 was considered significant.

#### 2.6. Imaging of biofilm penetration

Fluorescently labelled liposomes were prepared as described in section 2.4 but incorporating only 0.5 mol% Rho-PE in the formulation of 20 mM phospholipids. An *S. aureus* inoculum was prepared by suspending well-isolated colonies in 0.9 % NaCl until 0.5 McFarland was obtained, and the suspension was then diluted with TSB + 1 % (w/v) glucose to a final concentration of 10<sup>5</sup> CFU/ml. One ml of bacterial broth was added to each well in a 4-well chamber slides (Nunc Lab-Tek II CC<sup>2</sup>, Thermo Scientific) and allowed to grow for 72 h at 37 °C with shaking at 60 rpm. The medium was gently replaced every day without disrupting the biofilm. After incubation, medium was removed, and the biofilm was gently washed two times with sterile water before liposomes mixed with growth medium (1:1) were added to each well. A mixture of 5 mM phosphate buffer and growth medium (1:1) was added to the control wells. Liposomes were incubated with biofilms at 37 °C with shaking at 60 rpm for 24 h. After incubation, medium was removed, and wells were

washed twice with sterile water followed by staining with 100 µl of DAPI solution (0.1 µg/ml). DAPI stain was kept in contact with the biofilm for 30 min before removal and wells were again washed twice with sterile water. Subsequently, samples were fixed using 1 % paraformaldehyde in 0.9 % NaCl. The solution was then removed, and wells were washed twice with sterile water. Finally, 50 µl of antifade mounting solution was added to each well, covered by a glass coverslip and sealed with a clear nail polish. The slides were examined using a confocal microscope (TCS SP8 STED, Leica Microsystems, Germany). Fluorescence intensity measurements and visualisation of 3D structures of the biofilms were generated from z-stacks by using ImageJ software (National Institutes of Health, Maryland, USA). The experiment was performed three times as independent triplicates.

## 2.7. Hemocompatibility assay

Red blood cells were isolated from freshly collected blood samples from healthy human donors by centrifuging 1 ml blood at 4000 rpm for 5 min (5810R Centrifuge, Eppendorf, Germany). After removing the supernatants, pellets were resuspended in 10 ml PBS and centrifugation was repeated for a total of three cycles to ensure sample purity. In a 96-well round-bottom polystyrene plate (Corning®, USA), 100 µl red blood cell suspension was added to each well except for the blank wells (n = 12). Freshly prepared liposomes using PBS as hydration medium were serially diluted with PBS. One hundred µl of each liposomal concentration was added per well and mixed with red blood cell suspension to yield final concentrations in the range of 0.625 – 15 mM. The same volume of PBS and 1 % (w/v) Triton X-100 solutions were added to negative and positive control wells, respectively. The plate was incubated at room temperature for 3 h, then centrifuged at 4000 rpm for 5 min. Finally, 100 µl of the supernatant was transferred to a flat bottom 96-well polystyrene plate (Corning®, USA) and the haemoglobin content was determined spectrophotometrically at 405 nm (Victor Nivo, Perkin Elmer®, USA). The experiment was performed twice as independent duplicates (n = 8 in total for each liposomal concentration).

The degree of haemolysis was calculated as follow:

$$\% \text{Haemolysis} = \frac{(Abs_{\text{test}} - Abs_{\text{neg. control}}) / (Abs_{\text{pos. control}} - Abs_{\text{neg. control}})}{\times 100} \quad (2)$$

where Abs. test is the test absorbance, Abs. neg. control is the negative control absorbance and Abs. pos. control is the positive control absorbance.

## 2.8. Cytotoxicity study

A cytotoxicity study for selected liposomes was performed on adult human dermal fibroblasts (C-12302, PromoCell, Heidelberg, Germany). Cells were cultured in Fibroblast Growth Medium 2 supplemented with serum, insulin and basic fibroblast growth factor (C-23110, PromoCell, Heidelberg, Germany) in addition to antibiotic antimycotic solution (100 units penicillin, 100 µg streptomycin and 0.25 µg amphotericin B per ml, Merck, Germany). The tissue culture flasks were incubated at 37 °C and 5 % CO<sub>2</sub>. Starting medium was aspirated and fresh medium was added every two to three days. On reaching 70–90 % confluency, cells were detached and cultured in 96-well plates (black polystyrene flat bottom delta treated, Corning®, USA) by adding 250 µl cell suspension at a density of 3500 cells/cm<sup>2</sup>. Liposomes in PBS were diluted with growth medium to yield different concentrations (1.25, 2.5, 5, 10 and 15 mM). Cells were allowed to reach 50–60 % confluency before 250 µl of each concentration of liposomes was added to the wells and incubated for 20 h (n = 12). Cytotoxicity was induced in the positive control wells by addition of 1 % Triton X-100, while only growth medium was added to the negative control wells. After incubation, cytotoxicity was determined by the Alamar Blue assay as follows: the content of each well was removed, washed once with PBS and then 100 µl of Alamar Blue solution (10 % v/v in growth medium) was added to the

wells. Plates were incubated statically for 2 h at 37 °C and 5 % CO<sub>2</sub>. Cell viability was determined fluorometrically using a plate reader (Victor Nivo, Perkin Elmer®, USA) at an excitation wavelength of 560 nm and measuring the emission at 600 nm. Viability percentage was then calculated as follow:

$$\% \text{Cells Viability} = (F_{\text{test}} / F_{\text{neg. control}}) \times 100 \quad (3)$$

where F<sub>test</sub> is the test fluorescence and F<sub>neg. control</sub> is the negative control fluorescence. Analysis of variance (ANOVA) was used to determine significant differences (P-value < 0.05 was considered significant).

## 3. Results and discussion

### 3.1. Preparation, characterization and physical stability of fusogenic liposomes

In this study, large unilamellar vesicles (LUV) were prepared by the thin lipid film hydration – extrusion method (Lombardo and Kiselev 2022). Particle size, PDI and zeta potential measurements of all liposomal formulations at time point zero are shown in Table 1. Measured size of all liposomal preparations in the present study ranged approximately from 130 to 160 nm with PDI ≤ 0.1 immediately after preparation. The particle size is a critical parameter for determining the ability of the liposomes to penetrate the biofilm. It has been reported that particle size should not exceed 500 nm for optimal biofilm penetration through water channels within the EPS matrix (Liu et al. 2019). Thus, based on the obtained results, the particle size of the prepared liposomes is optimal for biofilm penetration. Generally, nanoparticles with less than 0.2 PDI value are considered to be monodispersed (Danaei et al. 2018). Therefore, the low PDI values demonstrated by the liposomal formulations indicate their monodispersity. Zeta potential measurements were proportional to the amount of charged phospholipid added to the formulation (Table 1). Increasing the amount of charged phospholipid from 2.5 mol% to 10 mol% resulted in an increase in the absolute zeta potential value from + 4.2 mV to + 25.7 mV with DOTAP and from −18.6 mV to −46.5 mV with DOPG, respectively, which was expected based on the phospholipids charge. Zeta potential values between −10 and + 10 mV are generally considered neutral (Wang et al. 2020), which was observed with the non-charged formulation (FL1) showing −5 mV.

**Table 1**

Results from particle size (presented as Z-average), PDI and zeta potential measurements (mean ± SD, n = 3) for different liposomal formulations after preparation at time point zero.

Liposomal formulation	Phospholipid composition (mol %)	Z-Average (nm) ± SD	Polydispersity index (PDI) ± SD	Zeta potential (mV) ± SD
FL1	DPPC:DOPE (50:50)	142 ± 1.9	0.103 ± 0.003	−5.01 ± 0.8
FL2	DPPC:DOPE:DOTAP (50:47.5:2.5)	160 ± 1.0	0.086 ± 0.025	+4.61 ± 0.5
FL3	DPPC:DOPE:DOTAP (50:45:5)	139 ± 1.5	0.102 ± 0.011	+16.4 ± 0.4
FL4	DPPC:DOPE:DOTAP (50:40:10)	135 ± 1.8	0.112 ± 0.064	+25.7 ± 1.3
FL5	DPPC:DOPE:DOPG (50:47.5:2.5)	133 ± 1.5	0.099 ± 0.009	−18.6 ± 0.6
FL6	DPPC:DOPE:DOPG (50:45:5)	133 ± 0.9	0.081 ± 0.019	−32.2 ± 1.2
FL7	DPPC:DOPE:DOPG (50:40:10)	131 ± 0.4	0.088 ± 0.006	−46.5 ± 0.7



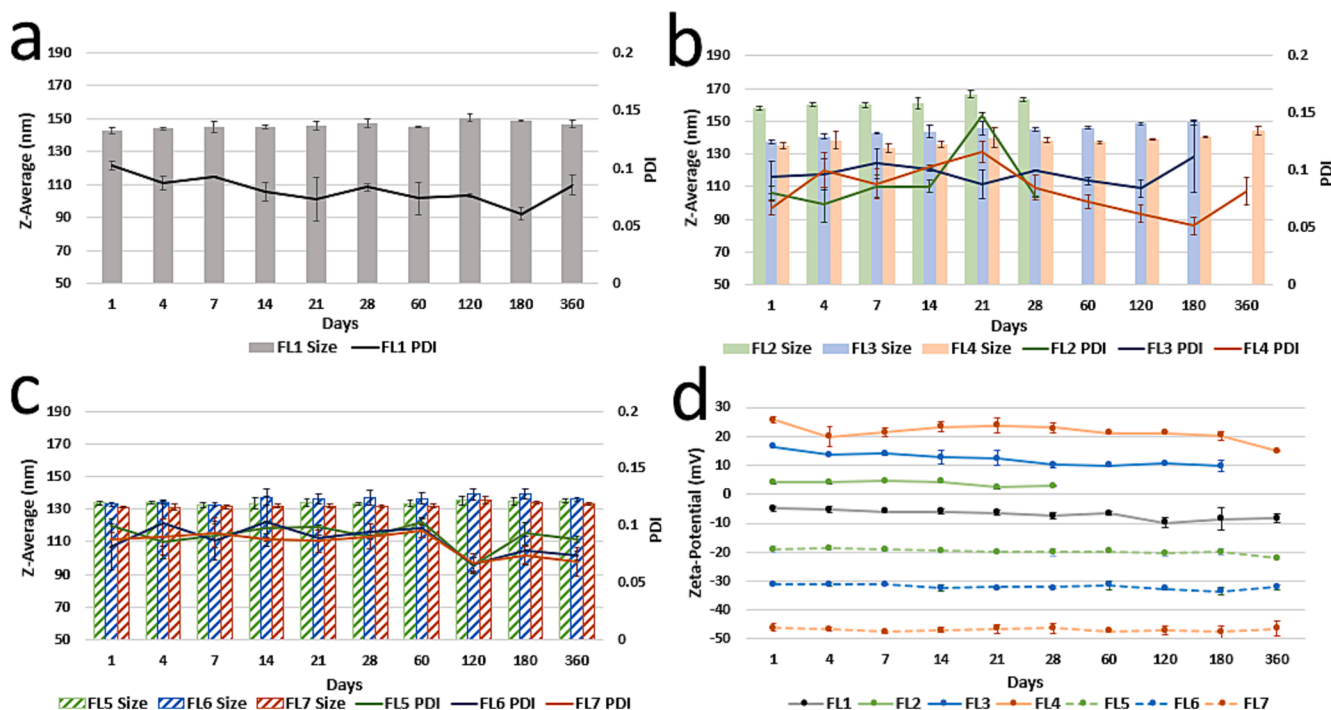


**Fig. 1.** One-year *in vitro* stability of fusogenic liposomes stored at 4 °C. The particle sizes (presented as Z-average) and polydispersity indices (PDIs) are shown for (a) neutral liposomes, (b) cationic liposomes, and (c) anionic liposomes. (d) shows the zeta potential for all liposomal formulations used in the study. The bars and the data points in the graphs represent mean  $\pm$  SD ( $n = 3$ ).

Particle size, PDI and zeta potential measurements at different time intervals after preparation over a period of one year are shown in Fig. 1. Despite the absence of cholesterol in the formulations, the particle size and PDI of the liposomes remained stable over a year of monitoring (Fig. 1a-c), except for the cationic liposomes FL2 and FL3 (Fig. 1b), which were only stable for 1 and 6 months, respectively. Physical instability was visually observed in these formulations at the specified time points. In terms of the impact of liposomal surface charge on the *in vitro* stability, the observed overall lower stability of cationic liposomes compared to the anionic ones (Fig. 1b and 1c) can probably be attributed to the valences of the counterions. According to Schulze-Hardy rule, the stability of colloidal dispersions is inversely proportional to counterion valency (Gambinossi et al. 2015, Muráth et al. 2018). At pH 7.4, the cationic liposome counterion is divalent ( $\text{HPO}_4^{2-}$ ), while the anionic liposome counterion is monovalent ( $\text{Na}^+$ ). This can result in a higher tendency for aggregation leading to decreased long term stability of cationic liposomes as observed. A similar effect of counterion valency has been reported with different type of colloidal dispersions (Badawy et al. 2010, Muráth et al. 2018). Although lacking cholesterol, the stability profile of the liposomes is maintained by the presence of the relatively high amount of DPPC lipid (50 mol %) in the formulations, which has a phase transition temperature ( $T_c$  41 °C) much higher than the storage temperature (4 °C) (Dorskoc et al. 2020). The improved stability provided by DPPC could be explained by increased membrane rigidity (Dorskoc et al. 2020). Although the stability experiments did not monitor drug leakage from the fusogenic liposomes, a previous study has shown that switching from a fluid phase phospholipid bilayer, e.g. containing egg-PC with  $T_c <$  physiological temperature, to a solid phase bilayer, such as DPPC, can reduce drug leakage (Storm et al. 1987). Moreover, hydrophilic drugs tend to have lower liposomal permeability than hydrophobic drugs (Allen and Cullis 2013). Since the retention properties of drugs in liposomes are drug-dependent, specific investigations of drug-loaded formulations are needed on a case-by-case basis to gain more information on system stability, particularly regarding drug leakage.

TEM imaging of the selected liposomal preparations is depicted in

Fig. 2. The TEM images confirm the presence of liposomal vesicles with a comparable size range to the DLS measurements. The shape of some liposomal vesicles was distorted due to the sample preparation processes required for TEM imaging. For studies focusing on liposomal morphology, cryo-TEM is often preferred over conventional TEM due to its ability to preserve the original structure of liposomes. However, in this study, TEM was not employed to examine detailed liposomal morphology. Instead, it complemented DLS measurements by providing visual confirmation and approximate size estimates.

Based on the initial characterization and promising long-term stability, one formulation from each liposome type (neutral FL1, cationic FL4, and anionic FL7) was selected for further investigation regarding their interactions with microbial cells and biofilm.

### 3.2. Liposomal fusion with planktonic microbial cells

In this study, liposomal fusion with planktonic microbial cells was measured using two different methods i.e., lipid mixing and flow cytometric assay. After 30 min of incubating microbial cells with liposomes, no fusion was detected with *S. aureus* and *C. albicans*, while measurable fusion was detected with *E. coli* based on the lipid mixing assay (data not shown). After 3 h of incubation, measurable fusion was observed with all microbial cells tested with using the lipid mixing assay (Fig. 3a). For each type of liposome tested, the fusion with microbial cells follows the order *E. coli* > *S. aureus* > *C. albicans*. Although the differences were not found to be statistically significant, a similar trend in the data was seen with the flow cytometric assay (Fig. 3b): liposomal fusion with *E. coli* was significantly higher than *S. aureus* for both neutral and cationic liposomes. No fusion was detected with *C. albicans* with flow cytometry which could be due to lower sensitivity of the method compared to lipid mixing assay. These results indicate that fusion with gram negative bacteria is higher than with gram positive bacteria and fungi, respectively, regardless of the liposomal charge and composition.

As observed in this study, a higher degree of liposomal fusion with gram negative bacteria was also reported in literature after evaluating the fusion of negatively charged liposomes with various gram negative

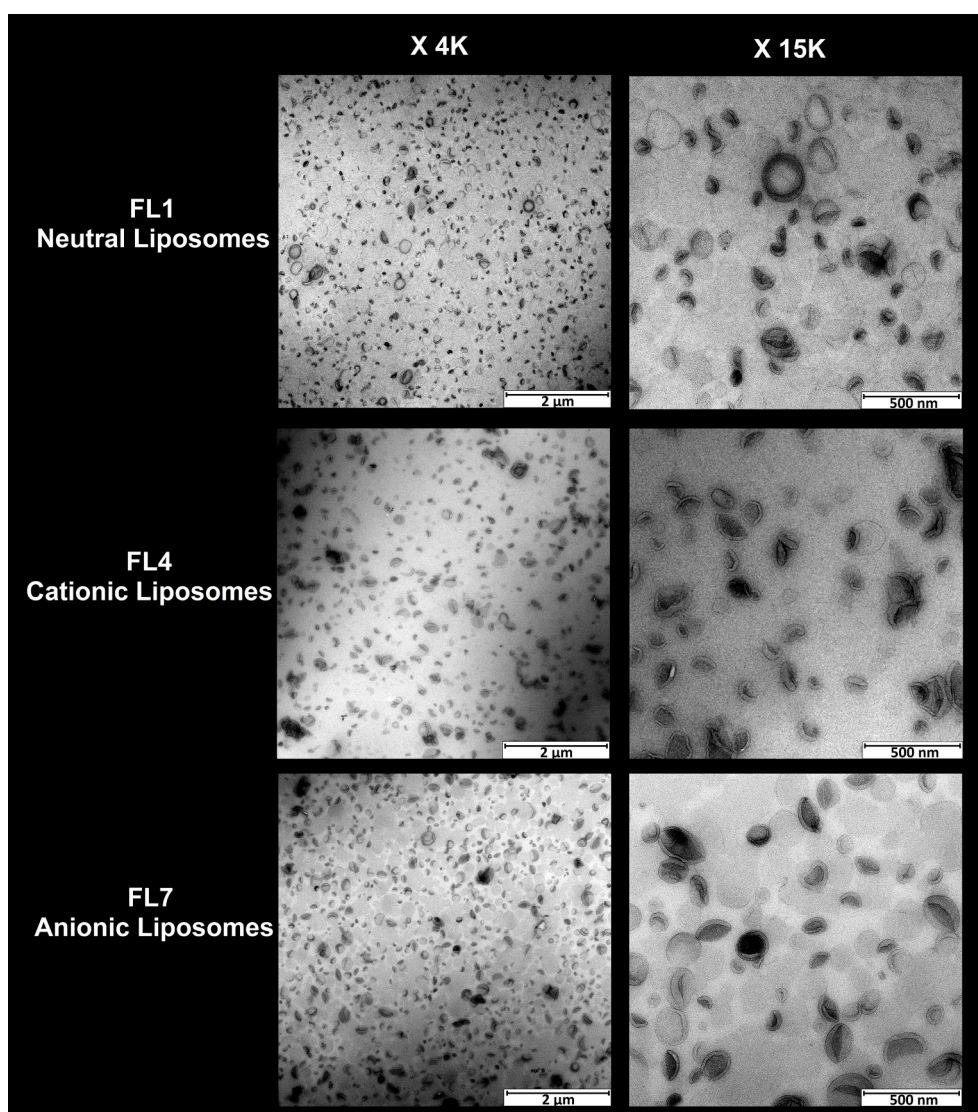


**Fig. 2.** TEM micrographs showing liposomal vesicles of neutral liposomes (DPPC:DOPE 50:50), cationic liposomes (DPPC:DOPE:DOTAP 50:40:10) and anionic liposomes (DPPC:DOPE:DOPG 50:40:10) after preparation.

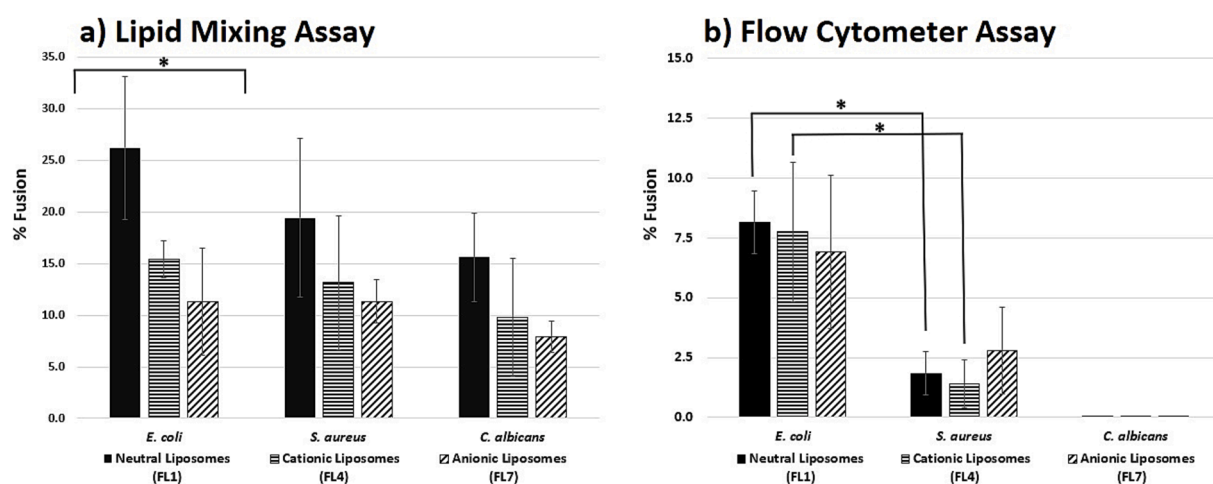


**Fig. 3.** The effect of liposomal charge on fusogenic behaviour with microbial cells measured as percentage fusion (mean  $\pm$  SD) by: (a) lipid mixing assay and (b) flow cytometry on *Escherichia coli*, *Staphylococcus aureus* and *Candida albicans* after 3 h of incubation. (\*) indicates statistically significant difference (P < 0.05).

and gram positive bacteria (Wang et al. 2016). The differences in the degree of liposomal fusion between the two types of bacterial cells could arise from the presence of the outer membrane in gram-negative bacteria, which contains a substantial amount of phospholipids in its inner leaflet (Silhavy et al. 2010, Ma et al. 2013, Wang et al. 2016). Studies investigating the mechanisms of liposomal fusion with gram positive and gram negative bacteria report that the processes occur through distinct approaches. With respect to gram negative bacteria, liposomes fuse with the outer membrane due to the chemical structural similarity (Wang et al. 2016, Scheeder et al. 2023). In contrast, gram positive bacteria and fungi lack an outer membrane. Therefore, liposomes are thought to either be internalized by gram positive bacteria or permeating through the cell wall pores followed by interaction with the cellular membrane (Scheeder et al. 2023). Bacterial biofilms have long been a primary focus of research in medical microbiology due to their significance in human disease. However, fungal biofilms are increasingly being recognized for their critical role in pathogenesis, particularly as a major contributor to hospital-acquired infections associated with medical devices (Ramage et al. 2012, Wang et al. 2024). Many clinically relevant fungi, such as *C. albicans*, are known to form biofilms and colonize prosthetic devices. *C. albicans* is the third most common cause of intravascular catheter-related infections (Martinez and Fries 2010). To our knowledge, interaction of fusogenic liposomes with fungal cells has not been reported in the literature up until now. Fusogenic liposomes may represent a promising novel delivery system for antifungals. Unlike the gram positive bacterial cell wall, which is composed of peptidoglycans and lipoteichoic acid, the fungal cell wall is composed of various layers of mannoproteins,  $\beta$ -glucan and chitin (Brown et al. 2015). The complexity of the fungal cell wall may limit liposomal internalization and interaction with the cell envelope, which could explain the lower liposomal fusion with *C. albicans* compared to *S. aureus* in this work. These findings suggest a potential tolerance of fungal cells to liposomal internalization and emphasize the necessity for further liposomal optimization to improve their uptake by fungal cells.

In the present work, a comparative analysis of different liposomal surface charges on microbial fusion revealed statistically significant difference only in the case of *E. coli*. Here, a significant difference was observed in the fusion percentage among liposomes with varying surface charges as detected by lipid mixing assay (Fig. 3a). Despite the differences observed with *S. aureus* and *C. albicans* being not statistically significant, the trend suggests that for each type of microbial cell, the extent of liposome fusion followed the order: neutral > cationic > anionic. More studies would be required to see if statistical significance emerges. However, this trend was not detectable with flow cytometry (Fig. 3b). This is possibly due to lower sensitivity of the method, which may be unable to discriminate between the different liposomal formulations. Electrostatic interaction between microbial cells and liposomes is thought to be the first step for fusion. Cationic liposomes are reported to attract to the negatively charged cell surface (Scheeder et al. 2023). While for anionic fusogenic liposomes, the interaction is believed to rely on the presence of divalent cations (e.g., calcium ions) in the surrounding environment, which neutralize the charge and facilitate the bridging of liposomal and cell surfaces (Wang et al. 2016). However, in our study, fusion of neutral and anionic liposomes occurred even in standard PBS, which lacks divalent cations. A similar observation was reported by Mugabe et al. (Mugabe et al. 2006), after measuring fusion of non-cationic liposomes with *Pseudomonas aeruginosa* using a flow cytometer assay in PBS (Mugabe et al. 2006). Fusion of negatively charged liposomes was observed in other studies, supporting their inherent ability to fuse with microbial cells in absence of divalent cations (Ma et al. 2013, Wang et al. 2016). The authors suggested that the main driving parameter for liposomal fusion is the chemical composition of the bacterial cell envelope (Wang et al. 2016). For instance, they attributed higher liposomal fusion with *E. coli*, as opposed to *P. aeruginosa*, to the greater abundance of phosphatidylethanolamine in the outer membrane composition in *E. coli* (91 %) compared to

*P. aeruginosa* (71 %) (Wang et al. 2016). The results obtained in our study suggest that both the chemical composition of the cell envelope and the liposomal membrane influence fusion. The increased fusion observed with neutral liposomes is likely due to the higher DOPE content in the neutral formulation (50 mol%) compared to the cationic formulation (40 mol%). Although both DOTAP and DOPE share identical carbon chains, their head groups differ significantly. DOPE's smaller head group promotes inward-curving structures that enhance the fusion (Scheeder et al. 2023). In contrast, DOTAP has a larger head group and positive curvature, which favours outward-curving structures. These results demonstrate that lipid composition plays a crucial role in facilitating fusion, while charge and electrostatic interactions primarily mediate the attraction between the liposome and microbial cell, enabling the fusion process to occur.

Although not all differences in liposomal fusion across microbial cells were statistically significant, consistent trends were observed in both the lipid mixing assay and flow cytometry. The lack of statistical significance may reflect limitations in the sensitivity of the methods and the inherent variability of biological samples, which can introduce additional error. Nonetheless, the observed trends are consistent with previous reports in the literature as discussed earlier. Given this, future work with improved methodologies and bigger sample size may likely show the trend to be statistically significant. Finally, as previously noted, liposomal fusion in this study was assessed by incubation in PBS, which does not fully represent the complexity of biological environments. The inclusion of complex microbiological media, which typically contain biological extracts with non-defined chemical compositions, could complicate the interpretation of the results. Subsequent studies should explore liposomal behaviour in more complex growth media, as these environments may affect the surface properties of the liposomes and liposome-cell interactions, for instance protein corona formation on the nanoparticle surface (Fleischer and Payne 2014, Graça et al. 2017).

### 3.3. Liposomal penetration into biofilm

In clinical settings, biofilms are complex and often polymicrobial (Yang et al. 2011). Nonetheless, *S. aureus* is considered to be one of the microbes most commonly involved in biofilm-related infections associated with medical implants (Zhao et al. 2023). With this in mind, *S. aureus* was chosen to evaluate the effect of liposomal charge on the liposome ability to penetrate and persist within a preformed biofilm. The ability of fusogenic liposomes to enhance antibiofilm activity of antimicrobial agents has been previously documented (Scriboni et al., 2019). However, to our knowledge this is the first study to investigate the interaction of fusogenic liposomes with preformed biofilms. In general, nanoparticle interactions with the biofilm matrix are mostly based on the physicochemical properties of the different nanoparticles. Particle size, surface charge, shape and hydrophobicity are among the critical factors (Fulaz et al. 2019). Images obtained by confocal laser scanning microscopy (CLSM) and 3D visualisations generated using ImageJ software are presented in Fig. 4. All three fusogenic liposomal formulations, each representing a different surface charge, were capable of penetrating and diffusing inside the different biofilm layers as demonstrated by the confocal images. However, the ability of fusogenic liposomes to interact with the biofilm varied, with cationic liposomes exhibiting fluorescence intensities two and three times higher than those of anionic and neutral liposomes, respectively. Similar findings were reported by Ibaraki et al. (Ibaraki et al. 2020) after testing non-fusogenic cationic and anionic liposomes on *P. aeruginosa* biofilms. Generally, cationic nanoparticles demonstrate higher interaction with the biofilm matrix due to the abundance of negatively charged molecules in the EPS composition, including extracellular DNA and negatively charged polysaccharides (Fulaz et al. 2019). Improved interaction of cationic liposomes with biofilms may also be attributed to the electrostatic attraction with negatively charged microbial cell surfaces (Malaekhe-Nikouei et al. 2020).



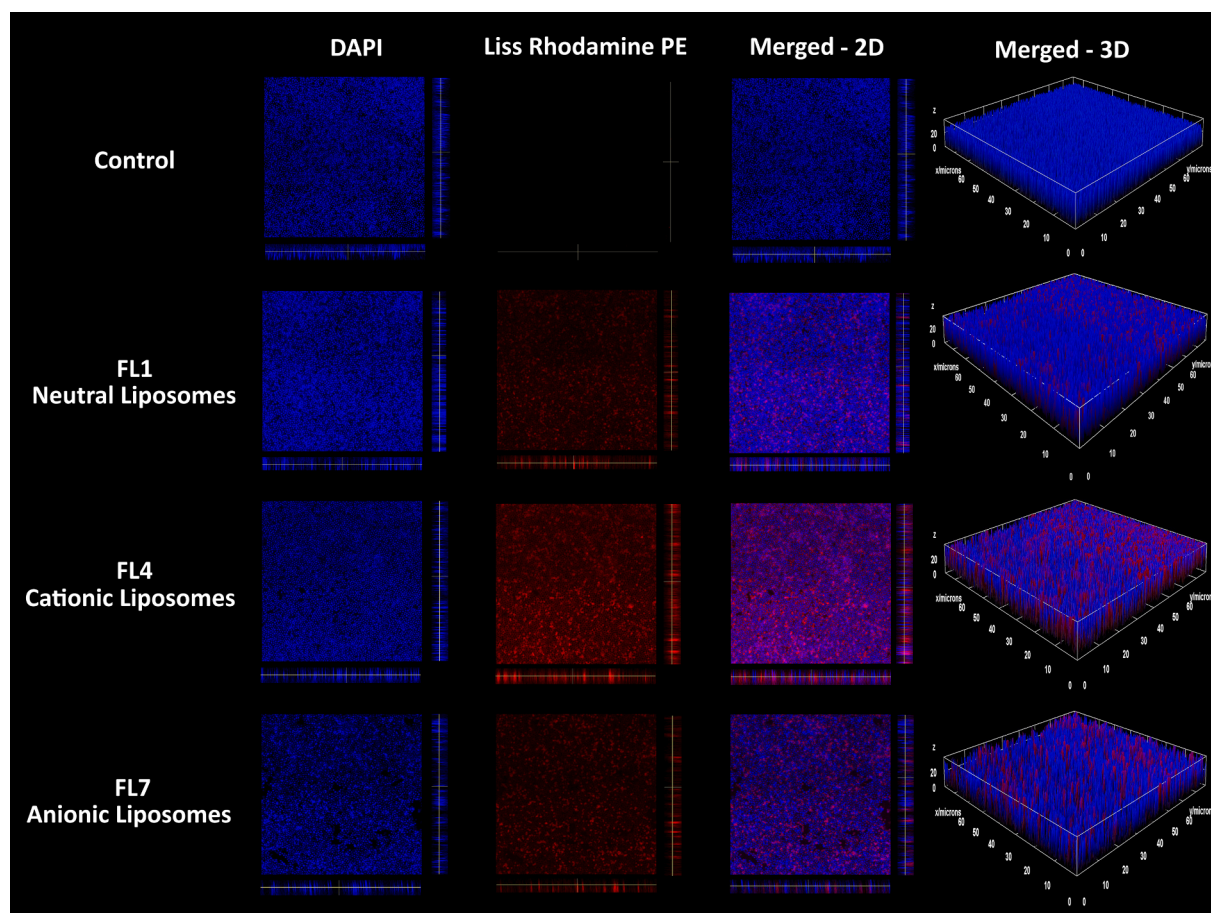


**Fig. 4.** Biofilm penetration of fusogenic liposomes with various surface charge; neutral liposomes (DPPC:DOPE 50:50), cationic liposomes (DPPC:DOPE:DOTAP 50:40:10) and anionic liposomes (DPPC:DOPE:DOPG 50:40:10) shown as 2D images representing biofilm cells (DAPI), liposomes (Liss Rhodamine) and 3D visualizations obtained from CLSM z-stacks.

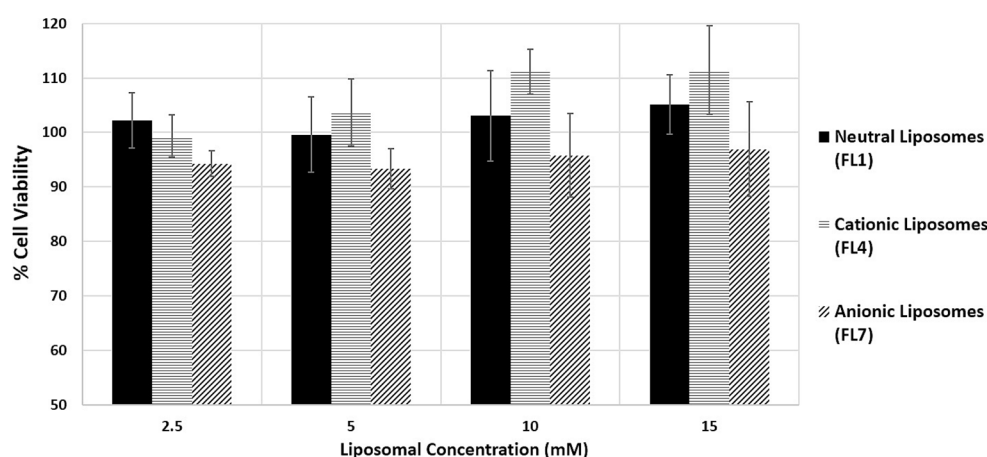


**Fig. 5.** Percentage cell viability (mean  $\pm$  SD,  $n = 18$ ) of human dermal fibroblasts after incubation with various concentrations of selected liposomal preparations for 20 h.

### 3.4. Hemocompatibility and cytotoxicity of cholesterol-free fusogenic liposomes

To evaluate cytotoxicity of the prepared liposomes, a cell viability study was performed on human dermal fibroblasts. The cell viability assay is based on irreversible enzymatic reduction of Alamar blue to resazurin by viable cells, which was then quantified using a fluorometric assay (Kamiloglu et al. 2020). The results obtained from testing various

concentrations of the liposomes indicate the tolerance of human fibroblast cells to liposomal exposure (Fig. 5). Cell viability was greater than 90 % even with the highest concentration (15 mM) of all three liposomal preparations tested. Generally, cell viability greater than 80 % is taken to indicate non-toxic effects of the tested material (López-García et al. 2014). Furthermore, no significant differences in cell viability were detected when comparing treatments with the different liposomal preparations.



Hemocompatibility of the liposomes was assessed by conducting a haemolysis assay. Unlike the colouration observed in control wells after inducing haemolysis with Triton X-100, no coloration was observed after incubation with the liposomes for 3 h. Additionally, after measuring the haemoglobin absorbance, the extent of haemolysis was found to be less than 1 % compared to the full haemolysis found in the presence of Triton X-100. Liposomal formulations offer outstanding flexibility in terms of dosage form and administration route. At this preliminary stage of development, where no antimicrobial agent is incorporated, potential delivery methods for treating biofilm-associated infections were investigated. This includes topical administration, such as direct application to infected wounds, or parenteral administration for systemic or inaccessible infection sites (Wu et al. 2015, Ciofu et al. 2017). The results from both the cytotoxicity and haemolysis assay demonstrate a promising biocompatibility of the fusogenic liposomes, supporting their potential application as antimicrobial drug delivery systems for both parenteral and topical administration.

#### 4. Conclusions

In this work, cholesterol-free fusogenic liposomes with neutral, cationic, and anionic surface charges were formulated and characterized as potential platforms for biofilm treatment. The high concentration of DPPC in the liposomal formulations compensated for the absence of cholesterol and contributed to improved *in vitro* stability. Liposomal fusion was found to be higher with gram negative bacteria, followed by gram positive bacteria and fungi. Neutral liposomes exhibited the greatest fusion capacity with microbial cells, followed by cationic and anionic liposomes respectively. Our investigations demonstrate that liposomal fusion with microbial cells is a multifactorial process influenced by the chemical composition of the liposomes, the liposomal surface charge, and probably the components and structure of the microbial cell surface. The developed cholesterol-free, fusogenic liposomes were found to be biocompatible and capable of penetrating the *S. aureus* biofilm regardless of the liposomal charge. However, cationic liposomes showed stronger interaction with the biofilm matrix. To summarise, this study demonstrates that the liposomes described hold promise as drug delivery platforms in antimicrobial treatment regimens and might enhance the efficacy of antimicrobials against biofilm-related infections.

#### CRediT authorship contribution statement

**Ahmed M. Amer:** Writing – review & editing, Writing – original draft, Methodology, Investigation, Data curation, Conceptualization. **Colin Charnock:** Writing – review & editing, Writing – original draft, Supervision, Methodology, Conceptualization. **Sanko Nguyen:** Writing – review & editing, Writing – original draft, Supervision, Methodology, Conceptualization.

#### Declaration of competing interest

The authors declare that they have no known competing financial interests or personal relationships that could have appeared to influence the work reported in this paper.

#### Acknowledgments

The authors thank Ellen Hagesæther (Hospital Pharmacies Enterprise, South-Eastern Norway) for her technical assistance with cytotoxicity study. The transmission electron microscopy photography was conducted by Jens Wohlmann at the Department of Biosciences, University of Oslo. Confocal laser scanning microscopy was performed at the core facility for advanced light microscopy, the Gaustad node, Oslo University Hospital with assistance from Anna Lång. Graphical abstract was created with Biorender.com

#### Data availability

No data was used for the research described in the article.

#### References

- Allen, T.M., Cullis, P.R., 2013. Liposomal drug delivery systems: from concept to clinical applications. *Adv. Drug Deliv. Rev.* 65 (1), 36–48.
- Al-Wrafy, F.A., Al-Gheethi, A.A., Ponnusamy, S.K., Noman, E.A., Fattah, S.A., 2022. Nanoparticles approach to eradicate bacterial biofilm-related infections: a critical review. *Chemosphere* 288, 132603.
- Arriaga, L.R., López-Montero, I., Monroy, F., Orts-Gil, G., Farago, B., Hellweg, T., 2009. Stiffening effect of cholesterol on disordered lipid phases: a combined neutron spin echo + dynamic light scattering analysis of the bending elasticity of large unilamellar vesicles. *Biophys. J.* 96 (9), 3629–3637.
- Badawy, A.M.E., Luxton, T.P., Silva, R.G., Scheckel, K.G., Suidan, M.T., Tolaymat, T.M., 2010. Impact of environmental conditions (pH, ionic strength, and electrolyte type) on the surface charge and aggregation of silver nanoparticles suspensions. *Environ. Sci. Tech.* 44 (4), 1260–1266.
- Bjarnsholt, T., 2013. The role of bacterial biofilms in chronic infections. *APMIS* 121 (s136), 1–58.
- Brown, L., Wolf, J.M., Prados-Rosales, R., Casadevall, A., 2015. Through the wall: extracellular vesicles in Gram-positive bacteria, mycobacteria and fungi. *Nat. Rev. Microbiol.* 13 (10), 620–630.
- Ciofu, O., Rojo-Moliner, E., Macià, M.D., Oliver, A., 2017. Antibiotic treatment of biofilm infections. *APMIS* 125 (4), 304–319.
- Costa, P.S., Prado, A., Bagon, N.P., Negri, M., Svidzinski, T.I.E., 2022. Mixed fungal biofilms: from mycobiota to devices, a new challenge on clinical practice. *Microorganisms* 10 (9).
- da Silva, R.A.G., Afonina, I., Kline, K.A., 2021. Eradicating biofilm infections: an update on current and prospective approaches. *Curr. Opin. Microbiol.* 63, 117–125.
- Danaei, M., Dehghankhold, M., Ataei, S., Hasanazadeh Davarani, F., Javanmard, R., Dokhani, A., Khorasani, S., Mozafari, M.R., 2018. Impact of particle size and polydispersity index on the clinical applications of lipidic nanocarrier systems. *Pharmaceutics* 10 (2), 57.
- Dong, D., Thomas, N., Thierry, B., Vreugde, S., Prestidge, C.A., Wormald, P.-J., 2015. Distribution and inhibition of liposomes on *Staphylococcus aureus* and *Pseudomonas aeruginosa* Biofilm. *PLoS One* 10 (6), e0131806.
- Doskocz, J., Dalek, P., Foryś, A., Trzebicka, B., Przybyło, M., Mesarek, L., Iglić, A., Langner, M., 2020. “The effect of lipid phase on liposome stability upon exposure to the mechanical stress.”. *Biochim. Biophys. Acta (BBA) - B Biomembranes* 1862 (9), 183361.
- Ferreira, M., Pinto, S.N., Aires-da-Silva, F., Bettencourt, A., Aguiar, S.I., Gaspar, M.M., 2021. Liposomes as a nanoplatform to improve the delivery of antibiotics into *Staphylococcus aureus* Biofilms. *Pharmaceutics* 13 (3), 321.
- Fleischer, C.C., Payne, C.K., 2014. Nanoparticle-cell interactions: molecular structure of the protein corona and cellular outcomes. *Acc. Chem. Res.* 47 (8), 2651–2659.
- Fulaz, S., Vitale, S., Quinn, L., Casey, E., 2019. Nanoparticle-biofilm interactions: the role of the EPS matrix. *Trends Microbiol.* 27 (11), 915–926.
- Furneri, P.M., Fresta, M., Puglisi, G., Tempera, G., 2000. Ofloxacin-loaded liposomes: in vitro activity and drug accumulation in bacteria. *Antimicrob. Agents Chemother.* 44 (9), 2458–2464.
- Gambinossi, F., Mylon, S.E., Ferri, J.K., 2015. Aggregation kinetics and colloidal stability of functionalized nanoparticles. *Adv. Colloid Interface Sci.* 222, 332–349.
- Ghosh, R., De, M., 2023. Liposome-based antibacterial delivery: an emergent approach to combat bacterial infections. *ACS Omega* 8 (39), 35442–35451.
- Graça, D., Louro, H., Santos, J., Dias, K., Almeida, A.J., Gonçalves, L., Silva, M.J., Bettencourt, A., 2017. Toxicity screening of a novel poly(methylmethacrylate)-Eudragit nanocarrier on L929 fibroblasts. *Toxicol. Lett.* 276, 129–137.
- Ibaraki, H., Kanazawa, T., Chien, W.-Y., Nakaminami, H., Aoki, M., Ozawa, K., Kaneko, H., Takashima, Y., Noguchi, N., Seta, Y., 2020. The effects of surface properties of liposomes on their activity against *Pseudomonas aeruginosa* PAO-1 biofilm. *J. Drug Delivery Sci. Technol.* 57, 101754.
- Kaddah, S., Khreich, N., Kaddah, F., Charcosset, C., Greige-Gerges, H., 2018. Cholesterol modulates the liposome membrane fluidity and permeability for a hydrophilic molecule. *Food Chem. Toxicol.* 113, 40–48.
- Kamiloglu, S., Sari, G., Ozdal, T., Capanoglu, E., 2020. Guidelines for cell viability assays. *Food Front.* 1 (3), 332–349.
- Kolašinac, R., Kleusch, C., Braun, T., Merkel, R., Csiszár, A., 2018. Deciphering the Functional Composition of Fusogenic Liposomes. *Int. J. Mol. Sci.* 19 (2), 346.
- Liu, Y., Shi, L., Su, L., van der Mei, H.C., Jutte, P.C., Ren, Y., Busscher, H.J., 2019. Nanotechnology-based antimicrobials and delivery systems for biofilm-infection control. *Chem. Soc. Rev.* 48 (2), 428–446.
- Lombardo, D., Kiselev, M.A., 2022. Methods of liposomes preparation: formation and control factors of versatile nanocarriers for biomedical and nanomedicine application. *Pharmaceutics* 14 (3), 543.
- López-García, J., Lehocký, M., Humpolíček, P., Sába, P., 2014. HaCaT keratinocytes response on antimicrobial atelocollagen substrates: extent of cytotoxicity, cell viability and proliferation. *J. Funct. Biomater.* 5 (2), 43–57.
- Ma, Y., Wang, Z., Zhao, W., Lu, T., Wang, R., Mei, Q., Chen, T., 2013. Enhanced bactericidal potency of nanoliposomes by modification of the fusion activity between liposomes and bacterium. *Int. J. Nanomed.* 8 (null), 2351–2360.
- Makhlof, Z., Ali, A.A., Al-Sayah, M.H., 2023. Liposomes-based drug delivery systems of anti-biofilm agents to combat bacterial biofilm formation. *Antibiotics* 12 (5), 875.

- Malaekheh-Nikouei, B., Fazly Bazzaz, B.S., Mirhadi, E., Tajani, A.S., Khameneh, B., 2020. The role of nanotechnology in combating biofilm-based antibiotic resistance. *J. Drug Delivery Sci. Technol.* 60, 101880.
- Martinez, L.R., Fries, B.C., 2010. Fungal biofilms: relevance in the setting of human disease. *Curr. Fungal Infect. Rep.* 4 (4), 266–275.
- Mountcastle, S.E., Cox, S.C., Sammons, R.L., Jabbari, S., Shelton, R.M., Kuehne, S.A., 2020. A review of co-culture models to study the oral microenvironment and disease. *J. Oral Microbiol.* 12 (1), 1773122.
- Mugabe, C., Halwani, M., Azghani, A.O., Lafrenie, R.M., Omri, A., 2006. Mechanism of enhanced activity of liposome-entrapped aminoglycosides against resistant strains of *Pseudomonas aeruginosa*. *Antimicrob. Agents Chemother.* 50 (6), 2016–2022.
- Muráth, S., Sáringer, S., Somosi, Z., Szilágyi, L., 2018. Effect of ionic compounds of different valences on the stability of titanium oxide colloids. *Colloids Interfaces* 2 (3), 32.
- Najafinobar, N., Mellander, L.J., Kurczy, M.E., Dunevall, J., Angerer, T.B., Fletcher, J.S., Cans, A.-S., 2016. Cholesterol alters the dynamics of release in protein independent cell models for exocytosis. *Sci. Rep.* 6 (1), 33702.
- Nicolosi, D., Cupri, S., Genovese, C., Tempera, G., Mattina, R., Pignatello, R., 2015. Nanotechnology approaches for antibacterial drug delivery: preparation and microbiological evaluation of fusogenic liposomes carrying fusidic acid. *Int. J. Antimicrob. Agents* 45 (6), 622–626.
- Panthi, V.K., Fairfull-Smith, K.E., Islam, N., 2024. Liposomal drug delivery strategies to eradicate bacterial biofilms: challenges, recent advances, and future perspectives. *Int. J. Pharm.* 655, 124046.
- Patil, R., Torris, A., Bhat, S., Patil, S., 2019. Mapping fusogenicity of ciprofloxacin-loaded liposomes with bacterial cells. *AAPS PharmSciTech* 20 (5), 180.
- Ramage, G., Rajendran, R., Sherry, L., Williams, C., 2012. Fungal biofilm resistance. *Int. J. Microbiol.* 2012 (1), 528521.
- Rukavina, Z., Vanić, Ž., 2016. Current trends in development of liposomes for targeting bacterial biofilms. *Pharmaceutics* 8 (2), 18.
- Sachetelli, S., Khalil, H., Chen, T., Beaulac, C., Sénéchal, S., Lagacé, J., 2000. "Demonstration of a fusion mechanism between a fluid bactericidal liposomal formulation and bacterial cells." *Biochim. Biophys. Acta (BBA) - B Biomembr.* 1463 (2), 254–266.
- Scheeder, A., Brockhoff, M., Ward, E.N., Kaminski Schierle, G.S., Mela, I., Kaminski, C.F., 2023. Molecular mechanisms of cationic fusogenic liposome interactions with bacterial envelopes. *J. Am. Chem. Soc.* 145 (51), 28240–28250.
- Scriboni, A. B., V. M. Couto, L. N. d. M. Ribeiro, I. A. Freires, F. C. Groppo, E. de Paula, M. Franz-Montan and K. Cogo-Müller (2019). "Fusogenic Liposomes Increase the Antimicrobial Activity of Vancomycin Against *Staphylococcus aureus* Biofilm." *Frontiers in Pharmacology* 10.
- Sharma, S., Mohler, J., Mahajan, S.D., Schwartz, S.A., Bruggemann, L., Aalinkel, R., 2023. Microbial biofilm: a review on formation, infection, antibiotic resistance, control measures, and innovative treatment. *Microorganisms* 11 (6), 1614.
- Silhavy, T.J., Kahne, D., Walker, S., 2010. The bacterial cell envelope. *Cold Spring Harb. Perspect. Biol.* 2 (5), a000414.
- Storm, G., Roerdink, F.H., Steerenberg, P.A., de Jong, W.H., Crommelin, D.J.A., 1987. Influence of lipid composition on the antitumor activity exerted by doxorubicin-containing liposomes in a rat solid tumor model. *Cancer Res.* 47 (13), 3366–3372.
- Wang, D., N. Zeng, C. Li, Z. Li, N. Zhang and B. Li (2024). "Fungal biofilm formation and its regulatory mechanism." *Heliyon* 10(12): e32766.
- Wang, Z., Ma, Y., Khalil, H., Wang, R., Lu, T., Zhao, W., Zhang, Y., Chen, J., Chen, T., 2016. Fusion between fluid liposomes and intact bacteria: study of driving parameters and in vitro bactericidal efficacy. *Int. J. Nanomed.* 11, 4025–4036.
- Wang, D.-Y., van der Mei, H.C., Ren, Y., Busscher, H.J., Shi, L., 2020. "Lipid-Based Antimicrobial Delivery-Systems for the Treatment of Bacterial Infections." *Frontiers Chemistry* 7.
- Webster, P., Webster, A., 2014. Cryosectioning fixed and cryoprotected biological material for immunocytochemistry. *Electron Microscopy: Methods and Protocols* 273–313.
- Wu, H., Moser, C., Wang, H.-Z., Høiby, N., Song, Z.-J., 2015. Strategies for combating bacterial biofilm infections. *Int. J. Oral Sci.* 7 (1), 1–7.
- Yang, L., Liu, Y., Wu, H., Høiby, N., Molin, S., Z. j. Song., 2011. Current understanding of multi-species biofilms. *Int. J. Oral Sci.* 3 (2), 74–81.
- Zhao, A., Sun, J., Liu, Y., 2023. Understanding bacterial biofilms: From definition to treatment strategies. *Front. Cell. Infect. Microbiol.* 13, 1137947.

## Paper II

Ahmed M. Amer, Colin Charnock, Kirill V. Ovchinnikov, Tage Thorstensen, Sanko Nguyen  
**Phospholipid Acyl Chain Length Modulation: A Strategy to Enhance Liposomal Drug  
Delivery of the Hydrophobic Bacteriocin Micrococcin P1 to Biofilms**

*European Journal of Pharmaceutical Sciences*, 211, article 107149 (2025).

DOI: <https://doi.org/10.1016/j.ejps.2025.107149>



Under review in the “**European Journal of Pharmaceutical Sciences**”



## **Phospholipid Acyl Chain Length Modulation: A Strategy to Enhance Liposomal Drug Delivery of the Hydrophobic Bacteriocin Micrococcin P1 to Biofilms**

Ahmed M. Amer <sup>a\*</sup>, Colin Charnock <sup>a</sup>, Kirill V. Ovchinnikov <sup>b</sup>, Tage

Thorstensen <sup>b</sup>, Sanko Nguyen <sup>a</sup>

<sup>a</sup> Department of Life Sciences and Health, Oslo Metropolitan University (OsloMet), Oslo, Norway

<sup>b</sup> AgriBiotix AS, Ås, Norway

\*Corresponding author

## Abstract

This study describes the development of fusogenic liposomes as a drug delivery system for the hydrophobic antimicrobial peptide micrococcin P1 (MP1). The liposomes were formulated using phospholipids with varying acyl chain lengths, with the goal of improving biofilm eradication. Entrapment of MP1 in liposomes effectively improved its stability in solution, as demonstrated by liquid chromatography-mass spectrometry monitoring over a two-month period. Liposomal entrapment lowered the minimum inhibitory concentration of MP1 against several *Staphylococcus aureus* strains, including clinical isolates, by 4- to 16-folds. Increasing the phospholipid acyl chain length (16-carbon to 20-carbon) in the liposomal composition, resulted not only in an improved entrapment of MP1, but also higher antibiofilm activity. Confocal laser scanning microscopy imaging revealed that the MP1-loaded liposomal effect was likely due to disruption of the biofilm matrix. At a concentration of 0.25 µg/mL, MP1 loaded in 1,2-diarachidoyl-sn-glycero-3-phosphocholine (DAPC)-based fusogenic liposomes reduced biofilm cell viability by approximately 55%, compared to only 15% with free MP1 equivalents. However, the increased liposomal bilayer hydrophobicity via the longer acyl chains compromised the physical stability of the fusogenic liposomes. While MP1-loaded liposomes based on the shorter 16-carbon acyl chain 1,2-dipalmitoyl-sn-glycero-3-phosphocholine (DPPC) remained stable for two months, the DAPC liposomes were only stable for two weeks. The physical stability was improved by increasing the concentration of the cationic phospholipid, 1,2-dioleoyl-3-trimethylammonium-propane (DOTAP), from 25 mol% to 50 mol% in the liposomal composition. Overall, these findings highlight the potential of liposomal systems for delivering hydrophobic peptides like MP1 to *Staphylococcus aureus* biofilms, offering promise for improving the treatment of biofilm-associated infections.

## Keywords

Fusogenic liposomes; Micrococcin P1; *Staphylococcus aureus*; Biofilm; Hydrophobic peptide

## 1. Introduction

The development of new antibiotics is struggling to keep pace with the alarming rise of antimicrobial resistance (1). In the last four decades, most of the antibiotics developed have been based on existing antimicrobial agents already in clinical use (2, 3). Strenuous efforts are being made to explore and develop new antibiotics for clinical application. Bacteriocins are ribosomally synthesized antimicrobial peptides produced mainly by gram positive bacteria and typically exhibit antimicrobial activity on closely-related bacterial species (4). Despite being discovered nearly a century ago, bacteriocins have primarily been explored in the food industry, resulting in the established use of nisin as a food preservative, rather than being investigated in pharmaceuticals (5, 6). This limited application is mainly due to inadequate toxicity data available for drug development, as well as the susceptibility of bacteriocins to enzymatic degradation, which reduces their stability and bioavailability (5, 7). Micrococcin P1 (MP1) is a 26-membered ring-based thiopeptide that is produced by bacterial strains from various genera, including *Micrococcus* and *Staphylococcus* (8). It exerts its antibacterial effect by targeting the 50S ribosomal subunit and disrupting protein synthesis (8-10). It has demonstrated antimicrobial activity against various infectious bacterial strains, including methicillin-resistant *Staphylococcus aureus* (MRSA) strains, which is designated as a high-priority global health threat by the World Health Organization (WHO) (11, 12). It has also been shown to work synergistically with other antimicrobial agents, reducing *S. aureus* cell viability within established biofilms (12, 13). MP1 has been found to be non-cytotoxic to human hepatic, monocytic, embryonic kidney and skin keratinocyte cell lines (14, 15). Given this background, MP1 holds promise as a safe and effective antimicrobial agent for use against antibiotic-resistant bacteria, and as such would be a valuable addition to current antibiotic treatments.

Being peptides, bacteriocins are highly prone to chemical degradation, which often leads to a substantial reduction in their antimicrobial efficacy (7). Despite its reported remarkable antibacterial activity, the hydrophobicity and poor water solubility of MP1 have restricted its development into a pharmaceutical product (14, 16). The use of nanoparticulate drug delivery systems offers a potential solution to overcome the limitations associated with bacteriocins as pharmaceutical therapeutics (7, 17). Most of the studies reported in the literature involve nanoparticle loading with the bacteriocin nisin, which resulted in enhanced antimicrobial

activity, reduced enzymatic degradation and improved bioavailability (7). Loading MP1 in polymeric polycaprolactone nanoparticles has been reported to enhance its antibacterial activity after *in vitro* and *in vivo* testing (14). Liposomes, as vesicles composed of phospholipid bilayers, are a versatile drug delivery system capable of entrapping hydrophobic drugs. They stand out as a promising nanoparticle platform due to their exceptional biocompatibility, ability to prevent drug degradation and enhanced biofilm penetration (18, 19). Several studies have reported the advantageous effects of nisin entrapment in liposomes (6, 7); however, the liposomal entrapment of MP1 has yet to be explored.

A recent study revealed that naturally secreted MP1 integrates into bacterial membrane vesicles, enhancing its ability to diffuse through aqueous environments despite MP1's hydrophobic nature (20). On reaching its target bacterial cell, the membrane vesicles carrying MP1 fuse with the cell, enabling MP1 to exhibit its antimicrobial effect (20). As such, using liposomes as drug delivery systems closely mimics this natural process (18). Additionally, the resemblance of liposomal structure to biological membranes, facilitates liposomal fusion with microbial cells (19). This fusion capability can be enhanced by integrating fusogenic phospholipids like 1,2-dioleoyl-sn-glycero-3-phosphoethanolamine (DOPE) into the liposome formulation, increasing their flexibility and forming fusogenic liposomes (21). The ability of fusogenic liposomes to enhance the antimicrobial and antibiofilm activity of various antimicrobial agents has been previously reported in the literature (22-24). Additionally, liposomal entrapment is beneficial to shield sensitive molecules, such as peptides, from inactivation and degradation (25). Incorporating MP1 in fusogenic liposomes may protect it from degradation, facilitate its diffusion in aqueous environments and promotes fusion with target cells, thus mimicking the behaviour of naturally secreted bacterial MP1 integrated into membrane vesicles.

In the present study, fusogenic liposomes based on phospholipids with various acyl chain lengths (C16, C18 and C20) were prepared for entrapping MP1. The liposomes were characterized and evaluated in terms of physicochemical properties, drug entrapment efficiency, and antimicrobial and antibiofilm activity on *S. aureus*, including a number of clinical isolates. To our knowledge, this study is the first to successfully develop a liposomal formulation of MP1 and investigate the effects of MP1 liposomal entrapment on its antimicrobial and antibiofilm activities.



## 2. Materials and methods

### 2.1. Materials

The lipids 1,2-dipalmitoyl-sn-glycero-3-phosphocholine (DPPC), 1,2-distearoyl-sn-glycero-3-phosphocholine (DSPC), 1,2-diarachidoyl-sn-glycero-3-phosphocholine (DAPC), 1,2-dioleoyl-3-trimethylammonium-propane (DOTAP), 1,2-dioleoyl-sn-glycero-3-phosphoethanolamine (DOPE) and 1,2-dioleoyl-sn-glycero-3-phosphoethanolamine-N-(lissamine rhodamine B sulfonyl) (18:1 Liss Rhod-PE) were purchased from Avanti Polar Lipids (Alabaster, AL, USA). Cation-adjusted Mueller Hinton broth (MHB), tryptic soy agar (TSA) and tryptic soy broth (TSB) were purchased from Oxoid/Thermo Fischer (MA, USA). Triton X-100, 4',6-diamidino-2-phenylindole (DAPI), dimethyl sulfoxide (DMSO), Tween 80, vancomycin hydrochloride (Product No. 94747) and phosphate buffered saline (PBS) tablets were purchased from Merck (Darmstadt, Germany). D-luciferin sodium salt was purchased from Gold Biotechnology (St Louis, MO, USA). Acetonitrile and formic acid, both HPLC/MS grade, and high purity chloroform and methanol were purchased from VWR BDH Chemicals (Oslo, Norway). PD-10 preppacked columns (Sephadex G-25M) were purchased from Cytiva/Merck (Darmstadt, Germany). Ultrapure water (Milli-Q, Merck Millipore, Germany) was used in the preparation of liposomes and high-performance liquid chromatography-mass spectrometry (HPLC-MS) analyses. *Staphylococcus aureus* (ATCC 29213) was purchased from American Type Culture Collection (Rockville, MD, USA). *S. aureus* Xen 29 bioluminescent bacteria derived from ATCC 12600 was purchased from Revvity (MA, USA). *S. aureus* clinical isolates P14 and P20 were obtained from the eyes of patients diagnosed with severe dry eye disease in a study conducted by our research group, as previously described (26). MP1 from *S. equorum* was purified and provided by AgriBiotix AS, Norway, as previously published (27).

### 2.2. Preparation of fusogenic liposomes

Fusogenic liposomes were prepared by a standard thin film hydration–extrusion method (28), incorporating 0.5 mg/mL MP1 and 75 mM total lipid concentration. Different combination of phospholipids and MP1 were dissolved in chloroform and the solutions evaporated to dryness in a rotary evaporator. To ensure complete removal of organic residues, lipid films were further dried under vacuum overnight. The lipid films were subsequently hydrated above the phase transition temperatures ( $T_m$ ) of the main saturated phospholipid incorporated in the

liposome: 41°C for DPPC, 55°C for DSPC, and 66°C for DAPC, as indicated by the phospholipids supplier (29). Hydration was performed using 5 mM phosphate buffer, pH 9. After preparation, samples were stored at 4°C to equilibrate overnight. Size reduction was performed by extrusion above the phase transition temperature first through 400 nm followed by 200 nm polycarbonate membranes (Avanti Polar Lipids, USA) using a Mini-Extruder (Avanti Polar Lipids, USA). Each extrusion step included 11 passes through the polycarbonate membrane. As controls, empty liposomes without MP1 were also prepared using the same method. Liposomal dispersions were stored under nitrogen at 4°C throughout the entire study.

### 2.3. Characterization of fusogenic liposomes

Before particle size and zeta potential measurements, liposomal preparations were diluted 1:40 with 5 mM phosphate buffer, pH 9. Particle size and polydispersity index (PDI) were measured by dynamic light scattering (DLS) using a Zetasizer Ultra (Malvern Panalytical Ltd, UK). Each sample was measured three times at 25°C with backscattering angle at 173° and a refractive index of 1.33. The zeta potential was determined based on electrophoretic light scattering (ELS) principles using the same instrument. Each sample was measured three times at 25°C with refractive index of 1.33. Liposomal characterization was carried out 24 h after preparation (i.e., time point zero) and at various time intervals over three months to evaluate the *in vitro* stability of the formulations (n = 3 for each formulation).

Transmission electron microscopy (TEM) micrographs of empty liposomal preparations were obtained using a negative-staining embedding technique. Samples were prepared following a previously published protocol (30), with some modifications. A 5 µL drop of each liposomal formulation was adsorbed onto a carbon-coated copper grid (300 mesh), which was glow discharged to create a charge opposite to that of the liposomes. After a 30-second contact time, the grid was washed twice with Milli-Q water for one minute each time. The samples were then exposed to a 20 µL drop of 1% (w/v) uranyl acetate for 30 seconds, followed by a second treatment of 30 seconds duration with a fresh drop of the same solution. For embedding, the grids were transferred to a 20 µL drop of a mixture of 0.4% (w/v) uranyl acetate and 1.8% (w/v) methylcellulose, followed by 2 minutes of incubation on a second drop of the same mixture. For drying, the grids were picked up with 3.5 mm metal loops, creating a thin layer of methylcellulose by gently dragging the loop's edge across filter paper to remove

excess liquid. The thin layer of methylcellulose was then allowed to air dry before imaging by TEM (JEM-1400, JEOL Ltd, Japan) at 120 kV.

#### 2.4. Quantification of MP1 in liposomes

After extrusion and equilibration over night at 4°C, unbound MP1 was separated from the liposomes using PD-10 prepacked columns and eluted with 5 mM phosphate buffer, pH 9. Eluted liposomes were then mixed with 1% Triton X-100 (1:1) and sonicated (Elmasonic S30, Elma Ultrasonic Technology, Germany) for 5 minutes to break the liposomal membrane and release the entrapped MP1. Subsequently, samples were diluted with a mixture of acetonitrile: water (1:1) + 0.1% formic acid and then analysed by HPLC (1290 Infinity II, Agilent Technologies, Germany). MP1 was quantified using a UV detector at 280 nm and a quadrupole mass spectrometry (MS) detector employing a C18 column (Gemini-NX - 3µm - 110A - 150 x 4.6 mm, Phenomenex, USA) and a gradient mobile phase method as described in the supplementary materials (**Supplementary Table S1**). Entrapment efficiency in percentage (EE%) was calculated using the following equation:

$$EE\% = \frac{\text{Amount of MP1 in liposomes (mg)}}{\text{Total amount of MP1 added (mg)}} \times 100 \quad (i)$$

The chemical stability of MP1 entrapped into liposomes, following the removal of free MP1, was monitored across different formulations at specified intervals over two months of storage at 4°C. The same sample preparation and quantification method described above was used. The chemical stability of liposomal-MP1 was compared with that of free MP1 prepared by dissolving MP1 in methanol, and diluting it with 5 mM phosphate buffer (pH 9) to a final concentration of 25 mg/mL. The free and liposomal-MP1 preparations were stored under identical conditions prior to analysis.

#### 2.5. Determination of minimum inhibitory concentration (MIC)

The minimum inhibitory concentration (MIC) was determined by the broth microdilution method. Stock solutions of MP1 and vancomycin (1600 µg/mL) were prepared in DMSO. Serial dilutions in DMSO were performed according to CLSI guidelines (31), yielding concentrations from 800 to 1.56 µg/mL. Each concentration was further diluted 1:100 in either MHB with or

without 0.002% Tween 80, resulting in final concentrations ranging from 8 to 0.0156 µg/mL. A 100 µL aliquot of each dilution was added to round-bottom polystyrene 96-well microtiter plates (Corning®, USA). For MP1-loaded liposomes, dilutions were prepared to obtain MP1 concentration of 8 µg/mL, based on the actual entrapment efficiency (EE%) quantified by HPLC-MS. Serial dilutions were then performed in MHB with or without 0.002% Tween 80 to achieve concentrations ranging from 8 to 0.0156 µg/mL. A 100 µL aliquot of each dilution was added to the microtiter plates. Equivalent amounts of empty liposomes were diluted with growth medium in separate wells as controls. Bacterial inoculums of *S. aureus* (DSM 2569, Xen 29, clinical isolates P14 and P20) were prepared from overnight TSA cultures incubated at 37 °C. Bacterial colonies were suspended in 0.9% NaCl to reach a 0.5 McFarland turbidity measured spectrophotometrically ( $\approx 10^8$  CFU/mL), then diluted in cation-adjusted MHB with or without 0.002% Tween 80 to achieve  $\approx 10^5$  CFU/mL in each well. Uninoculated wells served as negative controls, and inoculated wells without antibiotics as positive controls. Plates were incubated at 37 °C for 18 h, and MICs were determined visually by two researchers according to CLSI guidelines (31).

## 2.6. Screening of antibiofilm activity of MP1-loaded liposomes

The *S. aureus* Xen 29 strain was cultured to form biofilms in 96-well, flat-bottom, white polystyrene plates (Corning®, USA) as previously described (32). *S. aureus* (Xen 29) bacterial broth was prepared by suspending bacterial colonies from overnight TSA cultures in 0.9% NaCl to achieve a 0.5 McFarland standard. This was followed by dilution in tryptic soy broth (TSB) supplemented with 1% (w/v) glucose to a final concentration of  $10^5$  CFU/mL. Two hundred µL were then transferred to each well and incubated at 37°C for 72 h before treatment. Growth medium was carefully replaced every day with fresh medium taking care not to disrupt the biofilm. At the end of the incubation period, growth medium was gently removed, and wells were washed once with PBS. Then wells were treated by addition of vancomycin, free MP1 or MP1-loaded liposomes diluted with the growth medium to yield concentrations equivalent to  $\frac{1}{2} \times \text{MIC}$ , MIC,  $2 \times \text{MIC}$ ,  $4 \times \text{MIC}$ ,  $8 \times \text{MIC}$ ,  $16 \times \text{MIC}$  and  $32 \times \text{MIC}$  ( $n = 5$ ). Other wells were treated with empty liposomes, while only growth medium was added to the control wells. After 24 h incubation, wells were carefully washed twice with PBS. Subsequently, 150 µL of growth medium containing luciferin (150 µg/mL) was added to the wells and biofilm material was

dispersed in this by scrapping each well with a sterile dental micro applicator brush (Guangzhou Jaan Medical, China) to allow a uniform contact of cells with luciferin. Plates were then incubated for 1 h at 37°C followed by bioluminescence measurement using a multimode plate reader (Victor Nivo, Perkin Elmer®, USA). The experiment was independently repeated three times. The percentage change in biofilm metabolic activity after treatment was calculated based on the reduction in bioluminescence, which serves as an indication of biofilm viability as follows:

$$\% \text{ Change in Biofilm Metabolic Activity} = \frac{\text{Biolum.}_{\text{test}}}{\text{Biolum.}_{\text{control}}} \times 100 \quad (\text{ii})$$

where  $\text{Biolum.}_{\text{test}}$  and  $\text{Biolum.}_{\text{control}}$  are the measured test and control bioluminescence, respectively.

## 2.7. Treatment of established biofilm on polytetrafluoroethylene (PTFE)

PTFE, commonly used as a biomedical material for catheter production, was selected as the surface for biofilm formation. *S. aureus* (Xen 29) bacterial broth was prepared in TSB with 1% glucose, as detailed in **section 2.6**. Before inoculation, 1 cm PTFE rods were disinfected by immersion in sterile water at 70°C for 30 minutes, followed by a rinse with 70% ethanol and three washes with sterile water. Subsequently, rods were placed in a sterile Eppendorf tube (two rods per tube) and 0.5 mL of bacterial suspension was added. Biofilms were allowed to form on the PTFE rods over 72 h at 37°C, with orbital shaking at 60 rpm; fresh medium was supplied every 24 h.

After the incubation period, rods were rinsed once in PBS and transferred to new tubes. Treatment was performed by adding 0.5 mL of either free MP1 or MP1-loaded DAPC liposomes in growth medium at concentrations of  $\frac{1}{2} \times \text{MIC}$ , MIC,  $2 \times \text{MIC}$ ,  $4 \times \text{MIC}$ ,  $8 \times \text{MIC}$ ,  $16 \times \text{MIC}$ , and  $32 \times \text{MIC}$  ( $n = 3$ ). Other rods were incubated without antimicrobial agents as positive controls, while others were incubated without cells as negative controls. Rods were incubated for 24 h at 37°C, then washed twice in PBS and transferred to tubes prefilled with 0.2 mL of growth medium containing luciferin (150  $\mu\text{g/mL}$ ) and sterile 0.1 mm glass beads. Biofilms were dispersed by vortex mixing for 20 seconds, sonication for 5 minutes, and another 20 seconds vortex mixing. Tubes were then incubated statically for 1 h at 37°C. After incubation, tubes were vortex mixed again for 20 seconds, and 150  $\mu\text{L}$  biofilm suspension was

transferred to 96-well, flat-bottom, white polystyrene plates (Corning®, USA) for bioluminescence measurement. The percentage change in cellular metabolic activity after treatment was calculated as described in equation (ii), section 2.6. The experiment was independently repeated two times with newly prepared liposomal formulation and freshly cultured bacteria.

## 2.8. Biofilm analysis with confocal laser scanning microscopy (CLSM)

### 2.8.1. Biofilm preparation

Biofilms were prepared using *S. aureus* Xen 29 broth in TSB with 1% glucose, as detailed in **section 2.6**. One millilitre of the bacterial suspension was added to each well of 4-well chamber slides (Nunc Lab-Tek II CC2, Thermo Scientific) and incubated at 37°C with shaking at 60 rpm for 72 h to allow biofilm formation. The medium was carefully replaced daily without disrupting the biofilms. After incubation, biofilms were washed twice with sterile water before treatment.

### 2.8.2. Imaging of biofilm penetration by empty liposomes

To assess liposomal penetration, fluorescently labelled DPPC, DSPC, and DAPC liposomes were prepared as outlined in Section 2.2, with 0.5 mol% Rho-PE. Liposomes were diluted 1:1 in growth medium and added to biofilms. Slides were incubated at 37°C with shaking at 60 rpm for 24 h. Following incubation, biofilms were washed twice with sterile water and stained with 100 µL of DAPI solution (0.1 µg/mL) for 30 minutes. The stain was then removed, and wells were washed twice with sterile water before fixing the biofilms with 1% paraformaldehyde in 0.9% NaCl. After fixation, wells were washed twice with sterile water, and 50 µL of antifade mounting solution (AFR3, Citifluor Ltd, UK) was added. Confocal microscopy (TCS SP8 STED, Leica Microsystems, Germany) was used to examine the samples, and z-stacks were acquired for 3D visualisation of the biofilms using ImageJ software (National Institutes of Health, Maryland, USA).

### 2.8.3. Imaging of biofilm after treatment with MP1 and MP1-loaded DAPC liposomes

The antibiofilm effects were evaluated using CLSM as previously described (32, 33). Briefly, established biofilms were treated with free MP1 and MP1-loaded DAPC liposomes at concentrations equivalent to  $\frac{1}{2}\times$ MIC, MIC,  $2\times$ MIC,  $4\times$ MIC,  $8\times$ MIC,  $16\times$ MIC, and  $32\times$ MIC.

Control wells contained only fresh medium. Wells were incubated at 37°C with orbital shaking at 60 rpm for 24 h. After incubation, biofilms were washed twice with sterile water, followed by the addition of 200 µL of the FilmTracer™ LIVE/DEAD® Biofilm Viability Kit staining solution to each well. The staining solution was prepared by adding 3 µL of SYTO 9 stain and 3 µL of propidium iodide stain to 1 mL of sterile water. Slides were incubated at room temperature for 30 minutes, protected from light. The staining solution was then removed, and wells were rinsed twice with sterile water. Finally, 50 µL of antifade mounting solution (AFR3, Citifluor Ltd, UK) was added, and the slides were sealed with a coverslip.

Biofilms were imaged using the confocal microscope as previously mentioned (**section 2.8.2**), and image processing and 3D visualisation were performed using ImageJ software. The experiment was repeated twice with freshly prepared liposomal formulations and cultured bacteria. Cell viability was determined by counting SYTO 9-stained live (green) and propidium iodide-stained dead (red) cells in five randomly selected areas per well. The percentage of viable cells was calculated as follows:

$$\% \text{ Cell Viability} = \frac{\text{Number of live cells}_{(\text{green cells})}}{\text{Total number of cells}_{(\text{green \& red cells})}} \times 100 \quad (\text{iii})$$

## 2.9. Statistical analysis

Results are expressed as the mean ± standard deviation (SD). Significant differences between treatments were evaluated using analysis of variance (ANOVA), with the Bonferroni correction applied to adjust the significance level for multiple comparisons. For experiments involving only two treatments (**section 3.6**), significance was assessed using a t-test. A significance level of P-value = 0.05 was used to determine statistical significance.

### 3. Results and Discussion

#### 3.1. Characterization of fusogenic liposomes

Particle size, PDI, zeta potential and entrapment efficiency of empty and MP1-loaded liposomes after preparation are presented in **Table 1**. All liposomal formulations exhibited particle sizes less than 500 nm and narrow size distributions ( $PDI < 0.2$ ), which are considered favourable for biofilm penetration (34). The particle size increased slightly with increasing phospholipid carbon chain length from C16 in DPPC to C20 in DAPC for both empty and MP1-loaded liposomes. Incorporating MP1 within liposomes, however, led to a decrease in liposomal size. Similar findings have been reported by Jaradat *et al.* for liposomal formulation of the hydrophobic drug paclitaxel (35). The authors attributed this reduction in size to tighter packing of the drug within the liposomal bilayer (35). This explanation may also apply to the obtained results in our study, as hydrophobic interactions between MP1 and phospholipid molecules likely contribute to tight liposomal membrane packing effect. TEM imaging of empty liposomal vesicles is shown in **Fig. 1**. The vesicle sizes observed using TEM are comparable to the results obtained using the DLS method. The TEM image of DAPC liposomes shows larger particle size and broader size distribution compared to the images with the other liposomal formulations.

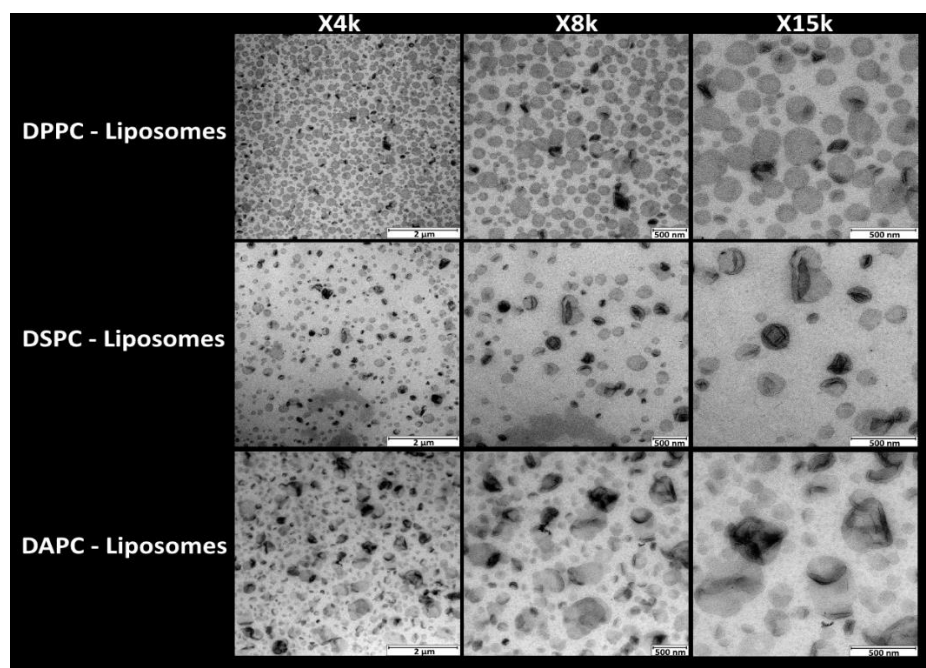


**Fig. 1.** TEM micrographs of empty liposomes containing different acyl chain length phospholipids: 1,2-dipalmitoyl-sn-glycero-3-phosphocholine (DPPC), 1,2-distearoyl-sn-glycero-3-phosphocholine (DSPC) and 1,2-diarachidoyl-sn-glycero-3-phosphocholine (DAPC).



**Table 1.** Particle size (presented as Z-average), PDI, zeta potential and percentage entrapment efficiency (EE%) presented as mean  $\pm$  SD (n = 3) for empty and drug-loaded liposomal formulations characterized at time point zero, following preparation.

	Liposomal formulation	Phospholipid composition (mol %)	Z-Average (nm) $\pm$ SD	Polydispersity index (PDI) $\pm$ SD	Zeta potential (mV) $\pm$ SD	Entrapment Efficiency (EE%)
MP1-Loaded Liposomes	MP1-DPPC	DPPC:DOPE:DOTAP (37.5:37.5:25)	105.0 $\pm$ 3.9	0.08 $\pm$ 0.016	+25.2 $\pm$ 0.8	16.36 $\pm$ 6.2
	MP1-DSPC	DSPC:DOPE:DOTAP (37.5:37.5:25)	116.4 $\pm$ 5.4	0.06 $\pm$ 0.015	+24.9 $\pm$ 1.6	18.77 $\pm$ 6.0
	MP1-DAPC	DAPC:DOPE:DOTAP (37.5:37.5:25)	159.7 $\pm$ 4.4	0.04 $\pm$ 0.016	+25.3 $\pm$ 1.7	21.03 $\pm$ 5.7
Empty Liposomes	DPPC	DPPC:DOPE:DOTAP (37.5:37.5:25)	135.4 $\pm$ 12.3	0.08 $\pm$ 0.014	+23.9 $\pm$ 4.2	-
	DSPC	DSPC:DOPE:DOTAP (37.5:37.5:25)	148.3 $\pm$ 12.5	0.07 $\pm$ 0.032	+23.8 $\pm$ 3.2	-
	DAPC	DAPC:DOPE:DOTAP (37.5:37.5:25)	219.7 $\pm$ 56.8	0.15 $\pm$ 0.067	+23.5 $\pm$ 1.4	-

The measured positive zeta potentials (**Table 1**) reflect the presence of the positively charged lipid DOTAP in the liposomal formulation. DOTAP was incorporated into liposomes to facilitate electrostatic attraction between the liposomes and anionic MP1 at pH 9, thus enhancing MP1 entrapment during preparation. Moreover, the entrapment of MP1, did not alter the zeta potential, suggesting that MP1 is predominantly entrapped within the liposomal membrane rather than adsorbed onto the surface. The EE% values indicate a trend, where increasing the phospholipid acyl chain length leads to a slight increase in EE%. The highest EE% was observed with 20-carbon DAPC liposomes (21%), followed by 18-carbon DSPC (19%) and 16-carbon DPPC liposomes (16%) (**Table 1**). Since the DOPE and DOTAP contents were consistent across all liposomal formulations, the observed differences in EE% can be attributed to the acyl chain length of phosphatidylcholine. Lipid composition is known to influence EE% of hydrophobic drugs based on their partitioning in the liposomal bilayer (36). In this case, stronger hydrophobic interactions between the longer DAPC chains and the hydrophobic peptide MP1

enhanced drug entrapment within the membrane. Additionally, the lipid composition is also known to influence liposomal properties such as membrane thickness and fluidity, which may also have consequences for the EE% and overall physical stability of the liposomal vesicles (36).

### 3.2. *In vitro* stability of MP1 and MP1-loaded liposomes

The physical stability of the liposomal formulations, both with and without MP1, over a two-month period is presented in **Fig. 2a-c**. Both empty and MP1-loaded DPPC liposomes exhibited robust physical stability, maintaining a consistent particle size with only a slight increase in PDI, which remained well below 0.2. However, the stability decreased with longer acyl chain lipids in the liposomal formulation. The particle size of empty DSPC liposomes gradually increased from 148 nm on day one to 196 nm after two months. MP1-loaded DSPC liposomes were even more unstable, with particle size doubling within four days and reaching on average 407 nm by the end of two months (**Fig. 2a-b**). The observed increase in PDI values corresponds with the particle size data, indicating reduced size uniformity across the liposomal formulations. Both empty and MP1-loaded DAPC liposomes exhibited a similar trend to DSPC but with a more rapid decline in stability. Their average particle size exceeded 800 nm, with a PDI approaching 0.4 after just 14 days. The appearance of visible particulates after 21 days prevented further monitoring (**Fig. 2a-b**).

Previous studies suggest that liposomes composed of saturated lipids with high transition temperatures ( $T_m$ ) generally exhibit greater stability than those with lower  $T_m$  (37, 38). Since  $T_m$  increases with acyl chain length, the poor stability of DAPC liposomes ( $T_m = 66^\circ\text{C}$ ) was unexpected. However, the liposomes in our study differ from previous formulations as they contain the fusogenic phospholipid DOPE. The high proportion (37.5 mol%) of this unsaturated and flexible lipid appears to impact the membrane stability. Based on the current data, it remains unclear whether the observed increase in particle size is due to aggregation, fusion, or a combination of both. Additionally, all formulations contained 25 mol% DOTAP, which should be sufficient to prevent aggregation via electrostatic repulsion. The stable zeta potential values throughout the study indicate no significant surface charge alterations, despite the observed changes in liposomes size and PDI (**Fig. 2c**). MP1-loaded liposomes exhibited even lower stability than their empty counterparts, likely due to MP1 incorporation into the liposomal bilayer, further destabilizing the membrane. This aligns with previous

reports linking peptide entrapment to liposomal instability, which can result in liposome aggregation, fusion or leakage (39).

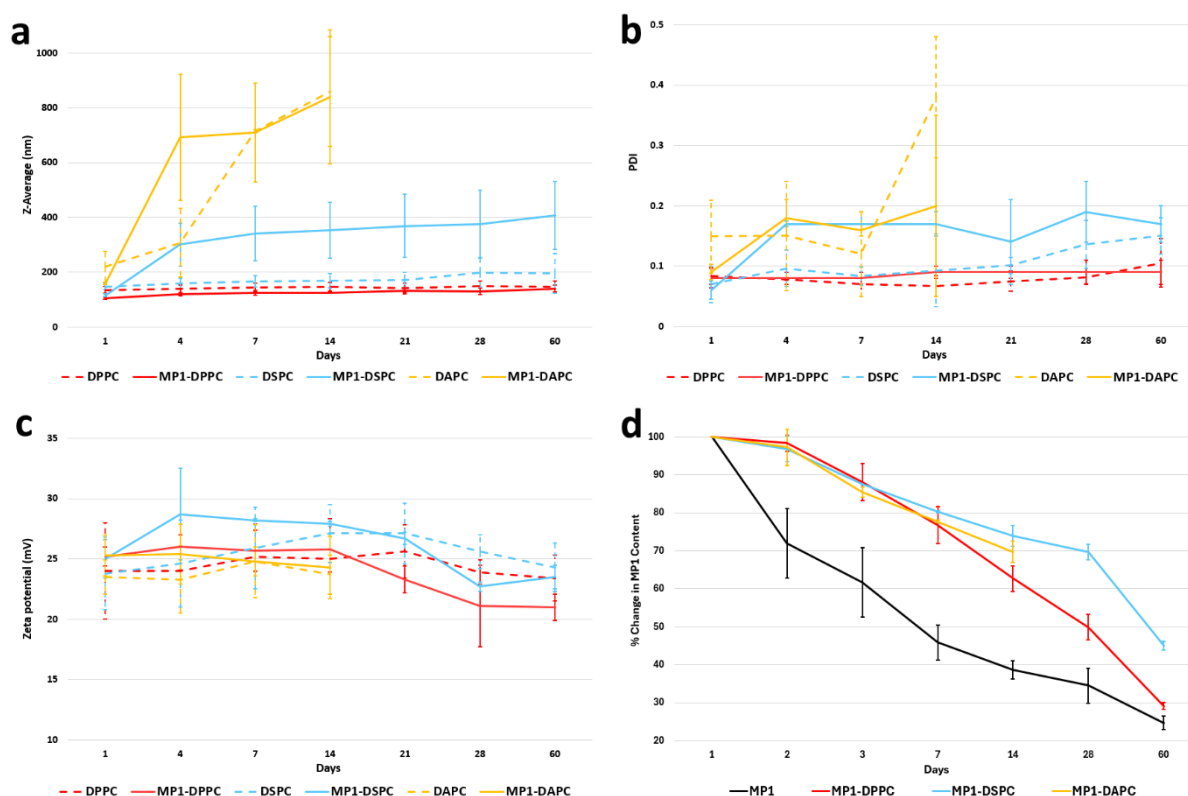


**Fig. 2.** *In vitro* stability of DPPC, DSPC, and DAPC phospholipids stored at 4°C over a period of two months. Empty lipids (dashed line) and MP1-loaded liposomes (solid line) were investigated in terms of (a) liposomal sizes presented as Z-average, (b) polydispersity indices (PDIs), (c) zeta potentials and (d) chemical stability of liposomal entrapped MP1 versus free MP1. The bars and the data points in the graphs represent mean  $\pm$  SD ( $n = 3$ ).

The stability of MP1 in aqueous solution was compared to its stability when incorporated into various liposomal formulations after the removal of unbound MP1 (**Fig. 2d**). The MP1 content measured by HPLC-MS gradually decreased over time across all samples. However, this decrease was significantly smaller for MP1-liposomal formulation. The peptide loss could result from the adsorption of the hydrophobic MP1 onto the container surface (40, 41) and/or chemical hydrolysis of MP1 over time. However, liposomal entrapment effectively minimized this effect, as MP1-loaded formulations retained significantly higher peptide content than free MP1 in solution throughout the study (**Fig. 2d**). No significant differences ( $P < 0.05$ ) in MP1 content were observed among the liposomal formulations during the first two weeks of the study. Monitoring of MP1-loaded DAPC liposomes was discontinued at this point due to their

previously described physical instability. By day 28, MP1-loaded DPPC liposomes showed a greater reduction in MP1 content than DSPC liposomes. This may be due to the shorter acyl chain of DPPC, which provides weaker hydrophobic interactions with MP1, leading to leakage and a faster decline in peptide content over time. Collectively, these findings demonstrate that liposomal entrapment effectively shields and protects MP1 during storage, with the degree of protection depending on the specific liposomal composition.

### 3.3. Minimum inhibitory concentration (MIC) of MP1 and MP1-loaded liposomes

In this study, fusogenic liposomes were prepared by the inclusion of DOPE at a uniform concentration of 37.5 mol% in all liposomal preparations. Fusogenic liposomes are expected to exhibit a higher tendency for liposomal fusion with microbial cells compared to conventional liposomes, potentially enhancing the delivery and antimicrobial activity of MP1 (22-24). The MIC assay was used to assess the effectiveness of MP1-liposomal entrapment against planktonic bacteria. MIC values for free MP1, MP1-loaded liposomes, and vancomycin, with and without 0.002% Tween 80, were measured across various *S. aureus* strains and presented in **Table 2**. The MIC for vancomycin against the quality control strain *S. aureus* ATCC 29213 fell within the CLSI guideline range (0.5–2 µg/mL) (31), confirming the validity of the experimental procedure. Empty liposomal formulations showed no antimicrobial activity, with bacterial growth similar to the positive control.

In a previous study using chemically synthesized MP1, the MIC against *S. aureus* ATCC 29213 was reported as 4 µg/mL (9), consistent with our findings for MP1 in the absence of Tween 80 (**Table 2**). Adding small amounts of surfactants like Tween 80 to MIC assays is a common approach to prevent antimicrobial adsorption to the plastic microplate surface (42), which is particularly relevant for the hydrophobic compounds as MP1. Our results showed that MIC values for the hydrophilic vancomycin remained unchanged in the presence of Tween 80 (**Table 2**), whereas those for hydrophobic MP1 and MP1-loaded liposomes varied.

Without Tween 80, MP1-loaded liposomes exhibited lower MIC values than free MP1 across all tested *S. aureus* strains, highlighting the role of liposomal entrapment in maintaining MP1's antimicrobial activity. This aligns with findings by Liu et al. (14), who reported that

incorporating MP1 into polycaprolactone nanoparticles reduced MIC values from 0.5 to 0.125 µg/mL against *S. aureus* in the absence of Tween 80.

The acyl chain length of the liposomal composition also influenced MIC values. Upon removal of Tween 80, MIC values increased. DSPC- and DAPC-based MP1 liposomes showed a 0- to 4-fold rise, while DPPC-based liposomes exhibited an increase of up to 8-fold (**Table 2**). The larger MIC increase observed with DPPC liposomes may be due to weaker hydrophobic interactions between MP1 and the shorter DPPC acyl chains, leading to greater MP1 leakage. In contrast, free MP1 was rapidly depleted due to adsorption onto the microplate surface in the absence of Tween 80, contributing to the observed MIC increase. These findings align with the conclusion by Liu et al. (20), that MP1's hydrophobicity limits its antimicrobial efficacy and that an effective drug delivery system is critical to overcoming this limitation (20).

**Table 2.** MIC (µg/mL) for different *S. aureus* strains tested with free MP1, MP1-loaded liposomes and vancomycin, both with and without addition of 0.002% Tween 80 to the growth medium (n = 3).

		<i>S. aureus</i> strain			
		ATCC 29213	Xen 29	P14	P20
Growth medium with 0.002% Tween 80	MP1	0.25 – 0.5	0.03 - 0.125	0.06 - 0.125	0.25 – 0.5
	MP1 – DPPC	0.25 – 0.5	0.03 - 0.06	0.03 - 0.06	0.125 – 0.25
	MP1 – DSPC	0.25 – 0.5	0.03 - 0.06	0.03 - 0.06	0.125 – 0.25
	MP1 - DAPC	0.25 – 0.5	0.03 - 0.06	0.03 - 0.06	0.125 – 0.25
	Vancomycin	1	1	1	0.5 - 1
Growth medium without Tween 80	MP1	2-4	1-2	1-2	2-4
	MP1 – DPPC	1	0.25	0.25	1
	MP1 – DSPC	0.5	0.125	0.125	0.25
	MP1 - DAPC	0.5	0.125	0.125	0.25
	Vancomycin	1	1	1	1

In the presence of Tween 80, a marked decrease in MIC was observed for all tested *S. aureus* strains with free MP1. This reduction suggests that Tween 80 minimized MP1 loss by

adsorption, thereby enhancing its antimicrobial activity. Moreover, free MP1 and MP1-loaded liposomes demonstrated similar MIC values, indicating that liposomal entrapment did not compromise the antimicrobial activity of MP1.

### 3.4. Microscopic evaluation of biofilm penetration by empty liposomes

The ability of empty fusogenic liposomes (based on DPPC, DSPC, and DAPC) to penetrate a mature *S. aureus* biofilm was evaluated using CLSM imaging. These liposomes also included the cationic lipid DOTAP in their composition. Generally, nanoparticle interactions with the biofilm matrix depend on their physicochemical properties, such as particle size, surface charge and hydrophobicity (43). CLSM 2D images and 3D visualizations generated with ImageJ software showed that all three liposomal formulations penetrated and diffused within the biofilm layers (**Fig. 3**). These results are in line with the importance of nanoparticulate size and positive surface charge for biofilm interaction. The positive surface charge of nanoparticles has been reported to facilitate strong electrostatic interactions with negatively charged biofilm components, such as extracellular DNA, and enhances binding to negatively charged microbial cell surfaces within the biofilm (43, 44). These findings indicate that the liposomal preparations described in this study have potential as effective drug delivery systems for antimicrobial agents targeting biofilm-associated infections.

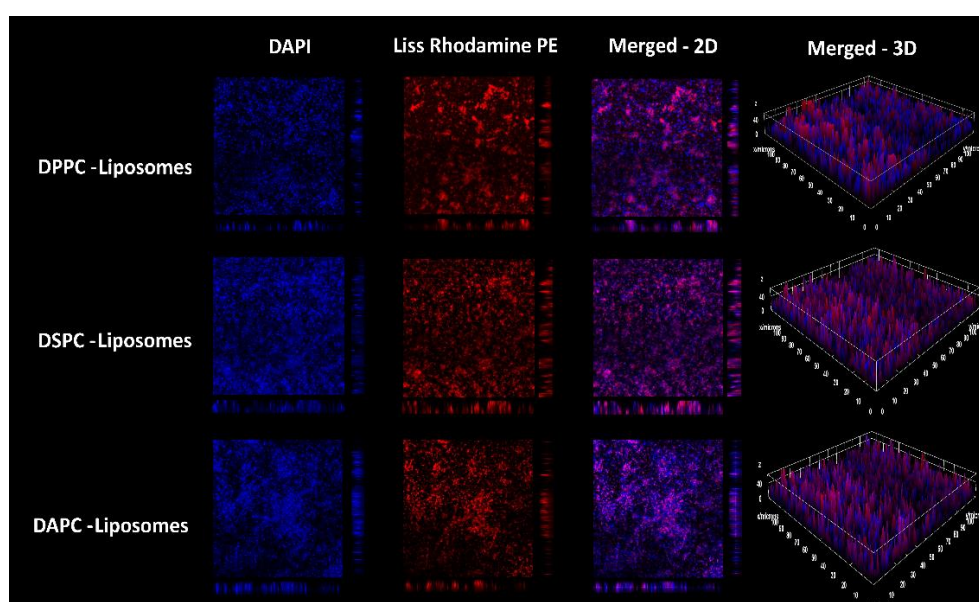


**Fig. 3.** Biofilm penetration of empty liposomes prepared using phospholipids with various acyl chain length (DPPC, DSPC and DAPC) shown as 2D images representing biofilm cells (DAPI) and liposomes (Liss Rhodamine) and as 3D visualizations obtained from CLSM z-stacks.

### 3.5. Screening of antibiofilm activity of MP1 and MP1-loaded liposomes

*S. aureus* is among the pathogens most commonly associated with implant-related biofilm infections (45). Screening the antibiofilm activity of free MP1, MP1-loaded liposomes and vancomycin was performed using bioluminescent *S. aureus* Xen 29. The results from three independent experimental rounds of testing are shown in **Fig. 4a-c**. For purposes of comparison, the effect of the empty liposomes on the biofilm is presented in **Fig. 4d**. The concentration of empty liposomes used as a control matches the amount of liposomal material present in MP1-loaded liposomes, ranging from 4×MIC to 32×MIC. As the concentration of empty liposomes increased, a gradual decrease in the measured metabolic activity of biofilm cells was seen (**Fig. 4d**). Since empty liposomes demonstrated no antimicrobial effect in MIC testing (**Section 3.3**), the observed reduction in metabolic activity is likely due to a decrease in biofilm mass rather than direct effects on cellular viability. Liposomal penetration into the biofilm may cause slight structural disruption, leading to cell detachment from the matrix, which in turn could reduce the measured metabolic activity of the biofilm. Mu *et al.* (46) reported the ability of gold nanoparticles to disrupt established biofilms after coating the particles with phosphatidylcholine. The ability of amphiphilic molecules, such as phospholipids, to disrupt biofilms is frequently reported in the literature (47-49). In another study involving cationic liposomes (50), scanning electron microscopy confirmed a significant reduction in biofilm mass following treatment with empty liposomes. In our work, the effect of empty, cationic liposomes on biofilm was more pronounced with DAPC-based liposomes. Here, a 0.6 mM lipid concentration (equivalent to 16×MIC) resulted in an approximately 40% decrease in the metabolic activity, whereas the corresponding values for both DPPC and DSPC liposomes were less than 10% (**Fig. 4d**). Moreover, by comparing the activity of various MP1-loaded liposomes (**Fig. 4a-c**), the antibiofilm activity was generally found to follow the order: MP1-DAPC > MP1-DSPC > MP1-DPPC. The greater effect of MP1-loaded DAPC liposomes is in agreement with the observed effect of the corresponding empty liposomes and suggests the influence of the phospholipid acyl chain length on the liposomal-biofilm matrix interaction. However, further research work is needed to clarify the reason for this effect.

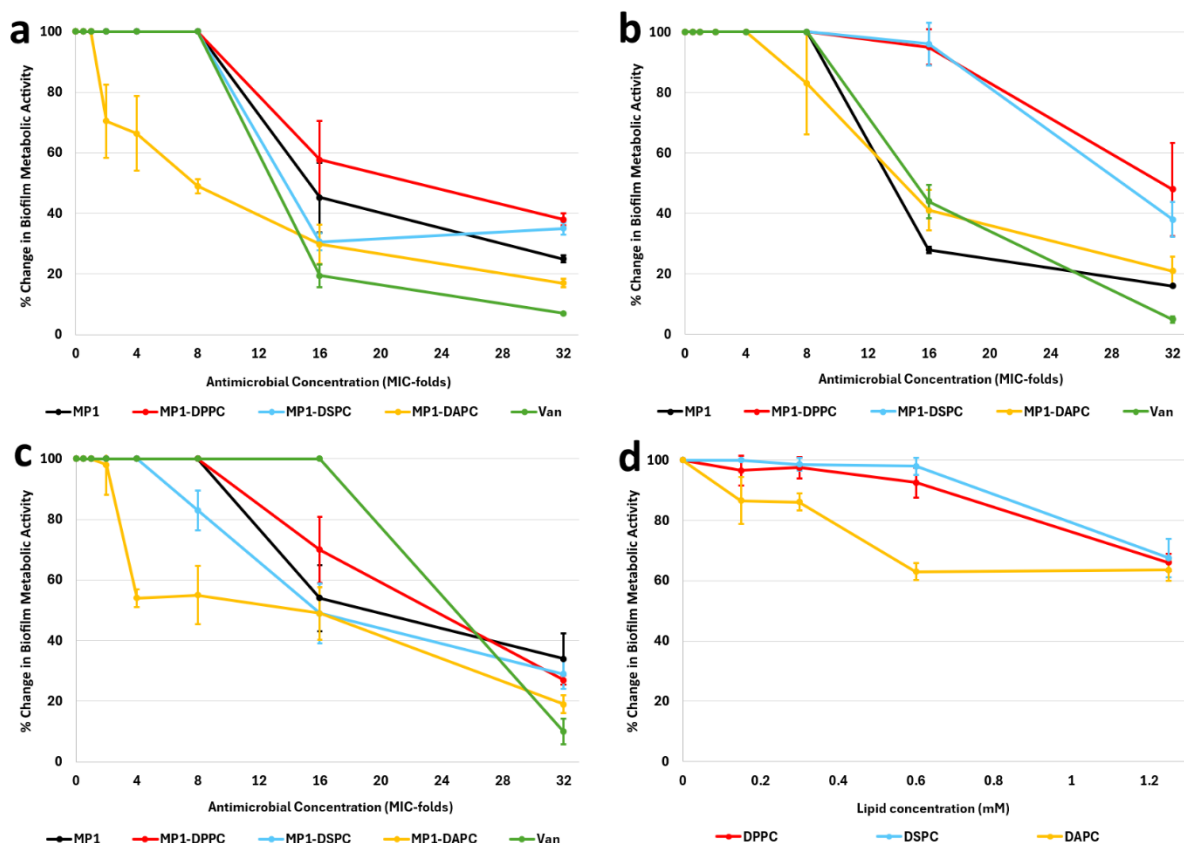


**Fig. 4.** The effect of various MP1-liposomal formulations, free MP1 and vancomycin on *S. aureus* preformed biofilm in 96-well plates measured as percentage changes in biofilm metabolic activity in three independent rounds of testing (a), (b) and (c). Panel (d) demonstrates the effect of empty liposomes on the biofilm. Data are presented as mean  $\pm$  SD (n = 5).

MP1-loaded DAPC liposomes showed a significant reduction ( $P < 0.05$ ) in biofilm metabolic activity at 8 $\times$ MIC concentration, decreasing by about 50% in two rounds of testing (**Fig. 4a, c**) and 20% in one round (**Fig. 4b**), while free MP1 showed no antibiofilm activity at this concentration. The difference in the effects of free MP1 and MP1-loaded DAPC liposomes became insignificant at and beyond 16 $\times$ MIC. At a concentration of 1  $\mu$ g/mL (equivalent to 32 $\times$ MIC), MP1-loaded DAPC liposomes reduced the biofilm metabolic activity by approximately 80% in all three rounds of testing. These findings suggest a promising antibiofilm application for MP1-loaded DAPC liposomes at low concentrations. Additionally, vancomycin showed antibiofilm activity at concentrations of 16 and 32  $\mu$ g/mL, which is equivalent to 16 $\times$ MIC and 32 $\times$ MIC, respectively (**Fig 4a-c**). Based on the screening results of



various MP1-loaded liposomes, the DAPC-based liposomes were selected for further investigations on established biofilms formed on a biomedical material (PTFE).

Despite the enhanced antimicrobial activity of MP1-loaded liposomes compared to free MP1 in MIC tests without Tween 80 (**Table 2**), the antibiofilm activity of free MP1 was comparable to or even superior to that of MP1-loaded DPPC and MP1-loaded DSPC liposomal formulations (**Fig. 4a-c**). This could be explained by the hydrophobic nature of MP1, which promotes its adsorption to hydrophobic surfaces such as the plastic microtiter wells. This adsorption may increase the concentration of MP1 in close proximity to the surface-attached biofilm, thereby enhancing its antibiofilm activity. In contrast, during MIC testing, free MP1 is more likely to adhere to the container surface rather than interact with planktonic cells freely suspended in the medium. Similar hydrophobic interactions influencing various antibiotics have been previously suggested in the literature (32, 42, 51). For instance, a previous study reported that higher concentrations of the hydrophilic vancomycin were required to treat *S. aureus* biofilm on PTFE surfaces compared to the more hydrophobic teixobactin analogues (32).

### 3.6. Effect of MP1 and MP1-loaded DAPC liposomes on established biofilm

The ability of MP1-loaded liposomes to eradicate biofilm was further investigated against a preformed *S. aureus* Xen 29 biofilm on PTFE, which is a biocompatible and inert material. PTFE is commonly used for production of biomedical devices and implants such as catheters and prosthetic joint implants (52). DAPC-based liposomes were selected due to their promising results in MIC testing and antibiofilm activity screening. The measured change in the biofilm metabolic activity after two independent rounds of testing is shown in **Fig. 5**. No changes were detected in the metabolic activity at concentrations below 0.25 µg/mL with either free MP1 or MP1-loaded DAPC liposomes. In the first round of testing, MP1-loaded DAPC liposomes demonstrated a significant ( $P < 0.05$ ) reduction in the biofilm metabolic activity by approximately 70% at 0.25 µg/mL, while free MP1 did not show an effect at the same concentration (**Fig. 5a**). In the second round of testing, both free MP1 and MP1-loaded DAPC demonstrated antibiofilm effect at 0.5 µg/mL with a decrease of approximately 70% and 85% in metabolic activity, respectively (**Fig. 5b**). Unlike the larger difference in antibiofilm activity between MP1-loaded DAPC liposomes and free MP1 observed in the 96-well plate screening (**section 3.5**), the difference on preformed biofilm on PTFE was smaller. This could be due to

the thinner biofilm formed on the PTFE rods, as evidenced by the lower level of bioluminescence measured in both experimental controls. This observation was expected given the inherent resistance of PTFE to biofilm formation compared to other surfaces (53, 54).

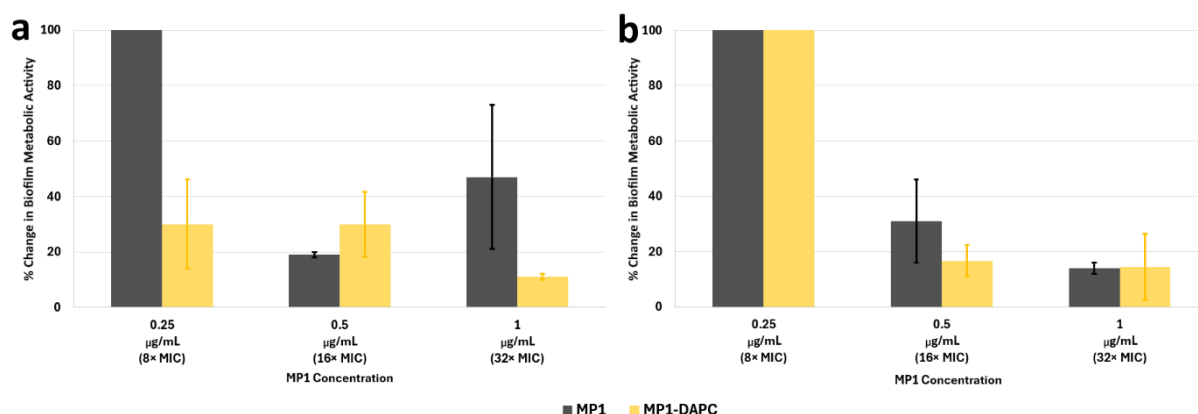


**Fig. 5.** The effect of free MP1 and MP1-DAPC liposomes on *S. aureus* preformed biofilm on a biomedical surface (PTFE) measured as percentage changes in cellular metabolic activity in two independent rounds of testing (a) and (b). Data are presented as mean  $\pm$  SD ( $n = 3$ ).

Live/dead cell staining with CLSM enabled direct evaluation of the effect of MP1-loaded DAPC liposomes on established biofilms, visualising biomass eradication and complementing the metabolic activity assessments (**section 3.5**). CLSM analysis of cellular viability following treatment with varying concentrations of free MP1 and MP1-loaded DAPC liposomes on preformed *S. aureus* biofilm is presented in **Fig. 6a**. Cell viability decreased with increasing concentrations of both free MP1 and MP1-loaded DAPC liposomes. However, the liposomal preparation exhibited a significantly greater reduction ( $P < 0.05$ ) at 0.25  $\mu\text{g/mL}$  ( $45.8 \pm 8.2\%$ ) compared to free MP1 ( $84.7 \pm 6.7\%$ ). A higher concentration (1  $\mu\text{g/mL}$ ) of free MP1 was required to reduce the cell viability below 50%. Additionally, MP1-loaded DAPC liposomes caused notably greater biofilm disruption compared to free MP1, as evident from CLSM images at 1  $\mu\text{g/mL}$  (**Fig. 6b**). These findings demonstrate that liposomal entrapment enhances MP1 efficacy against biofilm at lower concentrations. The combined cationic and fusogenic properties of the liposomes probably play a key role in promoting biofilm disruption and facilitating MP1 uptake into the biofilm-embedded cells, thereby enhancing antimicrobial and antibiofilm activity.

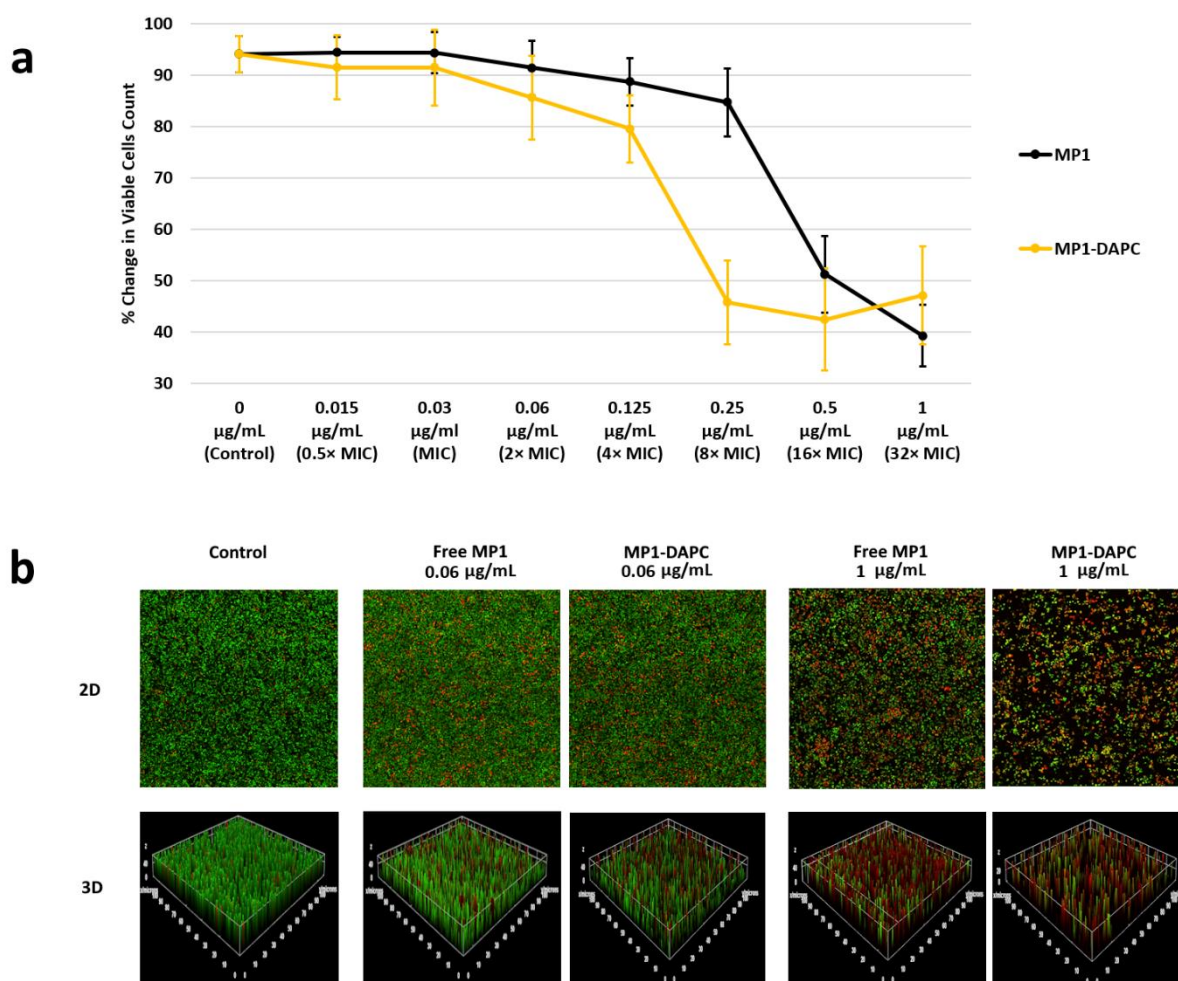


**Fig. 6.** Effect of different concentrations of free MP1 and MP1-loaded DAPC liposomes on percentage cell viability of *S. aureus* presented in (a) as mean  $\pm$  SD ( $n = 5$ ) and in (b) as 2D and 3D images obtained from CLSM z-stacks where live and dead cells are depicted in green and red, respectively. The control contains only growth medium.

### 3.7. Liposomal formulation optimization

Although MP1-loaded DAPC liposomes demonstrated superior drug delivery to biofilms compared to other MP1-liposomal formulations, they were physically unstable (**Fig. 2**). To enhance the *in vitro* stability of the formulation without compromising its antibiofilm activity, minor adjustments to the lipid composition were made and subsequently tested. This alteration in the composition also offered insights into the mechanisms underlying liposomal behaviour in aqueous media and their interaction with biofilms. In the modified formulation, denoted as “MP1-DAPC II”, the amount of cationic DOTAP was increased from 25 to 50 mol%, while both the fusogenic DOPE and DAPC components were reduced from 37.5 to 25 mol%. These modifications were intended to minimize potential aggregation by increasing

electrostatic repulsion between the liposomes, and to enhance membrane stability by decreasing the amount of flexible lipid (DOPE). The results of testing showed that the initial characteristics of both MP1-loaded DAPC liposomes were comparable (**Table 3**), but the physical stability of formulation II was significantly improved, with the modified liposomes remaining stable over two months of monitoring, confirming our hypothesis (**Fig. 7**). Additionally, the EE% of MP1 increased from  $21 \pm 5.7\%$  in MP1-loaded DAPC to  $27 \pm 2.6\%$  in the optimized formulation.

**Table 3.** Particle size (presented as Z-average), PDI, zeta potential and percentage entrapment efficiency (EE%) presented as mean  $\pm$  SD (n = 3) of MP1-DAPC and MP1-DAPC II liposomes characterized after preparation.

Liposomal formulation	Phospholipid composition (mol %)	Z-Average (nm) $\pm$ SD	Polydispersity index (PDI) $\pm$ SD	Zeta potential (mV) $\pm$ SD	Entrapment Efficiency (EE%)
MP1-DAPC	DAPC:DOPE:DOTAP (37.5:37.5:25)	159.7 $\pm$ 4.4	0.04 $\pm$ 0.016	+25.3 $\pm$ 1.7	21.03 $\pm$ 5.7
MP1-DAPC II	DAPC:DOPE:DOTAP (25:25:50)	132.7 $\pm$ 7.6	0.08 $\pm$ 0.013	+23.4 $\pm$ 1.1	27.04 $\pm$ 2.6

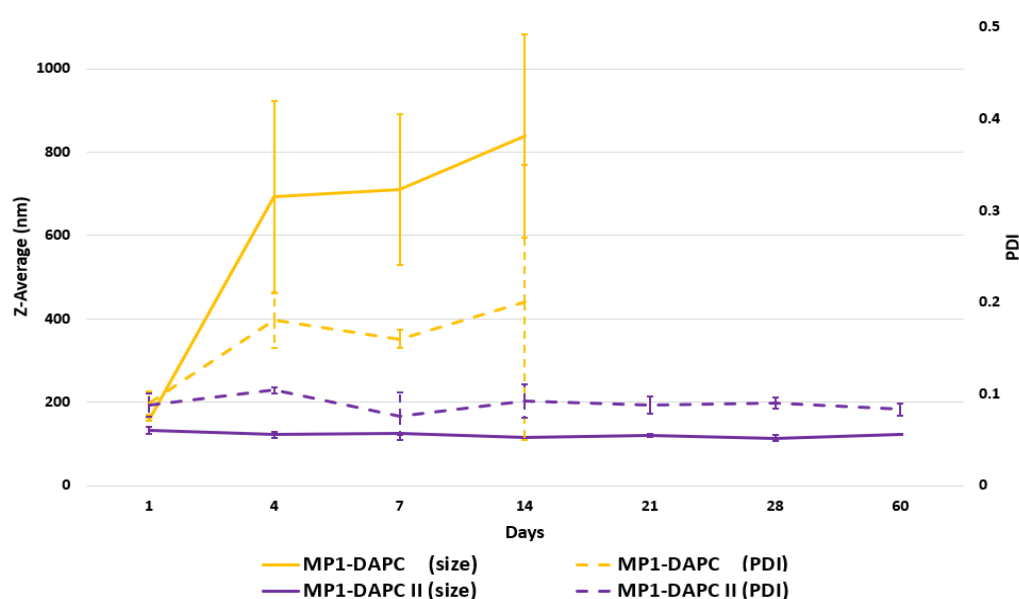


**Fig. 7.** *In vitro* stability of MP1-DAPC and MP1-DAPC II (modified composition) liposomes stored at 4°C over a period of two months. Physical stability was monitored by measuring liposome size as Z-average (solid line) and polydispersity index (PDI) (dashed line). Data points represent the mean  $\pm$  SD (n = 3).

Additionally, the modified liposomal formulation demonstrated improved chemical stability of MP1, with  $89 \pm 4.7\%$  of MP1 remaining stable after 14 days, compared to  $69.7 \pm 2.8\%$  in MP1-DAPC. Even after two months, the MP1 content of the optimized formulation remained relatively high at  $83 \pm 5.7\%$ . The enhanced chemical stability and entrapment efficiency of the optimized liposomal formulation may be attributed to the increased cationic DOTAP content (50 mol%), which strengthens electrostatic interactions with the negatively charged MP1 molecule, providing better entrapment and protection against loss of MP1.

Although the modified liposomes exhibited improved physicochemical properties, their antimicrobial activity, as determined by MIC assays, remained unchanged. The MIC values for the optimized liposomal composition (MP1-DAPC II) were identical to those of the original MP1-DAPC liposomes, both in the presence and absence of Tween 80, for all tested *S. aureus* strains. These findings are promising, as they indicate that the liposomal composition optimisation did not negatively impact the antimicrobial activity. However, the optimized liposomal preparation exhibited reduced antibiofilm activity compared to MP1-DAPC but remained comparable to free MP1 as documented in the supplementary material (**figure S1**). This decrease in antibiofilm activity may be attributed to the lower DAPC content (reduced from 37.5 to 25 mol%), emphasizing the influence of acyl chain length of phospholipids on liposomal-biofilm interactions, as discussed earlier in this study (**section 3.5**). Overall, while the modified MP1-DAPC liposomes enhanced physical stability, further optimization is required to fine-tune their antibiofilm activity for optimal performance.

## 4. Conclusions

In this work, fusogenic liposomes were developed as drug delivery systems for the bacteriocin MP1 targeting *S. aureus* biofilm. The effect of the fusogenic liposomes prepared with phospholipids of different acyl chain length on the antimicrobial and antibiofilm activity was investigated. Our study demonstrates that liposomal entrapment of MP1 improves its stability in aqueous solution and enhances the antimicrobial and antibiofilm activity. The latter effect was dependent on the acyl chain length of the phospholipid incorporated in the fusogenic liposomal composition. Increasing the acyl chain length from C16 to C20 (in DAPC-based liposomes) was found to further enhance MP1 entrapment efficiency. The MP1-loaded DAPC liposomes were superior in disrupting the *S. aureus* biofilm matrix. However, they were less stable *in vitro* compared to the liposomes containing shorter acyl chain phospholipids (DPPC and DSPC). The physical stability of DAPC-based liposomes was improved by increasing the concentration of the cationic phospholipid DOTAP while reducing DAPC. However, this adjustment led to a reduction in antibiofilm activity, highlighting the influence of the phospholipid acyl chain length on the liposome-biofilm interaction. In summary, the findings in this study highlight the potential of fusogenic liposomes as effective drug delivery systems for hydrophobic peptides, such as MP1, and may lead to improved treatment strategies for biofilm-associated infections.

## Authors contribution

**Ahmed M. Amer:** Conceptualization, Investigation, Data curation, Methodology, Writing – original draft, Writing – review & editing.

**Colin Charnock:** Conceptualization, Methodology, Supervision, Writing – review & editing.

**Kirill V. Ovchinnikov:** Conceptualization, Supervision, Writing – review & editing

**Tage Thorstensen:** Conceptualization, Supervision, Writing – review & editing

**Sanko Nguyen:** Conceptualization, Methodology, Supervision, Writing – review & editing.

## Declaration of competing interest

Tage Thorstensen is a cofounder of AgriBiotix company. Kirill V. Ovchinnikov is employed by AgriBiotix company. The remaining authors declare no conflict of interest.

## Acknowledgments

The authors would like to thank Jens Wohlmann at the Department of Biosciences, University of Oslo, who conducted transmission electron microscopy imaging. And Anna Lång at the core facility for advanced light microscopy, the Gaustad node, Oslo University Hospital, for assistance on imaging by confocal laser scanning microscopy. The Graphical abstract was created with Biorender.com

## References

1. Årdal C, Balasegaram M, Laxminarayan R, McAdams D, Outtersson K, Rex JH, et al. Antibiotic development — economic, regulatory and societal challenges. *Nature Reviews Microbiology*. 2020;18(5):267-74.
2. Browne K, Chakraborty S, Chen R, Willcox MD, Black DS, Walsh WR, et al. A New Era of Antibiotics: The Clinical Potential of Antimicrobial Peptides. *Int J Mol Sci*. 2020;21(19).
3. Miethke M, Pieroni M, Weber T, Brønstrup M, Hammann P, Halby L, et al. Towards the sustainable discovery and development of new antibiotics. *Nature Reviews Chemistry*. 2021;5(10):726-49.
4. Braem G, Stijlemans B, Van Haken W, De Vlieghe S, De Vuyst L, Leroy F. Antibacterial activities of coagulase-negative staphylococci from bovine teat apex skin and their inhibitory effect on mastitis-related pathogens. *Journal of Applied Microbiology*. 2014;116(5):1084-93.
5. Soltani S, Hammami R, Cotter PD, Rebuffat S, Said LB, Gaudreau H, et al. Bacteriocins as a new generation of antimicrobials: toxicity aspects and regulations. *FEMS Microbiology Reviews*. 2020;45(1):fuaa039.
6. Laridi R, Kheadr EE, Benech RO, Vuilleumard JC, Lacroix C, Fliss I. Liposome encapsulated nisin Z: optimization, stability and release during milk fermentation. *International Dairy Journal*. 2003;13(4):325-36.
7. Heinzinger LR, Pugh AR, Wagner JA, Otto M. Evaluating the Translational Potential of Bacteriocins as an Alternative Treatment for *Staphylococcus aureus* Infections in Animals and Humans. *Antibiotics*. 2023;12(8):1256.
8. de Freire Bastos MdC, Miceli de Farias F, Carlin Fagundes P, Varella Coelho ML. Staphylococins: an update on antimicrobial peptides produced by staphylococci and their diverse potential applications. *Applied Microbiology and Biotechnology*. 2020;104(24):10339-68.
9. Akasapu S, Hinds AB, Powell WC, Walczak MA. Total synthesis of micrococcin P1 and thiocillin I enabled by Mo(vi) catalyst. *Chemical Science*. 2019;10(7):1971-5.
10. Ongpipattanakul C, Desormeaux EK, DiCaprio A, van der Donk WA, Mitchell DA, Nair SK. Mechanism of Action of Ribosomally Synthesized and Post-Translationally Modified Peptides. *Chem Rev*. 2022;122(18):14722-814.
11. Wolden R, Ovchinnikov KV, Venter HJ, Oftedal TF, Diep DB, Cavanagh JP. The novel bacteriocin romsacin from *Staphylococcus haemolyticus* inhibits Gram-positive WHO priority pathogens. *Microbiol Spectr*. 2023;11(6):e0086923.
12. Kranjec C, Ovchinnikov KV, Grønseth T, Ebineshan K, Srikantham A, Diep DB. A bacteriocin-based antimicrobial formulation to effectively disrupt the cell viability of methicillin-resistant *Staphylococcus aureus* (MRSA) biofilms. *npj Biofilms and Microbiomes*. 2020;6(1):58.
13. Kranjec C, Kristensen SS, Bartkiewicz KT, Brønner M, Cavanagh JP, Srikantham A, et al. A bacteriocin-based treatment option for *Staphylococcus haemolyticus* biofilms. *Scientific Reports*. 2021;11(1):13909.
14. Liu Y, Liu Y, Du Z, Zhang L, Chen J, Shen Z, et al. Skin microbiota analysis-inspired development of novel anti-infectives. *Microbiome*. 2020;8(1):85.
15. Degiacomi G, Personne Y, Mondésert G, Ge X, Mandava CS, Hartkoorn RC, et al. Micrococcin P1 – A bactericidal thiopeptide active against *Mycobacterium tuberculosis*. *Tuberculosis*. 2016;100:95-101.



16. Park J, Kim LH, Lee JM, Choi S, Son YJ, Hwang HJ, et al. In vitro and intracellular activities of novel thiopeptide derivatives against macrolide-susceptible and macrolide-resistant *Mycobacterium avium* complex. *Microbiol Spectr*. 2023;11(5):e0182523.
17. Sulthana R, Archer AC. Bacteriocin nanoconjugates: boon to medical and food industry. *Journal of Applied Microbiology*. 2021;131(3):1056-71.
18. Liu H, Zhang Q, Wang S, Weng W, Jing Y, Su J. Bacterial extracellular vesicles as bioactive nanocarriers for drug delivery: Advances and perspectives. *Bioactive Materials*. 2022;14:169-81.
19. Ferreira M, Pinto SN, Aires-da-Silva F, Bettencourt A, Aguiar SI, Gaspar MM. Liposomes as a Nanoplatfrom to Improve the Delivery of Antibiotics into *Staphylococcus aureus* Biofilms. *Pharmaceutics*. 2021;13(3):321.
20. Liu Y, Liu Q, Zhao L, Dickey SW, Wang H, Xu R, et al. Essential role of membrane vesicles for biological activity of the bacteriocin micrococcin P1. *J Extracell Vesicles*. 2022;11(4):e12212.
21. Kolašinac R, Kleusch C, Braun T, Merkel R, Csiszár A. Deciphering the Functional Composition of Fusogenic Liposomes. *Int J Mol Sci*. 2018;19(2):346.
22. Nicolosi D, Cupri S, Genovese C, Tempera G, Mattina R, Pignatello R. Nanotechnology approaches for antibacterial drug delivery: Preparation and microbiological evaluation of fusogenic liposomes carrying fusidic acid. *International Journal of Antimicrobial Agents*. 2015;45(6):622-6.
23. Scriboni AB, Couto VM, Ribeiro LNDM, Freires IA, Groppo FC, de Paula E, et al. Fusogenic Liposomes Increase the Antimicrobial Activity of Vancomycin Against *Staphylococcus aureus* Biofilm. *Frontiers in Pharmacology*. 2019;10.
24. Beaulac C, Clément-Major S, Hawari J, Lagacé J. Eradication of mucoid *Pseudomonas aeruginosa* with fluid liposome-encapsulated tobramycin in an animal model of chronic pulmonary infection. *Antimicrobial Agents and Chemotherapy*. 1996;40(3):665-9.
25. Makhoul Z, Ali AA, Al-Sayah MH. Liposomes-Based Drug Delivery Systems of Anti-Biofilm Agents to Combat Bacterial Biofilm Formation. *Antibiotics (Basel)*. 2023;12(5).
26. Naqvi M, Fineide F, Utheim TP, Charnock C. Culture- and non-culture-based approaches reveal unique features of the ocular microbiome in dry eye patients. *The Ocular Surface*. 2024;32:123-9.
27. Ovchinnikov KV, Kranjec C, Telke A, Kjos M, Thorstensen T, Scherer S, et al. A Strong Synergy Between the Thiopeptide Bacteriocin Micrococcin P1 and Rifampicin Against MRSA in a Murine Skin Infection Model. *Frontiers in Immunology*. 2021;12:676534.
28. Amer AM, Charnock C, Nguyen S. The impact of surface charge on the interaction of cholesterol-free fusogenic liposomes with planktonic microbial cells and biofilms. *International Journal of Pharmaceutics*. 2025;669:125088.
29. Avanti Polar Lipids. 2025 [Available from: <https://avantiresearch.com/product-category/phospholipids>.]
30. Webster P, Webster A. Cryosectioning fixed and cryoprotected biological material for immunocytochemistry. *Electron Microscopy: Methods and Protocols*. 2014:273-313.
31. Clinical and Laboratory Standards Institute (CLSI). M100: Performance Standards for Antimicrobial Susceptibility Testing. 2020, 30th Edition.
32. Amer AM, Charnock C, Nguyen S. Novel Teixobactin Analogues Show Promising In Vitro Activity on Biofilm Formation by *Staphylococcus aureus* and *Enterococcus faecalis*. *Current Microbiology*. 2024;81(10):349.

33. Nafee N, Gaber DM, Abouelfetouh A, Alsequey M, Empting M, Schneider M. Enzyme-Linked Lipid Nanocarriers for Coping Pseudomonal Pulmonary Infection. Would Nanocarriers Complement Biofilm Disruption or Pave Its Road? *International Journal of Nanomedicine*. 2024;19(null):3861-90.
34. Liu Y, Shi L, Su L, van der Mei HC, Jutte PC, Ren Y, et al. Nanotechnology-based antimicrobials and delivery systems for biofilm-infection control. *Chemical Society Reviews*. 2019;48(2):428-46.
35. Jaradat E, Weaver E, Meziane A, Lamprou DA. Synthesis and Characterization of Paclitaxel-Loaded PEGylated Liposomes by the Microfluidics Method. *Molecular Pharmaceutics*. 2023;20(12):6184-96.
36. Jaradat E, Meziane A, Lamprou DA. Conventional vs PEGylated loaded liposomal formulations by microfluidics for delivering hydrophilic chemotherapy. *International Journal of Pharmaceutics*. 2024;655:124077.
37. Grit M, Crommelin DJA. Chemical stability of liposomes: implications for their physical stability. *Chemistry and Physics of Lipids*. 1993;64(1):3-18.
38. Anderson M, Omri A. The effect of different lipid components on the in vitro stability and release kinetics of liposome formulations. *Drug Deliv*. 2004;11(1):33-9.
39. Xia Y, Sun J, Liang D. Aggregation, Fusion, and Leakage of Liposomes Induced by Peptides. *Langmuir*. 2014;30(25):7334-42.
40. Goebel-Stengel M, Stengel A, Taché Y, Reeve JR, Jr. The importance of using the optimal plasticware and glassware in studies involving peptides. *Anal Biochem*. 2011;414(1):38-46.
41. Kristensen K, Henriksen JR, Andresen TL. Adsorption of cationic peptides to solid surfaces of glass and plastic. *PLoS One*. 2015;10(5):e0122419.
42. Kavanagh A, Ramu S, Gong Y, Cooper MA, Blaskovich MAT. Effects of Microplate Type and Broth Additives on Microdilution MIC Susceptibility Assays. *Antimicrob Agents Chemother*. 2019;63(1).
43. Fulaz S, Vitale S, Quinn L, Casey E. Nanoparticle-Biofilm Interactions: The Role of the EPS Matrix. *Trends in Microbiology*. 2019;27(11):915-26.
44. Malaekheh-Nikouei B, Fazly Bazzaz BS, Mirhadi E, Tajani AS, Khameneh B. The role of nanotechnology in combating biofilm-based antibiotic resistance. *Journal of Drug Delivery Science and Technology*. 2020;60:101880.
45. Zhao A, Sun J, Liu Y. Understanding bacterial biofilms: From definition to treatment strategies. *Frontiers in Cellular and Infection Microbiology*. 2023;13:1137947.
46. Mu H, Tang J, Liu Q, Sun C, Wang T, Duan J. Potent Antibacterial Nanoparticles against Biofilm and Intracellular Bacteria. *Scientific Reports*. 2016;6(1):18877.
47. Percival SL, Mayer D, Kirsner RS, Schultz G, Weir D, Roy S, et al. Surfactants: Role in biofilm management and cellular behaviour. *Int Wound J*. 2019;16(3):753-60.
48. Simões M, Pereira MO, Vieira MJ. Action of a cationic surfactant on the activity and removal of bacterial biofilms formed under different flow regimes. *Water Research*. 2005;39(2):478-86.
49. Chen X, Stewart PS. Biofilm removal caused by chemical treatments. *Water Research*. 2000;34(17):4229-33.
50. Fang J-Y, Chou W-L, Lin C-F, Sung CT, Alalaiwe A, Yang S-C. Facile Biofilm Penetration of Cationic Liposomes Loaded with DNase I/Proteinase K to Eradicate *Cutibacterium acnes* for Treating Cutaneous and Catheter Infections. *International Journal of Nanomedicine*. 2021;16(null):8121-38.

51. Mejías C, Martín J, Martín-Pozo L, Santos JL, Aparicio I, Alonso E. Adsorption of Macrolide Antibiotics and a Metabolite onto Polyethylene Terephthalate and Polyethylene Microplastics in Aquatic Environments. *Antibiotics (Basel)*. 2024;13(5).
52. Roina Y, Auber F, Hocquet D, Herlem G. ePTFE functionalization for medical applications. *Materials Today Chemistry*. 2021;20:100412.
53. Demling A, Elter C, Heidenblut T, Bach F-W, Hahn A, Schwestka-Polly R, et al. Reduction of biofilm on orthodontic brackets with the use of a polytetrafluoroethylene coating. *European Journal of Orthodontics*. 2010;32(4):414-8.
54. Berry JA, Biedlingmaier JF, Whelan PJ. In Vitro Resistance to Bacterial Biofilm Formation on Coated Fluoroplastic Tympanostomy Tubes. *Otolaryngology—Head and Neck Surgery*. 2000;123(3):246-51.

## Supplementary material

### HPLC-MS method for quantification of micrococcin P1 (MP1):

MP1 was quantified using UV detector at 280 nm and quadrupole mass spectrometry (MS) detector at positive polarity using single ion monitoring (SIM) mode at 572.7 (m/z) mass. Separation was done using a C18 column (Gemini-NX - 3 $\mu$ m - 110A - 150 x 4.6 mm, Phenomenex, USA), with a flow rate at 0.7 mL/min using a gradient method with mobile phase A (water + 0.1% formic acid) and mobile phase B (acetonitrile + 0.1% formic acid) as demonstrated in the following table.

**Table S1.** Chromatographic gradient mobile phase composition for MP1 analysis.

Time (min)	Mobile Phase A (%)	Mobile Phase B (%)
0	60	40
20	0	100
22	20	80
25	20	80
26	60	40
30	60	40

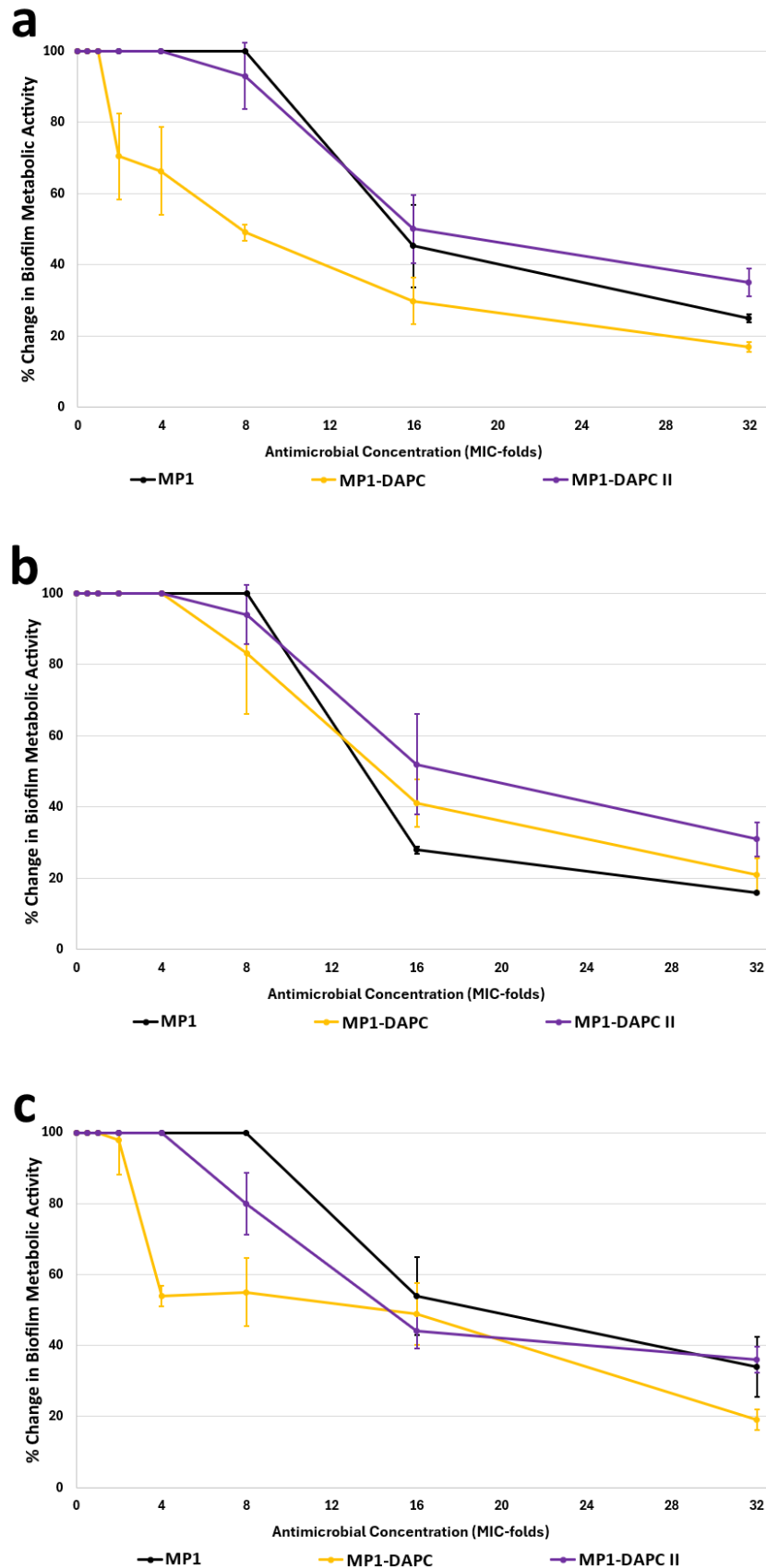


**Fig. S1.** The effect of MP1-loaded DAPC liposomes before and after liposomal composition optimization on *S. aureus* preformed biofilm in 96-well plates measured as percentage change in biofilm metabolic activity in three independent rounds of testing (a), (b) and (c). Data presented as mean  $\pm$  SD (n = 5).



## Paper III

Ahmed M. Amer, Colin Charnock, Sanko Nguyen

**Novel Teixobactin Analogues Show Promising In Vitro Activity on Biofilm Formation by *Staphylococcus aureus* and *Enterococcus faecalis***

*Current Microbiology*, 81, 349 (2024).

DOI: <https://doi.org/10.1007/s00284-024-03857-9>







# Novel Teixobactin Analogues Show Promising In Vitro Activity on Biofilm Formation by *Staphylococcus aureus* and *Enterococcus faecalis*

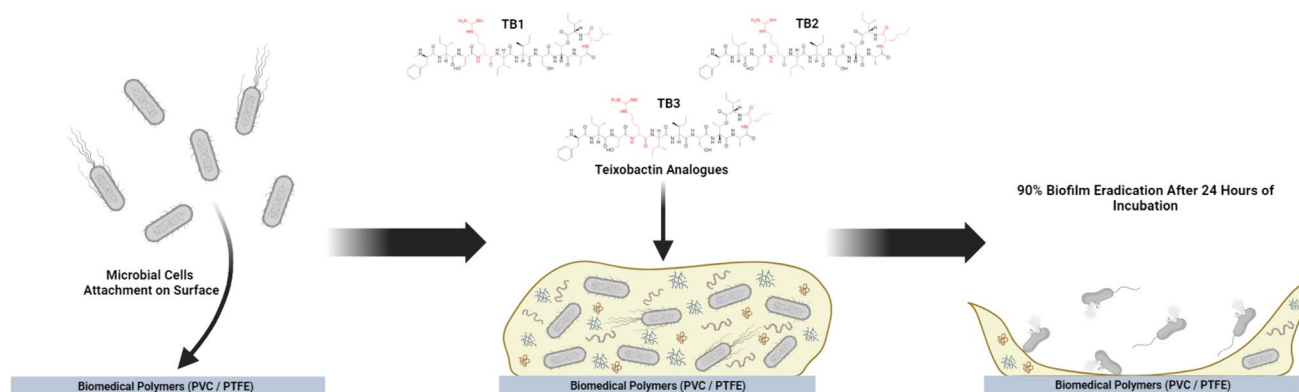
Ahmed M. Amer<sup>1</sup> · Colin Charnock<sup>1</sup> · Sanko Nguyen<sup>1</sup>

Received: 1 November 2023 / Accepted: 19 August 2024 / Published online: 10 September 2024  
© The Author(s) 2024

## Abstract

The treatment of infections caused by biofilm-forming organisms is challenging. The newly discovered antibiotic teixobactin shows activity against a wide range of biofilm-forming bacteria. However, the laborious and low-yield chemical synthesis of teixobactin complicates its further development for clinical application. The use of more easily synthesized teixobactin analogues may offer promise in this regard. In this article, three newly developed analogues were tested for efficacy against *Staphylococcus aureus* and *Enterococcus faecalis*. Minimum inhibitory and -bactericidal concentrations were investigated. MIC values for *S. aureus* and *E. faecalis* ranged from 0.5–2 and 2–4 µg/mL, respectively. Moreover, the ability of the analogues to prevent biofilm formation and to inactivate bacterial cells in already established *S. aureus* biofilm on medical grade materials (PVC and PTFE) used in the production of infusion tubing and catheters were also tested. The analogues showed an ability to prevent biofilm formation and inactivate bacterial cells in established biofilms at concentrations as low as 1–2 µg/mL. Confocal laser scanning microscopy showed that the most promising analogue (TB3) inactivated *S. aureus* cells in a preformed biofilm and gave a reduction in biovolume. The relative ease of synthesis of the analogues and their in vitro efficacy, makes them promising candidates for pharmaceutical development.

## Graphical Abstract



## Introduction

Biofilms are the main cause of approximately 80% of recurrent and chronic microbial infections [1]. They can be either associated with the use of medical devices or can be formed on tissues resulting in various types of chronic infections [2]. The tolerance of biofilms for antibiotics can be attributed to among other factors, limited drug diffusion through the

✉ Ahmed M. Amer  
ahmedame@oslomet.no

<sup>1</sup> Department of Life Sciences and Health, Oslo Metropolitan University (OsloMet), Pilestredet 50, 0167 Oslo, Norway

extracellular polymeric substances (EPS) and to cell conversion from the planktonic to dormant state with altered metabolic activities [2, 3]. The release of EPS and formation of the biofilm matrix is a fundamental step in the process of biofilm development. It protects the cells from the surrounding environment (e.g. components of the immune system and antibiotics) and provides mechanical and structural support. The EPS mostly consists of proteins, polysaccharides, extracellular DNA and lipids, all of which have a wide range of functions including adhesion, water retention, structural integrity and enzymatic activity [4]. In addition to being a physical barrier to antibiotic penetration, the biofilm matrix also plays a role in antibiotic degradation [5]. Bacterial cells inside the biofilm have in some cases been shown to be 1000 times more tolerant to antibiotics than planktonic cells [5].

Biofilm infections notably contribute to the emergence of antimicrobial resistance (AMR) through the transfer of resistance genes on mobile genetic elements, such as plasmids, inside the biofilm matrix [6]. Furthermore, biofilm formation is often associated with the development of hypermutator phenotypes of bacteria, which can show up to 1000-fold increases in mutation rates [1]. Mortality relating to AMR in 2019 was estimated at 1.27 million deaths based on data gathered from 204 countries [7]. Numbers are estimated to reach 10 million annually by 2050 if no firm actions are taken to resolve the problem [8, 9]. Unfortunately, the development of new antibiotics is being outpaced by the rapid increase of AMR. Over the past 40 years, most of the developed antibiotics were derived from antimicrobial agents already in clinical use. No antibiotics with novel modes of action have made it to the market since lipopeptide antibiotics emerged in the 1980s [10, 11].

In 2015, a novel class of antibiotics represented by the agent teixobactin was discovered. Teixobactin is produced by a newly discovered species provisionally named *Eleftheria terrae* [12]. Teixobactin is believed to exert its antimicrobial activity primarily by targeting lipid II and lipid III which are precursors for cell wall peptidoglycan and teichoic acid, respectively. The effect is generally limited to inhibition of cell wall synthesis in gram-positive bacteria, as the outer membrane of gram-negative bacteria prevents teixobactin penetration. Teixobactin demonstrated in vitro antimicrobial activity against multidrug resistant (MDR) bacteria, including methicillin-resistant *Staphylococcus aureus* (MRSA) and vancomycin-resistant *Enterococci* (VRE) [12]. Despite its potential as a new drug candidate, the chemical synthesis of teixobactin is challenging due to the presence of L-allo-enduracididine amino acid in the macrocyclic depsipeptide structure of teixobactin [13]. Methods for L-allo-enduracididine synthesis are multistep, laborious and with a relatively low yield. Therefore, new teixobactin analogues have been synthesised mainly by replacing L-allo-enduracididine with common and commercially available amino acids [14].

Structure–activity relationships (SAR) studies revealed that L-allo-enduracididine substitution by non-polar leucine at position 10 maintained significant antibacterial activity [13]. However, the substitution resulted in increased structural hydrophobicity, which is a common barrier to drug formulation and pharmaceutical development [13, 15]. To restore the hydrophilic/hydrophobic profile of the natural teixobactin molecule, a teixobactin analogue (D-Arg4-Leu10-teixobactin) was synthesised by replacing glutamine at position 4 with the cationic amino acid arginine [15]. This new, synthetic analogue demonstrated promising antimicrobial activity against both MRSA and VRE strains [15].

In the present study, the antimicrobial and antibiofilm activity of D-Arg4-Leu10-teixobactin along with two structurally related novel analogues, D-Arg4-Nle10-teixobactin and D-Arg4-Nva10-teixobactin (Fig. 1), on the clinically important species *S. aureus* and *Enterococcus faecalis* were investigated. To our knowledge, this is the first study looking at the effect of teixobactin analogues on biofilm formation and treatment of mature biofilms on biomedical polymers used for production of medical devices and implants.

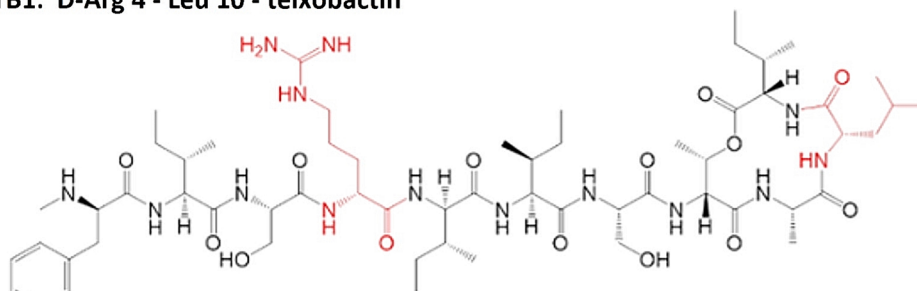
## Materials and Methods

### Materials

*S. aureus* (ATCC 29213) and *E. faecalis* (ATCC 29212) were purchased from American Type Culture Collection (Rockville, MD, USA). *S. aureus* clinical isolates P14 and P20 and *E. faecalis* clinical isolate P40 were isolated in our laboratory from the eyes of patients diagnosed with severe dry eye disease [16]. As previously described [16], the isolates were collected from the lower conjunctival sac and grown on a range of selective and non-selective agars. *E. faecalis* was identified after growing the isolate on *Enterococcus* selective agar and by partial sequencing of 16S rRNA. *S. aureus* was identified based on DNase production and latex slide agglutination (detecting clumping factor and protein A) in addition to 16S rRNA gene sequencing [16]. Additionally, the identity of the isolates was confirmed by whole genome sequencing. Protocols for 16S RNA and whole-genome sequencing are available in the supplementary data (Supplementary file 2). Cation-adjusted Mueller Hinton broth (MHB), tryptic soy broth (TSB), tryptic soy agar (TSA) and maximum recovery diluent (MRD) were purchased from Oxoid/Thermo Fischer (MA, USA). Vancomycin HCl (Product No. 94747), triphenyl tetrazolium chloride (TTC), crystal violet (CV) (ACS reagent C6158), Tween 80, dimethyl sulfoxide (DMSO) and phosphate buffered saline (PBS) tablets were purchased from Merck (Germany). FilmTracer™ LIVE/DEAD® Biofilm Viability Kit was purchased from

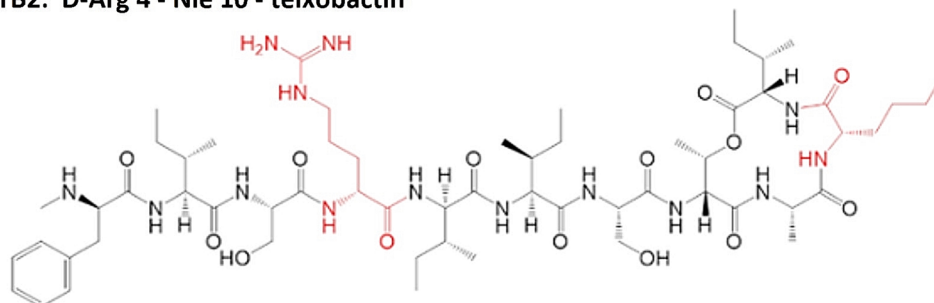
**Fig. 1** Chemical structures of the three teixobactin analogues (TB1, TB2 and TB3) investigated in this study. Red colour shows the substituted positions from the natural teixobactin structure. The L-allo-enduracididine amino acid residue at position 10 is replaced by an amino acid indicated by a three-letter code; *Leu* leucine, *Nle* norleucine, *Nva* norvaline. In all three analogues, the glutamine residue at position 4 is replaced by arginine (Arg)

**TB1: D-Arg 4 - Leu 10 - teixobactin**



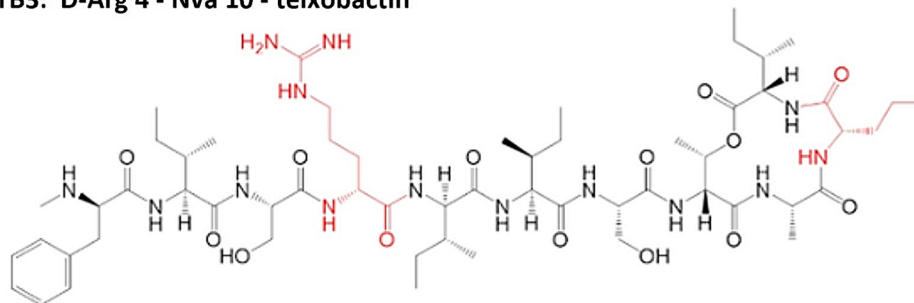
Chemical Formula:  $C_{59}H_{100}N_{14}O_{14}$   
Exact Mass: 1228.75

**TB2: D-Arg 4 - Nle 10 - teixobactin**



Chemical Formula:  $C_{59}H_{100}N_{14}O_{14}$   
Exact Mass: 1228.75

**TB3: D-Arg 4 - Nva 10 - teixobactin**



Chemical Formula:  $C_{58}H_{98}N_{14}O_{14}$   
Exact Mass: 1214.74

Invitrogen (USA). Natural teixobactin was provided by Novobiotic Pharmaceuticals (Cambridge, MA, USA). Teixobactin analogues were synthesized and provided by Dr. Ishwar Singh at Institute of Translational Medicine, University of Liverpool, as previously described [15]. All analogues were  $\geq 90\%$  pure as determined by HPLC-MS.

**Determination of Minimum Inhibitory Concentration (MIC) and Minimum Bactericidal Concentration (MBC)**

MIC was determined using the broth microdilution method. Briefly, a stock solution 1600  $\mu\text{g/mL}$  in DMSO of each antimicrobial compound was prepared. Vancomycin and natural teixobactin were used as quality controls. Serial dilutions were done in DMSO according to Clinical and Laboratory Standards Institute (CLSI) guidelines [17] to yield concentrations ranging from 1600 to

3.125 µg/mL. Each concentration was further diluted with MHB + 0.002% Tween 80 (1:100) to obtain final concentrations ranging from 16 to 0.03 µg/mL. One hundred µL of each final concentration was added to each well to round-bottom polystyrene and polypropylene 96-well microtiter plates (Corning®, USA) to investigate if plastic type affects the MIC results. Bacterial inoculums of *S. aureus* and *E. faecalis* were made from overnight cultures on TSA grown aerobically at 37 °C by suspending well-isolated colonies in 0.9% NaCl until 0.5 McFarland (approximately  $10^8$  CFU/mL) was obtained spectrophotometrically. Suspensions were then diluted with cation-adjusted MHB + 0.002% Tween 80 such that a final concentration of  $10^5$  CFU/mL was achieved in wells after inoculation [17]. As a negative control, some wells with growth medium were not inoculated with bacteria, while other wells were inoculated with bacteria and without any antibiotic as a positive control. Plates were incubated overnight at 37 °C and the MICs were determined visually by two researchers following the CLSI guidelines. After MIC determination, 100 µL from all wells containing TB analogues without visual bacterial growth (*S. aureus* ATCC 29213 and *E. faecalis* ATCC 29212) was spread out on TSA plates and incubated overnight at 37 °C. The number of colonies was counted to determine MBC, which is defined as the lowest antimicrobial concentration that kills  $\geq 99.9\%$  of the microorganism in the inoculum according to CLSI guidelines [18]. Experiments were repeated three times on separate occasions as independent experimental replicates.

### Effect of Teixobactin Analogues on Planktonic Growth

Inoculums of *S. aureus* (ATCC 29213) and *E. faecalis* (ATCC 29212) were prepared by suspending well-isolated colonies in 0.9% NaCl until 0.5 McFarland was obtained, followed by dilution with growth medium TSB + 1% glucose to a final concentration of  $10^5$  CFU/mL. Teixobactin analogues or vancomycin were added in concentrations equal to  $\frac{1}{2} \times \text{MIC}$ , MIC and  $2 \times \text{MIC}$ , and 2 mL of each mix was pipetted in into 24-well plates with a clear flat bottom (VisiPlates-24, PerkinElmer®, USA). Broth cultures without teixobactin or without cells were used as positive and negative growth controls, respectively. The optical density (OD) of the growth curves was measured with a multimode plate reader (Victor<sup>3</sup>, Perkin Elmer®, USA) at 590 nm every 15 min for 16 h at 37 °C. The curves were also plotted on a semi-logarithmic scale to determine the onset of the exponential growth phase and to calculate the culture doubling time (DT) as previously

described [19]. The experiment was performed twice on separate occasions as independent experimental replicates.

### Inhibition of Biofilm Formation

Inoculums of *S. aureus* (ATCC 29213) and *E. faecalis* (ATCC 29212) were prepared as described in “Effect of Teixobactin Analogues on Planktonic Growth” section. Teixobactin analogues or vancomycin were added to bacterial suspensions in concentrations equal to  $\frac{1}{2} \times \text{MIC}$ , MIC,  $2 \times \text{MIC}$  and  $4 \times \text{MIC}$ . Two hundred µL from each concentration for each mixture was transferred to wells ( $n=9$ ) in a 96-well polypropylene plate and incubated statically overnight at 37 °C to allow biofilm formation. Ten wells were incubated without antibiotic as positive controls. After incubation, wells were examined visually for bacterial growth and scored from 0 to +4, where 0 presents no growth and +4 is the maximum growth obtained with the positive control. Wells containing teixobactin analogues with significant visible growth reduction compared to the control were further assessed using three different methods i.e., colony counting, crystal violet (CV) assay and activity staining. The biofilm inhibitory concentration ( $\text{BIC}_{90}$ ), which is the lowest teixobactin analogue concentration inhibiting biofilm formation by  $> 90\%$ , was determined using the results obtained by the different analysis methods. Prior to testing, planktonic cells were carefully removed by pipetting out the contents of each well and gently washed three times with PBS. The experiment was performed twice on separate occasions as independent experimental replicates.

### Colony Counting

The biofilm was suspended into 0.1 mL MRD + 0.01% Tween 80 by scraping the wells' inner wall using a sterile dental micro applicator brush (Guangzhou Jaan Medical, China). The contents were transferred to a microtube containing sterile 0.1 mm glass beads. To ensure maximal biofilm recovery, the same procedure was repeated twice for each well to obtain a final volume of 0.3 mL using the same brush and pipette tip. Following this, the tubes were sonicated (Elmasonic S30, Elma Ultrasonic Technology, Germany) for 5 min and vortexed for 3 cycles of 30 s with intermittent cooling to homogenize biofilms and release cells prior to plating. The suspensions were then serially diluted in MRD, plated on TSA, and incubated overnight at 37 °C. After incubation, the number of colonies was recorded and the percentage reduction in cell viability was calculated compared to the control.

### Crystal Violet Assay

The assay was performed as previously described [20–22], with slight modifications: 0.1% w/v CV in purified water was prepared and filtered (0.22 µm) to remove any particles. Two hundred µl of the CV solution was added carefully to each well without disrupting the biofilm and the plate was incubated statically at 37 °C for 2.5 h. After incubation, the CV solution was removed, wells were washed carefully three times with PBS and 250 µl of 33% acetic acid was added to extract the colour from the biofilm by orbital shaking (Genie Temp-Shaker 100, Scientific Industries, USA) at 80 rpm for 15 min. Following extraction, 180 µl from each well was transferred to a flat-bottomed polystyrene 96-well plate and colour intensity was measured spectrophotometrically at 595 nm using the same plate reader (“[Effect of Teixobactin Analogues on Planktonic Growth](#)” section). The percentage reduction in biofilm formation was calculated compared to control wells using the following equation:

$$\% \text{ Reduction} = [(\text{control absorbance} - \text{test absorbance}) / \text{control absorbance}] \times 100 \quad (1)$$

### Activity Staining

The test was performed as previously described [23, 24], with slight modifications: 200 µL of 0.05% w/v triphenyl tetrazolium chloride (TTC) in TSB + 1% glucose was pipetted carefully into each well and incubated statically at 37 °C for 2.5 h. After incubation, the solution was removed, wells were washed three times with PBS and 250 µL of methanol was added to extract triphenyl formazan (TPF) colour from the biofilm by orbital shaking at 80 rpm for 15 min. Finally, 180 µL from each well was transferred to a new flat-bottomed polystyrene 96-well plate and colour intensity was measured spectrophotometrically at 490 nm. Percentage reduction in biofilm formation was calculated according to Eq. (1).

### Inactivation of Bacteria in Established Biofilms

Two structurally different materials used in biomedical applications were tested in this study i.e., polytetrafluoroethylene (PTFE for catheters production, Zeus Company, USA) and polyvinyl chloride (PVC for intravenous infusion tubing production, B. Braun, Germany). One cm rods of each type of plastic were disinfected by incubation at 70 °C in sterile water for 30 min followed by washing one time with 70% ethanol and three times with sterile water. An inoculum of *S. aureus* was prepared in TSB + 1% glucose as previously described (“[Effect of Teixobactin Analogues on Planktonic Growth](#)” section). Biofilm was allowed to grow on the rods for three days at 37 °C with gentle orbital

shaking at 80 rpm. Fresh medium was replaced every day without disrupting the biofilm. After three days, the plastic pieces were washed three times with fresh PBS to remove planktonic cells and transferred to 6-well polystyrene flat bottom plates (Corning®, USA). To each well, 5 mL of cation-adjusted MHB containing ½×MIC, MIC, 2×MIC, 4×MIC and 16×MIC of teixobactin analogues or vancomycin were added to cover the rods. Plates were incubated for 24 h at 37 °C with orbital shaking at 80 rpm. Three plastic rods of each material were incubated without antimicrobial agents as positive controls, while another three of each material were incubated without cells as negative controls. After incubation, rods were washed three times with PBS. The experiment was performed twice on separate occasions as independent experimental replicates. The extent of inactivation of biofilm bacteria was assessed quantitatively by colony counting and qualitatively by activity staining as described below:

### Colony Counting

Each rod was placed in a tube containing 1 mL MRD-broth + 0.01% Tween 80 and sterile 0.1 mm glass beads. The biofilm was then dispersed to free cells and plated on TSA using the same procedure described in “[Colony Counting](#)” section. After incubation, the number of colonies were recorded, and biofilm eradication concentration (BEC) was calculated as percentage reduction in CFU/mL relative to the control.

### Activity Staining

Plastic rods were placed individually in wells of 6-well plates and covered with 5 mL of 0.05% w/v TTC solution in TSB + 1% glucose and incubated at 37 °C with orbital shaking at 80 rpm for 2.5 h. After incubation, rods were transferred to clean wells and colour intensity was graded visually using a scoring system, where (–) represents no growth and (+++) is the maximum growth. The colour intensity scoring was performed separately by two researchers to ensure fidelity in the interpretation.

### Confocal Laser Scanning Microscopy (CLSM) Analysis of Biofilms

An inoculum of *S. aureus* (ATCC 29213) was prepared by suspending well-isolated colonies in 0.9% NaCl until 0.5 McFarland was obtained, and the suspension was then diluted with TSB + 1% glucose to a final concentration of



10<sup>5</sup> CFU/mL. Using 4-well chamber slides (Nunc Lab-Tek II CC2, Thermo Scientific), 1 mL of bacterial suspension was added to each chamber and allowed to grow for 72 h at 37 °C with shaking at 60 rpm. The medium was replaced carefully each day without disrupting the biofilm. After incubation, spent medium was replaced with 1 mL fresh medium containing 1, 2, 4 or 8 µg/mL of teixobactin analogue TB3 ( $n=3$ ). Other wells were incubated with only medium as control. TB3 was incubated with biofilms at 37 °C using low speed agitation (shaking at 60 rpm) for 24 h. After incubation, medium was again removed, and wells were washed twice with sterile water followed by addition of 200 µL of FilmTracer™ LIVE/DEAD® Biofilm Viability Kit working solution in each well. The working solution was prepared by adding 3 µL of SYTO 9 stain and 3 µL of propidium iodide stain to 1 ml of sterile water. Slides were incubated for 30 min at room temperature protected from light. Afterwards, staining solution was removed, and chambers were washed twice with sterile water. Finally, 50 µL of antifading mounting solution (AFR3, Citifluor Ltd, UK) was added to each well and sealed beneath a coverslip. The slides were examined using a confocal microscope (TCS SP8 STED, Leica Microsystems, Germany). Fluorescence intensity measurements and 3D structures visualisation of the biofilms were generated from z-stacks by using ImageJ software (National Institutes of Health, Maryland, USA). Percentage cell viability was calculated after counting the number of live (green) and dead (red) cells in 5 randomly picked spots from each well. Biovolume for each biofilm was determined by firstly measuring the area covered by cells (live and dead) in all stacks after changing the images to binary (black/white) and determining the pixels which corresponds with bacterial cells using ImageJ software [25]. Afterwards, biovolume was calculated as reported by Heydorn et al. [26], which is defined as the pixels corresponding to biomass multiplied by voxel size and divided by substratum area of the image [26].

## Statistical Analysis

Results are presented as the mean  $\pm$  standard deviation (SD). SD was calculated across all runs and replicates as the square root of the variance. The variance represents the data point's deviation from the mean and calculated by taking the average of the squared differences between each data point and the mean. Significant difference between various treatments was determined using analysis of variance (ANOVA) and Bonferroni correction is used to adjust the significance level as multiple sets of results were involved in the comparisons. This was done by dividing the significance level ( $P$  value = 0.05) by the number of comparisons made. Whenever the SD value is not reported in the tables,

it signifies that the experimental replicates yielded identical results with no observed variability.

## Accession Numbers of Clinical Isolates

The sequences of the clinical isolates used in this work have been deposited at the National Centre for Biotechnology Information (NCBI) repository under accession number SAMN40573642 for *E. faecalis* isolate P40 and accession numbers SAMN40573970 and SAMN40573973 for *S. aureus* isolates P14 and P20, respectively.

## Results

### Determination of MIC and MBC

The MIC values reported are the average obtained with polystyrene and polypropylene plates as no effect from the plate material on MIC was observed (Table 1). The measured MIC for natural teixobactin was similar to that previously reported by Ling et al. [12] for *S. aureus* ATCC 29213 (0.25 µg/mL). Furthermore, MIC values for vancomycin fell in the reported MIC range given in the CLSI guidelines for both *S. aureus* and *E. faecalis* [17], thus confirming the validity of the experimental approach. The newly developed teixobactin analogues MIC values were 1–2 and 2–4 µg/mL for *S. aureus* (ATCC 29213) and *E. faecalis* (ATCC 29212), respectively. The analogues demonstrated comparable microbiological activity on the clinical isolates of both bacterial strains as the MIC value for *S. aureus* clinical isolates ranged from 0.5 to 2 µg/mL and was found to be 2 µg/mL for the *E. faecalis* clinical isolate included in this study. The MIC of TB1 has previously been reported as <0.0625 µg/mL against the same *S. aureus* strain (ATCC 29213) by Parmar et al. [15]. This disagreement might be due to the adoption of different test procedures. The MIC values reported by Parmar et al. were generally lower than those reported in the literature [27, 28].

**Table 1** MIC (µg/mL) for *S. aureus* and *E. faecalis* with teixobactin analogues (TB1–3), natural teixobactin and vancomycin

	<i>S. aureus</i>			<i>E. faecalis</i>	
	ATCC 29213	P14	P20	ATCC 29212	P40
TB1	1 - 2	1	0.5 - 1	4	2
TB2	(1) - 2 <sup>a</sup>	1 - 2	1 - 2	2 - (4) <sup>a</sup>	2
TB3	1 - 2	1	0.5 - 1	2 - (4) <sup>a</sup>	2
Teixobactin	0.25 - (1)	1	0.25	2 - 4	1 - 2
Vancomycin	1	ND	ND	2	ND

ND not determined

<sup>a</sup>The non-bracketed number occurred most often

To determine whether an antimicrobial compound is likely to be bactericidal or bacteriostatic, the MBC/MIC ratio is usually calculated. Generally, an MBC/MIC ratio  $\leq 4$  indicates bactericidal action [29]. MBC results for *S. aureus* ATCC 29213 and *E. faecalis* ATCC 29212 with all three analogues was found to be 8  $\mu\text{g/mL}$  and  $> 16 \mu\text{g/mL}$ , respectively. No MBC values were determined for *E. faecalis* (ATCC 29212) at the concentrations investigated. However, since the MBC was  $> 16 \mu\text{g/mL}$  and the MIC was 2–4  $\mu\text{g/mL}$ , the teixobactin analogues are bacteriostatic against the *E. faecalis* strain used in the present study as MBC/MIC ratio will be  $> 4$ .

### Effect of Teixobactin Analogues on Planktonic Growth

As MIC values are endpoint measurements, growth curves were generated to gain information on the activity of the analogues during different phases of culture development. The same medium was used to study both growth curves and grow biofilms. The obtained growth curves (Fig. 2) were in accordance with the MIC results as no growth was observed in concentrations  $\geq \text{MIC}$ . At  $\frac{1}{2} \times \text{MIC}$ , a measurable delay in the onset of the exponential phase was observed for both *S. aureus* and *E. faecalis* for all three teixobactin analogues (Table 2). The doubling time (DT) is a variable that can be used as a measurement of bacterial fitness. The ratio

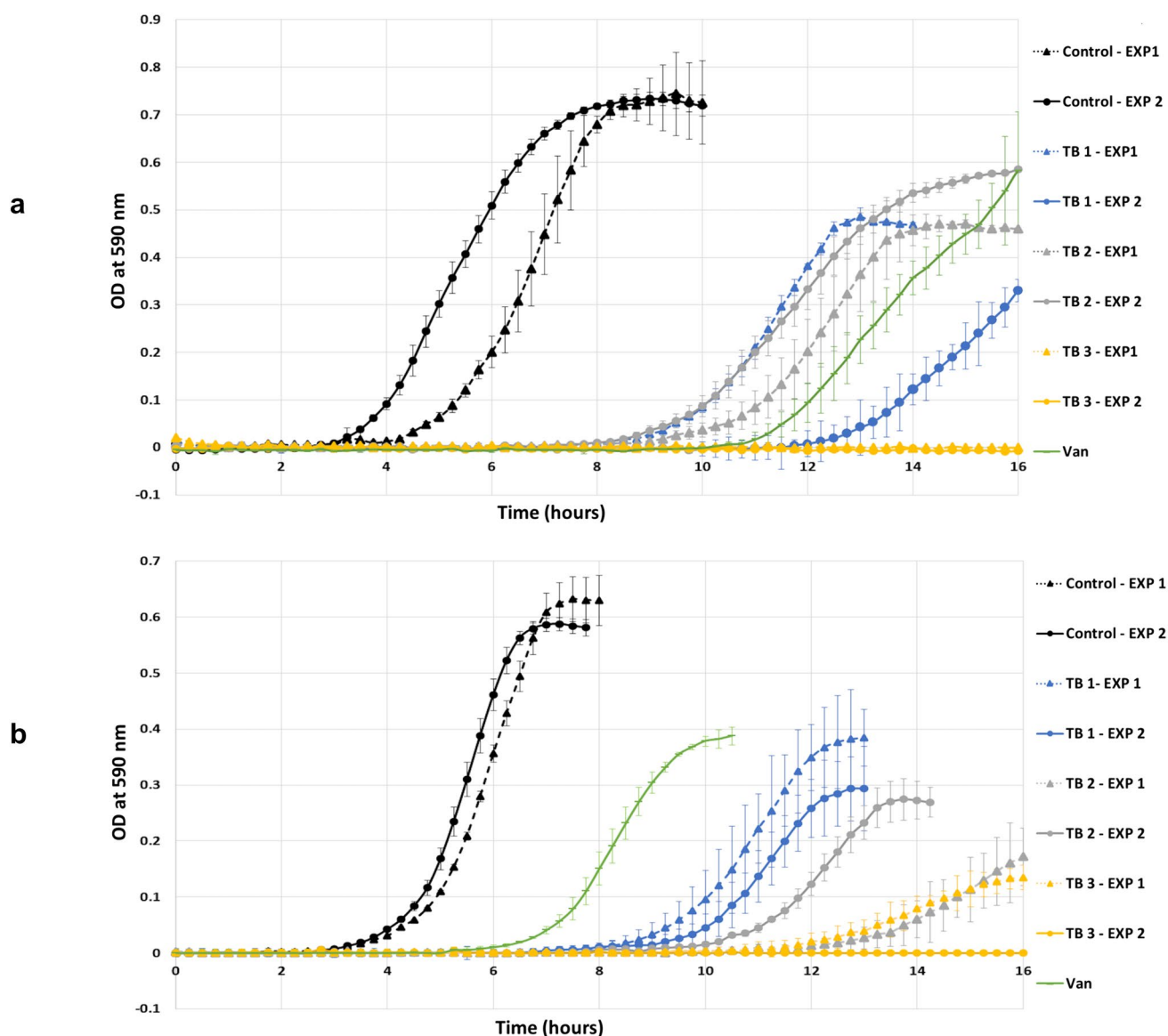


**Fig. 2** Growth curves of **a** *S. aureus* and **b** *E. faecalis* in the presence of  $\frac{1}{2} \times \text{MIC}$  equivalent concentration of teixobactin analogues and vancomycin (Van) presented as mean  $\pm$  SD

**Table 2** Time to onset of the exponential growth (log phase) and doubling times of *S. aureus* and *E. faecalis* without addition of any antibiotic (control) and after treatment with teixobactin analogues or vancomycin

	<i>S. aureus</i> ATCC 29213				<i>E. faecalis</i> ATCC 29212			
	Onset of exponential growth (h)		Doubling time (h)		Onset of exponential growth (h)		Doubling time (h)	
	Exp 1	Exp 2	Exp 1	Exp 2	Exp 1	Exp 2	Exp 1	Exp 2
Control	3±0.2	2.5±0.3	0.42±0.027	0.41±0.017	3.25±0.2	3.25±0.1	0.56±0.045	0.49±0.029
TB1	8.25±0.3	11.75±0.1	0.60±0.038 (1.43) <sup>a</sup>	0.69±0.042 (1.68) <sup>a</sup>	8.25±0.1	9±0.5	0.62±0.033 (1.12) <sup>a</sup>	0.61±0.052 (1.09) <sup>a</sup>
TB2	8.25±0.1	8±0.2	0.74±0.035 (1.76) <sup>a</sup>	0.85±0.061 (2.07) <sup>a</sup>	12.25±0.3	9.75±0.4	0.91±0.063 (1.63) <sup>a</sup>	0.67±0.049 (1.20) <sup>a</sup>
TB3	ND	ND	ND	ND	11.75±0.5	ND	0.84±0.048 (1.50) <sup>a</sup>	ND
Vancomycin	10±0.5		0.58±0.016 (1.41) <sup>a</sup>		5.5±0.2		0.54±0.027 (1.10) <sup>a</sup>	

Exp 1 and Exp 2 denote the two separate experiments performed. Results shown as mean±SD and significant difference was determined using analysis of variance (ANOVA) with Bonferroni correction (*P* value<0.05)

<sup>a</sup>Bracketed numbers are the fold increase in doubling time compared to the control

ND not determined

of increase in DT for each analogue compared to the control is given in Table 2. The period before the onset of the exponential phase was greatest with TB3 for both *S. aureus* and *E. faecalis*. In all but one experiment (experiment 1 with *E. faecalis*, Fig. 2), the onset of the exponential phase exceeded 16 h. By comparison, the time to onset of exponential growth ranged from 8 to 12 h with TB1 and TB2. From the calculated values for the doubling time (DT) presented in Table 2, the DT for *E. faecalis* had an average increase of 11% and 42% with TB1 and TB2, respectively, while with *S. aureus* the increase was notably higher at 56% and 92%, respectively for the same analogues. Statistical analysis of the results demonstrated significant delay in the exponential phase onset with teixobactin analogues compared to the control with both bacterial species. No significant differences were detected between the analogues tested. Moreover, the changes observed in the doubling time with the analogues were insignificant compared to the control. The results show that the analogues affect bacterial ability to adapt and grow

even at ½×MIC. The less profound effect of the teixobactin analogues on *E. faecalis* compared to *S. aureus* is in agreement with the MBC/MIC results.

### Inhibition of Biofilm Formation

The administration of prophylactic antibiotics and the use of antibiotic coated medical devices to prevent biofilm formation are among the currently implemented strategies for combating biofilms in the clinical setting [30, 31]. Therefore, testing the ability of antibiotics to prevent biofilm formation is pertinent. Biofilm experiments were performed in TSB + 1% glucose which is a commonly used growth medium for studies involving both *S. aureus* and *E. faecalis* biofilms [20–22, 32–35]. BIC<sub>90</sub> was determined by three different methods which are among the most common measures of biofilm quantification [36]. Results are summarized in

**Table 3** Summary of biofilm inhibitory concentration (BIC<sub>90</sub>) values in µg/mL (mean±SD) for teixobactin analogues and vancomycin determined with three different methods

	<i>S. aureus</i> ATCC 29213			<i>E. faecalis</i> ATCC 29212		
	Colony counting	Crystal violet	Activity staining	Colony counting	Crystal violet	Activity staining
TB1	4	4	4	8	8	ND
TB2	4	4	4	8	8	ND
TB3	3±1.41	3±1.41	3±1.41	4	4	ND
Vancomycin	1	1	1	2	> 8	ND

The absence of SD value signifies that the experimental replicates yielded identical results with no observed variability

ND not determined as no colour change was observed (see “Activity Staining” section)



Table 3 as biofilm inhibitory concentration (BIC90) values in µg/mL and presented for each method in detail below.

### Visual Scoring and Colony Counting

Regarding *S. aureus*, all analogues achieved greater than 90% reduction in the number of viable cells relative to the control at concentrations equal to  $2 \times \text{MIC}$  in both rounds of testing. TB3 even showed slightly higher activity by inhibiting biofilm formation at  $1 \times \text{MIC}$  in one round of testing. With respect to *E. faecalis*, similar results were obtained for TB1 and TB2. For TB3, no visual growth was observed at  $1 \times \text{MIC}$  equivalent concentration in two independent rounds of testing indicating higher antibiofilm activity than TB1 and TB2 (Supplementary file 1—Table S1). These results are in line with the growth curves observed for the teixobactin analogues (“Effect of Teixobactin Analogues on Planktonic Growth” section) suggesting the SAR effect of Nva substitution at position 10, which results in higher antimicrobial and antibiofilm effect with TB3.

### Crystal Violet Assay

CV staining is relatively easy to perform, less expensive and less laborious than colony counting [36]. However, CV is non-selective for cells and it stains negatively charged biofilm matrix molecules (e.g. nucleic acids, polysaccharides and proteins) [37]. Thus, the results represent the whole biofilm mass including both cells and extracellular components. In the present study, the calculated percentage reduction in biofilm formation by CV staining was similar to that obtained with colony counting (Supplementary file 1—Table S2). However, *E. faecalis* results with vancomycin did not reflect the actual biofilm reduction observed by colony counting. The deviation could be attributed to vancomycin-induced production of one or more biofilm matrix components which can possibly bind to crystal violet. Such deviations can occur especially after stressful treatment of bacteria with antibiotics [37]. These findings support the importance of also including colony counting or similar direct measures of cell viability when analysing biofilms.

### Activity Staining

The calculated reduction in TPF production compared to the control wells supports the colony counting and CV results for *S. aureus* (Supplementary file 1—Table S3). Results obtained with *E. faecalis* were inconclusive as no red colour development was observed even in the control wells without antibiotic treatment. The reason for this is not known but suggests a limitation of using TTC as a measure of biofilm production for this species. Biofilm formation may affect the cells metabolic activity, and this may have affected the assay outcomes.

### Inactivation of Bacteria in Established Biofilms

All three teixobactin analogues demonstrated a concentration-dependent effect on *S. aureus* biofilm eradication on both PVC and PTFE surfaces. Antibiotic concentrations resulting in 50% and 90% eradication of the biofilm,  $\text{BEC}_{50}$  and  $\text{BEC}_{90}$ , respectively, are presented in Table 4. All analogues showed effective inactivation of bacterial cells in the biofilm at concentrations as low as the MIC (1 µg/mL). The activity of the analogues increased slightly in the following order  $\text{TB3} > \text{TB2} > \text{TB1}$ . Results from the activity staining method (Table 5) showed similar patterns to colony counting, where the activity slightly increased in the same order ( $\text{TB3} > \text{TB2} > \text{TB1}$ ). Despite the low MIC value for vancomycin against *S. aureus* (1 µg/mL),  $\text{BEC}_{90}$  values of vancomycin were 4- and 16-folds higher than the MIC with PVC and PTFE, respectively.

### Confocal Laser Scanning Microscopy (CLSM) Analysis of Biofilms

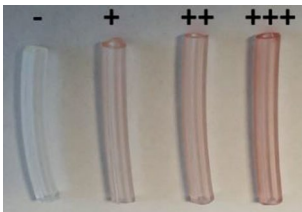
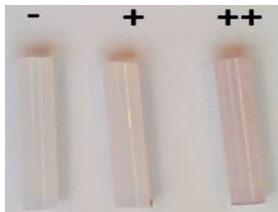
The results obtained from CLSM images analysis after testing different concentrations of TB3 on a preformed *S. aureus* biofilm on glass chamber are presented in Fig. 3. With respect to biofilm formation and inactivation, bacterial cell viability is the most critical operational parameter, as it directly influences biofilm production. Bacterial cell viability was investigated using a combination of dyes where actively metabolizing cells stain green and dead cells stain

**Table 4**  $\text{BEC}_{50}$  and  $\text{BEC}_{90}$  of *S. aureus* in µg/mL (mean  $\pm$  SD) after treatment of PVC and PTFE with teixobactin analogues and vancomycin

	PVC		PTFE	
	$\text{BEC}_{50}$ (µg/mL)	$\text{BEC}_{90}$ (µg/mL)	$\text{BEC}_{50}$ (µg/mL)	$\text{BEC}_{90}$ (µg/mL)
TB1	$1.5 \pm 0.71$	$5 \pm 4.24$	4	4
TB2	$1.5 \pm 0.71$	2	2	4
TB3	$1.5 \pm 0.71$	1	$1.5 \pm 0.71$	$3 \pm 1.41$
Vancomycin	4	4	4	16

The absence of SD value signifies that the experimental replicates yielded identical results with no observed variability

**Table 5** Qualitative scoring of *S. aureus* biofilm based on triphenyl formazan colour intensity on PVC and PTFE after treatment with teixobactin analogues

Plastic type	PVC				PTFE			
Scoring scale								
Concentration in µg/mL (MIC equivalent) <sup>a</sup>	Recorded colour scores							
	Exp 1	Exp 2	Exp 1	Exp 2	Exp 1	Exp 2	Exp 1	Exp 2
Control	+++	+++			+	++		
TB1								
1 (½ × MIC)	+	+			+	++		
2 (1 × MIC)	++	+			+	+		
4 (2 × MIC)	++	+			–	+		
TB2								
1 (½ × MIC)	+	+			+	++		
2 (1 × MIC)	++	+			–	++		
4 (2 × MIC)	+	+			–	–		
TB3								
1 (½ × MIC)	+	+			+	+		
2 (1 × MIC)	+	+			–	+		
4 (2 × MIC)	+	+			–	–		

<sup>a</sup>At and above 8 µg/mL (4 × MIC) no colouration was observed

red. Increasing the concentration of TB3 resulted in proportional significant decrease ( $P < 0.05$ ) in *S. aureus* viability which was  $34.2 \pm 5.3\%$  with the highest TB3 concentration tested (8 µg/mL). Additionally, biovolume was calculated to demonstrate the ability of TB3 to induce biofilm thinning and removal. Biovolume represents the overall volume occupied by the biofilm and is commonly used as a parameter in biofilm studies as it provides valuable information regarding the biofilm size and biomass [26, 38]. TB3 demonstrated the ability to significantly disrupt preformed biofilm after treatment for only 24 h. TB3 at 8 µg/mL concentration resulted in decreased biovolume by approximately 75% compared to the control.

## Discussion

Antibiotic resistance is a global health threat, prompting research aimed at the discovery and development of new agents with clinical potential. Here we show that three easily synthesized analogues of the natural antibiotic teixobactin, retain promising activity in vitro against the important pathogens *S. aureus* and *E. faecalis*. All three teixobactin

analogues gave similar MIC values of 1–2 and 2–4 µg/mL for *S. aureus* (ATCC 29213) and *E. faecalis* (ATCC 29212), respectively. The activity also extended to the clinical isolates of both species. Although the MIC values for the teixobactin analogues were slightly higher compared to the ones reported for natural teixobactin (this study and [12]), the advantage of the analogues for future drug development, lies in their relative ease of production compared with the natural product. Despite structural differences, the teixobactin analogues seem to retain most of the bactericidal activity of the natural teixobactin against *S. aureus* [12]. For *S. aureus* strain tested in this work, the teixobactin analogues were bactericidal, which is likely due to the inhibition of peptidoglycan and teichoic acid synthesis leading to disruption of cell wall formation and cell lysis [39]. However, no bactericidal effect was detected against *E. faecalis*, which can probably be attributed to an *E. faecalis* intrinsic tolerance mechanism against antibiotics targeting cell wall [40]. This suggests a potentially restricted application of teixobactin and its analogues in treating infections caused by this species. To our knowledge, Gebhard et al. study [41] is the only report on MBC values of teixobactin or its analogues for *E. faecalis*. They reported MIC and MBC of teixobactin as

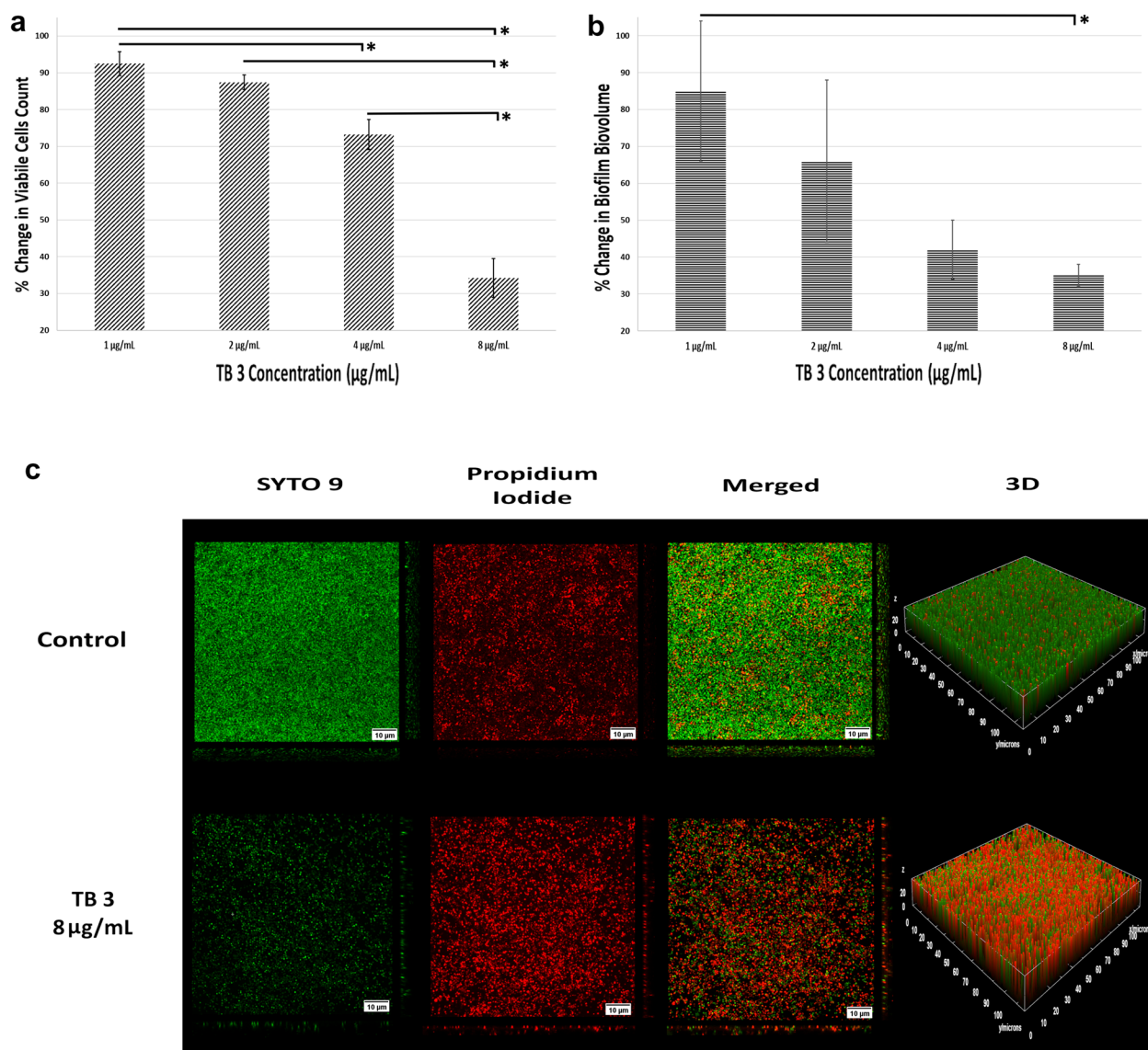


**Fig. 3** Effect of different concentrations of TB3 on **a** percentage bacterial cell viability presented as mean  $\pm$  SD and **b** percentage change in biovolume compared to control presented as mean  $\pm$  SD. **c** shows

2D images for live cells (SYTO 9), dead cells (propidium iodide) and 3D visualizations obtained from CLSM z-stacks for the control and 8 µg/mL of TB3. (\*) indicates significant difference ( $P < 0.05$ )

2 µg/mL and 16–32 µg/mL, respectively, which supports the findings of the current work. The same study also reported that vancomycin MBC for the same bacteria species was higher than 128 µg/mL. The authors attributed *E. faecalis* tolerance to teixobactin to a change in the CroRS two-component regulatory system. This change resulted in upregulation of the expression of major genes involved in cell wall biogenesis [41]. The same tolerance mechanism was also reported with vancomycin and bacitracin, indicating that it can be an intrinsic tolerance mechanism in *E. faecalis* against antibiotics targeting cell wall [40].

To our knowledge, details of the effect of sub-lethal concentrations of teixobactin on the development of bacterial

populations in liquid culture (growth curves) has not previously been investigated. The observed prolongation of the lag phase in the presence of teixobactin analogues might be attributed to a defence mechanism that allows the bacteria to tolerate cellular stress induced by the antimicrobial agent. This effect has been described as the “tolerance by lag” phenomenon [42]. Bacterial growth responses are agent-specific as they are affected by the antimicrobial’s mechanism of action. Theophel et al. [43] reported that antibiotics affecting cell wall or membrane integrity (e.g. vancomycin and daptomycin) delay the onset of bacterial growth. Conversely, antibiotics affecting DNA replication or protein synthesis (e.g. moxifloxacin and gentamicin) show initial normal growth

followed by induced alteration [43]. The observed delay in the onset of the exponential phase with both *S. aureus* and *E. faecalis* agrees with previously reported growth responses for antibiotics affecting cell envelope integrity [43, 44]. Additionally, it is noteworthy that even after the onset of the exponential growth, the maximum OD<sub>590</sub> reached was substantially lower for wells containing antibiotics compared to the antibiotic-free control for both types of bacteria (Fig. 2). The reason for this observation is not yet clear, but it has been reported by others [43]. It is possible that the prolonged lag phase consumes energy or generates products inhibitory for later growth, but these remain speculations. Although the MIC values for the three teixobactin analogues (Leu in TB1, Nle in TB2 and Nva in TB3) were equal (Table 1), bacterial growth in the presence of TB3 was more severely restricted than in the presence of the other analogues. This suggests that the length of the hydrophobic side chain at position 10 critically affects the structure–activity relationship (SAR). Although requiring further investigation, the finding receives support from Jin et al. [28], where a onefold decrease in MIC for *S. aureus* was reported when norvaline (Nva) was introduced in position 10 of the teixobactin structure compared to norleucine (Nle) and isoleucine (Ile) substitutions [28]. The authors proposed that the higher microbiological activity is associated with the presence of a linear three-carbon side chain in Nva [28]. This substitution is also present in TB3 (Fig. 1).

Three approaches (colony counting, CV and activity staining) were employed to test the ability of the analogues to inhibit biofilm formation. Results of the three analysis methods were consistent and generated the same BIC<sub>90</sub> values. BIC<sub>90</sub> for *S. aureus* with TB1 and TB2 was found to be 4 µg/mL (2 × MIC). While TB3 demonstrated slightly higher activity with an average BIC<sub>90</sub> of 3 µg/mL (Table 3). BIC<sub>90</sub> values for *E. faecalis* were 2 × MIC (8 µg/mL) for both TB1 and TB2, while for TB3 the BIC<sub>90</sub> was 1 × MIC (4 µg/mL). Although mutually supportive in analysis of biofilm formation, the three analytical approaches have individual weaknesses and strengths. The CV assay provides a measurement of total biofilm components (including cells and extracellular material). In contrast, colony counting and metabolic assays offer more selective measurements as they are not directly affected by extracellular material and essentially reflect the presence of viable cells. A particular advantage of activity staining is that viable cells may not form colonies on agar. Metabolically active cells will reduce the TTC substrate to TPF resulting in red colour development [23]. The consistent findings across all three methodologies strengthen the claim that teixobactin analogues possess the capability to prevent biofilm formation. Moreover, the increased efficacy observed with TB3 supports the proposed SAR.

The process of biofilm development on surfaces is multifactorial, depending on the bacterial strain, the surrounding

environment and physicochemical properties of the material surface [45]. Given this background, we decided to investigate two structurally different materials used in the production of medical devices, PVC and PTFE, for biofilm formation. Antibiofilm activity on both materials varied between the different teixobactin analogues. Activity increased in the following order TB3 > TB2 > TB1. This is also in line with previously discussed SAR. Moreover, the agreement of activity staining results with colony counting, suggests the possibility of using activity staining as an easy and time-saving qualitative method for preliminary screening of antibiotic activity against biofilms. The difference between MIC and BEC<sub>90</sub> with teixobactin analogues was much lower than that seen with vancomycin (e.g. only 2-folds with TB3 compared with 16-folds for vancomycin). This would suggest a better ability of teixobactin analogues to penetrate the biofilm matrix. This is highly interesting in terms of drug development, as insufficient antibiotic penetration is a main cause of treatment failure of biofilm based infections [2, 3]. Moreover, the higher hydrophobicity of teixobactin analogues compared to the water-soluble vancomycin may result in greater tendency of the analogues to adsorb onto plastic surfaces than vancomycin resulting in lower BEC<sub>90</sub> values. In a published study investigating peptide interaction with hydrophobic fluorocarbon surfaces, peptide adsorption on the surface occurred within a few minutes of incubation through hydrophobic attractions between leucine residues and the material surface [46].

Teixobactin analogue (TB3), which exhibited the most promising effect against established biofilm, was chosen for further analysis using CLSM. Biofilm cell viability and biovolume demonstrated a proportional decrease corresponding to an increase in TB3 concentration from 1 to 8 µg/mL (½ × MIC to 4 × MIC). Three dimensional visualisations for the collected image stacks show a considerable change in the biofilm population after treatment for 24 h with 8 µg/mL of TB3, as the count of viable cells (depicted in green in Fig. 3) decreased significantly ( $P < 0.05$ ) by 65% compared to the control wells, while the biovolume exhibited a reduction of approximately 75% relative to the control.

## Conclusion

All three novel teixobactin analogues proved to be effective at clinically relevant concentrations against the medically important, biofilm-forming species *S. aureus* and *E. faecalis*, including both culture-collection strains and some clinical isolates. The analogues were able to inhibit biofilm formation and demonstrated higher activity on pre-established *S. aureus* biofilms than vancomycin. This together with the relative ease of production of the analogues compared to the natural teixobactin makes them interesting candidates for



further pharmaceutical development. The impact of position 10 substitution on SAR of teixobactin analogues was also confirmed: substitution with norvaline resulted in a notable reduction in the agent concentration needed to eradicate biofilms. Future work could include investigations on a wider range of bacteria including more clinical isolates and the development of appropriate pharmaceutical formulations. We are currently working on incorporating teixobactin analogues in liposomal carriers to see if antibacterial efficacy and drug stability can be improved.

**Supplementary Information** The online version contains supplementary material available at <https://doi.org/10.1007/s00284-024-03857-9>.

**Acknowledgements** We acknowledge Dr. Ishwar Singh and his research group at Departments of Therapeutics and Chemistry at Institute of Translational Medicine, University of Liverpool for providing the teixobactin analogues investigated in this study.

**Author Contributions** AMA, CC and SN conceived and designed the study. AMA and CC performed the analyses. AMA, CC and SN were involved in interpretation of the data and writing the manuscript. All authors approved submission of the manuscript.

**Funding** Open access funding provided by OsloMet - Oslo Metropolitan University. This study was made possible through internal funding at Oslo Metropolitan University. No external funding was received.

**Data Availability** All data and material are available.

**Code Availability** Not applicable.

## Declarations

**Conflict of interest** The authors declare that they have no conflict of interest.

**Ethical Approval** Not required. Clinical isolates of *S. aureus* and *E. faecalis* were obtained from an investigation approved by the Regional Committee of Medical Research Ethics (REK number: 350387), adhering to the principles of the Declaration of Helsinki.

**Consent to Participate** Informed consent has been obtained from participants for sample collection.

**Consent for Publication** Informed consent has been obtained from participants for data publication.

**Open Access** This article is licensed under a Creative Commons Attribution 4.0 International License, which permits use, sharing, adaptation, distribution and reproduction in any medium or format, as long as you give appropriate credit to the original author(s) and the source, provide a link to the Creative Commons licence, and indicate if changes were made. The images or other third party material in this article are included in the article's Creative Commons licence, unless indicated otherwise in a credit line to the material. If material is not included in the article's Creative Commons licence and your intended use is not permitted by statutory regulation or exceeds the permitted use, you will need to obtain permission directly from the copyright holder. To view a copy of this licence, visit <http://creativecommons.org/licenses/by/4.0/>.

## References

1. Uruén C, Chopo-Escuin G, Tommassen J, Mainar-Jaime RC, Arenas J (2020) Biofilms as promoters of bacterial antibiotic resistance and tolerance. *Antibiotics* (Basel). <https://doi.org/10.3390/antibiotics10010003>
2. Da Silva RAG, Afonina I, Kline KA (2021) Eradicating biofilm infections: an update on current and prospective approaches. *Curr Opin Microbiol* 63:117–125. <https://doi.org/10.1016/j.mib.2021.07.001>
3. Gebreyohannes G, Nyerere A, Bii C, Sbhatu DB (2019) Challenges of intervention, treatment, and antibiotic resistance of biofilm-forming microorganisms. *Heliyon* 5(8):e02192. <https://doi.org/10.1016/j.heliyon.2019.e02192>
4. Fulaz S, Vitale S, Quinn L, Casey E (2019) Nanoparticle–biofilm interactions: the role of the EPS matrix. *Trends Microbiol* 27(11):915–926. <https://doi.org/10.1016/j.tim.2019.07.004>
5. Ceri H, Olson ME, Stremick C, Read R, Morck D, Buret A (1999) The Calgary Biofilm Device: new technology for rapid determination of antibiotic susceptibilities of bacterial biofilms. *J Clin Microbiol* 37(6):1771–1776. <https://doi.org/10.1128/jcm.37.6.1771-1776.1999>
6. Roberts MG, Burgess S, Toombs-Ruane LJ, Benschop J, Marshall JC, French NP (2021) Combining mutation and horizontal gene transfer in a within-host model of antibiotic resistance. *Math Biosci* 339:108656. <https://doi.org/10.1016/j.mbs.2021.108656>
7. Murray CJ, Ikuta KS, Sharara F, Swetschinski L, Aguilar GR, Gray A, Han C, Bisignano C, Rao P, Wool E (2022) Global burden of bacterial antimicrobial resistance in 2019: a systematic analysis. *The Lancet* 399(10325):629–655. [https://doi.org/10.1016/S0140-6736\(21\)02724-0](https://doi.org/10.1016/S0140-6736(21)02724-0)
8. Mestrovic T, Robles Aguilar G, Swetschinski LR, Ikuta KS, Gray AP, Davis Weaver N, Han C, Wool EE, Gershberg Hayoon A, Hay SI, Dolecek C, Sartorius B, Murray CJL, Addo IY, Ahinkorah BO, Ahmed A, Aldeyab MA, Allel K, Ancuceanu R, Anyasodor AE, Ausloos M, Barra F, Bhagavathula AS, Bhandari D, Bhaskar S, Cruz-Martins N, Dastiridou A, Dokova K, Dubljanin E, Durojaiye OC, Fagbamigbe AF, Ferrero S, Gaal PA, Gupta VB, Gupta VK, Gupta VK, Herteliu C, Hussain S, Ilıc IM, Ilıc MD, Jamshidi E, Joo T, Karch A, Kisa A, Kisa S, Kostyaneyev T, Kyu HH, Lám J, Lopes G, Mathioudakis AG, Mentis A-FA, Michalek IM, Moni MA, Moore CE, Mulita F, Negoii I, Negoii RI, Palicz T, Pana A, Perdigão J, Petcu I-R, Rabiee N, Rawaf DL, Rawaf S, Shakhmardanov MZ, Sheikh A, Silva LMLR, Skryabin VY, Skryabina AA, Socea B, Stergachis A, Stoeva TZ, Sumi CD, Thiagarajan A, Tovani-Palone MR, Yesiltepe M, Zaman SB, Naghavi M (2022) The burden of bacterial antimicrobial resistance in the WHO European region in 2019: a cross-country systematic analysis. *Lancet Public Health* 7(11):e897–e913. [https://doi.org/10.1016/S2468-2667\(22\)00225-0](https://doi.org/10.1016/S2468-2667(22)00225-0)
9. Hillock NT, Merlin TL, Turnidge J, Karnon J (2022) Modelling the future clinical and economic burden of antimicrobial resistance: the feasibility and value of models to inform policy. *Appl Health Econ Health Policy* 20(4):479–486. <https://doi.org/10.1007/s40258-022-00728-x>
10. Browne K, Chakraborty S, Chen R, Willcox MD, Black DS, Walsh WR, Kumar N (2020) A new era of antibiotics: the clinical potential of antimicrobial peptides. *Int J Mol Sci*. <https://doi.org/10.3390/ijms21197047>
11. Miethke M, Pieroni M, Weber T, Brönstrup M, Hammann P, Halby L, Arimondo PB, Glaser P, Aigle B, Bode HB, Moreira R, Li Y, Luzhetskyy A, Medema MH, Pernodet J-L, Stadler M, Tormo JR, Genilloud O, Truman AW, Weissman KJ, Takano E, Sabatini S, Stegmann E, Brötz-Oesterhelt H, Wohlleben W, Seemann M, Empting M, Hirsch AKH, Loretz B, Lehr C-M, Titz

- A, Herrmann J, Jaeger T, Alt S, Hestekamp T, Winterhalter M, Schiefer A, Pfarr K, Hoerauf A, Graz H, Graz M, Lindvall M, Ramurthy S, Karlén A, van Dongen M, Petkovic H, Keller A, Peyrane F, Donadio S, Fraisse L, Piddock LJV, Gilbert IH, Moser HE, Müller R (2021) Towards the sustainable discovery and development of new antibiotics. *Nat Rev Chem* 5(10):726–749. <https://doi.org/10.1038/s41570-021-00313-1>
12. Ling LL, Schneider T, Peoples AJ, Spoering AL, Engels I, Conlon BP, Mueller A, Schäberle TF, Hughes DE, Epstein S, Jones M, Lazarides L, Steadman VA, Cohen DR, Felix CR, Fetterman KA, Millett WP, Nitti AG, Zullo AM, Chen C, Lewis K (2015) A new antibiotic kills pathogens without detectable resistance. *Nature* 517(7535):455–459. <https://doi.org/10.1038/nature14098>
  13. Parmar A, Iyer A, Prior SH, Lloyd DG, Leng Goh ET, Vincent CS, Palmi-Pallag T, Bachrati CZ, Breukink E, Maddar A, Lakshminarayanan R, Taylor EJ, Singh I (2017) Teixobactin analogues reveal enduracididine to be non-essential for highly potent antibacterial activity and lipid II binding. *Chem Sci* 8(12):8183–8192. <https://doi.org/10.1039/C7SC03241B>
  14. Gunjal VB, Thakare R, Chopra S, Reddy DS (2020) Teixobactin: a paving stone toward a new class of antibiotics? *J Med Chem* 63(21):12171–12195. <https://doi.org/10.1021/acs.jmedchem.0c00173>
  15. Parmar A, Lakshminarayanan R, Iyer A, Mayandi V, Leng Goh ET, Lloyd DG, Chalasani MLS, Verma NK, Prior SH, Beuerman RW, Maddar A, Taylor EJ, Singh I (2018) Design and syntheses of highly potent teixobactin analogues against *Staphylococcus aureus*, methicillin-resistant *Staphylococcus aureus* (MRSA), and vancomycin-resistant enterococci (VRE) in vitro and in vivo. *J Med Chem* 61(5):2009–2017. <https://doi.org/10.1021/acs.jmedchem.7b01634>
  16. Naqvi M, Fineide F, Utheim TP, Charnock C (2024) Culture- and non-culture-based approaches reveal unique features of the ocular microbiome in dry eye patients. *Ocul Surf* 32:123–129. <https://doi.org/10.1016/j.jtos.2024.02.002>
  17. Clinical and Laboratory Standards Institute (CLSI) (2020) M100: performance standards for antimicrobial susceptibility testing, 30th edn. Clinical & Laboratory Standards Institute, Wayne
  18. Clinical and Laboratory Standards Institute (CLSI) (1999) M26-A: methods for determining bactericidal activity of antimicrobial agents, 1st edn. Clinical & Laboratory Standards Institute, Wayne
  19. Hall BG, Acar H, Nandipati A, Barlow M (2014) Growth rates made easy. *Mol Biol Evol* 31(1):232–238. <https://doi.org/10.1093/molbev/mst187>
  20. Narenji H, Teymournejad O, Rezaee MA, Taghizadeh S, Mehramuz B, Aghazadeh M, Asgharzadeh M, Madhi M, Gholizadeh P, Ganbarov K, Yousefi M, Pakravan A, Dal T, Ahmadi R, Samadi Kafil H (2020) Antisense peptide nucleic acids against *ftsZ* and *efaA* genes inhibit growth and biofilm formation of *Enterococcus faecalis*. *Microb Pathog* 139:103907. <https://doi.org/10.1016/j.micpath.2019.103907>
  21. Chaudhari PR, Masurkar SA, Shidore VB, Kamble SP (2012) Effect of biosynthesized silver nanoparticles on *Staphylococcus aureus* biofilm quenching and prevention of biofilm formation. *Nano-Micro Lett* 4(1):34–39. <https://doi.org/10.1007/BF03353689>
  22. El-Atrees DM, El-Kased RF, Abbas AM, Yassien MA (2022) Characterization and anti-biofilm activity of bacteriophages against urinary tract *Enterococcus faecalis* isolates. *Sci Rep* 12(1):13048. <https://doi.org/10.1038/s41598-022-17275-z>
  23. Etayash H, Qian Y, Pletzer D, Zhang Q, Xie J, Cui R, Dai C, Ma P, Qi F, Liu R, Hancock REW (2020) Host defense peptide-mimicking amphiphilic  $\beta$ -peptide polymer (Bu:DM) exhibiting anti-biofilm, immunomodulatory, and in vivo anti-infective activity. *J Med Chem* 63(21):12921–12928. <https://doi.org/10.1021/acs.jmedchem.0c01321>
  24. Haney EF, Trimble MJ, Cheng JT, Vallé Q, Hancock REW (2018) Critical assessment of methods to quantify biofilm growth and evaluate antibiofilm activity of host defence peptides. *Biomolecules* 8(2):29. <https://doi.org/10.3390/biom8020029>
  25. Mountcastle SE, Vyas N, Villapun VM, Cox SC, Jabbari S, Sammons RL, Shelton RM, Walmsley AD, Kuehne SA (2021) Biofilm viability checker: an open-source tool for automated biofilm viability analysis from confocal microscopy images. *NPJ Biofilms Microbiomes* 7(1):44. <https://doi.org/10.1038/s41522-021-00214-7>
  26. Heydorn A, Nielsen AT, Hentzer M, Sternberg C, Givskov M, Ersbøll BK, Molin S (2000) Quantification of biofilm structures by the novel computer program COMSTAT. *Microbiology (Reading)* 146(Pt 10):2395–2407. <https://doi.org/10.1099/00221287-146-10-2395>
  27. Velkov T, Swarbrick JD, Hussein MH, Schneider-Futschik EK, Hoyer D, Li J, Karas JA (2019) The impact of backbone N-methylation on the structure–activity relationship of Leu10-teixobactin. *J Pept Sci* 25(9):e3206. <https://doi.org/10.1002/psc.3206>
  28. Jin K, Po KHL, Kong WY, Lo CH, Lo CW, Lam HY, Sirinimal A, Reuven JA, Chen S, Li X (2018) Synthesis and antibacterial studies of teixobactin analogues with non-isostere substitution of enduracididine. *Bioorg Med Chem* 26(5):1062–1068. <https://doi.org/10.1016/j.bmc.2018.01.016>
  29. Mogana R, Adhikari A, Tzar MN, Ramliza R, Wiart C (2020) Antibacterial activities of the extracts, fractions and isolated compounds from *Canarium patentinervium* Miq. against bacterial clinical isolates. *BMC Complement Med Ther* 20(1):55. <https://doi.org/10.1186/s12906-020-2837-5>
  30. Tran HM, Tran H, Booth MA, Fox KE, Nguyen TH, Tran N, Tran PA (2020) Nanomaterials for treating bacterial biofilms on implantable medical devices. *Nanomaterials* 10(11):2253. <https://doi.org/10.3390/nano10112253>
  31. Ciofu O, Rojo-Molinero E, Macià MD, Oliver A (2017) Antibiotic treatment of biofilm infections. *APMIS* 125(4):304–319. <https://doi.org/10.1111/apm.12673>
  32. Seo S, Jung J, Kim CY, Kang H, Lee IH (2021) Antimicrobial peptides encounter resistance of aureolysin during their action on *Staphylococcus aureus* biofilm. *Biotechnol Bioprocess Eng* 26(2):216–222. <https://doi.org/10.1007/s12257-020-0384-z>
  33. Liu J, Li W, Zhu X, Zhao H, Lu Y, Zhang C, Lu Z (2019) Surfactin effectively inhibits *Staphylococcus aureus* adhesion and biofilm formation on surfaces. *Appl Microbiol Biotechnol* 103(11):4565–4574. <https://doi.org/10.1007/s00253-019-09808-w>
  34. Seidl K, Goerke C, Wolz C, Mack D, Berger-Bächi B, Bischoff M (2008) *Staphylococcus aureus* CcpA affects biofilm formation. *Infect Immun* 76(5):2044–2050. <https://doi.org/10.1128/IAI.00035-08>
  35. Cui P, Feng L, Zhang L, He J, An T, Fu X, Li C, Zhao X, Zhai Y, Li H, Yan W, Li H, Luo X, Lei C, Wang H, Yang X (2020) Antimicrobial resistance, virulence genes, and biofilm formation capacity among *Enterococcus* species from Yaks in Aba Tibetan Autonomous Prefecture, China. *Front Microbiol*. <https://doi.org/10.3389/fmicb.2020.01250>
  36. Wilson C, Lukowicz R, Merchant S, Valquier-Flynn H, Caballero J, Sandoval J, Okuom M, Huber C, Brooks TD, Wilson E, Clement B, Wentworth CD, Holmes AE (2017) Quantitative and qualitative assessment methods for biofilm growth: a mini-review. *Res Rev J Eng Technol*. <http://www.rroij.com/open-access/quantitative-and-qualitative-assessment-methods-for-biofilm-growth-a-minireview-.pdf>
  37. Latka A, Drulis-Kawa Z (2020) Advantages and limitations of microtiter biofilm assays in the model of antibiofilm

- activity of Klebsiella phage KP34 and its depolymerase. *Sci Rep* 10(1):20338. <https://doi.org/10.1038/s41598-020-77198-5>
38. Kannappan A, Gowrishankar S, Srinivasan R, Pandian SK, Ravi AV (2017) Antibiofilm activity of *Vetiveria zizanioides* root extract against methicillin-resistant *Staphylococcus aureus*. *Microb Pathog* 110:313–324. <https://doi.org/10.1016/j.micpath.2017.07.016>
  39. Homma T, Nuxoll A, Gandt AB, Ebner P, Engels I, Schneider T, Götz F, Lewis K, Conlon BP (2016) Dual targeting of cell wall precursors by teixobactin leads to cell lysis. *Antimicrob Agents Chemother* 60(11):6510–6517. <https://doi.org/10.1128/aac.01050-16>
  40. Darnell RL, Knottenbelt MK, Todd Rose FO, Monk IR, Stinear TP, Cook GM (2019) Genomewide profiling of the *Enterococcus faecalis* transcriptional response to teixobactin reveals CroRS as an essential regulator of antimicrobial tolerance. *mSphere*. <https://doi.org/10.1128/mSphere.00228-19>
  41. Todd Rose FO, Darnell RL, Morris S, Paxie O, Campbell G, Cook GM, Gebhard S (2022) The two-component system CroRS regulates isoprenoid flux to mediate antimicrobial tolerance in the bacterial pathogen *Enterococcus faecalis*. *bioRxiv*. <https://doi.org/10.1101/2022.12.05.519242>
  42. Bertrand RL (2019) Lag phase is a dynamic, organized, adaptive, and evolvable period that prepares bacteria for cell division. *J Bacteriol*. <https://doi.org/10.1128/JB.00697-18>
  43. Theophel K, Schacht VJ, Schlüter M, Schnell S, Stingu C-S, Schaumann R, Bunge M (2014) The importance of growth kinetic analysis in determining bacterial susceptibility against antibiotics and silver nanoparticles. *Front Microbiol*. <https://doi.org/10.3389/fmicb.2014.00544>
  44. Shlezinger M, Copenhagen-Glazer S, Gelman D, Beyth N, Hazan R (2019) Eradication of vancomycin-resistant enterococci by combining phage and vancomycin. *Viruses* 11(10):954. <https://doi.org/10.3390/v11100954>
  45. Pascual A (2002) Pathogenesis of catheter-related infections: lessons for new designs. *Clin Microbiol Infect* 8(5):256–264. <https://doi.org/10.1046/j.1469-0691.2002.00418.x>
  46. Weidner T, Samuel NT, McCrea K, Gamble LJ, Ward RS, Castner DG (2010) Assembly and structure of  $\alpha$ -helical peptide films on hydrophobic fluorocarbon surfaces. *Biointerphases* 5(1):9–16. <https://doi.org/10.1116/1.3317116>

**Publisher's Note** Springer Nature remains neutral with regard to jurisdictional claims in published maps and institutional affiliations.

# Supplementary material (file 1)

**Table S.1**

Visual scoring of growth intensity (in brackets) and percentage reduction in *S. aureus* and *E. faecalis* colonies after incubation for 24 hours with teixobactin analogues and vancomycin (Van). Exp 1 and exp 2 denote two independent rounds of testing.

S. aureus ATCC 29213												E. faecalis ATCC 29212																			
½ X MIC				MIC				2X MIC				4X MIC				½ X MIC				MIC				2X MIC				4X MIC			
Exp 1		Exp 2		Exp 1		Exp 2		Exp 1		Exp 2		Exp 1		Exp 2		Exp 1		Exp 2		Exp 1		Exp 2		Exp 1		Exp 2					
TB1	(4+)	(4+)	(4+)	(4+)	(4+)	(0)	(0)	99.85%	(0)	(0)	(0)	(0)	(0)	(0)	(0)	(3+)	(3+)	(2+)	(2+)	(3+)	(0)	(0)	99.56%	(0)	(0)	(0)	(0)				
TB2	(4+)	(4+)	(4+)	(4+)	(4+)	(0)	(0)	98.75%	(0)	(0)	(0)	(0)	(0)	(0)	(0)	(3+)	(3+)	(2+)	(2+)	(2+)	(0)	(0)	99.32%	(0)	(0)	(0)	(0)				
TB3	(4+)	(4+)	(3+)	(0)	(0)	(0)	(0)	99.87%	(0)	(0)	(0)	(0)	(0)	(0)	(0)	(3+)	(3+)	(0)	(0)	(0)	(0)	(0)	99.92%	(0)	(0)	(0)	(0)				
Van	(4+)	(0)	99.47%	(0)	(0)	(0)	(0)	99.96%	(0)	(0)	(0)	(0)	(0)	(0)	(0)	(3+)	(3+)	(0)	(0)	(0)	(0)	(0)	99.97%	(0)	(0)	(0)	(0)				



Table S.2

Percentage reduction in *S. aureus* and *E. faecalis* crystal violet absorbance after incubation for 24 hours with teixobactin analogues and vancomycin (Van). Exp 1 and exp 2 denote two independent rounds of testing.

	<i>S. aureus</i> ATCC 29213						<i>E. faecalis</i> ATCC 29212					
	$\frac{1}{2}$ X MIC		MIC		2X MIC		4X MIC		$\frac{1}{2}$ X MIC		MIC	
	Exp 1		Exp 2		Exp 1		Exp 2		Exp 1		Exp 2	
	Exp 1	Exp 2	Exp 1	Exp 2	Exp 1	Exp 2	Exp 1	Exp 2	Exp 1	Exp 2	Exp 1	Exp 2
<b>TB1</b>	ND	ND	ND	ND	96.08%	95.44%	99.06%	99.02%	ND	ND	ND	ND
											92.54%	100%
											100%	100%
<b>TB2</b>	ND	ND	ND	ND	97.04%	98.16%	100%	95.90%	ND	ND	ND	ND
											82.34%	94.51%
											100%	100%
<b>TB3</b>	ND	ND	ND	100%	100%	100%	99.01%	100%	ND	ND	100%	94.22%
											100%	99.91%
											100%	100%
<b>Van</b>	ND		97.10%		95.20%		99.14%		ND		69.60%	72.35%
												70.83%

\* ND: Not determined (testing was only done for wells without detectable visual growth).

**Table S.3**

Percentage reduction in *S. aureus* activity stain absorbance after incubation for 24 hours with teixobactin analogues and vancomycin. Exp 1 and exp 2 denote two independent rounds of testing.

<i>S. aureus</i> ATCC 29213									
	$\frac{1}{2}$ X MIC		MIC		2X MIC		4X MIC		
	Exp 1	Exp 2	Exp 1	Exp 2	Exp 1	Exp 2	Exp 1	Exp 2	
<b>TB1</b>	ND	ND	ND	ND	99.29%	98.45%	99.25%	99.34%	
<b>TB2</b>	ND	ND	ND	ND	99.72%	99.44%	99.81%	99.53%	
<b>TB3</b>	ND	ND	ND	100%	98.40%	100%	99.44%	99.15%	
<b>Van</b>	ND		98.87%		97.74%		100%		

\* ND: Not determined (testing was only done for wells without detectable visual growth).

## **Supplementary material (file 2)**

### **Identification of the clinical isolates**

#### **1. 16S rDNA amplification:**

The PCR reaction mixture (50 µL) contained 3 µL of 25 mM MgCl<sub>2</sub> (Promega), 1 µL dNTPS 10 mM (Promega), 10 µL HotStart DNA polymerase buffer, 0.2 µL HotStart DNA polymerase 5 U/µL (Promega), 0.25 µL of each of primers 27f (AGA GTT TGA TCA TGG CTC A) and 1492r (TAC GGT TAC CTT GTT ACG ACT T) [100 µM stock of standard à la carte sequencing primers from MWG Eurofins] and PCR-grade water to 50 µL. To provide the template, a flame-sterilized steel pin was touched onto a bacterial colony and the pinpoint of material was transferred to the reaction mix. PCR conditions were: one cycle at 95 °C (10 min) followed by 32 cycles of 95 °C/45s, 52 °C/45 s and 72 °C/1 min. This was followed by a final elongation of 72 °C/12 min. PCR products were checked for purity by agarose electrophoresis and DNA concentrations were measured using Qubit™ dsDNA BR Assay Kit (Thermo Fisher Scientific, Waltham, MA, USA). PCR products were sequenced with Sanger sequencing on both strands at a commercial laboratory (Eurofins Genomics, Germany) using the PCR primers. Sequences were aligned using Clustal Omega [3], and the consensus region of overlap was used for purposes of identification. Sequences were compared to deposited sequences in the GenBank sequence database using BLAST (Basic Tool Alignment Search Tool) (<https://blast.ncbi.nlm.nih.gov/Blast.cgi>). The curated 'Reference RNA sequence' setting in BLAST was used to assign the 16S sequences to a named taxon.

## 2. Whole genome sequencing

Whole genome sequences of the clinical isolates are available under accession number SAMN40573642 for *E. faecalis* isolate P40 and accession numbers SAMN40573970 and SAMN40573973 for *S. aureus* isolates P14 and P20, respectively. The two isolates form part of a larger study involving WGS of multiple dry eye isolates which is currently being prepared for publication. More details of the methodology can be made available on request. In brief, genomic DNA was extracted from the bacterial isolates after inoculation on brain heart infusion agar (ThermoFisher Scientific, CM1136B) using the GenElute Bacterial Genomic DNA kit (NA2120, Sigma-Aldrich-Merck) according to the manufacturer's instructions. DNA library preparation and sequencing were done by Eurofins Genomics (Germany). Briefly, DNA libraries with 150 base pair paired-end reads were generated through fragmentation, end-repair, A-tailing, adapter ligation, size selection and library amplification. Afterwards, sequencing was done by Illumina technology (NovaSeq6000, PE150 mode) and genome assembly and identification was performed by mapping the reads to reference genomes *S. aureus* NCTC 8532 and *E. faecalis* NCTC 775.

## **Errata list**

### **Page 6**

#### **Change from:**

Manuscript under review in the European Journal of Pharmaceutical Sciences

#### **To:**

European Journal of Pharmaceutical Sciences, 2025

DOI: 10.1016/j.ejps.2025.107149

### **Page 49**

#### **Change from:**

Manuscript under review in the European Journal of Pharmaceutical Sciences

#### **To:**

European Journal of Pharmaceutical Sciences, 2025